Privacy-Preserving Location-based Services

A DISSERTATION
SUBMITTED TO THE FACULTY OF THE GRADUATE SCHOOL
OF THE UNIVERSITY OF MINNESOTA
BY

Chi Yin Chow

IN PARTIAL FULFILLMENT OF THE REQUIREMENTS
FOR THE DEGREE OF
Doctor Of Philosophy

May, 2010

Acknowledgements

First and foremost, I would like to express my deepest gratitude to my advisors Dr. Mohamed F. Mokbel and Dr. Tian He. Especially, it has been an honor to be Dr. Mokbel's first Ph.D. student. They have taught me how high quality computer science research is done. I appreciate all their contributions of time, ideas, guidance, and funding to make my Ph.D. experience productive and stimulating. The joy and enthusiasm they have for their research was motivational for me, even during tough times in the Ph.D. pursuit. I am also thankful for the excellent example they have provided as a successful scholar and professor.

The members of the Data Management Lab, Jie Bao, Biplob Debnath, Abdeltawab Hendawi, Mohamed Khalefa, Justin Levandoski, Joe Naps, and Mohamed Sarwat, and the members of the Sensor System Group, Yu Gu, Shuo Guo, Jaehoon Jeong, Qingquan Zhang, Ziguo Zhong, and Ting Zhu, and other peers, Rene Bustamante, Colin DeLong, David Kuo-Wei Hsu, Taehyun Hwang, James Kang, Gaurav Pandey, Nishith Pathak, and Daniel Sandler, have contributed immensely to my personal and professional time at Minnesota. These people have been a source of friendships as well as good advice and collaboration.

I would also like to thank Dr. Xuan Liu, the mentor of my summer intern at the IBM Thomas J. Watson Research Center in 2008, and other great collaborators, Prof. Walid G. Aref (Purdue University), Dr. Jinchuan Chen (Renmin University), Dr. Reynold Cheng (The University of Hong Kong), Dr. Hong-Va Leong (The Hong Kong Polytechnic University), and Dr. Suman Nath (Microsoft Research) for giving their insight suggestions to my research and sharing their research experiences and knowledge with me.

For this thesis, I would like to thank my final oral examination committee members, Prof. Shashi Shekhar (the chair) and Dr. Gediminas Adomavicius (the external member), for their time, insight questions, and helpful comments.

Last but not the least, I would like to thank my fiancée Christine Liu, my sister Aster Chow, and my parents for all their endless love, support, and encouragement. This thesis is dedicated to all of them.

Dedication

To my fiancée Christine Liu, my sister Aster Chow, and my parents.

ABSTRACT

Location-based services (LBS for short) providers require users' current locations to answer their location-based queries, e.g., range and nearest-neighbor queries. Revealing personal location information to potentially untrusted service providers could create privacy risks for users. To this end, our objective is to design a privacy-preserving framework for LBS where users can obtain LBS and preserve their location privacy. In this thesis, we propose privacy-preserving LBS frameworks for different environments: (1) client-server environments in Euclidean space (the *Casper* system), (2) client-server environments in road networks, (3) mobile peer-to-peer environments, and (4) location monitoring services in wireless sensor networks (the *TinyCasper* system). In general, these frameworks have two main modules, namely, *location anonymization* and *privacy-aware query processing*. The location anonymization module blurs an user's exact location into a cloaked area (or a cloaked road segment set in road network environments) that satisfies the user's privacy requirements. The proposed frameworks support the two most popular privacy requirements, *k-anonymity*, i.e., a user is indistinguishable among k users, and *minimum area* A_{min} (or minimum total length of a cloaked road segment set), i.e., the size of a cloaked area is at least A_{min}. The user is able to specify his/her privacy requirements in a privacy profile and change the privacy profile at any time. The privacy-aware query processing module is embedded inside a database server to provide LBS based on cloaked areas (or cloaked road segment sets). To prove the concept of our privacy-preserving LBS frameworks, we implement system prototypes for Casper and TinyCasper. For each proposed privacy-preserving LBS framework, we conduct extensive experiments to evaluate the performance of its location anonymization and privacy-aware query processing modules. All experiment results show that the proposed frameworks are scalable and efficient with respect to large numbers of users, large numbers of queries, and various privacy requirements, and they provide high quality services in terms of the accuracy of query answers and the query response time.

Contents

List of Tables

List of Figures

Chapter 1

Introduction

Location-based services (LBS) combine the functionality of location-aware devices (e.g., GPS-like devices), wireless communication technologies, and information management to provide personalized services for users based on their current locations. Examples of LBS include location-aware emergency services, e.g., *"Dispatch the nearest ambulance"*, location-based advertisement, e.g., *"Send e-coupons to all cars that are within two miles of my gas station"*, live traffic reports, e.g., *"What is shortest path from my current location to a destination"*, and location-based store finders, e.g., *"Where is my nearest restaurant"*. The user registered with LBS continuously send his/her location to a location-based database server. Upon requesting LBS, the registered user issues a location-based query that is executed at the server based on the knowledge of the user's current location [1, 2, 3, 4]. Location-based queries can be categorized into either *snapshot* or *continuous* queries. Examples of snapshot queries include *"Where is my nearest gas station"* and *"What are the restaurants within one mile of my location"*, while examples of continuous queries include *"Continuously report my nearest police car"* and *"Continuously report the gas stations within one mile of my car"*.

Although LBS promise safety and convenience, they threaten the privacy and security of their users. The privacy threat comes from the fact that LBS providers rely mainly on an implicit assumption that the user agrees to reveal his/her private location to get LBS. In other words, the user trades his/her privacy with the service. If the user wants to keep his/her private location information, the user has to turn off the location-aware device and (temporarily) unsubscribe from the service. With potentially

untrusted servers, such a service subscription model poses several privacy threats to the user. For example, an employer may check on his/her employee's behavior by knowing the places where the employee visits and the time of each visit, the personal medical records can be inferred by knowing which clinic a person visits, or someone can track the locations of his/her ex-friends. In many real-life cases, people abuse GPS devices to stalk personal locations [5, 6, 7], and many people worry about their location privacy when they are using LBS [8]. Unfortunately, the traditional approach of *pseudonymity* (i.e., using a fake identity) [9] is not applicable to LBS, as the location information of a person can directly lead to the true identity. For example, asking about the nearest Pizza restaurant to the location of my house using a fake identity will reveal my true identity, as a resident of the house. In fact, many web-based tools are available to translate a location into a street address (e.g., Google Maps [10]) and find the resident of a street address (e.g., Intelius [11]).

In this thesis, we first present the *Casper* system [12, 13]; a query processing framework for privacy-preserving LBS. Casper consists of two main components, *location anonymizer* and *privacy-aware query processor*. The location anonymizer, which is a trusted third party placed between the user and the database server, blurs a user's exact location point into a *cloaked area* that satisfies the user's privacy requirements. Casper supports the two most popular privacy requirements, k-anonymity, i.e., a user is indistinguishable among k users, and minimum area A_{min}. Thus, a user's cloaked area contains at least $k-1$ other users and the size of the cloaked area is at least A_{min}. The privacy-aware query processor is embedded inside the database server to process both snapshot and continuous location-based queries based on cloaked areas rather than location points. The privacy-aware query processor supports three types of privacy-aware queries: (1) *private queries over public data*, (2) *public queries over private data*, and (3) *private queries over private data*. Data and/or queries are public if their exact location information is reported to the database server, while data and/or queries are private if only their cloaked location areas are reported to the database server. Since the privacy-aware query processor only knows that the query issuer and/or data are located in cloaked areas, the query processor can only returns a *candidate answer set* to the location anonymizer. Casper guarantees that the candidate answer set includes the exact answer to the user. As the location anonymizer knows the exact location of

the query issuer and data, it computes the exact answer for the user. To prove the concept of Casper, we implement a system prototype for Casper [14], where the location anonymizer is implemented as a stand-alone server placed between the user and the database server, and the privacy-aware query processor is implemented as query operators inside the PLACE server; a scalable location-aware database server developed by the Purdue University for spatio-temporal data streams [15, 16].

In some other privacy-preserving LBS frameworks, the user has to blur his/her location into a cloaked area without the help of the location anonymizer and contact the database server directly. Thus, the user has to receive the entire candidate answer set from the database server, and then computes the exact answers from the candidate answer set. Since the bandwidth of communication channels between the mobile user and the database server could be very limited (e.g., the downlink bandwidth of 3G mobile subscribers ranges from 128 kbps at vehicular speeds to 2 Mbps at stationary or very slow speeds), we propose an approximate range nearest-neighbor query, i.e., private queries over public data, with a quality guarantee [17]. It is important to note that the proposed query processing algorithm can also be used to deal with uncertain locations, where the user's location is modeled as a spatial area to capture its uncertainty. Given a query region and an approximation tolerance level t, the query processing algorithm returns a candidate answer set such that at least one of the t nearest objects of every point inside the query region is in the candidate answer set. The larger the value of t, the smaller the candidate answer set is returned to the user from the database server. Thus, the approximation tolerance level t can be served as a tuning parameter that trades off between the query response time and the quality of answers.

We extend the functionalities of Casper to road network environments [18], where a user's location is blurred into a set of connected road segments rather than a spatial area. Each user specifies two privacy parameters k and L_{min} in his/her privacy profile, such that the user's cloaked segment set contains at least k users and the total length of the cloaked segment set is at least L_{min}. The extended query processing framework is not only designed specifically for the road network environment, but it is also "query-aware" as it aims to balance between the query execution cost and the size of the candidate answer set returned to the user from the database server.

In mobile peer-to-peer (P2P) networks, where mobile users can only communicate

with other peers through multi-hop routing without any support of fixed communication infrastructure or centralized/distributed servers. The mobile P2P networks have many unique limitations, e.g., user mobility, limited transmission range, multi-hop communication, scarce communication resources, and network partitions[1] . With the advances in wireless communication technologies and mobile devices, the mobile P2P networks have become an important computing platform, so we propose a P2P spatial cloaking algorithm that mainly extends the functionality of the location anonymizer of Casper to the mobile P2P networks [19, 20]. The main idea of the P2P spatial cloaking algorithm is that when a mobile user wants to obtain services from an LBS provider, the user collaborates with other peers via multi-hop communication to blur his/her location into a cloaked area. Our algorithm guarantees that the cloaked area satisfies the user's k-anonymity and minimum area A_{min} privacy requirements. Then, the user sends his/her location-based query along with the cloaked area to the database server. After the user gets the candidate answer set from the database server, the user computes the exact answer from the candidate answer set.

This thesis finally presents the *TinyCasper* system; a privacy-preserving location monitoring system designed for wireless sensor networks [21]. In traditional location monitoring systems, sensors are deployed in the system to track personal locations. However, monitoring personal locations with a potentially untrusted system poses privacy threats to the monitored individuals, because an adversary could abuse the location information gathered by the system to infer personal sensitive information [22, 23, 24, 25]. To tackle the privacy breach in location monitoring systems, each sensor node blurs its sensing area into a cloaked area, in which at least k persons are residing. TinyCasper only allows each sensor node to report aggregate location information, which is in a form of a cloaked area along with the number of persons, N, located in the cloaked area, where $N \geq k$, to the server. It is important to note that the value of k achieves a trade-off between the strictness of privacy protection and the accuracy of monitoring services. A smaller k indicates less privacy protection, because a smaller cloaked area will be reported from the sensor node to the server; hence, more accurate monitoring services. However, a larger k results in a larger cloaked area, which will reduce the

[1] In a partitioned network, mobile users are partitioned into disjoint networks, in which a mobile user is only able to communicate with other peers residing in his/her network partition.

accuracy of monitoring services, but it provides better privacy protection. Although TinyCasper only knows the aggregate location information about the monitored persons, it can still provide monitoring services through answering aggregate queries, for example, *"What is the number of persons in a certain area"*. To support aggregate queries, we propose a *spatial histogram* that analyzes the aggregate locations reported from the sensor nodes to estimate the distribution of the monitored persons in the system. The estimated distribution is used to answer the aggregate queries. To prove the concept of TinyCasper, we implement a system prototype for TinyCasper [26] with 39 MICAz motes [27] on a physical test-bed, and the spatial histogram is implemented inside the base station computer with visualization.

1.1 Related Work

In this section, we highlight the related work to privacy-preserving LBS in four different areas, namely, location privacy, location-based query processing, privacy models, and privacy-aware query processing.

1.1.1 Location Privacy

Motivated by the privacy threats of location-detection devices [28, 29, 30, 31], recent attempts for providing location privacy in location-based services (LBS) (e.g., [32, 30, 19, 33, 34, 35, 36, 37, 38, 39, 40, 41, 42, 43, 44, 45, 46, 47, 48]) and other location-aware applications (e.g., context-aware computing [49] and sensor networks [23]) focus only on the location anonymizer part. Although such techniques would be valuable for protecting users' private locations in LBS, the practicality in real location-based database servers is doubtful as these techniques lack privacy-aware query processing capacity. By protecting users' location information from being disclosed to the location-based database server, processing these location privacy-preserving queries becomes challenging where new techniques need to be presented to provide efficient query processing while not being able to know users' exact locations.

In general, four different approaches have been explored: (1) False dummies [45]. For every location update, a user sends n different locations to the server with only one of them is true while the rest are dummies. Thus, the server cannot know which one of these

locations is the actual one. (2) Landmark objects [43]. Rather than sending the exact location to a location-based database server, the user refers to the location of a certain landmark or a significant object. (3) Location perturbation [32, 19, 33, 34, 35, 36, 37, 38, 39, 40, 41, 44, 46, 47, 48]. The main idea is to blur a user's exact location into a cloaked area using either spatial or temporal cloaking [32, 19, 33, 36, 37, 38, 39, 41, 44, 46, 47, 48] or location obfuscation [35]. The cloaked area can be based either on the k-anonymity concept [50, 51, 52] (i.e., the area should contain at least k users) or on a graph model that represents a road network [35]. (4) Avoid location tracking [30, 40]. While the previous three approaches focus only on hiding a certain instance of the user location, this approach aims to avoid tracking the user behavior.

Among these location anonymization techniques, our proposed privacy-aware query processor supports the location perturbation techniques that blur users' exact locations into rectilinear areas, i.e., cloaked areas, as this is the most commonly used form of location anonymization in many various environment settings, e.g., [32, 19, 36, 37, 38, 39, 41, 44] for snapshot locations, [33, 34, 47, 48] for continuous locations, [48] for spatial networks, and [26, 23] for wireless sensor networks.

1.1.2 Location-based Query Processing

A plethora of techniques has been proposed to deal with various *snapshot* location-based queries (e.g., [53, 54, 55, 56, 57, 58, 59]) and *continuous* location-based queries (e.g., [60, 61, 62, 63, 64, 3, 65, 66]). The main idea of snapshot queries is to provide an efficient and real-time execution of location-based queries using spatio-temporal index structures for frequently updated data. On the other hand, query processors for continuous location-based queries have mainly focused on efficiency and scalability. In terms of efficiency, several techniques have been proposed to use grid-based structures to support location-based services for moving data and moving queries (e.g., [61, 62, 3, 67, 65]). In terms of scalability, several techniques have proposed to employ a shared execution paradigm in which multiple concurrent continuous queries can be evaluated simultaneously at the location-based database server (e.g., [68, 60, 65, 69]). However, all these query processors for snapshot and continuous location-based queries rely on the knowledge of the users' exact locations as none of these techniques have considered private data and/or private queries.

1.1.3 Privacy Models

During the last decade, several paradigms of architecture have been explored to provide secure data transformation from the client to the server machines. Secure-multi-party communication [70, 71] organizes the communication among m parties such that each party can have the knowledge of only a certain function but not the actual data for other parties. However, the computational overhead of such a scheme prevents its direct application to database problems. Thus, the minimal information sharing [72] paradigm is proposed where it uses cryptographic techniques to perform join and intersection operations. However, the computational cost and the inability to serve other queries make such a paradigm not suitable for real time applications. The untrustworthy third party [73] paradigm has been proposed in the context of peer-to-peer systems. The main idea is to employ a third party that executes queries by collecting secure information from multiple data sources, i.e., peers. The most commonly used model is the trusted third party [74, 75] paradigm. The main idea is to employ a third party that is trusted by the users and acts as a middle layer between the user and the database server.

Among these models, our framework employs the trusted third party model as it requires less computational overhead and is more suitable for real-time query processing. The trusted third party model is already utilized by existing location privacy techniques (e.g., [30, 32, 19, 33, 36, 37, 41, 44, 46, 12, 47, 48]) and is commercially applied in other fields. For example, the Anonymizer [76] is for anonymous web surfing while the PayPal [77] system is a trusted third party where a user can buy products without giving his/her credit card information to the provider.

1.1.4 Privacy-Aware Query Processing

Recent research efforts have been dedicated to deal with location privacy-preserving queries, i.e., getting anonymous services from location-based applications (e.g., [34, 78, 44, 79, 80, 12, 81]). These query processing frameworks can be divided into three main categories. (1) Location obstruction [81]. The basic idea is that a querying user first sends a query along with a false location to a database server, and the database server keeps sending the list of nearest objects to the reported false location to his/her until the list of received objects satisfies the user's privacy and quality requirements. (2) Space

transformation [78, 79]. This approach converts the original location of data and queries into another space through a trusted third party. The space transformation maintains the spatial relationship among the data and query, in order to provide accurate query answers. (3) Cloaked area processing [34, 44, 80, 12]. In this framework, a privacy-aware query processor is embedded in the database server side to deal with the cloaked spatial area received either from a querying user [34, 80] or from a trusted third party [44, 12].

Among the existing cloaked area processing frameworks, the works [80, 44] are closest to ours. These works find the exact set of objects as a query answer based on the linear nearest neighbor search algorithm [82]. The difference between these two works is that the work [80] considers rectilinear cloaked areas while the other one considers circular cloaked areas [44]. The key distinctions between these two works and our proposed privacy-aware query processor are follows: (1) Our query processor has the ability to ease the optimality of query answers by finding a superset of the minimal answer set that contains the exact answer, in order to achieve system scalability. We use a tuning parameter to trade off between the system scalability and the candidate answer set size. (2) According to our classification of privacy-aware queries, these two previous works consider only private queries over public data, so they cannot be applied to the case of private data. (3) We consider continuous privacy-aware queries by proposing a *shared execution paradigm* that aims to improve system scalability when dealing with a numerous number of privacy-aware continuous queries. The shared execution paradigm also provides two other tuning parameters to trade off between system scalability and answer optimality. The detail of our privacy-aware query processor will be described in Section 4.

1.2 Organization of the Thesis

In this chapter, we have described the background of privacy-preserving LBS and the motivation and contribution of this thesis. The rest of this thesis is organized as follows:

- Chapter 2 describes the architecture and system model of the Casper system, and the Casper prototype.
- Chapter 3 presents the location anonymization algorithms used by the location

anonymizer of Casper to blur users' locations into cloaked areas.

- Chapter 4 gives the query processing algorithms proposed for the privacy-aware query processor of Casper to process the three introduced privacy-aware query types, i.e., private queries over public data, public queries over private data, and private queries over private data.
- Chapter 5 presents the query processing algorithm for approximate range nearest-neighbor queries with quality guarantees.
- Chapter 6 describes the query-aware location anonymization algorithms and query processing algorithms for privacy-preserving LBS in road network environments.
- Chapter 7 gives the spatial cloaking algorithm, designed for location anonymization, in mobile P2P environments.
- Chapter 8 describes the architecture and system model of the TinyCasper system, and the TinyCasper prototype.
- Chapter 9 presents the in-network location anonymization algorithms and the spatial histogram, designed for supporting aggregate query processing, in TinyCasper.
- Chapter 10 concludes this thesis and discusses future research directions in privacy-preserving LBS.

Chapter 2

The Casper System

This chapter describes the architecture of the *Casper* system and the Casper prototype. In Casper, mobile users can entertain location-based services (LBS) without the need to reveal their private location information. Upon registration with Casper, the mobile users specify their desired level of privacy through a user *privacy profile*. A user privacy profile includes two parameters k and A_{min}. k indicates that the mobile user wants to be k-anonymous, i.e., not distinguishable among other k users while A_{min} indicates that the user wants to hide her location information within an area of at least A_{min}. Large values for k and A_{min} indicate stricter privacy requirements. Our employed privacy profile matches the privacy requirements of mobiles users as depicted by several social science studies (e.g., see [29, 40, 42, 83, 84]).

Casper mainly consists of two components, namely, the *location anonymizer* and the *privacy-aware query processor*. The location anonymizer is a trusted third party that acts as a middle layer between the mobile user and the location-based database server in order to: (1) receive the user's exact location along with his/her privacy profile, (2) blur the user's exact location into a *cloaked area* based on the user's privacy profile, and (3) send the cloaked area to the location-based database server. The *privacy-aware query processor* is embedded inside the location-based database server to tune its functionality to deal with anonymous queries and cloaked areas rather than the exact location information. We identify three novel query types that are supported by Casper: (a) Private queries over public data, e.g., *"Where is my nearest gas station"*, in which the person who issues the query is a private entity while the data (i.e., gas stations) are

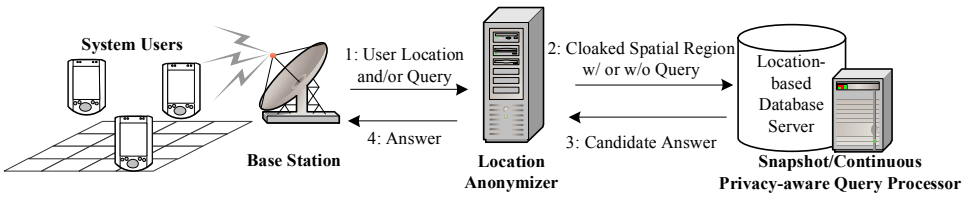

Figure 2.1: The Casper system architecture.

public, (b) Public queries over private data, e.g., *"How many cars in a certain area"*, in which a public entity asks about personal private locations, and (c) Private queries over private data, e.g., *"Where is my nearest buddy"* in which both the person who issues the query and the requested data are private. With this classification in mind, traditional location-based query processors can support only public queries over public data. Due to the lack of the exact location information at the server, the privacy-aware query processor returns a *candidate answer set* instead of a single exact answer to the location anonymizer. Since the location anonymizer knows the user's exact location, it computes the exact answer for the user. In Chapter 4, we prove that the candidate answer set returned by our privacy-aware query processor is *inclusive*, i.e., the candidate answer set contains the exact answer to the user, and is *minimal*, i.e., the candidate answer set size is minimal.

2.1 Architecture

Figure 2.1 depicts the system architecture of Casper, which has two main components: the location anonymizer and the privacy-aware query processor. The location anonymizer receives location updates from mobile users, blurs their locations to cloaked areas that match their user privacy profiles (k, A_{min}), and sends the cloaked areas to the location-based database server. While cloaking the user's location information, the location anonymizer also removes any user identity from the user's request to ensure the pseudonymity of the location information [9]. Similar to the exact point locations, the location anonymizer also blurs the query location information before sending a cloaked query area to the location-based database server.

The privacy-aware query processor is embedded inside the location-based database

server to deal with location-based queries based on cloaked areas rather than exact location points. Instead of returning an exact answer, the privacy-aware query processor returns a candidate answer set for the location-based query to the location anonymizer. As the location anonymizer knows the user's exact location, it computes the exact answer for the user. The privacy-aware query processor guarantees that the candidate answer set contains the exact query answer. The size of the candidate list heavily depends on the user privacy profile. A stricter privacy profile would result in a larger candidate list. With user privacy profiles, mobile users have the ability to adjust a personal trade-off between the amount of information they would like to reveal about their locations and the size of the candidate answer sets that they obtain from Casper. Location-based queries processed at the privacy-aware location-based database server may be received either from the mobile users or from public administrators. Queries that come from mobile users are considered as private queries and should pass by the location anonymizer to hide the query identity and blur the location of the user who issues the query. Location-based queries that are issued from public administrators are considered as public queries and do not need to pass through the location anonymizer, instead, they are directly submitted to the location-based database server. The database server will answer such public queries based on the stored blurred location information of all mobile users.

2.2 System Prototype

The system prototype of Casper consists of three different modules that can run on three different machines, namely, the client module (Figure 2.2), the location anonymizer module (Figures 2.3 and 2.4), and the location-based database server module (Figure 2.5). While both the client and the location anonymizer are implemented as stand alone applications, the privacy-aware query processor is implemented as query operators inside the PLACE server; a research prototype for location-based database services [2, 15]. Figure 2 gives a GUI screen shot of the client module. The GUI is divided into four parts: (1) A road network map that displays the position of the client roaming on the road network. In addition, query results that are requested by the client are displayed on the road network map. (2) The privacy profile interface where the user can update

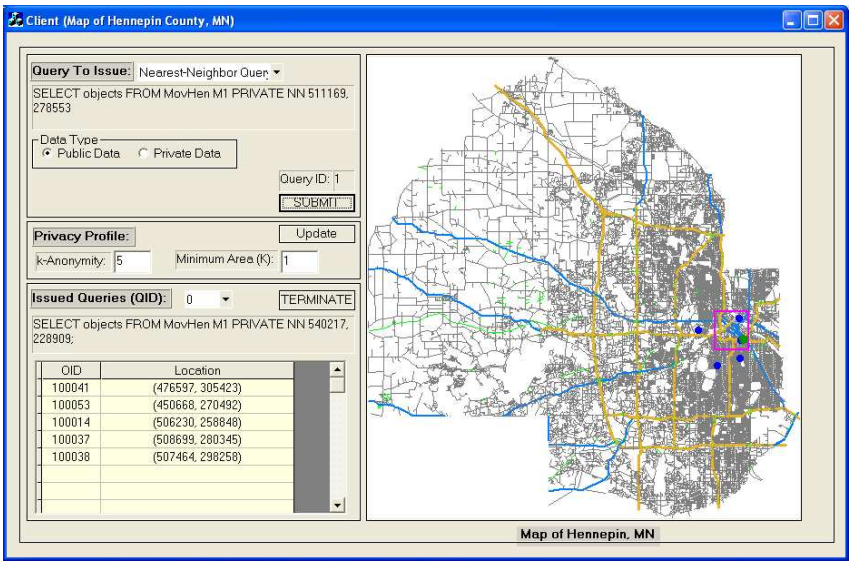

Figure 2.2: The client GUI.

the values of k and A_{min} at any time and submit the updated privacy profile to the location anonymizer. (3) The query submission interface in which the client has the ability to choose from four different query types, public query over public data, private query over public data, public query over private data, and private query over private data. Notice that the first query type is the traditional query type in location-based database servers while the latter three query types are unique to Casper. With each query type, there is a set of controls that appears to the clients to help in forming the required query without actually writing the SQL query. Figure 2.2 gives an example where the client selects a private query over public data. In this case, the client has the ability to choose either a range query or a nearest-neighbor query. In case of a range query, the client has to specify the range around its location. The SQL query will be displayed to the user for illustration. (4) The query result interface in which the query answer is tabulated to the user in addition to being shown on the road network map.

Figures 2.3 and 2.4 give the GUI screen shot for the *basic* and *adaptive* location anonymizers, respectively. The details of the basic and adaptive location anonymizers are described in Chapter 3. The GUI mainly shows the current exact locations of all participating mobile users over the road network. The level of the pyramid data structure is displayed as a grid over the road network. The number of mobile users at

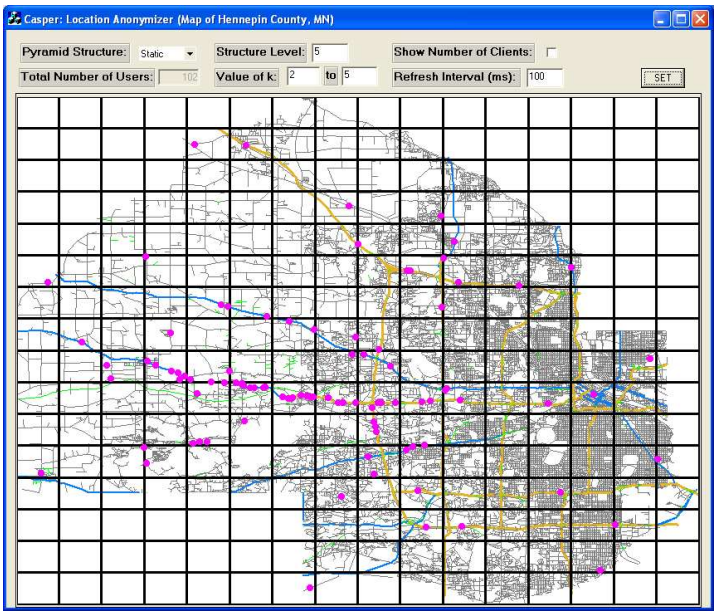

Figure 2.3: The basic location anonymizer.

each grid cell is displayed along with the grid level in the case of the adaptive anonymizer (Figure 2.4). As a default, the GUI displays only the lowest-level maintained cells. As a result, all grid cells in the basic location anonymizer GUI are of the same size (Figure 2.3) while in the adaptive location anonymizer GUI, grid cells have different sizes (Figure 2.4). For illustration, there is a set of controls at the top of the GUI for both location anonymizers that: (1) Alternates the GUI to show either the basic or the adaptive location anonymizer, (2) Controls the maximum level of the pyramid structure, (3) Turns on/off the counter display at each grid cell, and (4) Sets a parameter that refreshes the GUI every certain milliseconds in order to achieve better visualization. Figure 2.5 gives the GUI screen shot for the privacy-aware location-based database server which is implemented inside the PLACE server [2, 15]. The GUI shows the road network map with the exact locations of stationary public data (e.g., restaurants, gas stations, and hospitals) and moving public data (e.g., police cars). For private data (i.e., user location information), the server can show only the cloaked area that is received from the location anonymizer. The query processing steps are shown on the server console during the query life time.

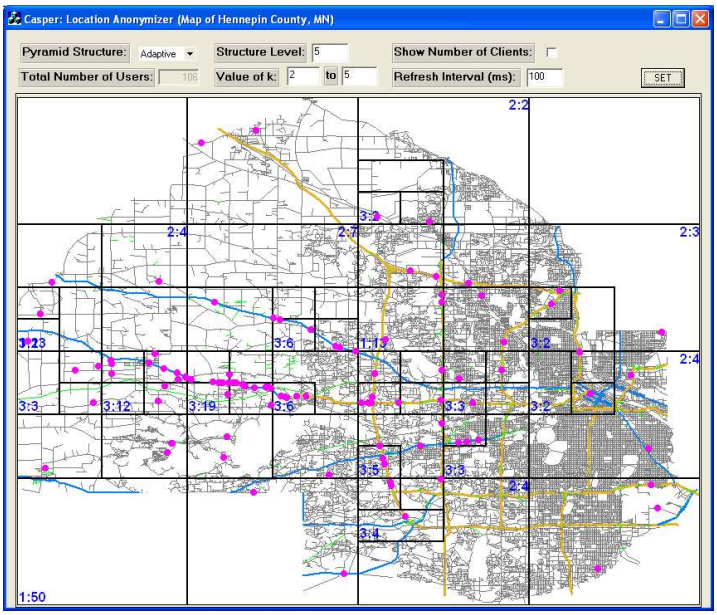

Figure 2.4: The adaptive location anonymizer.

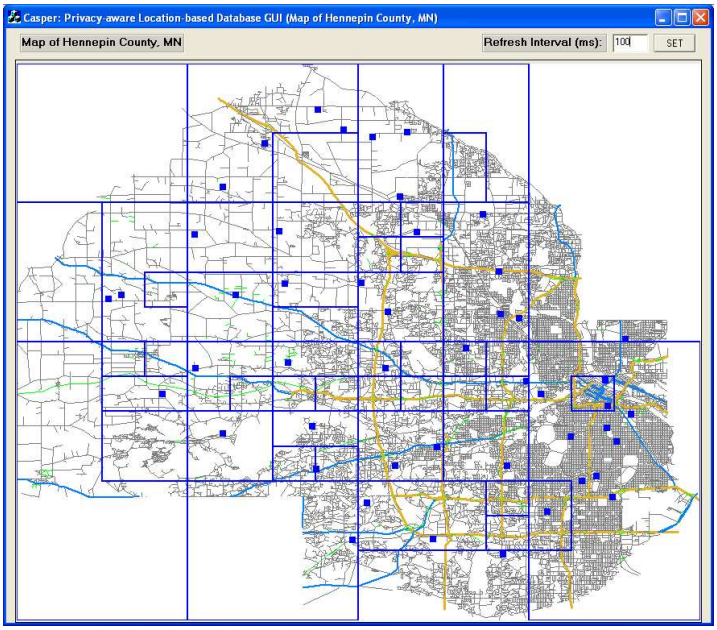

Figure 2.5: The server GUI.

Chapter 3

Location Anonymization in Casper

In this chapter, we describe the data structures designed for the location anonymizer in Casper. As depicted in Figure 2.1 (in Chapter 2), the location anonymizer blurs the exact location point of each mobile user to a cloaked area R that satisfies each user's privacy profile. To avoid the drawbacks of previous location anonymizers [85, 37], i.e., the assumption of a system-wide static k-anonymity for all users [37] and the support of only small k-anonymity levels ($k \approx 10$) [85], we identify the following four requirements that we aim to satisfy in our location anonymizer:

1. **Accuracy.** The cloaked area R should be of area A_R and contain k_R users that satisfy and as close as possible to the user profile (i.e., $k_R \gtrsim k$, $A_R \gtrsim A_{min}$).

2. **Quality.** An adversary can only know that the exact user location information could be equally likely anywhere within the cloaked area R.

3. **Efficiency.** The cloaking algorithm should be computationally efficient and scalable. It should be able to cope with the continuous movement of large numbers of mobile users and real-time requirements of spatio-temporal queries.

4. **Flexibility.** Each registered user with the location anonymizer should have (1) the ability to specify her own privacy requirements and (2) the ability to change her requirements at any time.

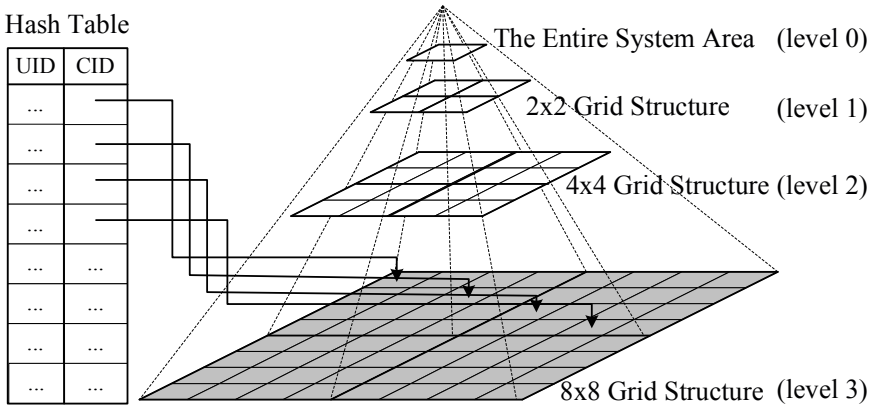

Figure 3.1: The basic location anonymizer.

Notice that the spatio-temporal cloaking algorithm in [37] can support only the quality requirement, while the CliqueCloak algorithm in [85] can partially support the accuracy and flexibility requirements in terms of the k-anonymity parameter. In the rest of this section, we present two alternative techniques for our location anonymizer that satisfy the above four requirements, namely, the *basic* location anonymizer and the *adaptive* location anonymizer.

3.1 The Basic Location Anonymizer

Data structure. Figure 3.1 depicts the data structure for the basic location anonymizer. The main idea is to employ a grid-based complete pyramid data structure [86] that hierarchically decomposes the spatial space into H levels where a level of height h has 4^h grid cells. The root of the pyramid is of height zero and has only one grid cell that covers the whole space. Each pyramid cell is represented as (cid, N) where cid is the cell identifier while N is the number of mobile users within the cell boundaries. The pyramid structure is dynamically maintained to keep track of the current number of mobile users within each cell. In addition, we keep track of a hash table that has one entry for each registered mobile user with the form $(uid, profile, cid)$ where uid is the mobile user identifier, $profile$ is the user's privacy profile, and cid is the cell identifier in which the mobile user is located. cid is always at the lowest level of the pyramid (the shaded level in Figure 3.1).

Algorithm 1 Bottom-up Cloaking Algorithm

```
1: Function BottomUp-Cloaking(k, A_min, cid)
2: if cid.N ≥ k and cid.Area ≥ A_min then
3:    return Area(cid);
4: end if
5: cid_V ← The vertical neighbor cell of cid.
6: cid_H ← The horizontal neighbor cell of cid.
7: N_V = cid.N + cid_V.N, N_H = cid.N + cid_H.N
8: if (N_V ≥ k OR N_H ≥ k) AND 2cid.Area ≥ A_min then
9:    if (N_H ≥ k AND N_V ≥ k AND N_H ≤ N_V) OR N_V < k then
10:      return Area(cid) ∪ Area(cid_H);
11:   else
12:      return Area(cid) ∪ Area(cid_V);
13:   end if
14: else
15:   BottomUp-Cloaking((k, A_min), Parent(cid));
16: end if
```

Maintenance. Due to the highly dynamic environment of location-based applications, any employed data structure should be sustainable to frequent updates. A location update is sent to the location anonymizer in the form (uid, x, y) where uid is the user identifier, x and y are the spatial coordinates of the user's new location. Once the update is received at the location anonymizer, a hash function $h(x, y)$ is applied to get the user cell identifier cid_{new} at the lowest grid layer. Then, the user entry in the hash table is checked to get its original cell identifier cid_{old}. If the old cell identifier matches the new one ($cid_{old} = cid_{new}$), then there is no need to do any more processing. If there is a change in the cell identifier ($cid_{old} \neq cid_{new}$), three operations should take place: (1) Update the new cell identifier in the hash table, (2) Update the counters N in both the old and new pyramid grid cells, and (3) If necessary, propagate the changes in the cell counters N for higher pyramid layers. If a new user is registered, a new entry will be created in the hash table and the counters of all the affected grid cells in the pyramid structure are increased by one. Similarly, if an existing user quits, its entry is deleted from the hash table and the counters of all affected grid cells are decreased by one.

The cloaking algorithm. Algorithm 1 depicts a bottom-up cloaking algorithm

for the grid-based pyramid structure. The input to the algorithm is the user privacy profile (k, A_{min}) and the cell identifier *cid* for the gird cell that the user is currently in. k and A_{min} should be less than the total number of users registered in the system and the total spatial area, respectively. If the initially given cell already satisfies the user privacy requirement, i.e., $cid.N \geq k$ (the number of users within the cell is greater than k) and $cid.Area \geq A_{min}$ (the cell area is larger than A_{min}), we return the cell *cid* as the cloaked area (Line 3 in Algorithm 1). If this is not the case, we check for the vertical and horizontal neighbor cells to cell *cid*. Two cells are considered neighbors to each other if they have the same parent and lie in a common row (horizontal neighbor) or column (vertical neighbor). Thus, each cell has only one horizontal and one vertical neighbors. If the combination of the cell *cid* with any of its neighbors yields a spatial region that satisfies the anonymity requirement, we return the combination that gives closer value to k (Lines 5 to 13 in Algorithm 1). If none of the neighbors can be combined with cell *cid*, then the algorithm is recursively executed with the parent cell of *cid* till a valid cell is returned (Line 15 in Algorithm 1).

3.2 The Adaptive Location Anonymizer

The basic location anonymizer incurs high cost for both location updates and cloaking time. For location updates, when a user changes her cell from cid_1 to cid_2, a set of updates need to be propagated from cid_1 and cid_2 at the lowest level till a common parent is reached. For the cloaking time, Algorithm 1 has to start from the lowest level regardless of the user privacy requirements. To avoid these drawbacks, we introduce the adaptive location anonymizer where the pyramid structure is adaptively maintained to certain levels that match the privacy requirements of existing users.

Data structure. Figure 3.2 depicts the data structure for the adaptive location anonymizer that mainly utilizes an incomplete pyramid structure [87]. The contents of each grid cell and the hash table are exactly similar to those of Figure 3.1. The main idea of the incomplete pyramid structure is to maintain only those grid cells that can be potentially used as cloaking regions for the mobile users. For example, if all mobile users have strict privacy requirements where the lowest pyramid level would not satisfy any user privacy profile, the adaptive location anonymizer will not maintain such

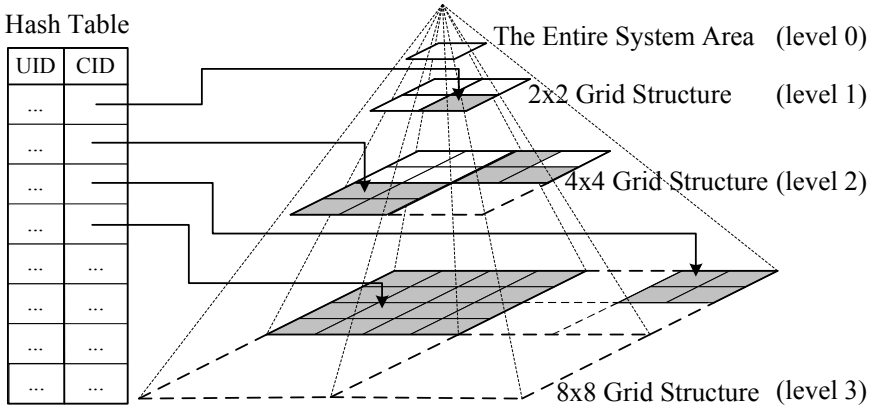

Figure 3.2: The adaptive location anonymizer.

level, hence, the cost of maintaining the pyramid structure is significantly reduced. The shaded cells in Figure 3.2 indicate the lowest level cells that are maintained (Compare to Figure 3.1 where all shaded cells are only in the lowest level). As an example, in the second topmost level, the right bottom quadrant is shaded indicating that all users in this quadrant have strict privacy requirements that will not be satisfied by any lower grid cell. Notice that it is not necessary to extend a whole quadrant. For example, in the lowest level, there are four shaded cells in the upper-right corner to indicate that these cells have the most relaxed user privacy requirements. Instead of having the hash table pointing to the lowest pyramid level as in Figure 3.1, in the adaptive location anonymizer, the hash table points to the lowest maintained cells which may not be at the lowest pyramid level.

Maintenance. In addition to the regular maintenance procedures as that of the basic location anonymizer, the adaptive location anonymizer is also responsible on maintaining the shape of the incomplete pyramid. Due to the highly dynamic environment, the shape of the incomplete pyramid may have frequent changes. Two main operations are identified to maintain the efficiency of the incomplete pyramid structure, namely, cell *splitting* and cell *merging*.

Cell splitting. A cell *cid* at level i needs to be split into four cells at level $i+1$ if there is at least one user u in *cid* with a privacy profile that can be satisfied by some cell at level $i+1$. To maintain such criterion, we keep track of the most relaxed user u_r for each cell. If a newly coming object u_{new} to the cell *cid* has more relaxed privacy

requirement than u_r, we check if splitting cell *cid* into four cells at level $i+1$ would result in having a new cell that satisfies the privacy requirements of u_{new}. If this is the case, we will split cell *cid* and distribute all its contents to the four new cells. However, if this is not the case, we just update the information of u_r. In case one of the users leaves cell *cid*, we just update u_r if necessary.

Cell merging. Four cells at level i are merged into one cell at a higher level $i-1$ only if all the users in the level i cells have strict privacy requirements that cannot be satisfied within level i. To maintain this criterion, we keep track of the most relaxed user u'_r for the four cells of level i together. If such user leaves these cells, we have to check upon all existing users and make sure that they still need cells at level i. If this is the case, we just update the new information of u'_r. However, if there is no need for any cell at level i, we merge the four cells together into their parent cell. In the case of a new user entering cells at level i, we just update the information of u'_r if necessary.

The high cost of cell splitting and merging is amortized by the huge saving in continuous updates and maintenance of large numbers of non-utilized grid cells as in the case of the *basic* location anonymizer. However, the basic assumption is that mobile users are moving at reasonable speeds. Thus, cell splitting and merging are not very frequent events. In the case of extremely high speed, e.g., each user movement results in a cell change, the basic location anonymizer would have less maintenance cost than the adaptive one.

The cloaking algorithm. The cloaking algorithm for the adaptive location anonymizer is exactly similar to Algorithm 1. The only difference is that the input to the algorithm is a cell *cid* from the lowest maintained level rather than a cell from the lowest pyramid level. Thus, the number of recursive calls of the algorithm (Line 15 in Algorithm 1) is greatly reduced. In fact, in many cases, we may not need any recursive calls.

3.3 Discussion

Both the *basic* and *adaptive* location anonymizers satisfy the four requirements that we have set at the beginning of this section, namely, *accuracy*, *quality*, *efficiency*, and *flexibility*. In terms of ***accuracy***, the ability to maintain large numbers of small size

grid cells along with searching for horizontal and vertical neighbor grid cells help in achieving higher accuracy for large number of users of various privacy requirements. For ***quality***, the fact that we utilize a pre-defined space partitioning scheme (i.e., the pyramid structure) guarantees that the cloaked area is completely independent form the data. Thus, an adversary cannot guess any information about the exact user location other than that the probability that the user is located at a certain point in the cloaked region R is $\frac{1}{Area(R)}$ for all points within R, i.e., the possible user location is uniformly distributed over the cloaked region R. Compared to previous algorithms [85, 37], the ***efficiency*** of the pyramid-based location anonymizer is obvious as its pre-computed grid cells scale well to large numbers of mobile users. The main idea is that the *cloaking* time is considerably low as the space is already partitioned while the update time is optimized through the efficient grid structure. With respect to ***flexibility***, our location-anonymizer allows each user to specify her convenient privacy requirements through the privacy profile (k, A_{min}). In addition, a user has the flexibility to change her privacy profile anytime.

3.4 Experiment Results

In this section, we evaluate and compare the efficiency and scalability of both the *basic* and *adaptive* location anonymizers with respect to the cloaking time, maintenance cost, and accuracy. We were unable to perform comparison with other approaches for the location anonymizer [85, 37] as these approaches are limited either for small numbers of users [37] or for privacy requirement (k is from 5 to 10) [85]. In all the experiments of this section, we use the Network-based Generator of Moving Objects [88] to generate a set of moving objects. The input to the generator is the road map of Hennepin County in Minnesota, USA (Figure 3.3). The output of the generator is a set of moving objects that move on the road network of the given city. Target objects are chosen as uniformly distributed in the spatial space. Unless mentioned otherwise, the experiments in this section consider 50K registered mobile users in a pyramid structure with 9 levels. We generate a random privacy profile for each user where k and A_{min} are assigned uniformly within the range [1-50] users and [.005,.01]% of the space, respectively.

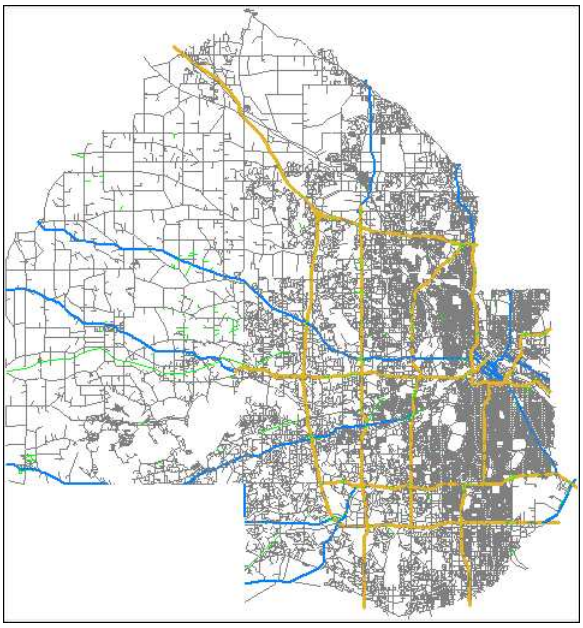

Figure 3.3: Map of Hennepin County, MN, USA.

3.4.1 The Pyramid Height

Figure 3.4 gives the effect of the pyramid height on the performance of both the *basic* and *adaptive* location anonymizers. The pyramid height varies from four to nine levels. Figure 3.4a gives the effect of the pyramid height on the average cloaking time per user request (Algorithm 1). For more than six pyramid levels, the performance of the *adaptive* approach is clearly better. The main reason is that the *adaptive* approach smartly decides about the lowest maintained level such that the number of pyramid levels to be searched is minimized. Figure 3.4b gives the effect of the pyramid height on the average number of updates required for each location update. For lower pyramid levels, the *basic* approach has a lower update cost as the cost of splitting and merging in the *adaptive* approach prevails the savings in updating the cell counters. However, for higher pyramid levels, the *adaptive* approach has less update cost as it encounters huge savings in updating large numbers of cell counters.

Optimally, a user wants to have a cloaked region that exactly matches her privacy profile. Due to the resolution of the pyramid structure, the *location anonymizer* may not be able to provide an exact match. Instead, a more restrictive cloaked region will

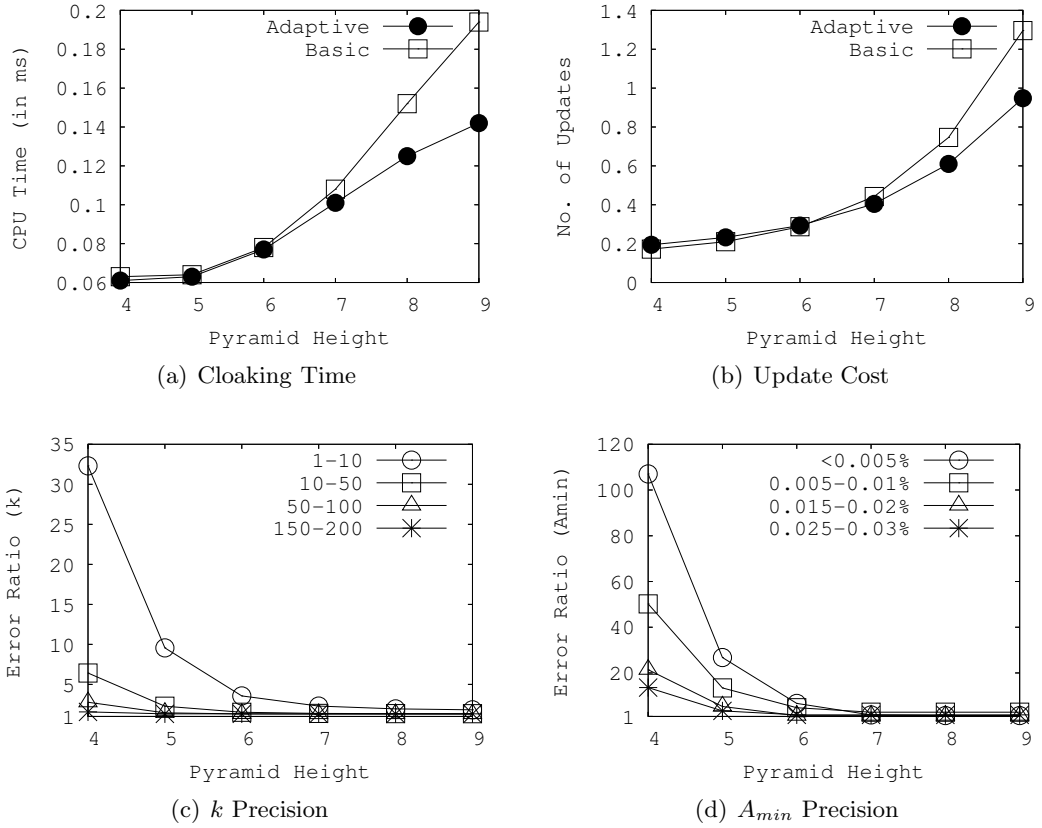

(a) Cloaking Time (b) Update Cost

(c) k Precision (d) A_{min} Precision

Figure 3.4: Effect of the pyramid structure height for the location anonymizer.

be given to the user which may result in a lousy service that the user is not comfortable with. Figures 3.4c and 3.4d give the effect of the pyramid height on the accuracy of the cloaked region in terms of k and A_{min}, respectively. Both the *basic* and *adaptive* approaches yield the same accuracy as they result in the same cloaked region from Algorithm 1. In Figure 3.4c, the accuracy is measured as k'/k, where k' is the number of users included in the cloaked spatial region while k is the exact user requirement. We run the experiment for various groups of users with most relaxed privacy requirements (k is from 1 to 10) to restrictive users (k is from 150 to 200) while setting A_{min} to zero. Lower pyramid levels give very inaccurate answer for relaxed users. However, higher pyramid levels give very accurate cloaked region that is very close to one (optimal case) even for relaxed users. Similar behavior is depicted in Figure 3.4d where the accuracy

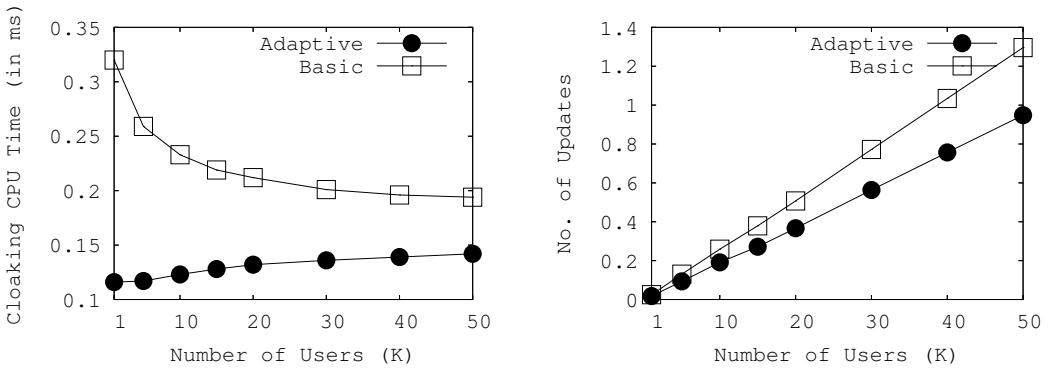

(a) Cloaking Time (b) Update Cost

Figure 3.5: Effect of the number of users for the location anonymizer.

is measured as A'/A_{min}, where A' is the computed cloaked area while A_{min} is the required one. Also, we run the experiment for several groups of users with various A_{min} requirements while setting k to one.

3.4.2 Scalability

Figure 3.5 gives the scalability of the *basic* and *adaptive* location anonymizers with respect to varying the number of registered users from 1K to 50K. With respect to the cloaking time (Figure 3.5a), the performance of the *basic* location anonymizer is greatly enhanced with the increase of the number of users. The main idea is that by increasing the number of users, the privacy requirements of mobile users will be likely to be satisfied in lower pyramid levels, i.e., less recursive calls to Algorithm 1. This is not the case for the *adaptive* location anonymizer where the large number of users increases the number of maintained grid cells to accommodate users with various requirements. However, the cloaking time of the *adaptive* approach is always less than that of the *basic* approach. For the update cost (Figure 3.5b), with the increase of the number of users, the performance of the *adaptive* approach is always better than that of the *basic* approach due to the less number of maintained cells.

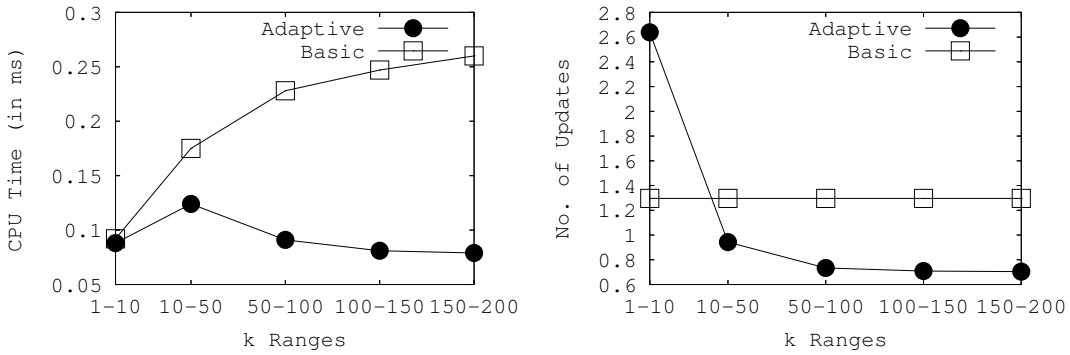

(a) Cloaking Time (b) Update Cost

Figure 3.6: Effect of the k-anonymity levels for the location anonymizer.

3.4.3 Effect of Privacy Profile

Figure 9.10 gives the effect of increasing the k anonymity parameter on both the *basic* and *adaptive* approaches. The range of k varies from [1-10] to [150-200]. For the cloaking time (Figure 9.10a), the *basic* location anonymizer incurs high cloaking cost with more restrictive privacy requirements as it has to traverse more pyramid levels in order to get the desired cloaked region. The *adaptive* location anonymizer has similar cost trend for relaxed users ($k < 50$). However, with more restrictive privacy profile, the performance of the *adaptive* approach gets much better as mobile users tend to cluster in higher pyramid levels, thus decreasing the cloaking time. For the update cost (Figure 9.10b), the *basic* approach is not affected by the privacy profile as it always maintains a complete pyramid structure. On the other hand, the *adaptive* approach has high update cost only for relaxed users as this will require maintaining lower pyramid levels in addition to the splitting and merging cost. However, the *adaptive* approach adopts its structure with more strict privacy requirements to give a much better performance than that of the *basic* approach. Similar figures and experiments give similar results for the case of changing A_{min}.

3.5 Summary

In Casper, the location anonymizer acts as a third trusted party that blurs the exact location information of each user into a cloaked area that matches the user privacy profile. This chapter describes the four requirements from the location anonymizer: accuracy, quality, efficiency, and flexibility. Two alternatives of the location anonymizer that achieve these requirements are proposed: the *basic* and *adaptive* location anonymizers. We use a complete pyramid structure for our basic location anonymizer, while a incomplete pyramid structure for our adaptive one. The performance of the basic and adaptive location anonymizers is evaluated through simulated experiments. The results show that the adaptive location anonymizer is more efficient than the basic one in terms of location anonymization time and location update cost.

Chapter 4

Query Processing in Casper

This chapter goes beyond the location anonymization problem as we address the challenging problem of providing *snapshot* and *continuous* LBS even when receiving the user's blurred location information from the location anonymizer rather than the exact locations from system users. Basically, we propose a *snapshot/continuous privacy-aware query processor* that is embedded inside the location-based database server to tune its functionalities to deal with anonymous location-based queries with *cloaked areas* received from the location anonymizer rather than the exact location information. Our privacy-aware query processor is completely independent of the underlying location anonymization algorithm. Thus, any existing location anonymization technique that cloaks users' locations into rectilinear areas can be employed. The proposed query processor supports three privacy-aware query types: (1) Private queries over public data, e.g., *"Where is my nearest gas station"*, in which the person who issues the query is a private entity while the data (i.e., gas stations) is public, (2) Public queries over private data, e.g., *"How many cars within a certain area"*, in which a public entity asks about personal private locations, and (3) Private queries over private data, e.g., *"Where is my nearest buddy"* in which both the person who issues the query and the requested data are private. With this classification in mind, traditional location-based query processors can support only public queries over public data. This query classification is applicable regardless of having the underlying query as *snapshot* or *continuous*.

Due to the lack of exact location information on the server side, the proposed privacy-aware query processor provides a *candidate answer set* instead of an exact answer. We

prove that the candidate answer set is *inclusive*, i.e., contains the exact answer, and is *minimal*, i.e., given certain conditions, the candidate answer set is of minimal size. In addition, our proposed query processor can be tuned through a tuning parameter to provide a trade-off between query processing cost and answer optimality, i.e., the candidate answer set size. For *continuous* location-based queries, we propose a *shared execution paradigm* that enables the privacy-aware query processor to scale to a large number of concurrent continuous queries. The shared execution paradigm maintains the answer of a set of selected static continuous queries, and the answer is shared by all outstanding continuous queries. The proposed shared execution paradigm provides two other tuning parameters to achieve a trade-off between system scalability and answer optimality.

4.1 Snapshot Privacy-Aware Query Processing

In this section, we present the privacy-aware query processing for snapshot queries. Although previous approaches can be used to compute a minimal candidate answer set for *private queries over public data* [80, 82], the minimal candidate answer set would be expensive to compute in many cases, e.g., private queries with large cloaked areas and the number of data is very large. On the other hand, our proposed algorithms for privacy-aware query processing provide a distinct feature to compute a superset of the minimal candidate answer set that contains the exact answer to the user with lower computational cost. We can adjust between the computational cost and the candidate answer set size through a tuning parameter *refine*. A larger value of *refine* gives a smaller candidate answer set, but incurs higher computational cost. When $refine = \infty$, our algorithm provides the same minimal candidate answer set as the previous approaches. Furthermore, although these previous approaches give conditions for pruning internal nodes with rectangular regions in an R-tree to obtain a set of candidate objects for query processing [80, 82], the given conditions are not sufficient for computing a minimal candidate answer set for *private queries over private data*, and simply returning all such candidate objects would result in a large candidate answer set that incurs high transmission time. Similar to *private queries over public data*, our algorithm for *private queries over private data* also supports the tuning parameter *refine*. When $refine = \infty$,

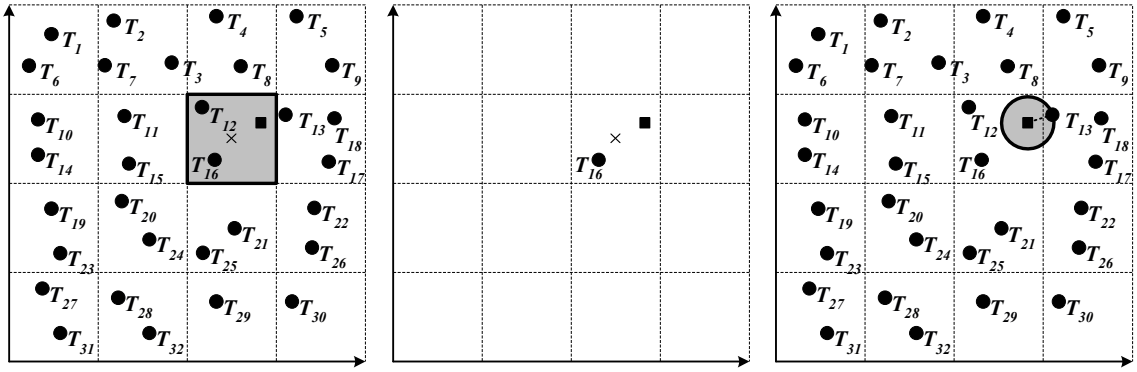

(a) The Server (b) Client: Trivial Approach I (c) Client: Trivial Approach II

Figure 4.1: Two trivial approaches for processing private queries over public data.

our algorithm provides a minimal candidate answer set for private data.

The rest of this section is organized as follows. First, we consider *private queries over public data*. Then, we extend the query processing algorithm to deal with *public queries over private data* and *private queries over private data*.

4.1.1 Private Queries over Public Data

In this section, we will consider a nearest-neighbor query issued by a user in a form *"What is my nearest gas station"*. In this case, the privacy-aware query processor does not know the exact location information of the user. Instead, the query processor knows only a cloaked area in which the user resides. On the other hand, the exact location of the gas stations is known. Figure 4.1a depicts such a scenario by showing the data stored on the server side. There are 32 target objects, i.e., gas stations, T_1 to T_{32} represented by circles. The shaded area represents the cloaked area of the user who issued the query. For clarity, the actual user location is plotted as a square inside the cloaked area, but this information is not revealed to the database server.

Figures 4.1b and 4.1c give two trivial approaches that represent two different extremes for evaluating private nearest-neighbor queries over public data. In the first approach (Figure 4.1b), the server computes the nearest object to the center of the *cloaked area*, i.e., T_{16}, as the query answer. Although this approach minimizes the data transmitted from the server to the client, it gives an inaccurate answer where the actual

nearest object to the client is T_{13}. In the second approach (Figure 4.1c), the server sends all target objects to the client. Then, the client evaluates her query locally to get T_{13} as the query answer. Although this approach provides the exact answer, it is not practical due to the overhead of transmitting large numbers of target objects and the limited processing and storage capabilities on the client side.

Our approach is to design a privacy-aware query processor that achieves a compromise between these two extremes. The main idea is to compute a candidate answer set that includes the exact answer, i.e., the nearest object to the user who issues the query. To guarantee efficiency and enhance utility, the computed candidate answer set should be of minimal size. In the rest of this section, we will describe our proposed privacy-aware query processor for the case of nearest-neighbor queries along with a detailed example. Then, we will prove that the candidate answer set produced by our algorithm does include the exact answer and of minimal size.

Algorithm for Nearest-Neighbor Queries

Algorithm 2 gives the pseudo code for private nearest-neighbor queries over public data. The inputs to Algorithm 2 are: (a) the *cloaked area A* that is received from the location anonymizer and (b) a tuning parameter, termed *refine*. A larger value of *refine* requires higher computational cost, yet it gives a smaller candidate answer set that reduces both the transmission time of sending the candidate answer set from the database server to the location anonymizer and the processing time of computing an exact answer from the candidate answer set at the location anonymizer. Setting *refine* to *zero* would result in a similar, yet better, algorithm to [12] that returns a candidate answer set with a size equal to or larger than our algorithm. On the other hand, setting *refine* to ∞ would result in a minimal candidate answer set with the highest computational cost. The output of Algorithm 2 is a candidate answer set to be sent to the location anonymizer. In this section, we consider *refine* as a system specified parameter, and we will describe how to adaptively adjust *refine* to minimize overall response time which includes processing and transmission time. For the ease of description, Figure 4.2 gives a running example for a private nearest-neighbor query over public data where it presents a zoom view of the shaded area of Figure 4.1a along with its neighbor cells and the tuning parameter *refine* is set to one. In general, our algorithm has the following three steps:

Algorithm 2 Private NN Queries over Public Data

```
1: function PrivateNNPublicData(CloakedArea A, Int refine)
2: for each vertex v_i of A
3:    t_i ← the nearest object to v_i
4: candidate_set ← {∅}; R ← {A}
5: for each edge e_ij = v_i v_j of region A do
6:    if t_i = t_j then
7:       candidate_set ← candidate_set ∪ {t_i}
8:    else
9:       R = R ∪ RecursiveRefinement(v_i v_j, t_i, t_j, refine, candidate_set)
10:   end if
11: end for
12: for each range search area R ∈ R
13:    candidate_set ← candidate_set ∪ {all target objects within R}
14: return candidate_set
```

Step 1: ***Filter selection step.*** The main objective of this step is to choose a set of filters that prunes the set of all target objects to a smaller set of objects that includes the exact answer. Basically, for each vertex v_i of the *cloaked area* A, we choose the nearest object of v_i as its filter t_i (Lines 2 to 3 in Algorithm 2). Thus, at most four filters can be chosen. In our example, Figure 4.2a depicts that the nearest objects for vertices v_1, v_2, v_3, and v_4 are T_{16}, T_{16}, T_{13}, and T_{12}, respectively, i.e., we end up selecting only three objects $\{T_{16}, T_{13}, T_{12}\}$.

Step 2: ***Range selection step.*** The input to this step is the set of filter objects chosen from the previous step. The output of this step has two components: (a) a set of areas, $\mathcal{R}$, encloses target objects that should be considered in the candidate answer set, and (b) a set of target objects should be included in the candidate answer set. Initially, we add the *cloaked area* A to the set of areas $\mathcal{R}$, and the candidate answer set is set to be empty (Line 4 in Algorithm 2). The initialization of $\mathcal{R}$ to A indicates that the object within A should be considered in the candidate answer set as the actual user object could be anywhere in A.

In this step, we deal with each edge $e_{ij} = v_i v_j$ of the *cloaked area* A separately. Based on the two filters t_i and t_j of the edge $v_i v_j$ and the tuning parameter *refine*, we have one of following four possibilities:

1. *The trivial edge condition* ($t_i = t_j$). We first check for the case that $t_i = t_j$, i.e., one object serves as the nearest object for both vertices v_i and v_j. If this is the case, we just add t_i to the candidate answer set (Lines 6 to 7 in Algorithm 2).

Algorithm 3 Private NN Queries over Public Data: Recursive Refinement

```
1: function RecursiveRefinement(Edge e_ij = v_i v_j, Obj t_i, Obj t_j, Int refine, Set candidate_set)
2: s_ij ← the intersection point of e_ij and the perpendicular bisector (⊥) of t_i and t_j
3: if refine > 0 then
4:     t_s ← the nearest object to s_ij
5:     if t_s = t_i or t_s = t_j then
6:         candidate_set ← candidate_set ∪ {t_i, t_j}
7:         return {∅}
8:     else
9:         refine ← refine − 1
10:        search_area ← search_area ∪ RecursiveRefinement(v_i s_ij, t_i, t_s, refine, candidate_set)
11:        search_area ← search_area ∪ RecursiveRefinement(s_ij v_j, t_s, t_j, refine, candidate_set)
12:    end if
13: else
14:    search_area ← a circle centered at s_ij of a radius dist(s_ij, t_i)
15:    return search_area
16: end if
```

Since we guarantee that t_i is the nearest object to any point on v_iv_j, we do not need to perform any additional search on v_iv_j, i.e., we do not need to consider any further steps for this edge. In our example (Figure 4.2a), this case is applied to edge v_1v_2 where $t_1 = t_2 = T_{16}$. In this case, we just add T_{16} to the candidate answer set as we guarantee that T_{16} is the nearest object to the user if the user location is anywhere on edge v_1v_2.

2. *The trivial split-point condition* ($t_i \neq t_j$, *refine* > 0, $t_s = t_i$). In the case that $t_i \neq t_j$, (i.e., the two vertices v_i and v_j have different filters), we will use Algorithm 3 to process the edge. Basically, we compute the split point s_{ij} of the edge v_iv_j as the intersection point of v_iv_j and the perpendicular bisector of t_i and t_j where $\mathsf{dist}(s_{ij}, t_i) = \mathsf{dist}(s_{ij}, t_j)$ (Line 2 in Algorithm 3). Since the *refine* parameter is greater than zero, we go ahead and find the nearest object t_s to the split point s_{ij}. If it ends up that $t_s = t_i$, we add both t_i and t_j to the candidate answer set and return an empty *range search area* (Lines 6 to 7 in Algorithm 3). It is important to note that if $t_s = t_i$, then $t_s = t_j$ as $\mathsf{dist}(s_{ij}, t_i) = \mathsf{dist}(s_{ij}, t_j)$. The idea behind returning the empty *range search area* is that if $t_s = t_i$, then we guarantee that t_i is the nearest object of any point on line segment v_is_{ij}, while t_j is the nearest object of any point on line segment $s_{ij}v_j$. This means that there is no need to have more search on the edge v_iv_j. In our example, this case takes place for two

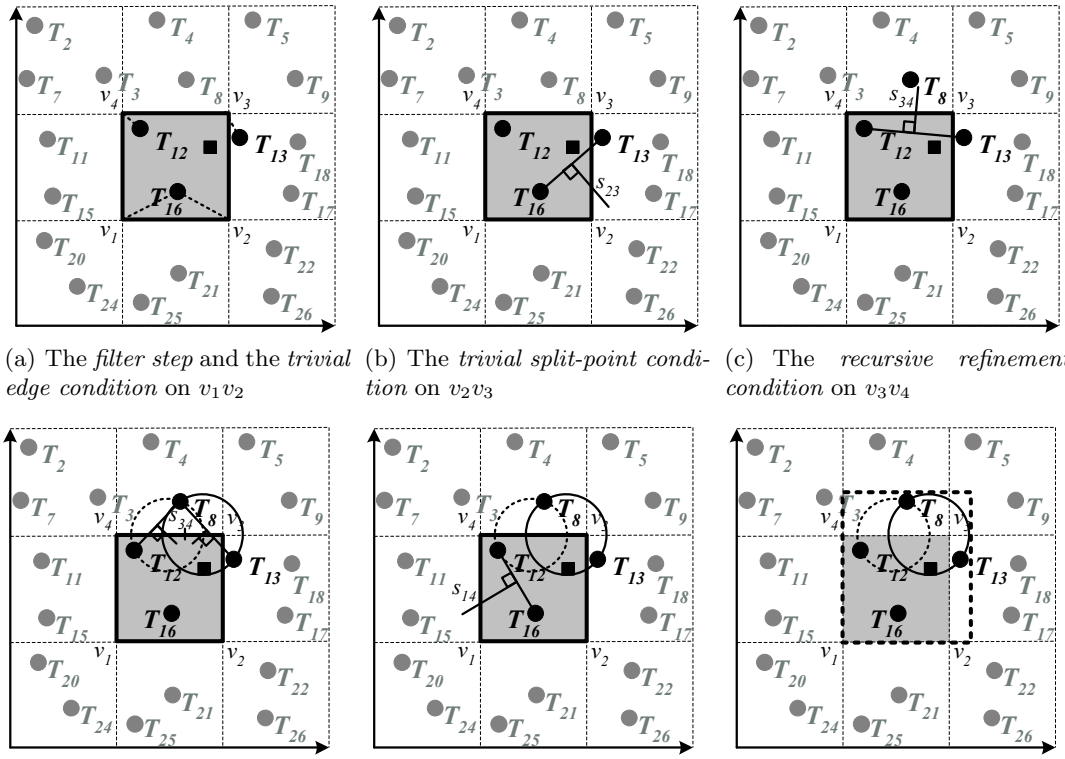

(a) The *filter step* and the *trivial edge condition* on v_1v_2

(b) The *trivial split-point condition* on v_2v_3

(c) The *recursive refinement condition* on v_3v_4

(d) The *stopping criterion condition* on v_3s_{34} and $s_{34}v_4$

(e) The *trivial split-point condition* on v_1v_4

(f) Range search step

Figure 4.2: Example of a private nearest-neighbor query over public data (*refine* = 1).

edges, v_2v_3 and v_1v_4. For edge v_2v_3, since $t_2 = T_{16} \neq t_3 = T_{13}$, we compute the split point s_{23} (Figure 4.2b). Since the nearest object of s_{23} could be either T_{13} or T_{16}, i.e., both T_{13} and T_{16} are of the same distance from s_{23}, we just add T_{13} and T_{16} to the candidate answer set. Similarly, for edge v_1v_4, we figure out that both T_{12} and T_{16} could be the nearest object to the split point s_{14} (Figure 4.2e). Thus, we just add T_{12} to the candidate answer set because T_{16} is already there.

3. *The recursive refinement condition* ($t_i \neq t_j$, *refine* > 0, $t_s \neq t_i$). In the case that the nearest object t_s to the split point s_{ij} is different from t_i and t_j, we split the edge v_iv_j into two separate line segments v_is_{ij} and $s_{ij}v_j$. Then, we decrease the tuning parameter *refine* by one while recursively splitting each edge separately until we either: (a) the tuning parameter *refine* reaches zero, or (b) we end up at

the *trivial split-point condition* (Lines 9 to 11 in Algorithm 3). In our example, edge v_3v_4 depicts this case where $t_3 = T_{13} \neq t_4 = T_{12}$. The nearest object to the split point s_{34} is T_8 (Figure 4.2c). Since T_8 is different from T_{12} and T_{13} and the *refine* parameter is one, we decrease *refine* by one to zero while dividing the edge v_3v_4 into two separate segments v_3s_{34} and $s_{34}v_4$ (Figure 4.2d). Since *refine* reaches zero for the two separate line segments, we end up with the next case of the *stopping criterion condition*.

4. *The stopping criterion condition* ($t_i \neq t_j$, *refine* $= 0$). Once the tuning parameter *refine* reaches zero, we terminate our algorithm by returning a *range search area* as a circle centered at the split point s_{ij} with a radius of $\mathsf{dist}(s_{ij}, t_i)$, i.e., $\mathsf{dist}(s_{ij}, t_i) = \mathsf{dist}(s_{ij}, t_j)$ (Line 14 in Algorithm 3). The idea behind this circular *range search area* is that all target objects within that area could be the answer of some point on v_iv_j, so these objects should be added to the candidate answer set. It is important to note two main issues in this step: (a) We may not reach to this step as repetitive recursive splitting of the edges may always result in either the *trivial edge condition* or the *trivial split-point condition*; and (b) Based on the number of recursive calls and the tuning parameter *refine*, we may end up with a large number of circular *range search areas* that include target objects to be added to the candidate answer set. In our running example, we end up having the two separate line segments v_3s_{34} and $s_{34}v_4$ with *refine* set to zero. Thus, we conclude these segments by returning two circular *range search areas* of their split points. The *range search area* of line segment v_3s_{34} is represented by a circle, while the *range search area* of $s_{34}v_4$ is represented by a dotted circle, as depicted in Figure 4.2d.

Step 3: ***Range search step.*** In this step, we can have one of two options that either provide a candidate answer set with the minimal size (minimality will be proved later) or provide a larger candidate answer set with less computation. In both cases, the candidate answer set is guaranteed to include the exact answer (inclusion will be proved later). The two options are:

1. To get the candidate answer set of the minimal size, we issue a range query for each *range search area* R in the *range query set* $\mathcal{R}$. All the results of these range

queries are added to the candidate answer set (Lines 12 to 13 in Algorithm 2), and the candidate answer set is sent to the location anonymizer. In our example, we will execute three range queries as one range query for the shaded *cloaked area* A and two range queries for the two circles depicted in Figure 4.2f.

2. To reduce computational cost while getting a larger candidate answer set, we execute only one range query that corresponds to the minimum boundary rectangle of all *range search areas* in $\mathcal{R}$. In our example, we will execute only one range query with the minimum bounding rectangle (represented by a bold dotted rectangle) as the query region that covers the circles and the *cloaked area* A (Figure 4.2f).

In our example, both options give the same candidate answer set (i.e., four target objects T_8, T_{12}, T_{13}, and T_{16}) that contains the actual query answer T_{13}.

Finally, it is important to know that our privacy-aware query processor is independent of the underlying nearest-neighbor and range query algorithms used in the nearest-neighbor search for filters or the nearest object of each split point in Step 1 and Step 2 and the range search in Step 3, respectively. These algorithms are assumed to be implemented in traditional location-based database servers. We do not have any assumptions about these algorithms as they can be employed using an R-tree or any other methods. In fact, our approach can be seamlessly integrated with any traditional location-based database servers to turn them to be *privacy-aware*.

Proof of Correctness

In this section, we show the correctness of the algorithm of *private nearest-neighbor queries over public data* (Algorithm 2) by proving that: (1) **Minimality** - the algorithm is *optimal*, i.e., it returns the minimal candidate answer set when the tuning parameter *refine* is set to ∞, and (2) **Inclusion** - the algorithm is *inclusive*, i.e., it returns the exact answer within the candidate answer set.

Theorem 1. Minimality. *Given a cloaked area A, a user U who issues a query within A, and a tuning parameter refine which is set to ∞, the algorithm computes a minimal candidate answer set for A.*

Proof. The algorithm results in a candidate answer set of objects which reside in A and/or the nearest object of some point on the edge of A. We will show that a minimal

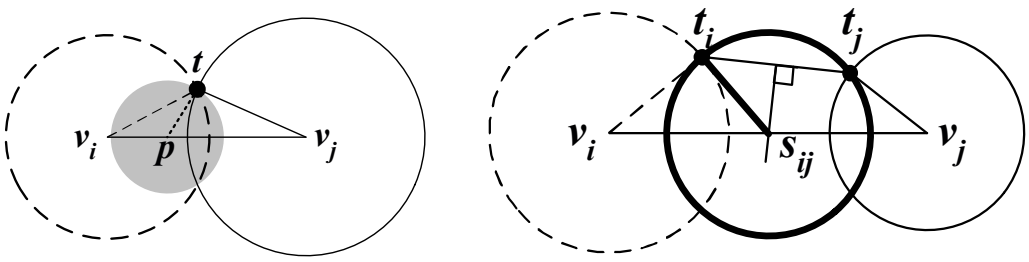

(a) Trivial edge condition ($t_i = t_j$) (b) Trivial split-point condition ($t_i \neq t_j$, $t_s = t_i$)

Figure 4.3: Two termination cases for the query processing of private queries over public data.

candidate answer set contains all such objects. First, U could be located anywhere within A. An object within A is the nearest object to U, when the object and U are at the same location. Thus, the object within A could be the exact answer to U. Second, U could be located at any point on the edge of A. For each line segment v_iv_j with objects t_i and t_j as the nearest object of its endpoints v_i and v_j, respectively, the algorithm ends up having the line segment with either the *trivial edge condition* (i.e., $t_i = t_j$) or the *trivial split-point condition* (i.e., $t_i \neq t_j$, $t_s = t_i$). This is because the *stopping criterion condition* will not take place as *refine* $= \infty$. We will show that the algorithm finds the nearest object to any point on the line segment where either the *trivial edge condition* or the *trivial split-point condition* takes place.

1. *The trivial edge condition.* Figure 4.3a depicts this case where t is the nearest object to any point p on v_iv_j, the dotted, shaded and solid circles are the required nearest-neighbor search space of v_i, p, and v_j, respectively. The shaded circle touches the intersection points of the dotted and solid circles, and it is totally covered by the dotted and solid circles. Suppose that there is another object t' that is closer to p than t; and hence, t' is within the shaded circle (i.e., t' is within the dotted and/or solid circles). However, if t' is within the dotted circle (or solid circle), it contradicts to the minimality, i.e., t is the nearest object to v_i (or v_j). Therefore, t is the nearest object to any point on v_iv_j.

2. *The trivial split-point condition.* Figure 4.3b depicts this case where s_{ij} is the split point of the edge v_iv_j and the nearest object of s_{ij} could be either t_i or t_j. For the line segment v_is_{ij}, v_i and s_{ij} have the same nearest object t_i. The proof of

the *trivial edge condition* shows that t_i is the nearest object to any point on $v_i s_{ij}$. Similarly, for the line segment $s_{ij} v_j$, t_j is the nearest object to any point on $s_{ij} v_j$.

Since we guarantee that only the objects within A and the nearest objects to some point on the edge of A are added to the candidate answer set, the candidate answer set contains the minimal set of objects that could be the exact answer to U. □

Theorem 2. Inclusion. *Given a cloaked area A, a user U who issues a query within A, and a tuning parameter refine ≥ 0, the algorithm computes a candidate answer set for A that contains the exact answer to U.*

Proof. When *refine* is set to ∞, the proof of Theorem 1 shows that the target objects which could be the nearest object to U are added to the candidate answer set, so the exact answer to U is included in the candidate answer set. On the other hand, when *refine* is finite, the *stopping criterion condition* could take place for some line segments. We will show that the exact answer of any point on such line segments is included in the candidate answer set. When the *stopping criterion condition* is applied to a line segment $v_i v_j$, we do not find the nearest object to the split point s_{ij} of $v_i v_j$. Thus, we distinguish two cases.

Case 1: If t_i and t_j are the nearest objects of s_{ij}, the proof of the *trivial split-point condition* in Theorem 1 can be applied to this case. Thus, t_i is the nearest object to any point on the line segment $v_i s_{ij}$, while t_j is the nearest object to any point on the line segment $s_{ij} v_j$. In this case, the algorithm adds the objects within the *range search area* of s_{ij} to the candidate answer set. Since t_i and t_j are the only objects within the *range search area*, these two objects are added to the candidate list.

Case 2: If neither t_i nor t_j is the nearest object of s_{ij}. There is an object t that is closer to some point on $v_i v_j$ than t_i and/or t_j. For the line segment $v_i s_{ij}$, if t is closer to some point on $v_i s_{ij}$ than t_i, the proof of the *trivial edge condition* in Theorem 1 gives that t must be within the dotted and/or bold circles (Figure 4.3b). This is because if t is outside the dotted and bold circles, t_i is closer to any point on $v_i s_{ij}$ than t. Similarly, for the line segment $s_{ij} v_j$, if t is closer to some point on $s_{ij} v_j$ than t_j, t is within the thin and/or bold circles. Since t_i and t_j are the nearest objects to v_i and v_j, respectively, there is no other objects within the dotted and/or thin circles. Therefore, t must be

within the bold circle, i.e., the *range search area* of s_{ij}. In this case, the algorithm adds the objects within the *range search area* of s_{ij} to the candidate answer set.

For both cases, the nearest object to any point on a line segment where the *stopping criterion condition* takes place is included in the candidate answer set. Therefore, the exact answer to U is included in the candidate answer set whenever *refine* ≥ 0. □

4.1.2 Public Queries over Private Data

In this section, we will consider a public nearest-neighbor query over private data issued by a user in a form *"What is the nearest customer to my taxi"*. In this case, the privacy-aware query processor is aware of the exact location of the query issuer, i.e., the taxi. However, the query processor does not know the exact location of the data, i.e., customers' locations. Instead, the query processor knows only a *cloaked area* in which each customer resides. The query processor returns a candidate answer set that includes the exact query answer. The query processing of *public queries over private data* is a very simple one as we are describing it here just as a basis for processing *private queries over private data* in Section 4.1.3.

Algorithm for Nearest-Neighbor Queries

As the idea of the algorithm is very simple, we just show the modifications that we need to have in Algorithm 2 to deal with *public queries over private data*. The input to the algorithm is a point-size area A where the four vertices are the same as the query location point. Since the query location point has no edges, the tuning parameter *refine* takes no effect on the algorithm; and thus, the *range selection step* (Step 2) in Algorithm 2 is neglected. The other two steps will be slightly modified as follows. Figure 4.4 acts as a running example where the location of the user who issues the query is represented by a square while four private target objects, i.e., T_1 to T_4, are represented by rectangles.

Step 1: *Filter selection step.* This step is similar to the *filter selection step* in Algorithm 2. The only modification is in the nearest object search where we consider that the location of a private object T is its furthest corner from the user's location. In other words, the distance between a user's location U and a private object t with a *cloaked area* A_t, $\mathsf{dist}_{\mathsf{max}}(U, A_t)$, is the distance from U to the furthest corner of A_t from

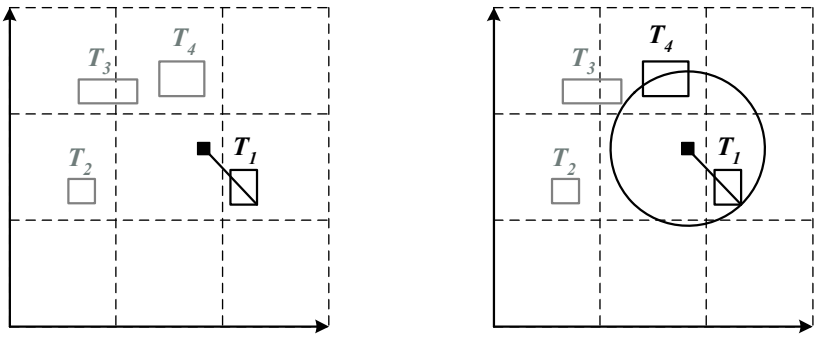

(a) Filter selection step (b) Range selection step

Figure 4.4: Example of a public nearest-neighbor query over private data.

U. Figure 4.4a depicts that T_1 is a *filter* object and the distance between the user and T_1, i.e., $\mathsf{dist}_{\mathsf{max}}(U, A_{T_1})$, is represented by a line.

Step 2: ***Range search step.*** In this step, we compute only one circular *range search area* centered at the user's location U with a radius of the maximum distance between U and the *filter* object t, i.e., $\mathsf{dist}_{\mathsf{max}}(U, A_t)$. All objects which intersect the *range search area* could be the exact query answer, so they are added to the candidate answer set. Figure 4.4b depicts the *range search area* represented by a circle. The objects which intersect the *range search area*, i.e., T_1 and T_4, are added to the candidate answer set.

After the location anonymizer gets the candidate answer set from the privacy-aware query processor, the exact location of a private object in the candidate answer set can be disclosed to the user who issues the query, if (1) the user has the required privilege, e.g., police, to access these objects' exact location information; and/or (2) the private object has granted the user the required privilege, e.g., the user is on the object's friend list. However, if the user does not have the required privilege to access the exact location of an object, the user can only get a *cloaked area* as the object's location, in order to preserve the object's location privacy.

Proof of Correctness

In this section, we show the correctness of the algorithm of *public nearest-neighbor queries over private data* by proving that: (1) **Minimality** - the algorithm returns the

minimal candidate answer set, and (2) **Inclusion** - the algorithm returns the exact answer within the candidate answer set.

Theorem 3. Minimality. *Given a user U who issues a query, a filter object t with a cloaked area A_t, and a range search area R centered at U with a radius of the distance between U and the furthest corner of A_t from U, the set of objects which intersects R constitutes a minimal candidate answer set.*

Proof. If t is the only object in R, t is the exact answer to U. However, if there is another object t' and its cloaked area $A_{t'}$ intersects R, t' could be the exact answer to U. Since t' intersects R, t' is added to the candidate answer set. Since only the objects which could be the exact answer are added to the candidate answer set, the result candidate answer set is the minimal set of objects that contains the exact answer. □

Theorem 4. Inclusion. *Given a user U who issues a query, a filter object t with a cloaked area A_t, and a range search area R centered at U with a radius of the distance between U and the furthest corner of A_t from U, the exact answer intersects R.*

Proof. We know that the distance between the exact answer and U is not larger than $\mathsf{dist}_{\mathsf{max}}(U, A_t)$, and all objects intersecting R are added to the candidate answer set. Suppose that t' is the exact answer to U and t' is not included in the candidate answer set. Thus, we know that the distance between U and t' is larger than $\mathsf{dist}_{\mathsf{max}}(U, A_t)$, i.e., t must be closer to U than t', that contradicts to the assumption that t' is the exact answer. Thus, the candidate answer set includes the exact answer. □

4.1.3 Private Queries over Private Data

In this section, we will consider the case of private nearest-neighbor queries over private data in which the query issued by the user is in a form *"What is my nearest buddy"*. In this case, the privacy-aware query processor does not know the exact location information of both the user who issued the query and the data, i.e., her buddies. Instead, the query processor knows only a *cloaked area* in which the user or each of her buddies resides. The query processor returns a candidate answer set that includes the exact query answer to the query issuer. The query processing of *private queries over private data* is similar to Algorithm 2, as described in Section 4.1.1, while using the query processing

of *public queries over private data*, as presented in Section 4.1.2, for nearest neighbor searches.

Algorithm for Nearest-Neighbor Queries

As the basic idea of the algorithm is to employ the algorithm of *public queries over private data* for nearest neighbor searches in Algorithm 2. Thus, we show only the modifications that we need to have in Algorithm 2 to deal with *private queries over private data*. The input to the algorithm is exactly the same as Algorithm 2, i.e., the *cloaked area* A received from the location anonymizer and a tuning parameter *refine*, where a larger value of *refine* gives a candidate answer set with a smaller size, but incurs higher query processing time. The output of the algorithm is a candidate answer set to be sent to the location anonymizer. Figure 4.5 depicts a running example for a private nearest-neighbor query over private data where the *cloaked area* A is represented by a shaded area and the private data is represented by rectangles. For clarity, the actual location of the user who issued the query is represented by a square within A, but this information is not revealed to the database server. Also, we show only the private data that is involved in the query processing for the sake of simplicity. In this example, the tuning parameter *refine* is set to one. The algorithm has the same three steps as in Algorithm 2 with following modifications:

Step 1: ***Filter selection step.*** The only modification in this step is that we use the algorithm of *public queries over private data* to find a filter t_i for each vertex v_i of the *cloaked area* A. This means that t_i with a *cloaked area* A_{t_i} has the smallest distance $\mathsf{dist}_{\mathsf{max}}(v_i, A_{t_i})$, i.e., the distance between v_i and the furthest corner of A_{t_i} from v_i, among all objects. In our example, Figure 4.5a depicts that the nearest objects for vertices v_1, v_2, v_3, and v_4 are T_1, T_1, T_2, and T_4, respectively. The distance between each vertex and its filter is represented by a dotted line.

Step 2: ***Range selection step.*** The basic idea of this step is similar to the *range selection step* in Algorithm 2, but we have some modifications for each possible condition.

1. *The trivial edge condition* ($t_i = t_j$). The only modification of this condition is that we add two *range search areas* to the *range query set* $\mathcal{R}$. One *range search area* is

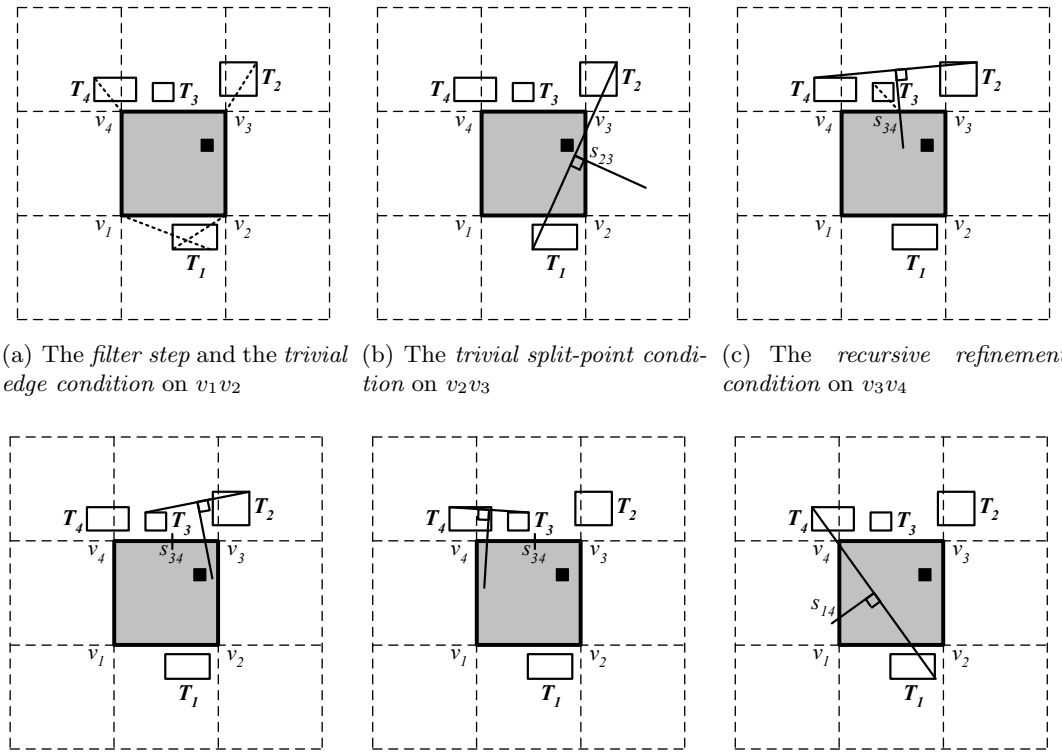

(a) The *filter step* and the *trivial edge condition* on v_1v_2

(b) The *trivial split-point condition* on v_2v_3

(c) The *recursive refinement condition* on v_3v_4

(d) The *stopping criterion condition* on v_3s_{34}

(e) The *stopping criterion condition* on $s_{34}v_4$

(f) The *trivial split-point condition* on v_1v_4

Figure 4.5: Example of a private nearest-neighbor query over private data (*refine* = 1).

a circular region centered at v_i with a radius of $\mathsf{dist}_{\mathsf{max}}(v_i, A_{t_i})$ and the other *range search area* is a circular region centered at v_j with a radius of $\mathsf{dist}_{\mathsf{max}}(v_j, A_{t_j})$. The idea of adding these two *range search areas* to $\mathcal{R}$ instead of adding t_i and t_j to the candidate answer set is that all objects intersecting these *range search areas* could be the answer of some point on the edge v_iv_j. Thus, these objects should be added to the candidate answer set. In our example, this condition takes place for edge v_1v_2 where $t_1 = t_2 = T_1$, so we add the *range search areas* of v_1 and v_2 to $\mathcal{R}$.

2. *The trivial split-pint condition* ($t_i \neq t_j$, *refine* > 0, $t_s = t_i$). We have two modifications for this case. The first modification is in the computation of the split point s_{ij} of the edge v_iv_j. s_{ij} is computed as an intersection point of v_iv_j and

the perpendicular bisector of t_i and t_j in which we consider the furthest corners of t_i and t_j from the opposite vertices v_j and v_i, respectively. Since the tuning parameter *refine* is greater than zero, we find the nearest object t_s to the split point s_{ij}. The second modification is that if it results in a case $t_s = t_i$, we add the *range search areas* of t_i, t_s, and t_j, i.e., these areas are the circles centered at v_i, s_{ij}, and v_j with a radius of $\mathsf{dist}_{\mathsf{max}}(v_i, A_{t_i})$, $\mathsf{dist}_{\mathsf{max}}(s_{ij}, A_{t_i}) = \mathsf{dist}_{\mathsf{max}}(s_{ij}, A_{t_j})$, and $\mathsf{dist}_{\mathsf{max}}(v_j, A_{t_j})$, respectively, to the *range query set* $\mathcal{R}$. The reason of returning these three *range search areas* is that the set of objects intersecting the *range search areas* of v_i and s_{ij} constitutes the minimal set of objects that could be the answer of some point on $v_i s_{ij}$. On the other hand, the set of objects intersecting the *range search areas* of s_{ij} and v_j is the minimal set of objects that could be the answer of some point on $s_{ij} v_j$. In our example, this case is applied to two edges v_2v_3 and v_1v_4. For edge v_2v_3, since $t_2 = T_1 \neq t_3 = T_2$, and the tuning parameter *refine* is larger than zero, we compute the split point s_{23} (Figure 4.5b). Since the nearest object of s_{23} is T_1 or T_2, i.e., $\mathsf{dist}_{\mathsf{max}}(s_{23}, A_{T_1}) = \mathsf{dist}_{\mathsf{max}}(s_{23}, A_{T_2})$, we add the *range search areas* of v_2, s_{23}, and v_3 to the *range query set* $\mathcal{R}$. Likewise, for edge v_1v_4, we know that the nearest object to the split point s_{14} is T_1 or T_4 (Figure 4.5f). Since the *range search area* of v_1 is already added to $\mathcal{R}$, we merely add the *range search areas* of s_{14} and v_4 to $\mathcal{R}$.

3. *The recursive refinement condition* ($t_i \neq t_j$, *refine* > 0, $t_s \neq t_i$). This step is exactly the same as the *recursive refinement condition* in Algorithm 2. In our example, this case is applied to edge v_3v_4 where v_3, s_{34}, and v_4 have different nearest objects, i.e., $t_3 = T_2$, $t_{s_{34}} = T_3$, and $t_4 = T_4$, and *refine* is larger than zero. We split v_3v_4 into two separate line segments v_3s_{34} and $s_{34}v_4$, and then recursively execute this step on these two separate line segments while decreasing *refine* by one to zero, as illustrated in Figures 4.5d and 4.5e, respectively. In this example, *refine* reaches zero after the first recursive refinement for both line segments, we end up with the next case of the *stopping criterion condition*.

4. *The stopping criterion condition* ($t_i \neq t_j$, *refine* $= 0$). The only modification of this step is the same as the second modification of the *trivial split-point condition*. When the tuning parameter *refine* reaches zero, we add the *range search areas* of

the endpoints v_i and v_j, and the split point s_{ij} of the edge v_iv_j to the *range query set* $\mathcal{R}$.

Step 3: ***Range search step.*** The basic idea of this step is the same as in Algorithm 2. The only modification for each option is follows:

1. To get the candidate answer set of the minimal size, we issue a range query for each *range search area* R in the *range query set* $\mathcal{R}$. For each range query, all objects intersecting R are returned as the answer. The answers of these range queries are added to the candidate answer set.

2. To reduce computational cost while getting a larger candidate answer set, we execute only one range query with a query region that corresponds to the minimum boundary rectangle of all *range search areas* in $\mathcal{R}$. Then, all objects intersecting the query region are added to the candidate answer set.

Proof of Correctness

In this section, we show the correctness of the *private nearest-neighbor queries over private data* algorithm by proving that: (1) **Minimality** - the algorithm is *optimal*, i.e., it returns the minimal candidate answer set, when the tuning parameter *refine* is set to ∞, and (2) **Inclusion** - the algorithm is *inclusive*, i.e., it returns the exact answer within the candidate answer set.

Theorem 5. Minimality. *Given a cloaked area A, a user U who issues a query within A, and a tuning parameter refine which is set to ∞, the algorithm computes a minimal candidate answer set for A.*

Proof. The algorithm results in a candidate answer set of objects which intersect with A or could be the nearest object to some point on the edge of A. We will show that the minimal candidate answer set contains all such objects. First, U could be anywhere within A. The object intersecting A could be the exact answer because the object and U could be at the same location. Second, U could be located at any point on the edge of A. For each line segment v_iv_j with objects t_i and t_j as the nearest object of its endpoints v_i and v_j, respectively, the algorithm ends up having the line segment with

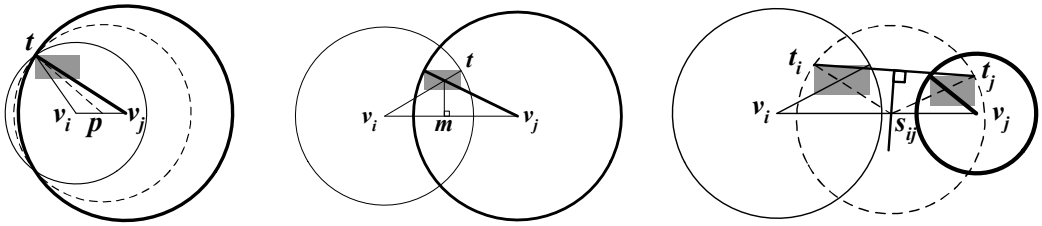

(a) $t_i = t_j$: same vertex (b) $t_i = t_j$: different vertices (c) $t_i \neq t_j$, $t_s = t_i$ and $t_s = t_j$

Figure 4.6: Some termination cases for private queries over private data.

either the *trivial edge condition* (i.e., $t_i = t_j$) or the *trivial split-point condition* (i.e., $t_i \neq t_j$, $t_s = t_i$). This is because the *stopping criterion condition* will not take place when *refine* $= \infty$. We will show that the algorithm finds all objects that could be the exact answer of some point on a line segment where either the *trivial edge condition* or the *trivial split-point condition* takes place.

1. *The trivial edge condition.* We distinguish two cases.

   Case 1: *The furthest corner of the cloaked area of the same filter t of v_i and v_j, A_t, from v_i and v_j is the same* (Figure 4.6a). The *search range area* of any point p on v_iv_j is a circle with a radius of a distance from p to the furthest corner of A_t from p (represented by a dotted circle). By Theorems 3 and 4, the nearest object to p intersects the *range search area* of p. All possible *range search areas* of p are within the *range search areas* of v_i and v_j, so the objects intersecting the *range search area* of v_i and v_j constitute the minimal set of objects that could be the exact answer to p.

   Case 2: *The furthest corners of A_t from v_i and v_j are different* (Figure 4.6b). Let l_i be the line from v_i to the furthest corner of A_t from v_i (represented by a thin line) and l_j be the line from v_j to the furthest corner of A_t from v_j (represented by a bold line). m is a point on v_iv_j projected from the intersection point of l_i and l_j. The point p on the line segment v_im has the same furthest corner, while p on the line segment mv_j also has the same furthest corner. Thus, the first case can be applied to both line segments v_im and mv_j.

2. *The trivial split-point condition.* We split v_iv_j into two separate line segments

$v_i s_{ij}$ and $s_{ij} v_j$. Since both the line segments have the same nearest object, as depicted in Figure 4.6c, the proof of the *trivial edge condition* can be applied to this case.

Since we guarantee that only the objects within A and the objects that could be the exact answer of some point on the edge of A are added to the candidate answer set, the candidate answer set is minimal. □

Theorem 6. Inclusion. *Given a cloaked area A, a user U who issues a query within A, and a tuning parameter refine ≥ 0, the algorithm computes a candidate answer set that contains the exact answer to U.*

Proof. When *refine* is set to ∞, the proof of Theorem 5 shows that target objects that could be the nearest object to U are added to the candidate answer set, so the exact answer to U is included in the candidate answer set. When *refine* is finite, the *stopping criterion condition* could take place for some line segments. The proof of the *trivial split-point condition* in Theorem 5 shows that the nearest object to any point on the line segment $v_i v_j$ interests the *range search areas* of v_i, v_j, and/or the split point s_{ij} of $v_i v_j$. Since the *stopping criterion condition* adds these three *range search areas* to the *range query set* $\mathcal{R}$, the algorithm adds all objects intersecting these *range search areas* to the candidate answer set. This means that the nearest object to any point on a line segment where the *stopping criterion condition* takes place is included in the candidate answer set. Therefore, the exact answer to U is included in the candidate answer set whenever the tuning parameter *refine* ≥ 0. □

4.2 Continuous Privacy-aware Query Processing

In this section, we propose a *shared execution paradigm* that turns the *snapshot* privacy-aware query processor proposed in Section 4.1 into a scalable and efficient query processor for *continuous* privacy-aware queries. Examples of continuous queries include *"Continuously send e-coupons to the car that is within one mile of my restaurant"* and *"Continuously report my nearest police car"*. The user issues a continuous query by registering the query with a database server for a specified period of time. After the user gets an initial query answer from the database server, she is notified with the

changes in the query answer. Since a numerous number of *continuous* privacy-aware queries could be lasted for a long time at the database server, the most important challenges for processing such continuous queries are system scalability and computational efficiency. However, a *basic paradigm* that simply extends the *snapshot* privacy-aware query processing algorithm to deal with continuous queries individually is not scalable and efficient. To this end, we propose a shared execution paradigm that aims to share computational resources among *continuous* privacy-aware queries, in order to improve system scalability and efficiency.

The rest of this section is organized as follows. First, we use a *basic paradigm* that extends the *snapshot* privacy-aware query processor to deal with *continuous* privacy-aware queries and analyze the computational cost of maintaining their query answers. Then, we give the detail of our proposed shared execution paradigm, analyze the computational cost of employing the shared execution paradigm to process *continuous* privacy-aware queries, and describe how to modify the *snapshot* privacy-aware query processing algorithm to incorporate the shared execution paradigm for all introduced privacy-aware query types.

4.2.1 Basic Continuous Privacy-aware Query Processing

This section describes a *basic paradigm* that extends the *snapshot* privacy-aware query processing algorithm proposed in Section 4.1 to deal with *continuous* privacy-aware queries. The main idea of the *basic paradigm* is that the *snapshot* privacy-aware query processor computes an initial query answer. Due to mobility, the query answer would become stale at any time. Thus, the query processor has to continuously detect the change in the query answer and notify the user with the change immediately. Continuously maintaining the answer of a privacy-aware query needs to detect two cases of changes: (1) The nearest object of the vertex of a *cloaked area* A or the split point of the edge of A changes its location or there is a new nearest object for the vertex or split point, and (2) Some objects move to or out from a *range search area* in the *range query set* $\mathcal{R}$. For the first case of changes, we issue a *continuous nearest-neighbor (NN) query* for each vertex or split point to monitor its nearest object. For the second case of changes, we issue a *continuous range query* for each *range search area* in $\mathcal{R}$ to detect

the change of the target objects within the area. We will describe how the query processor maintains the answer of continuous privacy-aware queries. Whenever the query processor is notified with some changes in the *continuous NN query*, the query processor re-evaluates the query answer. Then, we only send the changes in the query answer to the location anonymizer, i.e., an incremental query answer update, in order to reduce communication overhead. On the other hand, when we detect changes only in the *continuous range queries*, we simply send the changes in the query answer to the location anonymizer without re-evaluating the query answer. If we re-evaluate a query answer due to the change in a *continuous NN queries*, any change in *continue range queries* can be neglected. This is because all *range search areas* will be removed from $\mathcal{R}$ before the re-evaluation.

Analysis. We will study the computational cost of the *basic paradigm* for each privacy-aware query type. In our analytical model, we consider the second option of the *range search step* in Algorithm 2, i.e., only one *continuous range query* is issued to monitor the minimum bounding rectangle of all *range search areas* in the *range query set* $\mathcal{R}$ and let N_Q be the number of continuous privacy-aware queries in the system. Hence, the total number of *continuous range queries* is N_Q. The computational cost of each privacy-aware query type in terms of the number of *continuous NN queries* is analyzed as follows:

- *Private queries over public data.* For each query, we issue one *continuous NN query* to monitor the nearest object of each vertex of the *cloaked area* A, i.e., four *continuous NN queries* for each query. For each edge of A, we have to monitor the nearest object of at most $2^{refine} - 1$ split points of the edge; and hence, we issue at most $4 \times (2^{refine} - 1)$ *continuous NN queries* for all the split points of A. Thus, the computational cost is $O(N_Q \times [4 + 4 \times (2^{refine} - 1)]) = O(N_Q \times 2^{refine+2})$.

- *Public queries over private data.* For each query, we issue only one *continuous NN query* to monitor its filter object, Thus, the computational cost is N_Q.

- *Private queries over private data.* The computational cost of this query type is exactly the same as that of the *private queries over public data*, i.e., $O(N_Q \times 2^{refine+2})$.

4.2.2 Shared Execution Paradigm for Continuous Privacy-aware Query Processing

Although the *basic paradigm* is simple, the computational cost is dependent on the number of continuous privacy-aware queries and the tuning parameter *refine*. The *basic paradigm* would suffer from a scalability issue when a location-based database server processes a numerous number of continuous privacy-aware queries with a strict requirement on the answer optimality, i.e., a large value of *refine*. To this end, we propose a shared execution paradigm for continuous privacy-aware queries to improve system scalability and computational efficiency. The basic idea is that we maintain a set of *static query points* whose nearest objects would be utilized as part of the query processing for all continuous privacy-aware queries.

Static query points. In the shared execution paradigm, we maintain a set of *static query points* that is uniformly distributed in the system. A *static query point* is either in an *on* or *off* state. Initially, all *static query points* are in the *off* state. When the query processor needs to find the nearest object of the vertex of a *cloaked area* A or the split point of the edge of A, it finds the nearest *static query point* of the vertex or split point, and then turns the *static query point* on and finds the nearest object to the *static query point* as an approximate answer for the vertex or split point. We maintain the answer of this *static query point* until it is no longer needed by any continuous privacy-aware queries, i.e., we turn the *static query point* off. Since the answer of a *static query point* may not be the actual nearest object of the vertex of a *cloaked area* A or the split point of the edge of A, using the *static query point* would result in a larger candidate answer set. Although the number of *static query points* can be served as a system-wide performance tuning parameter, it would not satisfy the need of individual queries. Thus, we introduce another tuning parameter δ for individual continuous privacy-aware queries. The idea is to use the answer of a *static query point* as the nearest object of the vertex or split point of A if the distance between the vertex or split point and its nearest *static query point* is less than δ. When we set $\delta = \delta_{max}$, where δ_{max} is the maximum value of δ, we always use the *static query points* for query processing. At the other extreme case $\delta = 0$, we will not use any *static query points* for query processing.

The *privacy-aware query processor* benefits from the shared execution paradigm in three aspects. (1) The number of *static query points* can be served as a performance

tuning parameter to trade off between system scalability and query answer optimality. In other words, a larger number of *static query points* gives better quality of query answers, i.e., a smaller candidate answer set, but it incurs higher computational cost. It is important to note that the shared execution paradigm guarantees that the exact query answer is included in the candidate answer set, regardless of the number of *static query points*. (2) The shared execution paradigm provides a fashion to bound the total number of *continuous NN queries* maintained at the database server by the number of *static query points* when $\delta = \delta_{max}$. (3) When we use the answer of a *static query point* as the nearest object of the vertex of a *cloaked area* A or the split point of the edge of A, the answer is immediately available for the query processor without performing any nearest-neighbor search, and thus reducing computational overhead.

Analysis. Table 4.1 summarizes the computational cost of the *basic paradigm* and the shared execution paradigm with different values of δ for each privacy-aware query type. Similar to the analysis of the *basic paradigm*, we let N_Q be the number of continuous privacy-aware queries and maintain a *continuous range query* for all *range search areas* in the *range query set* $\mathcal{R}$ of each continuous privacy-aware query. Furthermore, we assume that there are N_S *static query points* that are uniformly distributed in the system. Figure 4.7a depicts a cell (represented by a rectangle) enclosed by four *static query points* (represented by triangles) where the length and width of the cell are l and w, respectively, and the *coverage area* of each *static query point* is represented by a shaded circle. A *coverage area* of a *static query point* is a circular area centered at the query point with a radius of δ. We first develop a function to determine the probability of using the answer of a *static query point* for the vertex of a *cloaked area* A or the split point of the edge of A with respect to δ, $P_A(\delta)$, and then analyze the computational cost of each privacy-aware query type for different values of δ.

Figure 4.7b gives the case of the maximum value of δ, δ_{max}, i.e., the distance from a *static query point* to the center of the cell. Thus, $\delta_{max} = |\overline{bc}| = \sqrt{|\overline{ab}|^2 + |\overline{ac}|^2} = \sqrt{(l^2 + w^2)/4}$, where c is the center of the cell and $|\overline{bc}|$ represents the distance of line segment $\overline{bc}$. For simplicity, we assume that $P_A(\delta)$ of the vertices and split points of a *cloaked area* A is independent; and thus, $P_A(\delta)$ can be computed as a ratio of the area of the union of the *coverage area* of the four *static query points* of a cell to the cell area. To determine $P_A(\delta)$ for different values of δ, we distinguish three cases:

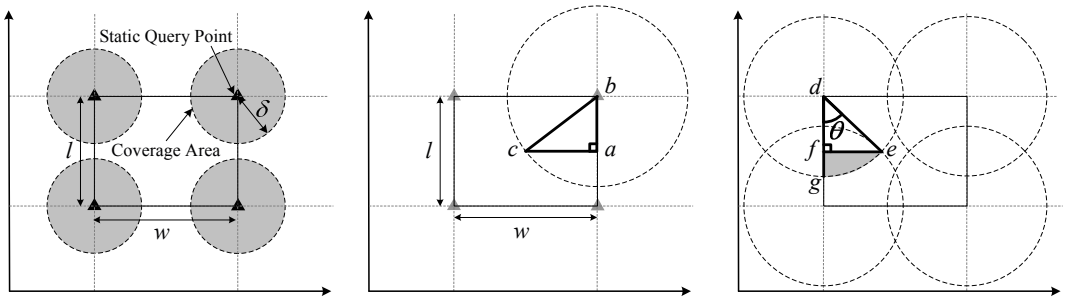

(a) Static query points (b) Maximum value of δ (c) Intersection area

Figure 4.7: The effect of δ for the shared execution paradigm.

Case 1: $0 \leq \delta \leq \min(w, l)$. In this case, there is no intersection among the *coverage area* of the four *static query points* of a cell (e.g., see Figure 4.7a); and hence, $P_A(\delta) = [4 \times (\delta^2\pi \times 90/360)]/(w \times l) = \delta^2\pi/(w \times l)$.

Case 2: $\min(w, l) < \delta < \delta_{max}$. Figure 4.7c illustrates this case where $|\overline{de}| = |\overline{dg}| = \delta$, $|\overline{fg}| = (2\delta - l)/2 = \delta - l/2$, $|\overline{df}| = |\overline{dg}| - |\overline{fg}| = \delta - (\delta - l/2) = l/2$, $|\overline{ef}| = \sqrt{|\overline{de}|^2 - |\overline{df}|^2} = \sqrt{\delta^2 - (l/2)^2}$, and $\theta = \cos^{-1}(|\overline{df}|/|\overline{de}|) = \cos^{-1}[(l/2)/\delta]$. The area of the shaded area is equals to the area of the triangle EDF subtracted from the area of the sector EDG. The area of the sector EDG is $\delta^2\pi(\theta/360)$ and the area of the triangle EDF is $(|\overline{df}| \times |\overline{ef}|)/2$; and hence, the shaded area is $\delta^2\pi(\theta/360) - (|\overline{df}| \times |\overline{ef}|)/2 = \delta^2\pi(\cos^{-1}[(l/2)/\delta]/360) - [(l/2)\sqrt{\delta^2 - (l/2)^2}]/2$. In general, the intersection area of the *coverage area* of the two *static query points* on the vertical or horizontal edge of a cell is $A_{Int}(s) = 2 \times \{\delta^2\pi(\cos^{-1}[(s/2)/\delta]/360) - [(s/2)\sqrt{\delta^2 - (s/2)^2}]/2\}$, where $s = l$ and $s = w$ for the vertical and horizontal edge of a cell, respectively. Thus, $P_A(\delta) = [\delta^2\pi - 2(A_{Int}(w) + A_{Int}(l))]/(w \times l)$.

Case 3: $\delta \geq \delta_{max}$. In this case, the cell area is totally covered by the *coverage area* of the four *static query points* that enclose the cell; and hence, the query processor always uses the answer of *static query points* for query processing, $P_A(\delta) = 1$.

Therefore, the probability of using the answer of a *static query point* as the nearest object for the vertex or split point of a *cloaked area* A, $P_A(\delta)$, can be summarized as

Table 4.1: The computational cost of each privacy-aware query type.

Privacy-aware Query Types	Basic Paradigm	Shared Execution Paradigm ($\delta = \delta_{max}$)	Shared Execution Paradigm ($\delta < \delta_{max}$)
Private Queries over Public Data	$O(N_Q \times 2^{refine+2})$	$O(\min(N_Q \times 2^{refine+2}, N_S))$	$O((1-P_A(\delta)) \times N_Q \times 2^{refine+2} + \min(P_A(\delta) \times N_Q \times 2^{refine+2}, N_S))$
Public Queries over Private Data	N_Q	$O(\min(N_Q, N_S))$	$((1-P_A(\delta)) \times N_Q + \min(P_A(\delta) \times N_Q, N_S))$
Private Queries over Private Data	$O(N_Q \times 2^{refine+2})$	$O(\min(N_Q \times 2^{refine+2}, N_S))$	$O((1-P_A(\delta)) \times N_Q \times 2^{refine+2} + \min(P_A(\delta) \times N_Q \times 2^{refine+2}, N_S))$

the following equations:

$$P_A(\delta) = \begin{cases} \delta^2\pi/(w \times l), & 0 \le \delta \le \min(w, l); \\ \left[\delta^2\pi - 2(A_{Int}(w) + A_{Int}(l))\right]/(w \times l), & \min(w, l) < \delta < \delta_{max}; \\ 1, & \delta_{max} \le \delta < \infty. \end{cases}$$

The computational cost of each privacy-aware query type with different values of δ is analyzed as follows:

- *Private queries over public data.* For a set of N_Q queries, we use a total of at most $\min(P_A(\delta) \times N_Q \times 2^{refine+2}, N_S)$ *static query points* for query processing and maintain at most $(1 - P_A(\delta)) \times N_Q \times 2^{refine+2}$ *continuous NN queries*. Thus, the computational cost is $O((1 - P_A(\delta)) \times N_Q \times 2^{refine+2} + \min(P_A(\delta) \times N_Q \times 2^{refine+2}, N_S))$.

- *Public queries over private data.* For a set of N_Q queries, we use a total of at most $\min(P_A(\delta) \times N_Q, N_S)$ *static query points* for query processing and maintain at most $(1 - P_A(\delta)) \times N_Q$ *continuous NN queries*. Thus, the computational cost is $O((1 - P_A(\delta)) \times N_Q + \min(P_A(\delta) \times N_Q, N_S))$.

- *Private queries over private data.* The computational cost of this query type is exactly the same as that of the *private queries over public data*.

Algorithm for Private Nearest-Neighbor Queries over Public Data

In this section, we extend Algorithm 2 to employ the shared execution paradigm to compute the query answer of a private continuous nearest-neighbor query over public data. Figure 4.8 depicts a running example of the shared execution paradigm for a private continuous nearest-neighbor query over public data where the *cloaked area* A is represented by a shaded area, the four *static query points* of the cell intersecting A are represented by triangles, and the tuning parameter *refine* is set to one. If a *static query point* has been turned on by the query processor, the *static query point* is represented by a black triangle; otherwise, the *static query point* is represented by a gray triangle. For simplicity, we show only the objects that will be used by the algorithm. The actual location of the user who issued the query is represented by a square for illustration only, but this actual location information is not revealed to the database server. Initially, the candidate answer set is set to be empty and the *range query set* $\mathcal{R}$ is set to the *cloaked area* A. Then, the same idea of Algorithm 2 can be applied to the shared execution paradigm with the following modifications:

Step 1: ***Filter selection step.*** The only modification is that for each vertex v_i of A, if the distance between v_i and the nearest *static query point* is less than δ, we use the answer of the nearest *static query point* as the filter t_i of v_i. Although the filter may not be the actual nearest object to the vertex, we guarantee that the exact answer to the user is included in the candidate answer set (inclusion will be proved later). Otherwise, we find the actual nearest object of v_i as the filter t_i as in Algorithm 2. Note that if the *static query point* has been turned on, its answer is immediately available for the query processor without performing any nearest-neighbor search. In our example, Figure 4.8a depicts that only the vertices v_3 and v_4 with a distance to their nearest *static query point* is less than δ. Thus, the query processor needs to find the actual nearest object to the other vertices v_1 and v_2 as their filters, i.e., $t_1 = t_2 = T_{16}$. Since the distance between v_3 and the top right *static query point* is less than δ, the filter of v_3 is the answer of the top right *static query point*, i.e., $t_3 = T_{13}$. Likewise, the filter of v_4 is the answer of the top left *static query point*, i.e., $t_4 = T_3$.

Step 2: ***Range selection step.*** We will present the minor modification for each possible condition.

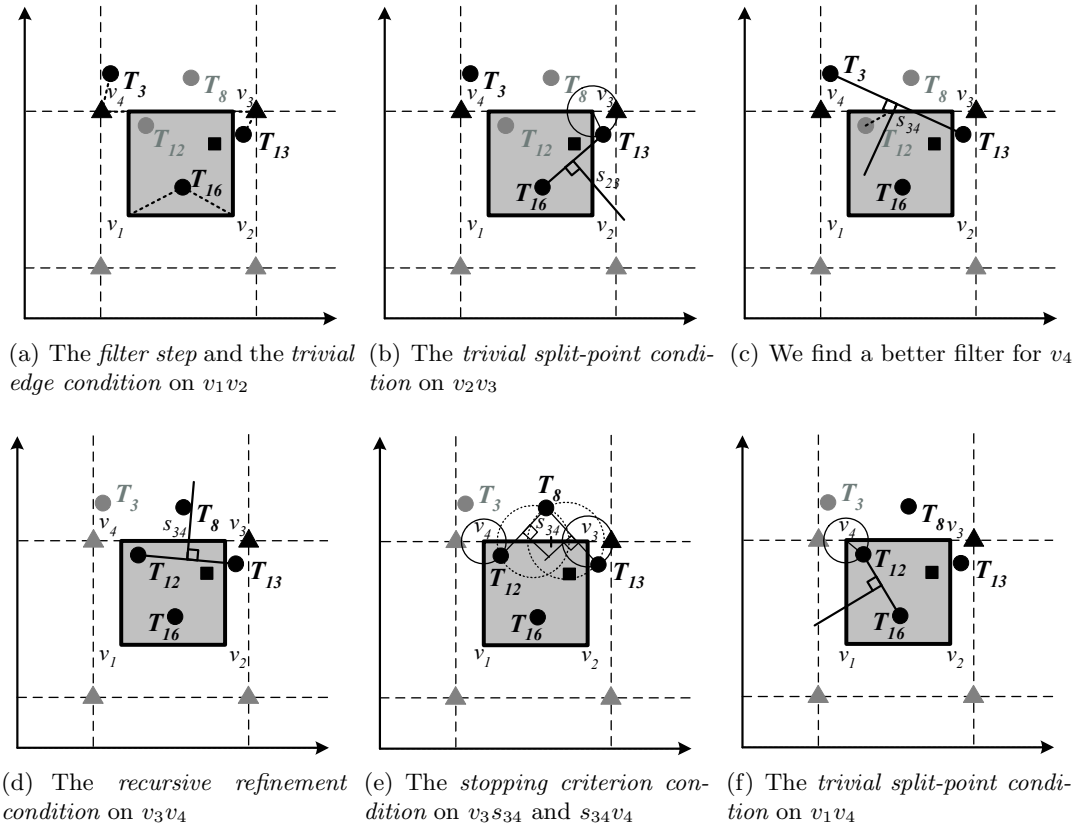

(a) The *filter step* and the *trivial edge condition* on v_1v_2

(b) The *trivial split-point condition* on v_2v_3

(c) We find a better filter for v_4

(d) The *recursive refinement condition* on v_3v_4

(e) The *stopping criterion condition* on v_3s_{34} and $s_{34}v_4$

(f) The *trivial split-point condition* on v_1v_4

Figure 4.8: Example of the shared execution paradigm for a private continuous nearest-neighbor query over public data (*refine* = 1).

The trivial edge condition ($t_i = t_j$). This condition takes place for an edge v_iv_j when the same object serves the filter of v_i and v_j. In this condition, the only modification is that if we use the answer of a *static query point* as the filter of v_i, we do not add t_i to the candidate answer set. Instead, we add a *range search area* of v_i that is a circle centered at v_i with a radius of the distance from v_i to t_i to the *range query set* $\mathcal{R}$. The idea behind this modification is that when we use a *static query point*, its answer may not be the actual nearest object of the vertex. In fact, the objects that could be the actual nearest object of v_i are within the *range search area*. Thus, all these objects should be added to the candidate answer set. The same scenario is also applied to the vertex v_j. In our example, this condition takes place for edge v_1v_2 because the same object T_{16} serves the filter of both vertices v_1 and v_2 (Figure 4.8a). Since T_{16} is the

actual nearest object to v_1 and v_2, we simply add T_{16} to the candidate answer set and no further refinement on v_1v_2 is needed.

The trivial split-point condition ($t_i \neq t_j$, *refine* > 0, $t_s = t_i$). We have two modifications before checking for this condition, and one modification when this condition holds for an edge v_iv_j. The first modification is similar to the *filter step*. If the distance between the split point s_{ij} of v_iv_j and the nearest *static query point* is less than δ, we use the answer of the nearest *static query point* as the nearest object t_s of s_{ij}. The second modification is that if t_s is closer to v_i than v_i's current filter t_i, t_s is considered as the filter of v_i. Then, we start over this step on v_iv_j with the new filter. The idea behind this modification is that if we find t_i for v_i based on a *static query point*, t_s could be closer to v_i than t_i, i.e., t_s is a better filter for v_i. The same scenario is also applied to the vertex v_j. We update the filter of v_i and/or v_j whenever we find a better one. The third modification that is similar to the modification of the *trivial edge condition* is for the case that this condition takes place. If we use the *static query point* to find the nearest object of v_i, we add a *range search area* of v_i to the *range query set* $\mathcal{R}$. This is because the objects within *range search area* could be the actual nearest object of v_i. The same scenario is also applied to the vertex v_j and the split point s_{ij} of v_iv_j. In our example, this condition takes place for edges v_2v_3 and v_1v_4. For edge v_2v_3, we compute the split point s_{23} of v_2v_3. Since the distance between s_{23} and the nearest *static query point* is larger than δ, we find the actual nearest object to s_{23}. Figure4.8b gives that the nearest object of s_{23} is the same as the filter of v_2 and v_3. Since we use only the answer of the top right *static query point* as the filter of v_3, we add the *range search area* of v_3 to the *range query set* $\mathcal{R}$ and T_{13} to the candidate answer set. Similarly, for edge v_1v_4, the actual nearest object of the split point s_{14} is the same as the filter of v_1 and v_4, as depicted in Figure 4.8f. As we use the answer of the top left *static query point* for v_4, only the *range search area* of v_4 and T_{16} are added to $\mathcal{R}$ and the candidate answer set, respectively.

The recursive refinement condition ($t_i \neq t_j$, *refine* > 0, $t_s \neq t_i$). The query processing of this condition is exactly the same as in Algorithm 2. In our example, this condition takes place on edge v_3v_4 where we compute the split point s_{34} of v_3v_4, and then find the actual nearest object to s_{34}, i.e., the distance between s_{34} and the nearest *static query point* is larger than δ. Figure 4.8c depicts that the nearest object of s_{34} is

T_{12}. Since T_{12} is closer to v_4 than v_4's current filter $t_4 = T_3$, we set T_{12} as v_4's filter, i.e., $t_4 = T_{12}$. If the left top *static query point* is no longer used by any other continuous privacy-aware queries, we turn off this *static query point*. Then, we start over the *range selection step* on v_3v_4 with $t_3 = T_{13}$ and $t_4 = T_{12}$. Since the *trivial edge* and *stopping criterion conditions* still do not take place, we recompute the split point s_{34} and find the actual nearest object to s_{34}, i.e., T_8, as depicted in Figure 4.8d. T_8 is different from the filters of v_3 and v_4, so this condition takes place for edge v_3v_4 again. We split v_3v_4 into two separate line segments v_3s_{34} and $s_{34}v_4$, and execute the *range selection step* on these two separate line segments while decreasing the tuning parameter *refine* by one to zero. In the recursive calls on these line segments, since *refine* $= 0$, we end up with the next case of the *stopping criterion condition* for these line segments.

The stopping criterion condition ($t_i \neq t_j$, *refine* $= 0$). The only modification for this condition is similar to the *trivial edge condition*. As in Algorithm 2, we first add the *range search area* of the split point s_{ij} of the edge v_iv_j to the *range query set* $\mathcal{R}$. However, if we use the answer of a *static query point* as the nearest object of v_i, we add the *range search area* of v_i to the *range query set* $\mathcal{R}$. The same scenario is also applied to the other vertex v_j. In our example, we end up with this condition for edge v_3v_4, in which we compute the split point of each of the two separate line segments v_3s_{34} and $s_{34}v_4$ without finding the nearest object of these two split points. For the line segment v_3s_{34}, we add the *range search areas* of v_3 and the split point of v_3s_{34} that are represented by solid and dotted circles, respectively, at the right side in Figure 4.8e to the *range query set* $\mathcal{R}$ and T_8 to the candidate answer set. The idea of not adding the *search range area* of s_{34} to $\mathcal{R}$ is that T_8 is the actual nearest object to s_{34}, so s_{34}'s *range search area* contains only T_8. Likewise, for the line segment $s_{34}v_4$, we add the *range search areas* of v_4 and the split point of $s_{34}v_4$ to $\mathcal{R}$ and T_8 to the candidate answer set.

Step 3: *Range search step.* This step is exactly the same as in Algorithm 2. In our example depicted in Figure 4.8, the examples for the two options are:

1. We get the minimal candidate answer set by issuing a *continuous range query* for each *range search area* in the *range query set* $\mathcal{R}$, i.e., the *cloaked area* A and four distinct *range search areas* represented by circles, and then adding the answer to the candidate answer set.

2. We issue only one *continuous range query* with a query region that corresponds to a minimum bounding rectangle covering all the *range search areas* in $\mathcal{R}$, and then add the answer to the candidate answer set.

Proof of Correctness. In this section, we show the correctness of the shared execution paradigm for private queries over public data by proving that the paradigm is *inclusive*, i.e., it returns the exact answer within the candidate answer set.

Theorem 7. Inclusion. *Given a cloaked area A, a user U who issues the query within A, the algorithm of private queries over public data employing the shared execution paradigm computes the candidate answer set that contains the exact answer to U.*

Proof. We first show that the exact nearest object t_p to some point p on an edge v_iv_j is included in the candidate answer set for the *trivial edge*, *trivial split-point*, or *stopping criterion condition*.

The trivial edge condition. By Theorem 1, t_p is within the dotted and/or solid circles (Figure 4.3a). We distinguish three cases. Case 1: We use the answer of a *static query point*, t, as the nearest object of v_i, while t is the actual nearest object of v_j. Since t is the actual nearest object of v_j, there is no other objects within the solid circle. If the actual nearest object of v_i is t, there is no other objects within the dotted circle; and hence, $t = t_p$. On the other hand, if the actual nearest object of v_i is not t, t_p is closer to p than t, t_p is within the *range search area* of v_i, i.e., the dotted circle. Thus, t_p is included in the candidate answer set. Case 2: We use the answer of a *static query point*, t, as the nearest object of v_j while t is the actual nearest object of v_i. This case is symmetric with Case 1. Case 3: We use the answer of *static query points*, t, as the nearest object of both v_i and v_j. The proof of Case 1 is applied to the case that t is the actual nearest object of v_i and/or v_j. If t is not the actual nearest object of v_i or v_j, t_p is closer to p than t, t_p is within the *range search area* of v_i and/or v_j. Thus, t_p is included in the candidate answer set.

The trivial split-point condition. As depicted in Figure 4.3b, we consider that the edge v_iv_j is split into two separate line segments v_is_{ij} and $s_{ij}v_j$. For both the line segments, the endpoints have the same nearest object, so the proof of the *trivial edge condition* can be applied to these two line segments.

The stopping criterion condition. In this case, the *range search area* R of s_{ij} is added to the *range query set* $\mathcal{R}$, i.e., all objects within R are added to the candidate answer set. For line segment $v_i s_{ij}$, the proof of the Case 1 and Case 3 of the *trivial edge condition* is applied to the case that we find the actual nearest object of v_i and use the answer of a *static query point* as the nearest object of v_i, respectively. The proof for the line segment $s_{ij} v_j$ is symmetric with that for the line segment $v_i s_{ij}$.

Then, we show that the exact answer to U is within the candidate answer set. When *refine* is set to ∞, each line segment ends up with having either the *trivial edge condition* or the *trivial split-point condition.* When *refine* is finite, the *stopping criterion condition* could take place for some line segments. We already show that the nearest object to any point on each line segment is added to the candidate answer set for these three conditions. The objects within A are also added to the candidate answer set. Therefore, the exact answer to U is included in the candidate answer set. □

Algorithms for Public Nearest-Neighbor Queries over Private Data

The query processing algorithm for *public queries over private data* presented in Section 4.1.2 can be applied to the shared execution paradigm with only one modification in the *filter selection step.* The modification is that if the distance between the user who issues the query and the nearest *static query point* is less than δ, we use the answer of the nearest *static query point* as the filter. Otherwise, we find the actual nearest object of the user as the filter. The *range search step* is the same as in Section 4.1.2.

Proof of Correctness. We will show the correctness of the proposed shared execution paradigm for public queries over private data by proving that the paradigm is *inclusive*, i.e., it returns the exact answer within the candidate answer set.

Theorem 8. Inclusion. *Given a cloaked area A, a user U who issues the query within A, the algorithm of public queries over private data employing the shared execution paradigm computes the candidate answer set that contains the exact answer to U.*

Proof. We use the answer of a *static query point*, t, as the nearest object of U. Let t' be the actual nearest object of U. If $t = t'$, the proof is the same as in Theorem 4. However, if $t \neq t'$, $\mathsf{dist}_{\mathsf{max}}(U, A_{t'}) < \mathsf{dist}_{\mathsf{max}}(U, A_t)$, i.e., t' intersects the *range search area* of U. Thus, t' is added to the candidate answer set. □

Algorithms for Private Nearest-Neighbor Queries over Private Data

The *private queries over private data* algorithm presented in Section 4.1.3 only returns *range search areas*, so we have only three minor modifications to apply the shared execution paradigm to this algorithm. The modifications are as follows.

Step 1: *Filter selection step.* The only modification for this step is that for each vertex v_i of a *cloaked area* A, if the distance between v_i and the nearest *static query point* is less than δ, we use the answer of the *static query point* as the filter t_i of v_i. Otherwise, we find the actual nearest object of v_i as its filter t_i.

Step 2: *Range selection step.* We have only two modifications in the *trivial split-point condition*. These modifications are exactly the same as the first two modifications in the *trivial split-point condition* of the *range selection step* in the *private queries over public data* algorithm (Section 4.2.2).

Step 3: *Range search step.* We do not have any modification in this step.

Proof of Correctness. We will show the correctness of the proposed shared execution paradigm for private queries over private data by proving that the paradigm is *inclusive*, i.e., it returns the exact answer within the candidate answer set.

Theorem 9. Inclusion. *Given a cloaked area A, a user U who issues the query within A, the algorithm of private queries over private data employing the shared execution paradigm computes the candidate answer set that contains the exact answer to U.*

Proof. We first show that the exact nearest object t_p to some point p on an edge v_iv_j is included in the candidate answer set for the *trivial edge*, *trivial split-point*, or *stopping criterion condition*.

The trivial edge condition. We distinguish two cases.

Case 1: *The furthest corner of the cloaked area of the same filter t of v_i and v_j, A_t, from v_i and v_j is the same* (Figure 4.6a). By Theorem 5, the *cloaked area* of t_p intersects the thin and/or bold circles. We distinguish three cases. Case I: We use the answer of a *static query point*, t, as the nearest object of v_i while the actual nearest object of v_j is t. Since the distance from the actual nearest object of v_i to v_i is either the same as the distance from t to v_i, i.e., t is the actual nearest object of v_i, or smaller that the distance from t to v_i, so the *cloaked area* of the actual nearest object of v_i is totally covered by the thin circle; and thus, the actual *range search area* of v_i is within the thin

and/or bold circles. As the *trivial edge condition* adds both the thin and bold circles to the *range query set* $\mathcal{R}$, all objects within the thin and/or bold circles are added to the candidate answer set. This means that all objects intersecting the actual *range search area* of v_i will be added to the candidate answer set. Case II: We use the answer of a *static query point*, t, as the nearest object of v_j while the actual nearest object of v_i is t. This case is symmetric with Case I. Case III: We use the answer of *static query points* as the nearest object of both v_i and v_j. The thin and bold circles are the *range search areas* of v_i and v_j, respectively. Since the actual *range search areas* of v_i and v_j are within the thin and/or bold circles, all objects within these two circles are added to candidate answer set.

Case 2: *The furthest corners of A_t from v_i and v_j are different* (Figure 4.6b). The proof of this case is the same as the Case 2 of the *trivial edge condition* in Theorem 5.

The trivial split-point condition. The proof of the *trivial split-point condition* in Theorem 7 is applied to this case.

The stopping criterion condition. The proof of the *stopping criterion condition* in Theorem 7 is applied to this case.

Then, we show that the exact answer to U is within the candidate answer set. When *refine* is set to ∞, each line segment ends up with having either the *trivial edge condition* or the *trivial split-point condition*. When *refine* is finite, the *stopping criterion condition* could take place for some line segments. We already show that the nearest object to any point on each line segment is added to the candidate answer set for these three conditions. The objects within A are added to the candidate answer set. Therefore, the exact answer to U is included in the candidate answer set. □

4.3 Experiment Results

In this section, we evaluate the performance of the *basic paradigm* using the *snapshot* privacy-aware query processing algorithm and the *shared execution paradigm* for all privacy-aware query types, i.e., *private queries over public data*, *public queries over private data*, and *private queries over private data*, in our *Casper** framework. Since the *basic paradigm* uses exact nearest-neighbor queries to compute candidate answer sets, this paradigm is denoted as "Exact" in this section, while the shared execution paradigm

is denoted as "Shared". We evaluate our algorithms with respect to performance tuning parameters, system scalability, and privacy requirements. In all experiments, the performance evaluation is in terms of (a) *total processing time*, which includes the query processing time of computing an candidate answer set at the database server, the transmission time of sending the candidate answer set from the database server to the location anonymizer, and the filtration time of computing an exact answer from the candidate answer set, and (b) *candidate answer set size*. However, the filtration time is much less than both the query processing time and the transmission time, so we do not show the filtration time in all the figures. For the experiments of performance tuning parameters, we vary the value of *refine*, and the number of *static query points* and the value of δ for the shared execution paradigm. These experiments are important to evaluate the performance trade-off of the three tuning parameters. Then, we perform experiments to show the scalability of the proposed algorithms with respect to large numbers of users and data, and various data object sizes. Finally, we show the performance of the proposed algorithms with respect to various levels of k-anonymity which is the most commonly used privacy requirement.

We use two baseline algorithms to evaluate the performance of our algorithms. For *private queries over public data*, we compare our algorithms with an existing range nearest-neighbor algorithm that finds the minimal set of nearest objects of a rectangular query region [80] (denoted as "RNN"). For private data, since none of existing approaches works for private data, we design a baseline algorithm for *private queries over private data* (denoted as "Base"). The basic idea of the Base algorithm is that we first find the nearest object t to the center of a cloaked area A and determine the maximum distance d_{max} between each vertex v of A and the furthest corner of t from v. Then, we determine a circular range search area centered at the center of A with a radius of the sum of the distance between the center of A and one of its vertex and d_{max}. The set of private data that intersects the range search area constitutes an answer set. Thus, the Base algorithm requires only one nearest neighbor search for t and one range search for the extended A. Since *public queries over private data* is very simple, we do not design any baseline algorithm for this query type. At the location anonymizer, we use a nearest neighbor search to compute the exact answer from a candidate answer set.

In all experiments, we generate a set of moving objects on the road map of Hennepin

Table 4.2: Summary of parameter settings.

Parameters	Default Values	Ranges
Number of users	200K	100K to 500K
Number of data	20K	10K to 50K
Data size	2 Kbytes	2 to 10 Kbytes
Number of static query points	$2^{10} \times 2^{10}$	$2^6 \times 2^6$ to $2^{10} \times 2^{10}$
refine	1	0 to ∞
δ	60% of $\delta_{max} = 500$	20% to 100% of δ_{max}
k-anonymity privacy requirement	[10-50]	[10-50] to [10-250]

County in Minnesota, USA. The input road map is extracted from the Tiger/Line files that are publicly available [89]. Furthermore, the location anonymizer employs the *PrivacyGrid* algorithm that is the state-of-the-art location anonymization algorithm to blur users' locations into cloaked areas [32]. These cloaked areas are the input of our privacy-aware query processor. Unless mentioned otherwise, the experiment considers 200K mobile users in which 100K users issue continuous privacy-aware queries, and 20K data objects with a size of 2 Kbytes. The continuous queries are simulated similar to the work [65], but we consider a more dynamic environment. Each moving object or query reports its new location information (if changed) every five seconds. *Casper** is adopted to refresh query results every five seconds. The communication bandwidth between the database server and the location anonymizer is 1 Mbits per second (Mbps). We generate a random k-anonymity privacy requirement for each user where k is assigned uniformly within a range $[10 - 50]$. For both the *basic* and shared execution paradigms, *refine* is set to one. For the shared execution paradigm, we consider $2^{10} \times 2^{10}$ *static query points* and δ is set to 60% of $\delta_{max} = 500$. Table 9.1 summarizes the parameter settings.

4.3.1 Effect of Performance Tuning Parameters

In this section, we study the effect of three performance tuning parameters, i.e., *refine*, the number of *static query points*, and δ, on our proposed *basic paradigm* (Exact) and shared execution paradigm (Shared) with respect to *total processing time* and candidate answer set size. In our framework, the tuning parameter *refine* is for both the *basic* and shared execution paradigms, while the number of *static query points* and the parameter δ are dedicated for the shared execution paradigm.

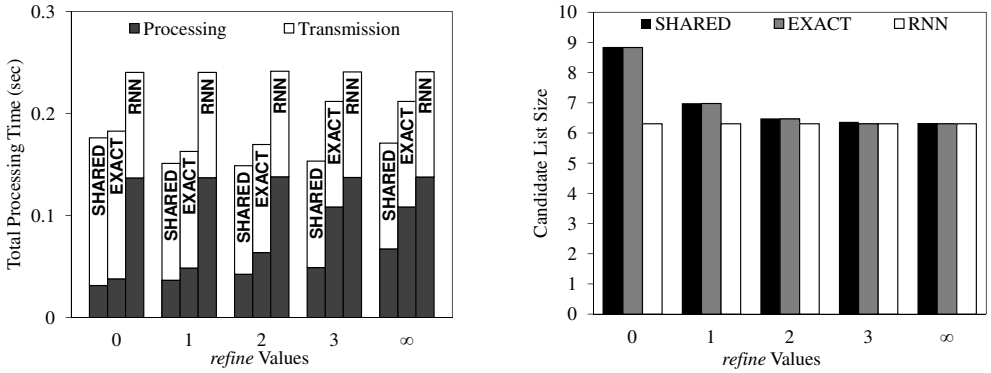

(a) Total Processing Time (b) Candidate Answer Set Size

Figure 4.9: *refine* values (private queries over public data).

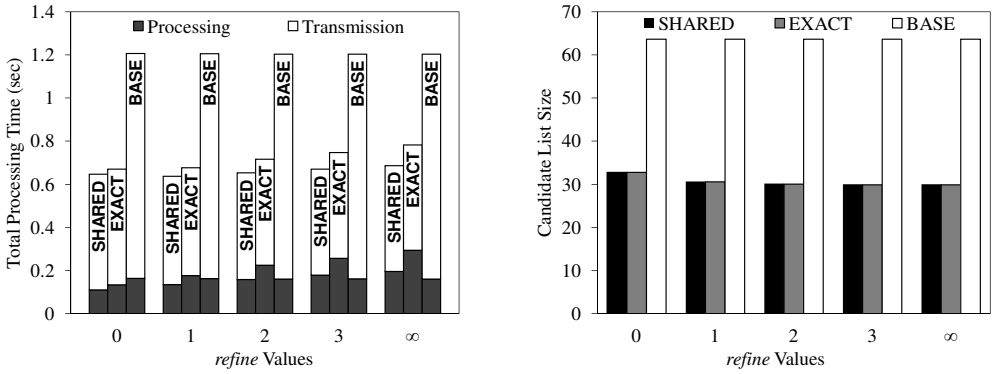

(a) Total Processing Time (b) Candidate Answer Set Size

Figure 4.10: *refine* values (private queries over private data).

Figures 4.9 and 4.10 depict the performance of the Shared and Exact algorithms with respect to increasing the value of *refine* from zero to infinity. Figures 4.9a and 4.10a give the effect of *refine* on total processing time which includes the *processing time* of a candidate answer set at the database server (represented by gray bars) and the *transmission time* of sending the candidate answer set to the location anonymizer (represented by white bars). Since the parameter *refine* has no effect on public queries over private data, we show only the performance of private queries over public and private data. The results show that the query processing time of our Shared and Exact algorithms increases when *refine* gets larger. The results also indicate that Shared effectively improves query

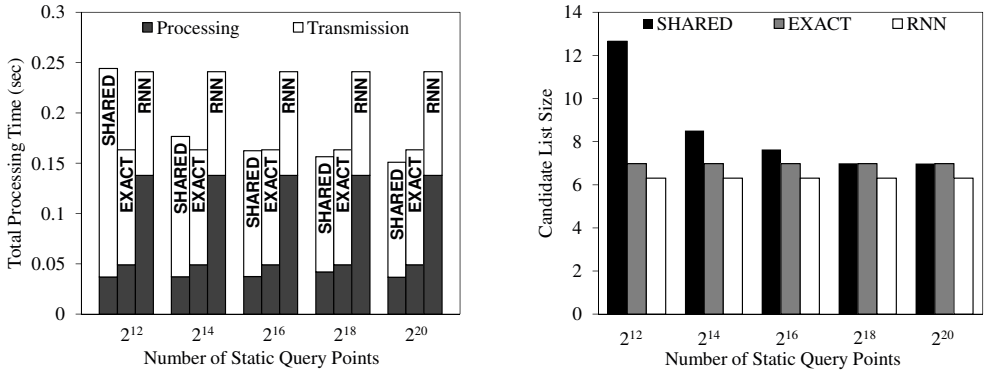

(a) Total Processing Time (b) Candidate Answer Set Size

Figure 4.11: Number of static query points (private queries over public data).

processing time, i.e., Shared reduces the query processing time of Exact by from 17% to 55% for private queries over public data and by from 18% to 33% for private queries over private data, as depicted in Figures 4.9a and 4.10a, respectively. The main reason of the improvement is that Shared significantly reduces the number of nearest-neighbor searches in Exact by sharing the answer of a set of *static query points* as approximate nearest-neighbor searches among all continuous queries. It is important to note that Shared only slightly increases the candidate answer set size (Figures 4.9b and 4.10b). The total processing time of Shared and Exact is better than the baseline algorithms RNN and Base for public and private data, respectively. The total processing time of Shared and Exact increases and the candidate answer set size slightly reduces when *refine* is larger than one. The main reason is that the first two iterations of refinements already prune the object set to a small set of objects which includes the exact answer to the user. Further refinements can only slight improve transmission time, but they incur higher query processing time. Thus, we set *refine* to one as a default value for other experiments.

Figures 4.11-4.13 depict the performance of Shared with respect to increasing the number of *static query points* from 2^{12} to 2^{20}. In general, when the number of *static query points* gets larger, Shared only slightly increases the query processing time (Figures 4.11a-4.13a) while significantly improving the candidate answer set size (Figures 4.11b-4.13b). The decrease of the candidate answer set size is due to the fact

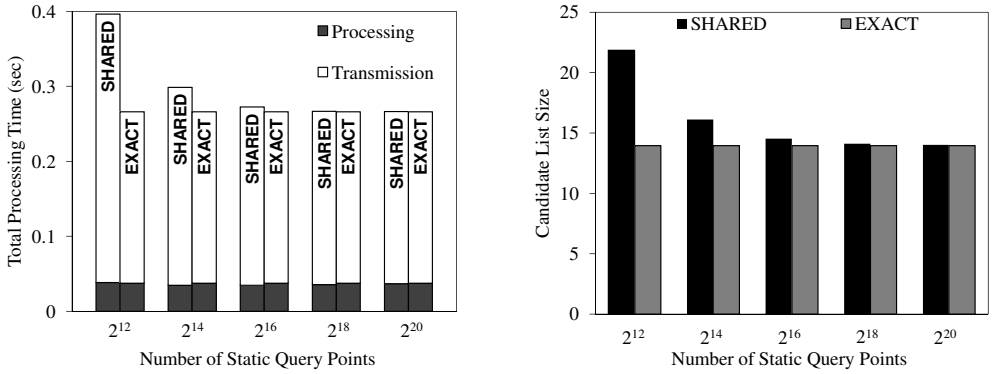

(a) Total Processing Time (b) Candidate Answer Set Size

Figure 4.12: Number of static query points (public queries over private data).

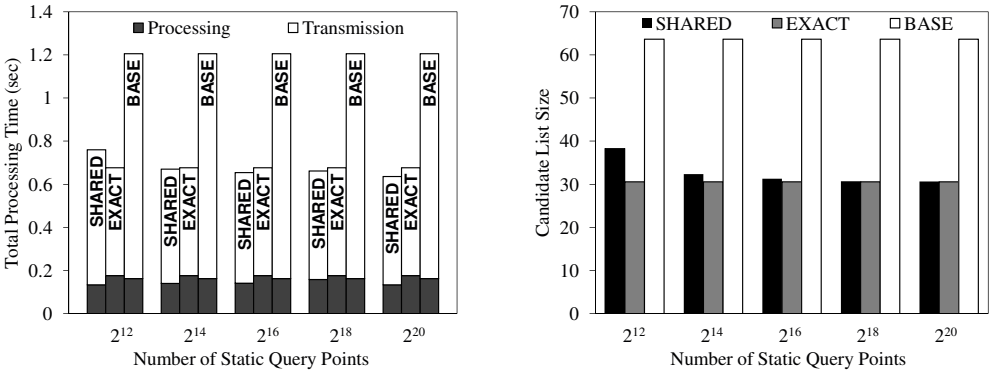

(a) Total Processing Time (b) Candidate Answer Set Size

Figure 4.13: Number of static query points (private queries over private data).

that Shared provides more accurate approximate nearest neighbor searches as there are more *static query points*, i.e., the vertex of a cloaked area A or the split point of the edge of A is closer to its nearest *static query point*. As Shared reduces the candidate answer set size, it also improves the transmission time; and thus, increasing the number of *static query points* results in better total processing time.

Figures 4.14-4.16 give the performance of Shared with respect to increasing δ from 20% to 100% of $\delta_{max} = 500$, i.e., from 100 to 500. In general, the results show that when δ gets larger, the query processing time of Shared decreases (Figures 4.14a-4.16a) while the candidate answer set size slightly increases (Figures 4.14b-4.16b). The reason for

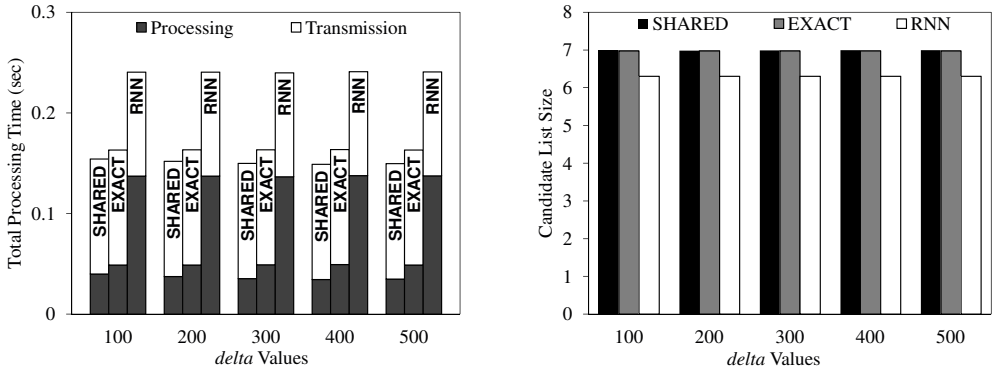

(a) Total Processing Time (b) Candidate Answer Set Size

Figure 4.14: δ values (private queries over public data).

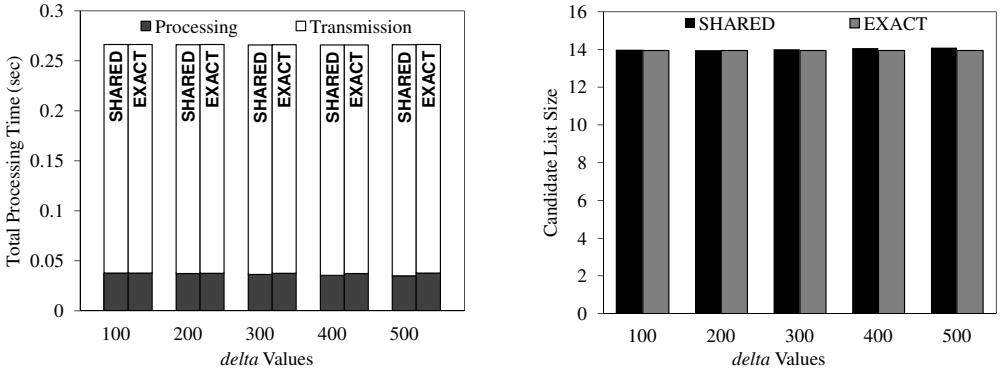

(a) Total Processing Time (b) Candidate Answer Set Size

Figure 4.15: δ values (public queries over private data).

the improvement in query processing time is that the answer of static query points can be shared with more queries. However, as δ gets larger, Shared provides more inaccurate approximate nearest-neighbor searches for the query processor; and thus, the size of the range search areas in the range query set $\mathcal{R}$ gets larger. Larger range search areas would give larger candidate answer sets that lead to higher transmission time and filtration time. Therefore, δ can be served as a tuning parameter for a trade-off between query processing time and candidate answer set size.

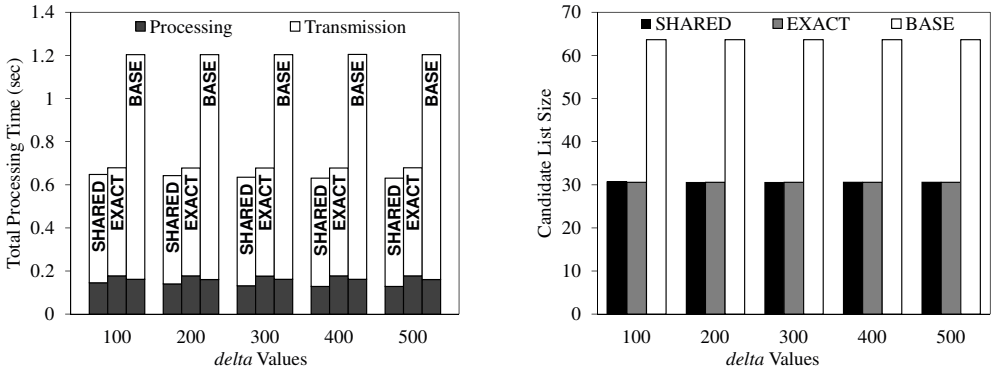

(a) Total Processing Time (b) Candidate Answer Set Size

Figure 4.16: δ values (private queries over private data).

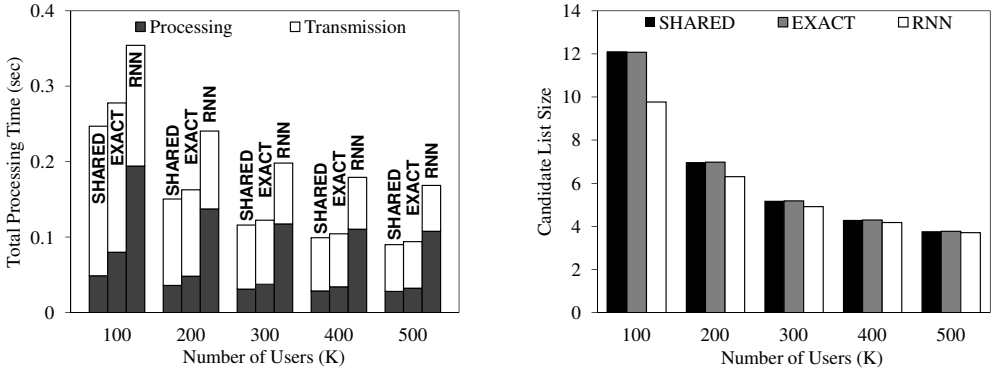

(a) Total Processing Time (b) Candidate Answer Set Size

Figure 4.17: Number of users (private queries over public data).

4.3.2 Scalability

In this section, we evaluate the scalability of our algorithms with respect to three dimensions, i.e., the number of users, the number of data, and data size.

Figures 4.17 and 4.18 depict the scalability of our algorithms with respect to varying the number of mobile users from 100K to 500K. As there are more users, the total processing time of all approaches improves (Figures 4.17a and 4.18a). The main reasons for this are that (a) increasing the number of users results in smaller cloaked areas that incur lower query processing time; and (2) such smaller cloaked areas lead to smaller candidate answer sets that reduce transmission time (Figures 4.17b and 4.18b).

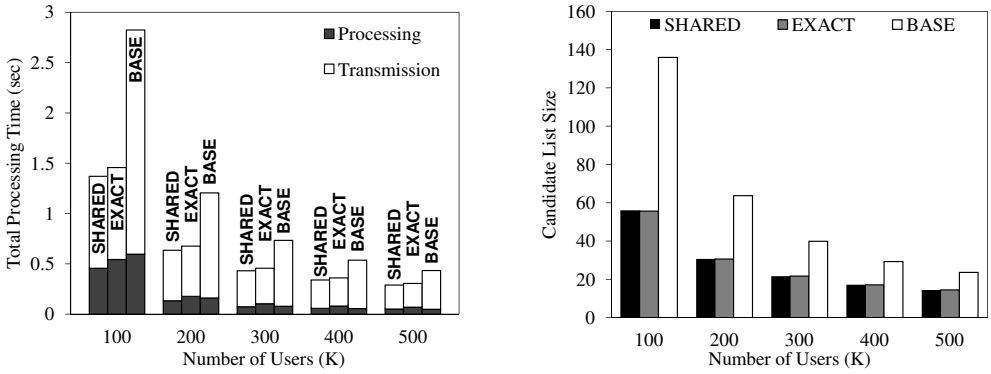

(a) Total Processing Time (b) Candidate Answer Set Size

Figure 4.18: Number of users (private queries over private data).

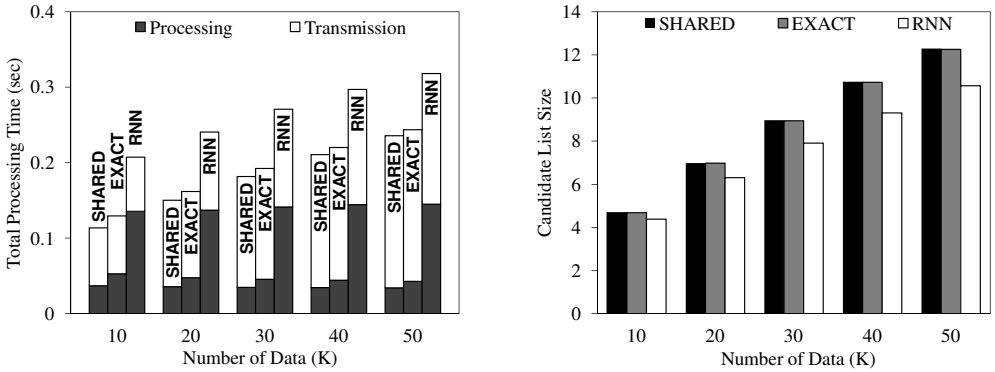

(a) Total Processing Time (b) Candidate Answer Set Size

Figure 4.19: Number of data (private queries over public data).

Figures 4.19 and 4.20 give the scalability of our algorithms with respect to increasing the number of public/private data from 10K to 50K. The results show that the total processing time and candidate answer set size of all approaches increase when the number of data gets larger, as depicted in Figures 4.19a-4.20a and Figures 4.19b-4.20b, respectively. The increase of the total processing time is due to higher transmission time of sending larger candidate answer sets from the database server to the location anonymizer. When the number of data increases, there are more objects within a cloaked area A and each edge of A has more nearest target objects; and hence, the candidate

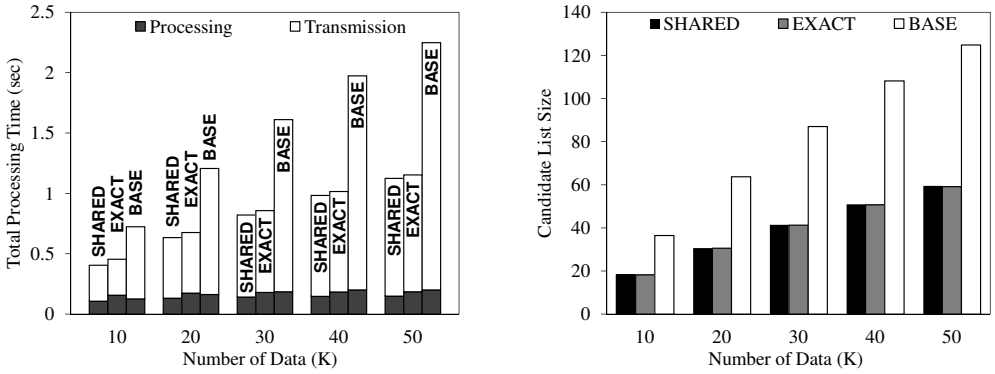

(a) Total Processing Time (b) Candidate Answer Set Size

Figure 4.20: Number of data (private queries over private data).

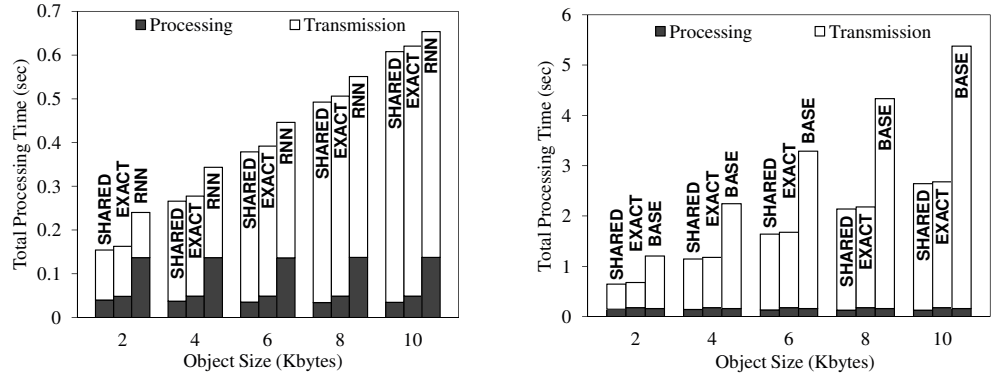

(a) Private Queries over Public Data (b) Private Queries over Private Data

Figure 4.21: Data object size (total processing time).

answer set size increases. Since the transmission time is higher than the query processing time and filtration time, when there are more data, we should increase the value *refine* to reduce candidate answer set size to improve the total processing time.

Figure 4.21 gives the effect of data object size on the total processing time of our algorithms with respect to increasing the object size from 2 to 10 Kbytes. Increasing the object size results in higher transmission time for all approaches, so the total processing time of all approaches increases. For public data, since our algorithms improve the query processing time by giving larger candidate answer sets of answers, i.e., $refine = 1$, the improvement in the total processing time becomes smaller when the object size gets

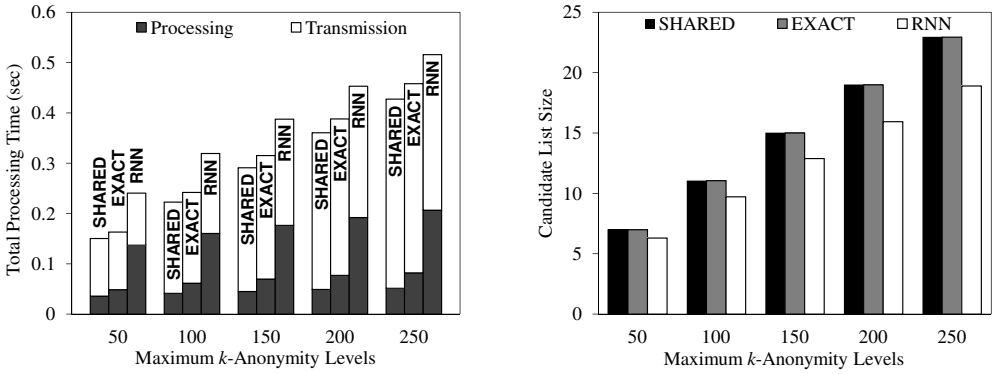

(a) Total Processing Time (b) Candidate Answer Set Size

Figure 4.22: k-anonymity requirements (private queries over public data).

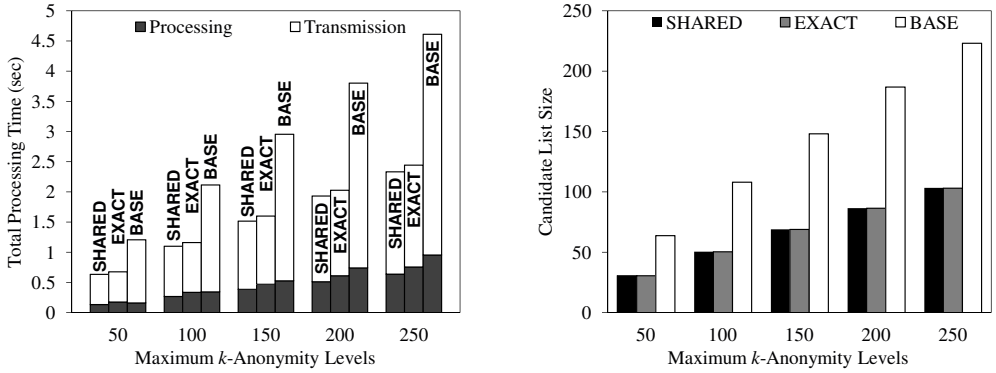

(a) Total Processing Time (b) Candidate Answer Set Size

Figure 4.23: k-anonymity requirements (private queries over private data).

larger (Figure 4.21a). For private data, our algorithms always (Shared and Exact) give smaller candidate answer sets than Base, so our algorithms perform much better than Base when the data object size increases (Figure 4.21b).

4.3.3 Effect of Privacy Requirements

Figures 4.22 and 4.23 depict the performance of our algorithms with respect to increasing the maximum k-anonymity level from 50 to 250 (the minimum k-anonymity level is 10). The results show that the query processing time of all approaches increases as k gets larger (Figures 4.22a and 4.23a). This is because increasing the k-anonymity

level results in larger cloaked areas that lead to higher query processing time. Larger cloaked areas also pose larger candidate answer sets that lead to higher transmission time (Figures 4.22b and 4.23b). Thus, the total processing time of all approaches increases, as the k-anonymity level gets stricter.

4.4 Summary

This chapter focuses on the privacy-aware query processor in Casper. The privacy-aware query processor is embedded into traditional location-based database servers to tune their functionalities to be privacy-aware by dealing with cloaked areas rather than exact location points. Three new query types that are supported by Casper are identified, private queries over public data, public queries over private data, and private queries over private data. To deal with these three privacy-aware query types, the privacy-aware query processor provides a candidate answer set rather than an exact answer for the user. We prove that the returned candidate answer set contains the exact answer and is of minimal size. Then, we propose a shared execution paradigm that aims to share computational resources among continuous privacy-aware queries, in order to improve system scalability and computational efficiency of the query processor for continuous privacy-aware queries. In addition, the performance of the query processor can be tuned through several parameters to achieve a trade-off between system scalability, i.e., query processing time, and query answer optimality, i.e., candidate answer set size. Extensive experimental evaluation studies the performance of the privacy-aware query processor in Casper. The results show the scalability and efficiency of the privacy-aware query processor with a large number of mobile users, continuous queries, and data, various privacy requirements, and various performance tuning settings.

Chapter 5

Approximate Range Nearest Neighbor Queries

In this chapter, we present a new query type, termed approximate range nearest-neighbor (NN) queries. Although the approximate range NN query is similar to the private queries over private data, as described in Chapter 4, the approximate range NN query does not assume a third party placed between the user and the database server and it can also be applied to the case of users with uncertain location information. NN queries have been widely used in location-based services (e.g., see [90, 61, 3, 65, 91]). The problem of traditional NN queries can be defined as follows: "given a set of objects and a query location point p, find the nearest object(s) to p"; and thus, they are referred to as *point* NN queries. *Point* NN queries have been extended to find all NNs for line segments [82] and spatial regions [80, 44, 12] that are referred to as *linear* and *range* NN queries, respectively. A *linear* NN query returns an answer set that includes the nearest object(s) to every point in a given line segment. On the other hand, a *range* NN query returns an answer set that includes the nearest object(s) to every point in a given spatial region, where the spatial region can be either a rectangular region [80, 12] or a circular region [44].

Recent research efforts have shown the importance of *range* NN queries in location-based services, as it can be applied to the following realistic scenarios:

- **Uncertain locations.** We have two kinds of location uncertainty, *measurement*

imprecision and *sampling imprecision*. The measurement imprecision is due to the limitation of the underlying positioning techniques of network environments, e.g., 2G/3G and Wi-Fi. On the other hand, the sampling imprecision is due to continuous motion, network delays, and location update frequency even with highly accurate positioning devices, e.g., GPS. Thus, we have to use a spatial region where the user is guaranteed to be therein to represent the user location information in order to capture location uncertainty (e.g., see [92, 93, 94, 95, 96]).

- **Privacy-preserving queries.** Mobile users are not willing to reveal their exact location information to location-based service providers, as they want to preserve their location privacy. The most commonly used privacy-enhancing technique is to blur the user's exact location into a spatial region, i.e., spatial cloaking, that satisfies the user's specified privacy requirements (e.g., see [44, 12, 32, 34, 39, 36, 97]).

In these two scenarios, the mobile user sends her NN query along with a spatial region as the query location, i.e., a *range* NN query. Then, a database server returns an answer set that includes the nearest object(s) to every point within the spatial region. The answer set size would substantially increase as the query region gets larger. Unfortunately, the communication bandwidth between the user and the database server is very limited in a mobile environment, i.e., the downlink bandwidth ranges from 128 kbps at vehicular speeds to 2 Mbps at stationary or very slow speeds for 3G mobile subscribers. Transmitting large answer sets to the user would pose very high query response time. Furthermore, as mobile users receive their answer handheld devices with a small screen, it is convenient to return to the users very few answers with high quality.

In this chapter, we propose a new *approximate range* NN query processing algorithm that enables the user to tune a trade off between query response time and the quality of query answers. Our proposed algorithm allows the user to specify an *approximation tolerance level* t, where we return an answer set $\mathcal{A}$ such that each object in $\mathcal{A}$ is one of the t nearest objects of every point in the query region. The larger the value of t, the smaller the answer set returned by a database server. Thus, the approximation tolerance level is a tuning parameter that trades off between query response time and the quality of answers. In the case that $t = 1$, we return the exact range NN answer of

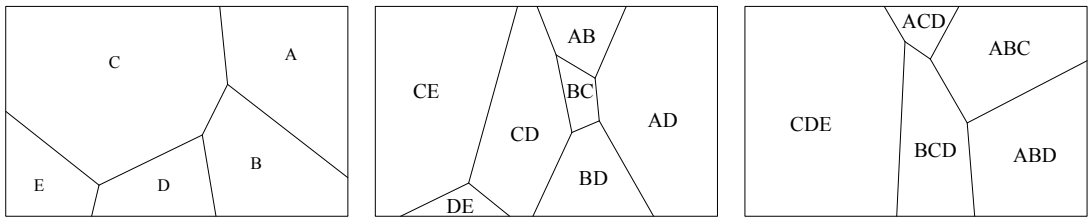

(a) 1-NN of each region (b) 2-NN of each region (c) 3-NN of each region

Figure 5.1: A motivating example for approximate range NN queries.

maximal size to the user. On the other hand, if $t > 1$, we return an approximate answer set, which is smaller than the exact answer, to the user; and thus, the transmission time of sending the answer set to the user is reduced. Since query response time is dominated by the communication overhead between the user and the database server, a larger value of t incurs lower query response time.

Figure 5.1 depicts a motivating example for our problem where we decompose the query region $Q.R$ of a range NN query Q into disjoint regions and label each region with its t-NN(s). Figure 5.1a shows the NN of each region. If a user wants to find the nearest object(s) to $Q.R$, i.e., the exact range NN query answer, the required answer set contains the nearest object(s) to every point in $Q.R$, i.e., $\mathcal{A}_1 = \{A, B, C, D, E\}$. Figure 5.1b shows the 2-NN of each region. If the user is satisfied with the 2-nd nearest object(s) to $Q.R$, the answer set $\mathcal{A}_2$ should contain at least one object among the 2 nearest objects to every point in $Q.R$. For example, if $\mathcal{A}_2 = \{A, B, C, D\}$, regardless of the actual user location within $Q.R$, the user is guaranteed to receive an object among her 2 nearest objects. However, we can still do better. For example, if $\mathcal{A}'_2 = \{A, C, D\}$, the user is still guaranteed to receive an object among her 2 nearest objects, regardless of her actual location within $Q.R$. Thus, the answer set of minimal size is a minimal set of objects such that there is at least one object among the 2 nearest objects of each region. Furthermore, if the user is satisfied with the 3-rd nearest object(s) to $Q.R$, i.e., the required answer set $\mathcal{A}_3$ should contain at least one object among the 3 nearest objects of each region, as depicted in Figure 5.1c, where the minimal answer set is $\mathcal{A}_3 = \{A, C\}$. Therefore, if a user accepts a higher approximation tolerance in a range NN query answer, the user will receive a smaller answer set and more user convenience.

The main idea of our proposed range NN query processing algorithm is to have an

off-line process to pre-compute a set of t-order Voronoi diagrams, from order one to a predefined maximum order t_{max}, for a set of stationary data objects, e.g., restaurants, gas stations and hotels. For a t-order Voronoi diagram, each Voronoi cell is associated with a distinct set of t objects that are the t nearest objects to every point in the cell. To efficiently search in a Voronoi diagram, we propose an *incomplete pyramid structure* as an access method to index the Voronoi cells. Given a *range* NN query Q and an approximation tolerance level t, our proposed *on-line* range NN query processing algorithm first determines a set of Voronoi cells $\mathcal{V}$ that intersects the query region by accessing the *incomplete pyramid structure* of the relevant t-order Voronoi diagram. Then, the remaining query processing is reduced to a well-known set-covering problem where we use a greedy approach to select the minimal set of objects, i.e., the answer set $\mathcal{A}$, from the objects associated with the Voronoi cells in $\mathcal{V}$ such that at least one object from each Voronoi cell in $\mathcal{V}$ is selected. As a result, each object in $\mathcal{A}$ is one of the t nearest objects to every Voronoi cell in $\mathcal{V}$, i.e., each object in $\mathcal{A}$ is one of the t nearest objects to every point in the query region. With a larger value of t, there are more common objects associated among the Voronoi cells in $\mathcal{V}$; and hence, we would get smaller answer sets that incur lower query response time.

5.1 System Model

In this section, we first formally define our problem, and then present the basic concept of Voronoi diagrams and the underlying system architecture.

Problem definition. Our problem is defined as follows: *given a set of objects, a range nearest-neighbor query Q with a query region $Q.R$, and an approximation tolerance level t, find the minimal set of objects $\mathcal{A}$ such that each object in $\mathcal{A}$ is one of the t nearest objects to every point in $Q.R$.*

Voronoi diagrams. Given a set of points $\mathcal{S}$ on the plane, which are the Voronoi *sites*, the Voronoi diagram of $\mathcal{S}$, denoted as $V(\mathcal{S})$, is a decomposition of the space into disjoint regions, *cells*, such that each site s_i is associated with a cell V_j, denoted as $V_j = \{s_i\}$, containing all the points in the plane that are closer to s_i than any other site in $\mathcal{S}$. In other words, s_i is the nearest site to every point in V_j. Figure 5.2a depicts a Voronoi diagram of a set of five sites $\mathcal{S} = \{s_1, s_2, s_3, s_4, s_5\}$, $V(\mathcal{S})$. $V(\mathcal{S})$ decomposes

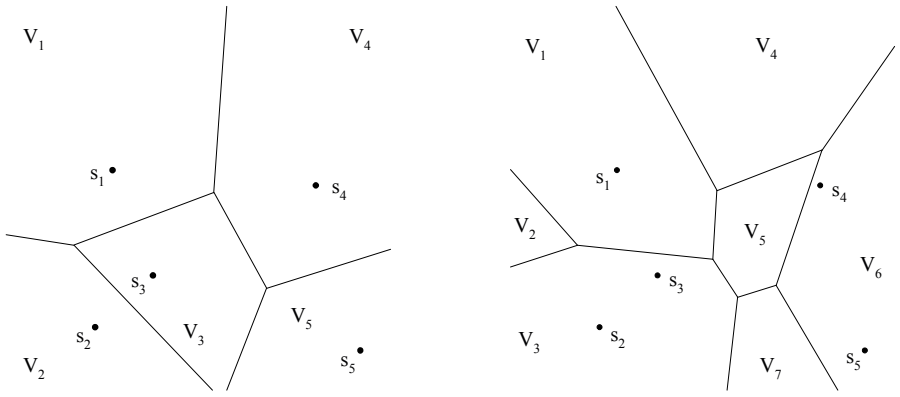

(a) 1-order Voronoi diagram (b) 2-order Voronoi diagram

Figure 5.2: The 1-order and 2-order Voronoi diagrams for five sites s_1 to s_5.

the space into five cells V_1, V_2, V_3, V_4, and V_5 that are associated with the sites s_1, s_2, s_3, s_4, and s_5, respectively. For example, given a point p in cell V_1, s_1 is the nearest site to p.

Higher-order Voronoi diagrams. The t-order Voronoi diagram extends the concept of the Voronoi diagram by defining cells based on the t nearest neighbors. The t-order Voronoi diagram of $\mathcal{S}$, where $1 < t \leq |\mathcal{S}|-1$, denoted as $V_t(\mathcal{S})$, is a decomposition of the space into disjoint cells, such that a distinct set of t sites $S_i = \{s_{i_1}, s_{i_2}, \ldots, s_{i_t}\}$ is associated with a cell V_j, $V_j = \{S_i\}$, containing all the points in the plane that have the sites in S_i as their t nearest sites. In other words, S_i contains t nearest sites to every point in V_j. Figure 5.2b depicts the 2-order Voronoi diagram of $\mathcal{S}$, $V_2(\mathcal{S})$, that decomposes the space into seven cells, i.e., $V_1 = \{s_1, s_3\}$, $V_2 = \{s_1, s_2\}$, $V_3 = \{s_2, s_3\}$, $V_4 = \{s_1, s_4\}$, $V_5 = \{s_3, s_4\}$, $V_6 = \{s_4, s_5\}$, and $V_7 = \{s_3, s_5\}$. For example, given a point p in cell V_3, the sites s_2 and s_3 are the two nearest sites to p.

System architecture. We consider a mobile environment where mobile users communicate with a location-based database server through a (2G/3G) cellular network. The data/control flow of our system is as follows: The mobile user sends range NN queries to the database server. Our proposed approximate range NN query processing algorithm that is implemented in the database server computes an answer set, and then the server sends the answer set to the user. We use the Euclidean distance as our distance metric.

5.2 Approximate Range NN Query Processing

In this section, we first describe an *off-line* process to compute Voronoi diagrams, from order one to order t_{max}, where t_{max} is the maximum allowable user specified approximation tolerance level, and present our proposed *incomplete pyramid structure* that is used as an access method for each Voronoi diagram. Then, we present an *on-line* query processing algorithm for approximate range NN queries.

5.2.1 Building Voronoi Diagrams

We use an off-line process to build t Voronoi diagrams for a set of objects, e.g., restaurants, hotels and gas stations, from order one to order t_{max}, where t_{max} is the maximum user specified approximation tolerance level. Thus, the user can specify her desired approximation tolerance level t from one to t_{max}. Notice that if $t = 1$, our algorithm provides an exact answer set of the minimal size for range NN queries. Given a set of objects $\mathcal{S}$, building a set of Voronoi diagrams, from order one to order t_{max}, i.e., $V_1(\mathcal{S}), V_2(\mathcal{S}), \ldots,$ and $V_{t_{max}}(\mathcal{S})$, takes $O(t_{max}^2 N \log N)$ time and $O(\sum_{t=1}^{t_{max}} t^2(N-t))$ space, where N is the number of objects in $\mathcal{S}$ [98]. After we build the t Voronoi diagrams, they are stored for later use in our proposed range NN query processing algorithm. For each Voronoi diagram, we maintain a table to store each Voronoi cell with its associated objects.

5.2.2 Access Method for Voronoi Diagrams

We will construct an *incomplete pyramid structure* for each Voronoi diagram to support efficient range search among Voronoi cells. The idea of our proposed *incomplete pyramid structure* is that we need to find a set of Voronoi cells $\mathcal{V}$ that intersects a given range query region in order to retrieve their associated objects. Without any index structure, we have to scan every cell in a Voronoi diagram to find $\mathcal{V}$. When the number of objects and/or t is large, scanning all cells in a Voronoi diagram would pose a scalability issue. To this end, we propose an *incomplete pyramid structure* to overcome this issue. The construction of an *incomplete pyramid structure* for each Voronoi diagram includes two main steps.

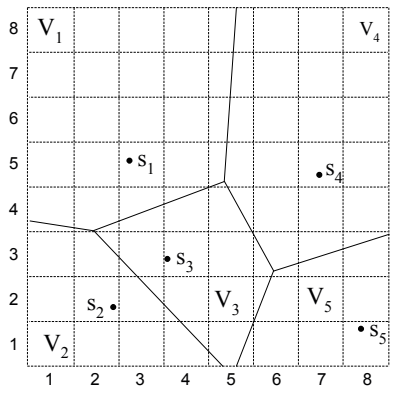

Mapping Table

Cell ID	Voronoi Cells
C(1,1)	V_2
C(2,1)	V_2
C(3,1)	V_2
C(4,1)	V_2,V_3
C(5,1)	V_2,V_3,V_5
C(6,1)	V_5
C(7,1)	V_5
C(8,1)	V_5
…	…
C(8,8)	V_4

Figure 5.3: The base level of an incomplete pyramid structure.

Step 1: ***Base level step.*** This step decomposes the space into grid cells where each grid cell $C(c, r)$ is uniquely identified by its column number c and row number r. Also, we use a hash table, *mapping table*, that associates each grid cell identity with a list of Voronoi cells that intersects the grid cell. Figure 5.3 depicts an 8×8 grid structure for the Voronoi diagram given in Figure 5.2a and the corresponding *mapping table*. For example, given a grid cell identity $C(5, 1)$, we can retrieve a set of Voronoi cells that intersects $C(5, 1)$, i.e., V_2, V_3, and V_5.

Step 2: ***Merge step.*** This step merges quadtree-like neighbor cells to their parent if they intersect the same set of Voronoi cells. The idea of this step is to adaptively determine the height of an *incomplete pyramid structure* for a Voronoi diagram to minimize search time. This is due to the fact that the t Voronoi diagrams we maintain have different structures, e.g., the number of Voronoi cells and Voronoi cell size distribution, with respect to the number of objects, the object distribution and the degree of order (t). Thus, the shape of an *incomplete pyramid structure* would be different for each computed Voronoi diagram. Other than the base level, each cell $C(l, c, r)$ at upper levels is identified by the level of the *incomplete pyramid structure* l, column number c and row number r. This step uses a bottom-up approach to construct the upper levels of an *incomplete pyramid structure*. Starting from the base level, if all quadtree-like sibling cells (i.e., the cells have the same parent) intersect the same set of Voronoi cells, they are merged to their parent. The merge process includes three tasks, (i) adding an entry that associates the parent cell identity with the set of intersected Voronoi cells

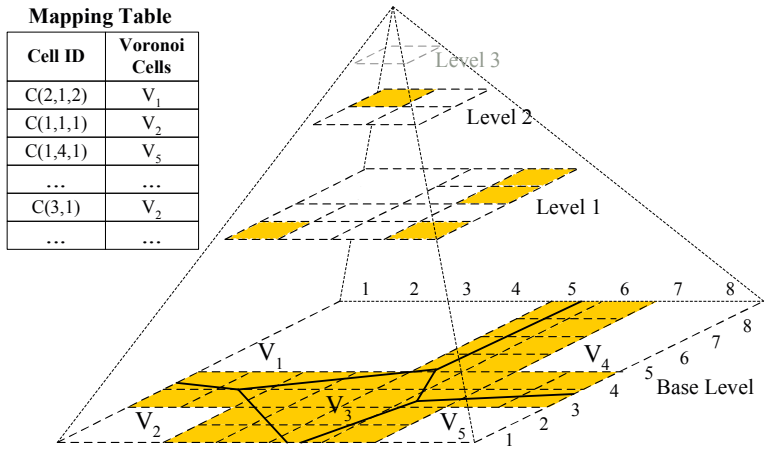

Figure 5.4: Incomplete pyramid structure.

of its children to the *mapping table*, (2) removing the entries of the merged child cells from the *mapping table*, and (3) annihilating the merged child cells by removing their pointers at their parent.

Figure 5.4 depicts an *incomplete pyramid structure* with a *mapping table* for the base level given in Figure 5.3, where the underlying Voronoi diagram is shown at the base level for the sake of illustration. Starting from the base level, we merge the quadtree-like sibling cells to their parent if they intersect the same set of Voronoi cells. For example, the four cells at the left bottom corner ($C(1,1)$, $C(2,1)$, $C(1,2)$, and $C(2,2)$) intersect the same Voronoi cell V_2, these cells are merged to their parent. To complete the merge process, we add an entry with the parent identity $C(1,1,1)$ with the intersected Voronoi cell V_2 to the *mapping table*, remove the entries of the merged child cells from the *mapping table*, and annihilate the merged child cells. We illustrate merged child cells by removing the grid cells. Similarly, we merge the cells at the other corners. At level one, the sibling cells at the left top corner (i.e., $C(1,1,3)$, $C(1,2,3)$, $C(1,1,4)$, and $C(1,2,4)$) intersect the same Voronoi cell V_1, so they are merged to their parent at level two, i.e., $C(2,1,2)$. At level two, since all cells intersect different sets of Voronoi cells, we cannot merge any cells and this step terminates. In this example, the shaded cells depict the lowest maintained cells of the *incomplete pyramid structure*, and there is an entry for each shaded cell in the *mapping table*. The height of the *incomplete pyramid structure* is two.

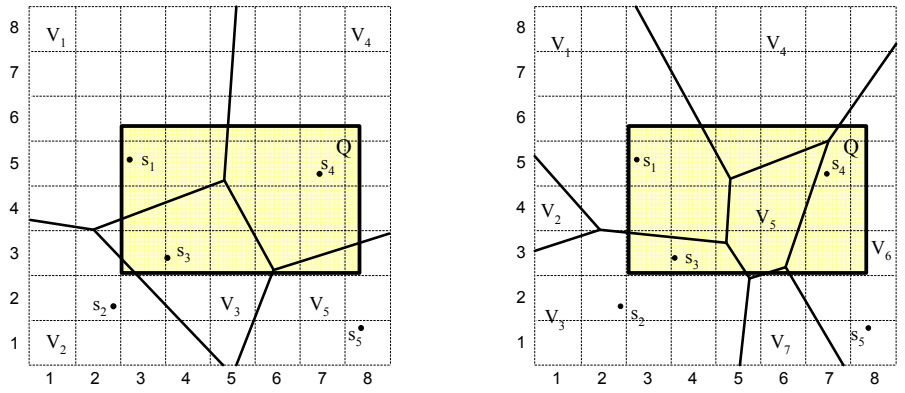

(a) Voronoi diagram (b) 2-order Voronoi diagram

Figure 5.5: Range NN query processing using Voronoi diagrams.

5.2.3 Online Query Processing Algorithm

The distinct feature of our proposed approximate range NN query processing algorithm is to enable the user to specify an approximation tolerance t for a range NN query, so that we provide a minimal answer set $\mathcal{A}$ where each object is guaranteed to be one of the t nearest objects to every point in the query region. If $t = 1$, we return an exact answer set with the maximal size to the user. In the case that $t > 1$, we return an approximate answer set with a smaller size than the exact one to the user; and thus, the transmission time of the answer set is reduced. The input of our proposed algorithm is a range NN query Q, a user specified approximation tolerance level t, and a t-order Voronoi diagram that is pre-computed by an off-line process (as described in Section 5.2.1). Figure 7.5 depicts a running example for our proposed algorithm where the query region of the input range NN query Q is represented as a bold rectangle and the maximum approximation tolerance level t_{max} is two. The algorithm consists of two key steps, *range search* step (Section 5.2.3) and *query-covering* step (Section 5.2.3).

Range Search Step

In this step, we retrieve a set of Voronoi cells $\mathcal{V}_t = \{V_1, V_2, \ldots, V_n\}$ that intersects the query region $Q.R$ and each Voronoi cell in $\mathcal{V}_t$ associates with t objects, i.e., $V_i = \{s_{i_1}, \ldots, s_{i_t}\}$ $(1 \leq i \leq n)$. We use a top-down approach to traverse an *incomplete*

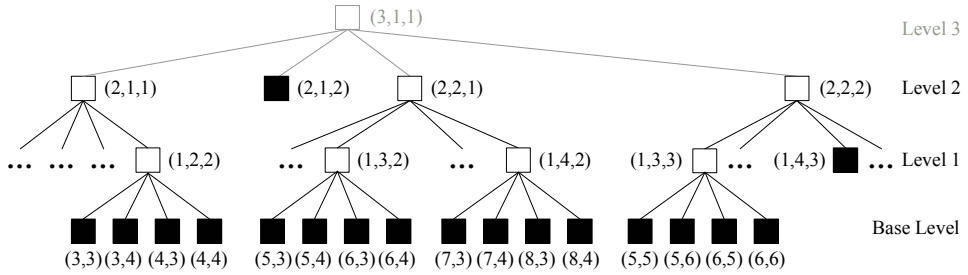

Figure 5.6: Example of a range search in the incomplete pyramid structure (Figure 5.4).

pyramid structure. Initially, at the highest maintained level of the *incomplete pyramid structure* of the t-order Voronoi diagram, we find a set of grid cells that intersects $Q.R$, and then recursively search each of these grid cells. During a recursive search, if an encountered grid cell C that intersects $Q.R$ is at the lowest maintained level or base level of the *incomplete pyramid structure*, we retrieve the set of Voronoi cells that intersects C from the *mapping table*, and then return it. Otherwise, we recursively search the four child cells of C.

Figure 5.6 illustrates the *range search* step for the running example depicted in Figure 7.5a where $t = 1$. For the sake of illustration, we only show the grid cells intersecting the query region $Q.R$, and the grid cells at the lowest maintained level or base level of the *incomplete pyramid structure* (as depicted in Figure 5.4) are represented shaded nodes. As shown in Figure 5.4, the highest maintained level of the *incomplete pyramid structure* is level two where we start the *range search* step. Since all grid cells at level two, i.e., $C(2,1,1)$, $C(2,1,2)$, $C(2,2,1)$ and $C(2,2,2)$, intersect $Q.R$, we will recursively search these grid cells. For $C(2,1,1)$, only one child cell $C(1,2,2)$ intersects $Q.R$, so we search their child cells $C(3,3)$, $C(3,4)$, $C(4,3)$, and $C(4,4)$ at the base level. Since all these child cells intersect $Q.R$, we retrieve the Voronoi cells that intersect them from the *mapping table* and return the set of retrieved Voronoi cells. As $C(2,1,2)$ is at the lowest maintained level, we retrieve the Voronoi cells that intersects $C(2,1,2)$ from the *mapping table* without further search. Then, we search the grid cell $C(2,2,1)$ where it has two child cells $C(1,3,2)$ and $C(1,4,2)$ intersecting $Q.R$. Since all child cells of $C(1,3,2)$ and $C(1,4,2)$ at the base level intersect $Q.R$, we retrieve the Voronoi cells that intersect them from the *mapping table* and return the retrieved Voronoi cells. Similarly, we search the grid cell $C(2,2,2)$. As a result, the set of Voronoi cells that

Algorithm 4 Query-Covering Step

```
1: function QueryCovering (RNNQuery Q, ToleranceLevel t, VoronoiCellSet V_t)
2: AnswerSet A ← {∅}
3: Construct an inverted list of V_t, i.e., L(V_t) = {L(s_1), L(s_2), ..., L(s_m)}, where
   L(s_i) = {V_{i_1}, V_{i_2}, ..., V_{i_|L(s_i)|}} and 1 ≤ i ≤ m
4: while L(V_t) ≠ {∅} do
5:    Select the object s_i ∈ L(V_t) with the largest |L(s_i)|
6:    for each object s_j ∈ L(V_t) (i ≠ j) do
7:       L(s_j) ← L(s_j) − L(s_i)
8:       if L(s_j) = {∅} then
9:          L(V_t) ← L(V_t) − {L(s_j)}
10:      end if
11:   end for
12:   A ← A ∪ {s_i}
13:   L(V_t) ← L(V_t) − {L(s_i)}
14: end while
15: return A
```

intersects $Q.R$ is $\mathcal{V}_1 = \{V_1, V_2, V_3, V_4, V_5\}$. For the other running example where $t = 2$, the *range search* step searches the *incomplete pyramid structure* of the 2-order Voronoi diagram and the set of Voronoi cells that intersects $Q.R$ is $\mathcal{V}_2 = \{V_1, V_3, V_4, V_5, V_6, V_7\}$.

Query-Covering Step

Algorithm 4 gives the pseudo code of this step where we aim to compute the minimal set of objects in which each object is one of the t nearest objects to every point in the query region $Q.R$. First, we construct an inverted list of the set of Voronoi cells $\mathcal{V}_t$ retrieved from the previous step, $\mathcal{L}(\mathcal{V}_t)$ (Line 3). In the inverted list $\mathcal{L}(\mathcal{V}_t)$, each object s_i has a list of Voronoi cells $L(s_i) = \{V_{i_1}, \ldots, V_{i_m}\}$ $(m \leq n)$, where s_i is associated with V_{i_j} $(1 \leq j \leq m)$.

Figure 5.7a depicts the inverted list of our running example for $t = 1$, as given in Figure 7.5a, where the Voronoi cells in $\mathcal{V}_1$ with their associated objects retrieved from the *range search* step are $V_1 = \{s_1\}$, $V_2 = \{s_2\}$, $V_3 = \{s_3\}$, $V_4 = \{s_4\}$, and $V_5 = \{s_5\}$. The inverted list of $\mathcal{V}_1$ is $\mathcal{L}(\mathcal{V}_1) = \{L(s_1) = \{V_1\}, L(s_2) = \{V_2\}, L(s_3) = \{V_3\}, L(s_4) = \{V_4\}, L(s_5) = \{V_5\}\}$. On the other hand, Figure 5.7b depicts the inverted list of our running example for $t = 2$, as shown in Figure 7.5b where the Voronoi cells in $\mathcal{V}_2$

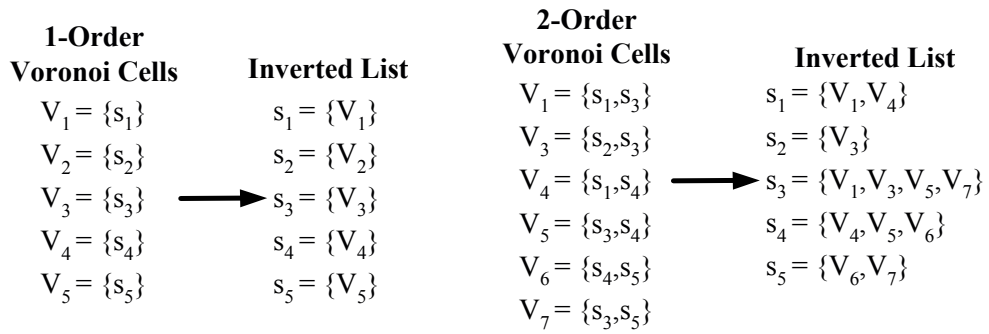

(a) Voronoi cell set $\mathcal{V}_1$ (b) Voronoi cell set $\mathcal{V}_2$

Figure 5.7: Inverted lists.

with their associated objects retrieved from the *range search* step are $V_1 = \{s_1, s_3\}$, $V_3 = \{s_2, s_3\}$, $V_4 = \{s_1, s_4\}$, $V_5 = \{s_3, s_4\}$, $V_6 = \{s_4, s_5\}$, and $V_7 = \{s_3, s_5\}$. The inverted list of $\mathcal{V}_2$ is $\mathcal{L}(\mathcal{V}_2) = \{L(s_1) = \{V_1, V_4\}, L(s_2) = \{V_3\}, L(s_3) = \{V_1, V_3, V_5, V_7\}, L(s_4) = \{V_4, V_5, V_6\}, L(s_5) = \{V_6, V_7\}\}$.

After constructing the inverted list of $\mathcal{V}_t$, $\mathcal{L}(\mathcal{V}_t)$, our objective is to select the minimal set of objects from $\mathcal{L}(\mathcal{V}_t)$ such that every Voronoi cell in $\mathcal{V}_t$ has at least one associated object selected in the answer set. In other words, we consider the items in the inverted list as sets and the Voronoi cells in $\mathcal{V}_t$ as elements, and then select a minimum number of sets so that the selected sets contain all the elements that are contained in any of the sets in the inverted list. Thus, our problem can be reduced to a well-known *set-covering problem*. Since computing the optimal solution for the set-covering problem is NP-hard [99], we use a greedy approach to compute an answer set. Basically, the greedy approach selects an object with the largest set of Voronoi cells, and then remove the Voronoi cells associated with the selected object from other objects' lists. Then, the selected object and the objects with an empty list are removed from the inverted list. We repeat this procedure until the inverted list is empty (Lines 4 to 14 in Algorithm 4). The set of selected objects is returned as the answer set to the user.

In our running example for $t = 1$, i.e., the user wants to have an exact query answer, the *query-covering* step simply add all objects in the inverted list $\mathcal{L}(\mathcal{V}_1)$ (Figure 5.7a) to the answer set, i.e., $\mathcal{A}_1 = \{s_1, s_2, s_3, s_4, s_5\}$. On the other hand, Figure 5.8 depicts the *query-covering* step for our running example for $t = 2$, based on the inverted list of

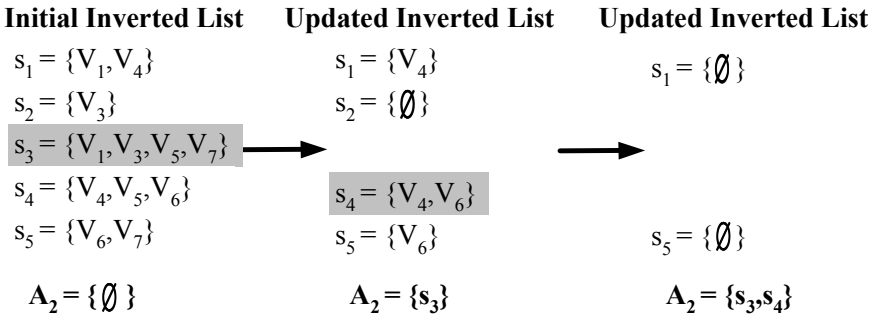

Figure 5.8: Example of the query-covering step, based on Figure 5.7b.

$\mathcal{V}_2$, $\mathcal{L}(\mathcal{V}_2)$, as given in Figure 5.7b. Since $L(s_3)$ has the largest size, we select s_3 and remove the Voronoi cells in $L(s_3)$, i.e., V_1, V_3, V_5, and V_7, from other objects' lists, i.e., $L(s_1)$, $L(s_2)$, $L(s_4)$, and $L(s_5)$. Then, we add s_3 to an answer set $\mathcal{A}_2$ and remove $L(s_3)$ from $\mathcal{L}(\mathcal{V}_2)$. The updated inverted list is $\mathcal{L}(\mathcal{V}_2) = \{L(s_1) = \{V_4\}, L(s_2) = \{\emptyset\}, L(s_4) = \{V_4, V_6\}, L(s_5) = \{V_6\}\}$. After we remove the empty list $L(s_2)$ from $\mathcal{L}(\mathcal{V}_2)$, $L(s_4)$ has the largest size. Thus, we select s_4 and remove the Voronoi cells in $L(s_4)$, i.e., V_4 and V_6, from other objects' lists, i.e., $L(s_1)$ and $L(s_5)$. Then, we add s_4 to $\mathcal{A}_2$ and remove $L(s_4)$ from $\mathcal{L}(\mathcal{V}_2)$. The updated inverted list is $\mathcal{L}(\mathcal{V}_2) = \{L(s_1) = \{\emptyset\}$ and $L(s_5) = \{\emptyset\}\}$. Since all lists are empty, they are removed from the inverted list, and the *query-covering* step terminates and returns the answer set $\mathcal{A}_2 = \{s_3, s_4\}$ to the user. From this example, we can see that our proposed approximate range NN query processing algorithm reduces the answer set size by 60%, i.e., from five objects in the exact answer set to two objects in the approximate answer set.

5.3 Experimental Results

In this section, we evaluate our Approximate Range nearest-neighbor (NN) query processing algorithm (denoted as ARNN) with respect to user specified approximation tolerance levels (t), query region size, the number of objects, downlink bandwidth, and object size. We compare our ARNN algorithm with two state-of-the-art range NN query processing algorithms as baseline algorithms. The first baseline algorithm computes an exact answer set of the minimal size for range NN queries (denoted as Exact) [80], while the other baseline algorithm computes a candidate answer set that contains the exact

Table 5.1: Parameter settings.

Parameter	Default Value	Range
Approximation tolerance (t)	4	1 to 10
Number of objects	200	100 to 300
Query region size	$(0.05l)^2$	$(0.008l)^2$ to $(0.256l)^2$ (where $l = 1000$)
Downlink bandwidth	384 kbps	128 kbps to 2 Mbps
Object size	10 Kbytes	0.5 Kbytes to 20 Kbytes

answer for range NN queries (denoted as Casper) [12].

We have two performance measures: (1) *total processing time* that includes the query processing time at the database server and the transmission time of sending the answer set to the user, and (2) *answer set size* that is the average number of objects returned in the answer sets. The *answer set size* is important as it indicates communication overhead and the power consumed by the user device to receive the answer set and user convenience.

In all experiments, we assume that the user communicates with a database server through a 3G cellular network. The downlink (i.e., from the database server to the user) bandwidth varies with respect to the user mobility speed, i.e., 128 kbps (i.e., kbits per second) at vehicular speeds, 384 kbps at pedestrian speeds, 2 Mbps at stationary or very slow movement speeds. Unless mentioned otherwise, the experiments consider 200 objects in a square space of a length $l = 1000$. The mobile user moving at pedestrian speeds (i.e., the downlink bandwidth is 384 kbps) issues 1,000 range NN queries, and the object size is 10 Kbytes. The default user specified approximation tolerance level (t) is four and the query region size is $0.05l \times 0.05l$. Table 9.1 summarizes the parameter settings.

5.3.1 Effect of Approximation Tolerance Levels

Figure 9.10 depicts the performance of our proposed algorithm (ARNN) with respect to varying the approximation tolerance level (t) from 1 to 10. The performance of the baseline algorithms (Casper and Exact) is not affected by varying the value of t. Figure 9.10a gives the number of objects returned in the answer set, while Figure 9.10b indicates the total processing time that includes the query processing time at the database server and

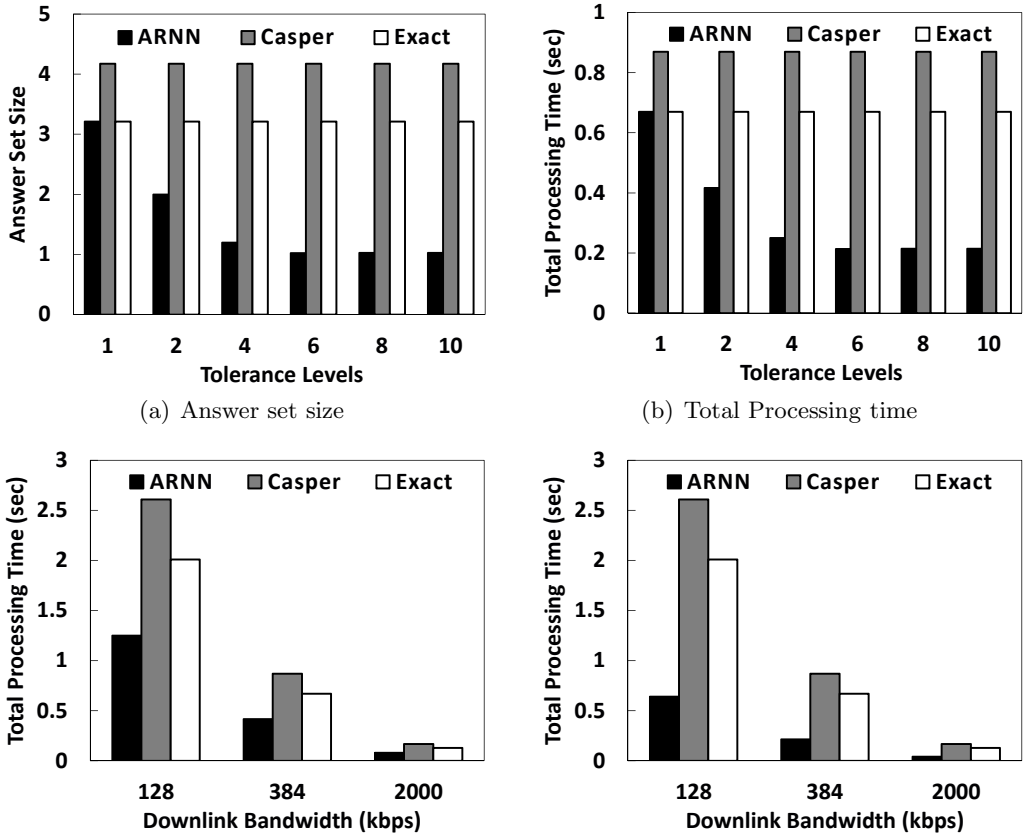

(a) Answer set size

(b) Total Processing time

(c) Tolerance level: $t = 2$

(d) Tolerance level: $t = 10$

Figure 5.9: Approximation tolerance levels (t).

the transmission time of sending the answer set to the user. Figure 9.10a shows that ARNN effectively reduces the answer set size as t gets larger. When $t = 2$ ($t = 10$), ARNN reduces the size of the answer sets given by Casper and Exact by 34.3% and 66% (79.3% and 89.3%), respectively. Since the transmission time is much higher than the total processing time, the total processing time of ARNN decreases as t gets larger (Figure 9.10b). Figures 9.10c and 9.10d show that ARNN performs better than the baseline algorithms for all mobility speeds. Since ARNN effectively reduces the answer set size, when the downlink bandwidth is more limited, ARNN performs much better than Casper and Exact.

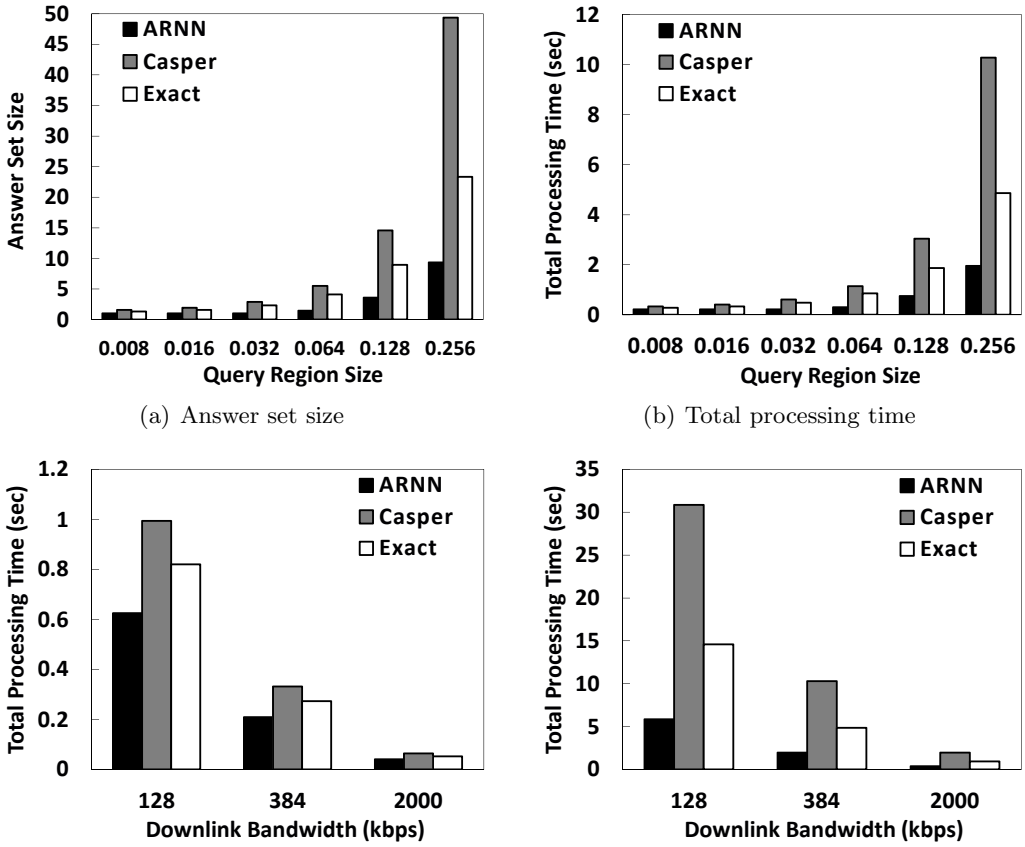

(a) Answer set size

(b) Total processing time

(c) Query region size: $(0.008l)^2$

(d) Query region size: $(0.256l)^2$

Figure 5.10: Query region size.

5.3.2 Effect of Query Region Size

Figure 5.10 depicts the performance of our proposed algorithm (ARNN) with respect to increasing the query region size from $(0.008l)^2$ to $(0.256l)^2$, where $l = 1000$. Figure 5.10a shows that the answer set of all algorithms gets larger as the query region size increases. With small query regions, i.e., $(0.008l)^2$, the answer set size of ARNN is 94.7% and 59.8% smaller than Casper and Exact, respectively. For large query regions, i.e., $(0.256l)^2$, the answer set size of ARNN is 442.1% and 145.3% smaller than Casper and Exact, respectively. Thus, ARNN performs much better than the baseline algorithms for larger query regions. Since the transmission time is much higher than the total processing time, ARNN outperforms the baseline algorithms in terms of query response

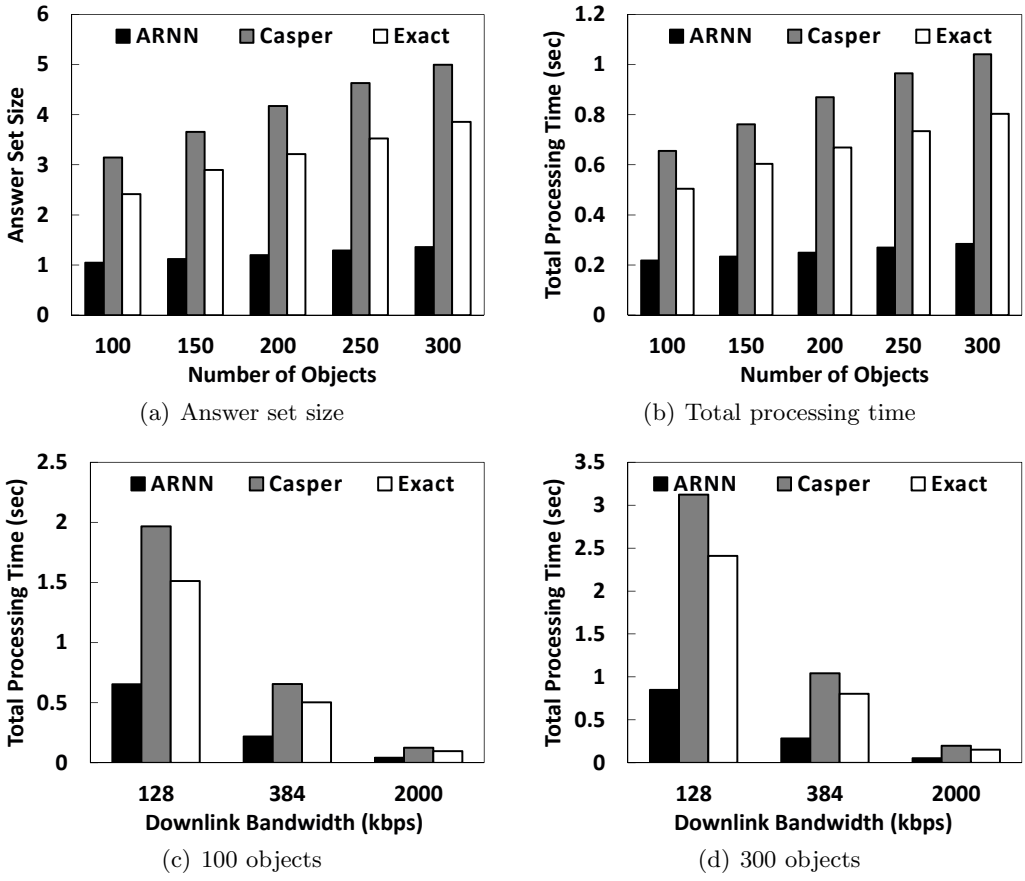

(a) Answer set size

(b) Total processing time

(c) 100 objects

(d) 300 objects

Figure 5.11: Number of objects.

time (Figure 5.10b). Figures 5.10c and 5.10d depict that ARNN effectively reduces the total processing time of the baseline algorithms regardless of user mobility speeds.

5.3.3 Effect of Number of Objects

Figure 5.11 gives the performance of our proposed algorithm (ARNN) with respect to varying the number of objects from 100 to 300. When the number of objects increases, there are more nearest objects to the query region; and thus, the answer set size of all algorithms gets larger (Figures 5.11a). Similar to the previous experiments, the transmission time is much higher than the total processing time. Since the answer set size of ARNN is smaller than the baseline algorithms Casper and Exact, ARNN incurs the

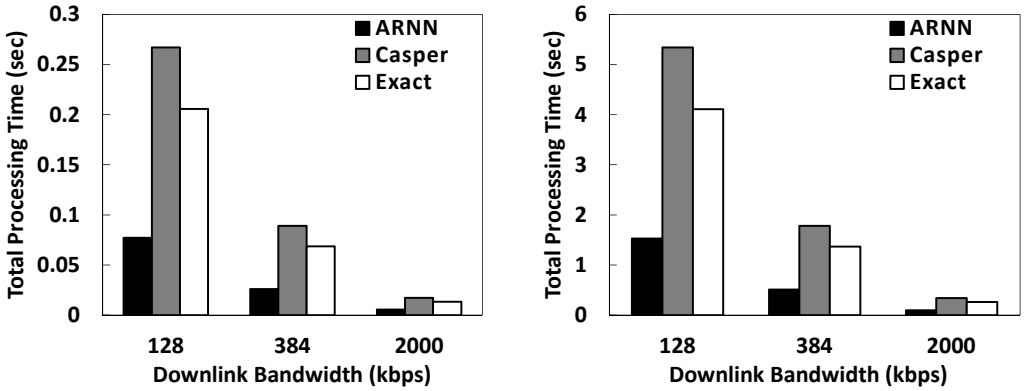

(a) 0.5 KB (b) 20 KB

Figure 5.12: Object size.

lowest total processing time for any number of objects (Figures 5.11b). Likewise, ARNN effectively reduces the answer set size, the total processing time of ARNN is better than Casper and Exact for all user mobility speeds, as depicted in Figures 5.11c and 5.11d.

5.3.4 Effect of Object Size

Figure 5.12 depicts the performance of our proposed algorithm (ARNN) with respect to the object size of 0.5 and 20 Kbytes. Since varying the object size does not affect the answer set size, the answer set size of all algorithms is the same as the case that $t = 4$ in Figure 9.10a. It is interesting to see that the transmission time is much higher than the total processing time even if the object size is small and the answer set is sent to the user through the downlink with the largest possible bandwidth, i.e., 2 Mbps. Therefore, the results indicate that reducing the answer set size is an effective way to improve query response time. This is the motivation of our proposed algorithm ARNN that aims to minimize the answer set size while guaranteeing that the answer set is satisfied with the user specified approximation tolerance level t.

5.3.5 Effect of Communication Bandwidth

Figures 5.13 and 5.14 give the comprehensive evaluation of our proposed algorithm (ARNN) with respect to all parameters for users moving at vehicular speeds and very slow speeds, respectively. Although Casper gives the best query processing time, it

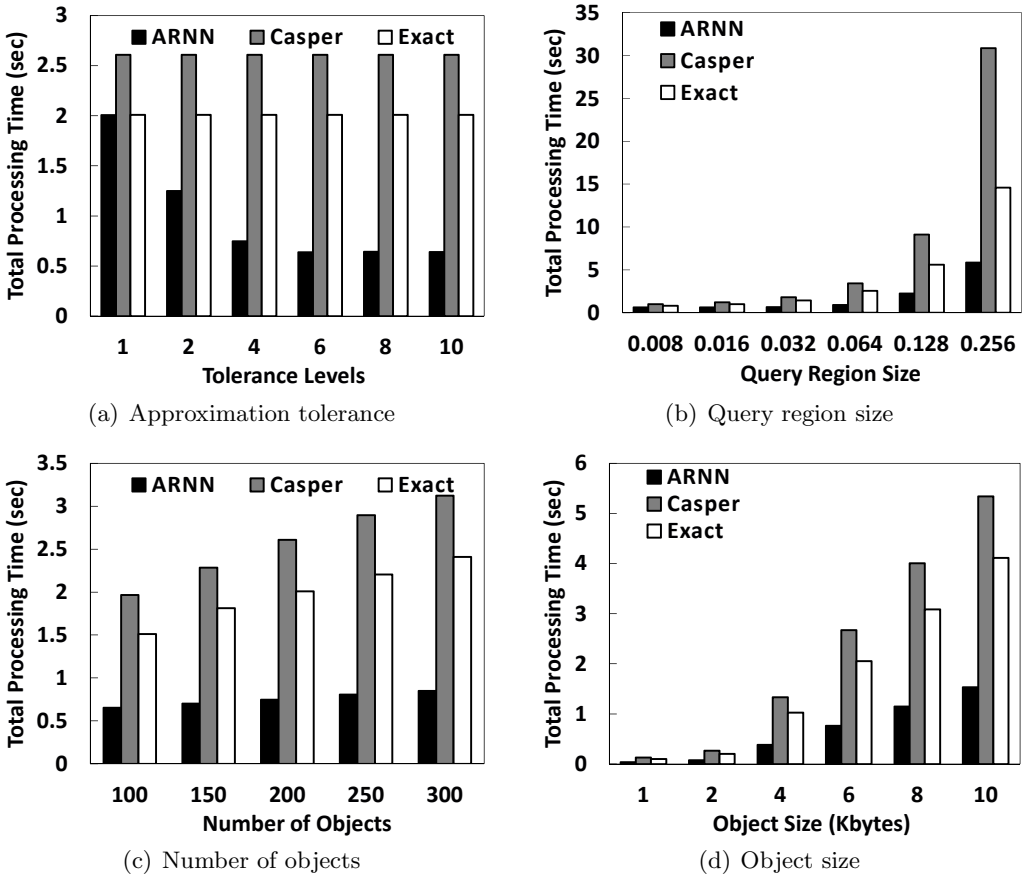

(a) Approximation tolerance

(b) Query region size

(c) Number of objects

(d) Object size

Figure 5.13: Downlink bandwidth at vehicular speeds (128 kbps).

suffers from very high transmission time. This is because the candidate answer set provided by Casper is much larger than the answer set of ARNN and Exact. Thus, the total processing time of Casper is always worse than ARNN and Exact. Since ARNN provides approximate answers that satisfy the user specified approximation tolerance level, the answer set size of ARNN is smaller than the exact answer set provided by Exact. As a result, ARNN performs better than Casper and Exact in terms of the total processing time for all parameter settings.

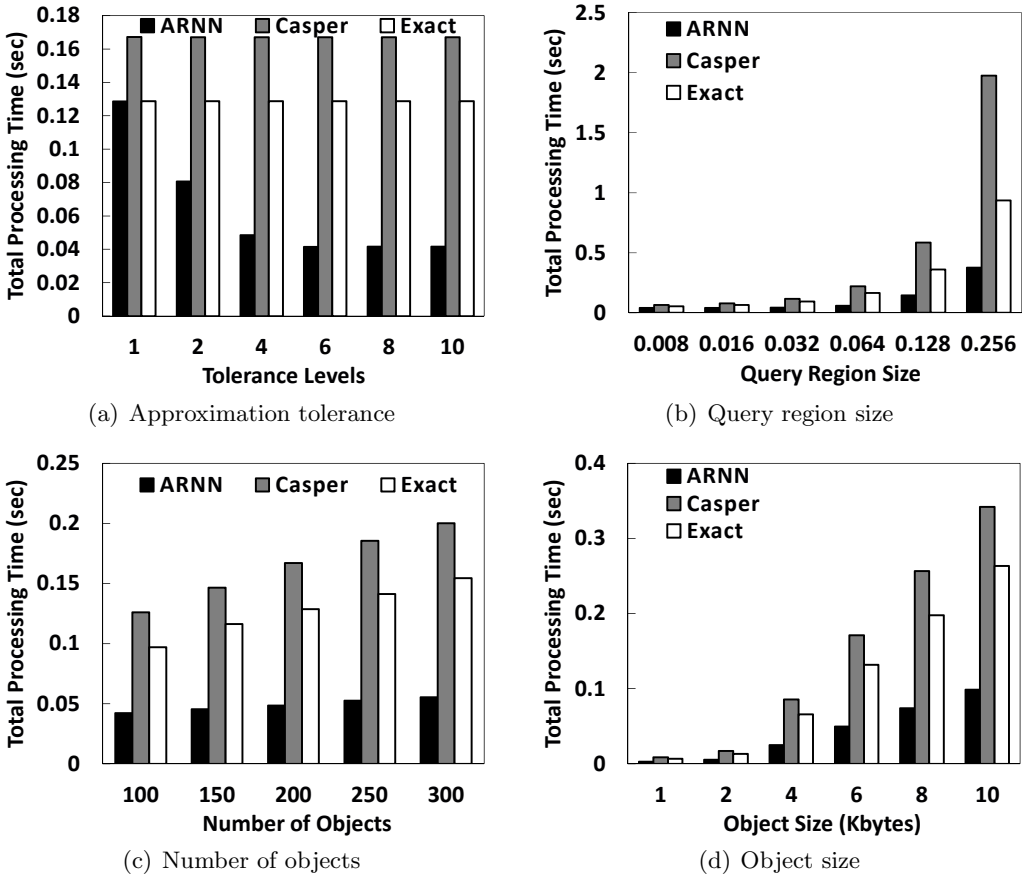

(a) Approximation tolerance

(b) Query region size

(c) Number of objects

(d) Object size

Figure 5.14: Downlink bandwidth at stationary or very slow speeds (2 Mbps).

5.4 Summary

In this chapter, we present a new query type, *approximate range nearest-neighbor (NN) query*, for location-based services. The distinct features of this new query type are that (1) It aims to minimize the number of objects returned to the user so as to reduce the transmission time of sending the answer to the user; and (2) It provides quality guarantee for the query answer, i.e., each object in an answer set is one of the t nearest objects to every point in a given query region, where t is a user specified tuning parameter for a tradeoff between query response time (that is dominated by transmission time as shown in all experimental results) and the quality of answers. To achieve these two features, we propose an *approximate range NN query processing* algorithm. The main idea is to

have an *off-line* process to compute Voronoi diagrams, from order one to order t_{max}, where t_{max} is the maximum allowable user specified approximation tolerance level, and then build our proposed *incomplete pyramid structure* as an access method for each Voronoi diagram. Given a range NN query and an approximation tolerance level t, our *on-line* query processing algorithm accesses the *incomplete pyramid structure* of the t-order Voronoi diagram to retrieve a set of Voronoi cells that intersects the query region and the t nearest objects to each Voronoi cell. Then, the remaining query processing is reduced to a set-covering problem where we use a greedy approach to find a minimal answer set. Extensive experimental results show that our proposed algorithm is scalable in terms of query processing time, and effective to reduce query response time compared with the state-of-the-art techniques while guaranteeing that the answer set satisfies the user desired approximation tolerance level.

Chapter 6

Query-Aware Location Anonymization in Road Networks

In this chapter, we extend the functionalities of the Casper system, i.e., the *location anonymizer* and the *privacy-aware query processor*, in road network environments. Several techniques are proposed to anonymize the user location information through *false locations* (e.g., [43, 45, 81]), *space transformation* (e.g., [78, 79]), or *spatial cloaking* (e.g., [32, 34, 33, 19, 35, 36, 38, 39, 37, 23, 44, 12, 47, 48]). This chapter focuses on the spatial cloaking technique as it is the most commonly used technique and is applicable to various problem settings (e.g., distributed/peer-to-peer environments [19, 38, 39], sensor networks [23], trajectories [48], and continuous queries [33, 47]).

Unfortunately, almost all previously proposed location anonymization techniques suffer from two main drawbacks: (1) The location anonymization process is designed completely independent from the underlying query processor. As a result, some of these techniques may end up anonymizing the user location to an extent where it is either very inefficient to execute a location-based query as a large number of queries need to be sent to the server [45, 81] or specialized query processing techniques need to be developed [78, 44, 79, 12]. (2) All techniques are designed only for the Euclidean space. Applying these techniques to the road network environment results in privacy leakage. Figure 6.1a depicts such a case where user q needs to be four anonymous with a cloaked area of at least four grid cells. The gray area represents the cloaked area that could

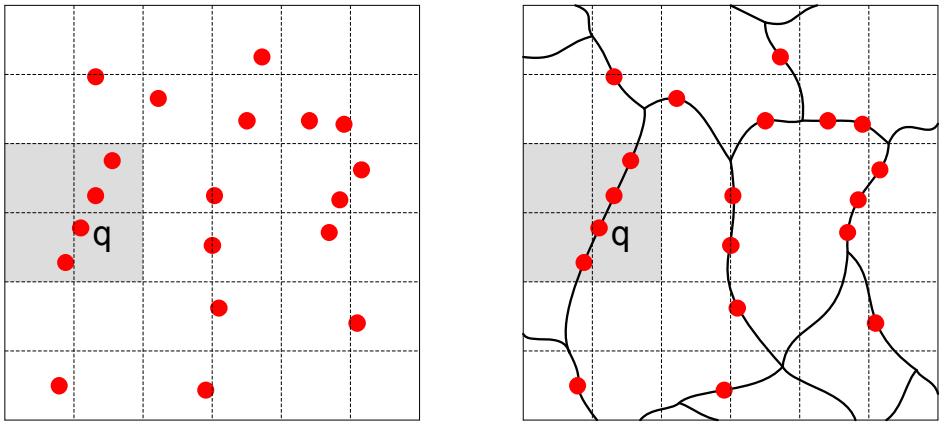

(a) Euclidean Space (b) Road Network

Figure 6.1: Spatial cloaking for the Euclidean space.

be provided by a location anonymization technique designed for the Euclidean space (e.g., [32, 36, 37, 44, 12]). With such a cloaked area, an adversary knows that the user can be anywhere in the gray area. Figure 6.1b shows the same example with the drawing of the underlying road network. Since all the four users are in the same road segment, an adversary can pinpoint the exact road segment of user q. Thus, the cloaked area violates the area privacy requirement, i.e., the user cannot be anywhere in the cloaked area, as the user has to be in a single road segment only. The only previous work that addresses location privacy in a road network [100] suffers from the same drawbacks as it solely relies on using an Euclidean-based anonymization technique while considering the road network in the query processing only.

In this chapter, we overcome the above two main drawbacks by proposing a new location anonymization algorithm that (a) is designed specifically for the road network environment, and (b) not only aims to satisfy the user privacy requirements, but it is also "query-aware" as it aims to balance between the query execution cost and the quality of services that we can get from the server. The main idea of our proposed "query-aware" location anonymization technique is to blur a user location into a cloaked set of connected road segments S such that S satisfies the user specified privacy requirements, k-anonymity and minimum length L_{min}. The k-anonymity requirement indicates include at least k users while the minimum length l length L_{min} requirement indicates

that the total length of in S must be at least l. As the database server only database server only knows about a cloaked segment set S as a user's location information, it has to compute an answer set A includes the exact query answer should the user be anywhere within S. The smaller the size of the returned answer set A, the better quality the server will provide. Thus, the quality of services is measured by the size of the returned answer set. To achieve our goals, we design a new objective cost function that encapsulates the query execution cost for both $\mathcal{K}$-nearest-neighbor and range queries with the answer quality. Then, the objective of our road network location anonymization algorithm boils down to finding a cloaked set of road segments S that minimizes our developed objective cost function while satisfying the user privacy requirements.

We present two versions of our proposed location anonymization algorithm. The first version is a *pure greedy* approach where we repeatedly select road segments to be included in a cloaked segment set S based on minimizing our developed objective cost function. Although the pure greedy approach is simple and efficient, its deterministic property may suffer from a reverse engineering attack where an adversary may crack the system to know the objective cost function. To avoid such an attack, we propose another version of our algorithm, termed *randomized greedy* approach, where we inject some randomness into the greedy approach. To accommodate for cases of high workloads, e.g., traffic congestions and rush hours, we propose a *shared execution* paradigm that boosts the system scalability in terms of supporting large numbers of queries received within a short time period. The main idea of the shared execution paradigm is to maximize the number of shared road segments among the users' cloaked segment sets. By doing so, location-based queries at the shared road segments will be executed only once for multiple queries.

6.1 System Model

In this section, we first give the preliminaries of this paper. Then, we describe the underlying system architecture that consists of three main entities, mobile users, location anonymizer, and location-based database server.

Preliminaries. The proposed location anonymization algorithm mainly blurs a user's location into ***a cloaked set of road segments*** S that is defined as a set of

connected road segments where the requesting user is residing therein, such that S satisfies the user specified privacy requirements. In a cloaked set S, a vertex v is a ***closed vertex*** if all edges connected to v are included in S; otherwise, v is an ***open vertex***. The underlying road network is modeled as a connected graph $G = (V, E)$, where V is a vertex set that represents the intersection and endpoints of the road segments, while E is an edge set that represents the road segments.

Mobile users/privacy requirements. Mobile users register with the system by specifying their personalized privacy requirements, i.e., *k-anonymity* and *minimum length* L_{min}. k-anonymity privacy requirement indicates user wants to be k-anonymous, i.e., indistinguishable among k users. The minimum length privacy requirement L_{min} indicates that the minimum resolution of the blurred location the total length of the road segments in S is at least . Thus, a user's location must be blurred into a cloaked set a cloaked set S that contains at least k users and the total length of the road segments in S is at least L_{min}.

Location anonymizer. The location anonymizer is a trusted third party placed between *mobile users* and the *location-based database server*. We assume that the location anonymizer is placed at some cellular service provider through which the *mobile users* have access to location-based service providers. Furthermore, the location anonymizer maintains an *edge table* that is a hash-table on edge ID [67]. For each edge e, the tuple in the *edge table* stores (a) its endpoints, (b) its length, (c) the set of edges connected to each of its endpoints, and (d) the list of objects currently residing in e. Basically, the location anonymizer blurs the location information of a user's query into a cloaked set of road segments S such that S satisfies the user's privacy requirements. While *blurring* the location information, the location anonymizer also removes any user identity to ensure the pseudonymity of the location information [9]. Then, the location anonymizer sends the anonymized query with the cloaked segment set to the database server. After the location anonymizer gets a *candidate answer set* from the database server, it computes the exact answer from the candidate answer set and sends the exact answer to the user.

Location-based database server. The location-based database server is placed at an untrustworthy service provider and has the capacity to deal with private queries along with cloaked sets of road segments. Since the private queries can be easily boiled down to traditional $\mathcal{K}$-nearest-neighbor ($\mathcal{K}$-NN) and range queries (described in Section 6.2), the

query processor embedded inside the database server only needs to employ any existing $\mathcal{K}$-NN and range query algorithms designed for road networks (e.g., [101, 102, 103]). Furthermore, the database server also maintains an *edge table* as in the location anonymizer. Instead of returning an exact answer, the database server returns a candidate answer set that is guaranteed to contain the exact answer to the location anonymizer regardless of the exact user location within the given cloaked segment set S.

6.2 Cost Model for Private Queries

This section develops the cost model for both private $\mathcal{K}$-nearest-neighbor ($\mathcal{K}$-NN) and range queries. This cost model will be used later by the location anonymizer (Section 6.3) to find a cloaked set of road segments S that balances between minimizing the developed cost function and the query answer quality while satisfying the user privacy requirements. Throughout this section, we use the following terminologies and assumptions: (a) We assume only an existing spatio-temporal query processor embedded inside the database server to deal with private $\mathcal{K}$-NN and range queries. Thus, the query processor can employ any existing $\mathcal{K}$-NN and range query processing algorithms designed for road networks (e.g., [101, 104, 102, 103]). (b) For any cloaked set of road segments S, we define two functions $V_o(S)$ and $E(S)$ that return the number of *open vertices* (i.e., vertices where some of its connected edges are not included in S) and the number of edges in S, respectively. (c) Without loss of generality, we assume that all $\mathcal{K}$-NN and range queries ask about the same type of target objects (e.g., gas stations, taxis, or restaurants). There are T such target objects and R road segments in the system. The information about the number of target objects is given by the database server as hints. For all vertices and edges in the road network, d and l represent the average degree of connectivity of a vertex v (i.e., the number of edges connected to v) and the average edge length, respectively.

6.2.1 Private $\mathcal{K}$-Nearest-Neighbor Queries

A typical example of a $\mathcal{K}$-nearest-neighbor ($\mathcal{K}$-NN) query is *"find the $\mathcal{K}$ nearest objects of my location $q = (x, y)$"*. However, with the anonymization process, the $\mathcal{K}$-NN query is transformed to a *private* one, i.e., *"find the $\mathcal{K}$ nearest objects of my location, given*

that my location is somewhere in a cloaked set of road segments S".

Algorithm. An algorithm for a *private* $\mathcal{K}$-NN query with a cloaked set of road segments S will find a candidate answer set where the exact answer of the original query is guaranteed to be in the candidate answer set regardless of the actual user location within S. To facilitate the development of the query cost model, given a cloaked set of road segments S, we divide the query processing algorithm of *private* $\mathcal{K}$-NN queries into two steps: (1) *Range Search Step.* In this step, we mainly execute a traditional range query of the form *"find all target objects located within the road segments in S"* where we add all target objects within S to the candidate answer set. (2) *External Search Step.* In this step, we mainly execute a traditional $\mathcal{K}$-NN query at each *open vertex* in S, i.e., *"find the closest $\mathcal{K}$ target objects to a vertex v"*, where we add the answers of these queries to the candidate answer set.

Thus, the execution of one *private* $\mathcal{K}$-NN query boils down to executing one *traditional* range query and a set of *traditional* $\mathcal{K}$-NN queries. Figure 6.2 depicts a *private* $\mathcal{K}$-NN query ($\mathcal{K} = 1$), where the actual query location Q is represented as a triangle located in edge v_4v_6. The cloaked segment set S of Q includes three edges v_3v_4, v_4v_6, and v_4v_9, one *closed vertex* v_4, and three *open vertices* v_3, v_6, and v_9. Figure 6.2a depicts the *range search step* where we add all target objects of the three edges in S, o_3 to o_7, to the candidate answer set. Figure 6.2b depicts the *external search step* where the nearest target object to each *open vertex* in S (enclosed in rectangles) is added to the candidate answer set. The nearest target object of the *open vertices* v_3, v_6, and v_9 are o_2, o_7, and o_8, respectively. As a result, the answer of the *private* $\mathcal{K}$-NN query is a candidate answer set that contains seven objects o_2 to o_8. Notice that the exact answer, according to the exact location of Q, is o_7 which is included in the candidate answer set.

Cost model. The execution cost of a *private* $\mathcal{K}$-NN query is the sum of the execution cost of the *range search* and *external search* steps. We will present the cost in terms of the number of edges whose information is retrieved through the *edge table* data structure as described in Section 6.1. For the *range search* step, we need to retrieve the information (i.e., target objects) of all edges in S. This step results in a straightforward cost of $E(S)$, i.e., the number of edges in S. For the *external search* step, we will first consider the cost of issuing a *traditional* $\mathcal{K}$-NN query at one *open vertex*. Without the knowledge

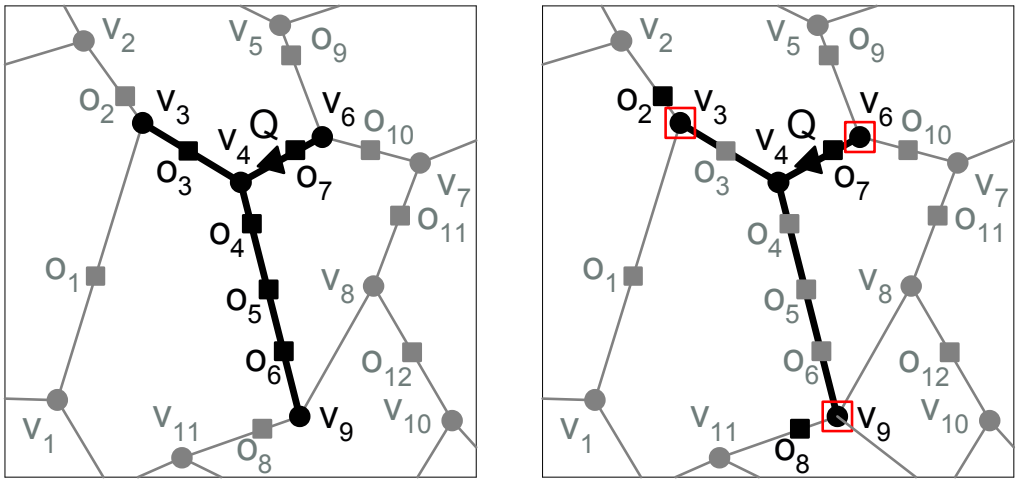

(a) Range Search Step (b) External Search Step

Figure 6.2: Private $\mathcal{K}$-nearest-neighbor query.

of the actual distribution of the target objects, we assume a uniform distribution of the T target objects over all the road segments R in the road network. Thus, we will need to search within R/T segments to find one closest target object to an *open vertex*. Thus, to find $\mathcal{K}$ nearest target objects, we need to retrieve the information of $R/T \times \mathcal{K}$ road segments, as we do the same for each *open vertex* in S. The total cost of the *external search* step is $V_o(S) \times R/T \times \mathcal{K}$, where $V_o(S)$ represents the number of *open vertices* in S. Thus, given a cloaked segment set S, the query execution cost of a *private* $\mathcal{K}$-NN query is:

$$Cost_{PKNN}(S, \mathcal{K}) = E(S) + V_o(S) \times R/T \times \mathcal{K}.$$

6.2.2 Private Range Queries

A typical example of a range query is *"find all target objects within a network range distance r of my location $q = (x, y)$"*. However, with the anonymization process, the range query is transformed into a *private* one, i.e., *"find all target objects within a network range distance r of my location, given that my location is somewhere in a cloaked set of road segments S"*.

Algorithm. Similar to the case of *private* $\mathcal{K}$-NN queries, an algorithm for a *private* range query consists of two steps: (1) *Range Search Step.* The target objects residing in the edges in S are added to the candidate answer set. (2) *External Search Step.* The target objects within a network range distance r from each *open vertex* in S are added to the candidate answer set. Thus, a *private* range query boils down to $V_o(S)+1$ *traditional* range queries.

Cost model. The execution cost of the *range search step* of a *private* range query is exactly the same as in the case of *private* $\mathcal{K}$-NN queries, i.e., $E(S)$. The execution cost of the *external search* step is the sum of the cost of finding the target objects within a network range distance r of each *open vertex* in S. For each *open vertex* in S, we need to expand the search to $\lceil r/l \rceil$ edges in all directions where l is the average edge length. Given that the average degree of connectivity of a vertex is d, then, approximately, we need to search a total of $\lceil r/l \rceil \times d$ road segments for each *open vertex* in S. Thus, given a cloaked set of road segments S, the query execution cost of a *private* range query is:

$$Cost_{PRange}(S, r) = E(S) + V_o(S) \times \lceil r/l \rceil \times d.$$

6.3 Query-Aware Anonymization

As we have indicated earlier, there are two main factors that control the quality of a cloaked set of road segments S, namely, the query execution cost and the answer quality. To realize the first factor, query execution cost, we will need to select S that satisfies the user privacy requirements while minimizing the query cost models that are developed in Section 6.2. On the other hand, to realize the second factor, the quality of answers, we need to select S that satisfies the user privacy requirements and has the number of users and length as close as possible to the anonymity k and minimum length L_{min} privacy requirements, respectively. The main idea is that the shorter the length of S, the smaller the size of the candidate answer set, and hence the better quality of answers the query processor will provide.

In this section, we start by showing that realizing any of these two important factors for S may significantly deteriorate the other factor (Section 6.3.1). Then, we develop an objective cost function that aims to balance these two desired factors, query execution

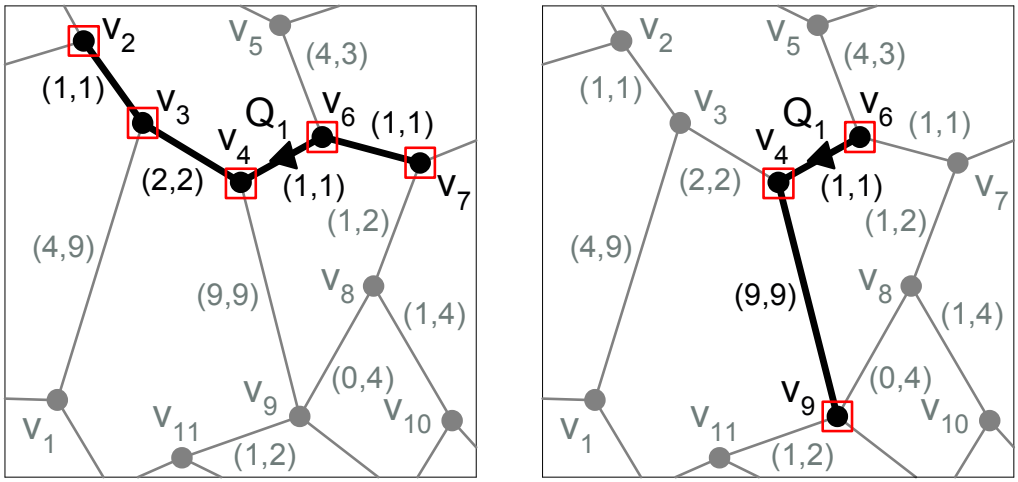

(a) Optimal Query Quality (b) Optimal Query Cost

Figure 6.3: A trade-off between query quality and cost.

cost and the quality of answers (Section 6.3.2). Finally, we propose two greedy-based anonymization approaches, namely, *pure greedy* and *randomized greedy*, that aim to find a cloaked set of road segments S that minimizes our developed objective cost function (Section 6.3.3).

6.3.1 Motivation: A Trade-off between Query Cost and Query Quality

Figure 6.3 gives a trade-off between query execution cost and query quality for a cloaked set of road segments S with privacy requirements $k = 5$ and $L_{min} = 5$. Each edge in the road network has a pair (a, b) where a indicates the number of users in that edge while b indicates the edge length. For example, the edge v_1v_3 has four users and of length nine. Figure 6.3a gives a cloaked segment set $S_q = \{v_2v_3, v_3v_4, v_4v_6, v_6v_7\}$ that is optimal in terms of query quality. In this case, S_q has the minimum possible length, i.e., $Length(S_q) = 5$, and the minimum possible number of users, i.e., $NumUser(S_q) = 5$. In terms of query execution cost, S_q has five *open vertices* (enclosed in rectangles) and four edges (represented as black lines), i.e., $V_o(S_q) = 5$ and $E(S_q) = 4$. On the other hand, Figure 6.3b gives a cloaked segment set $S_c = \{v_4v_6, v_4v_9\}$ that is optimal in terms of query execution cost as it is the one that has the minimum possible number of *open vertices*, i.e., $V_o(S_c) = 3$, and edges, i.e., $E(S_c) = 2$, while still satisfying the user privacy

requirements. However, S_c may result in very bad answer quality S_c is 10 which is way above the minimum length l privacy requirement.

From these examples, we can see that trying to find the optimal S_q, i.e., maximizing the query quality, results in having five *open vertices* and four edges (Figure 6.3a) which is 66.7% and 100% worse than what we can get from S_c (Figure 6.3b). On the other hand, trying to find the optimal S_c that gives the minimal query execution cost, i.e., the minimum possible number of *open vertices* and edges, results in the total segment length of 10 (Figure 6.3b) which is 100% worse than what we can get from S_q (Figure 6.3a). This raises the issue of finding an objective cost function that balances between query execution cost and query quality.

6.3.2 Objective Cost Function

As we have discussed in the previous section, we need an objective cost function that balances between query execution cost and query quality. The query execution cost is measured by the cost models described in Section 6.2. On the other hand, the query quality is measured by the number of candidate target objects returned by a database server given that the query location is within a cloaked set of road segments S. In general, the number of candidate target objects is proportional to the total length of the road segments in S. Thus, the objective cost function aims to find a cloaked segment set S, such that S not only satisfies the user privacy requirements, but it also minimizes the query execution cost and the total segment length.

Based on these contradicting requirements, we distinguish between two cases for the objective cost function based on whether the privacy requirements are achieved or not. If the privacy requirements are not yet met, we try to minimize the query execution cost while maximizing the number of users and total length of the road segments in S as this will increase the query quality. On the other hand, if only one of the privacy requirement is already met, we attempt to minimize the query execution cost and the total length of S as further increase of the total length of S will unnecessarily degrade the answer quality. Notice that in the second case, if k-anonymity privacy requirement is already met, we do not have to worry about the number of users in S as maximizing or minimizing the number of users will not affect the query quality. Then, we will discuss the incorporation of each privacy requirement in our proposed objective cost function.

For the k-anonymity privacy requirement, when this requirement is not yet met, we should select some edges that contain more users to S. For example, if adding edge e_i or e_j to S incurs the same query execution cost $QCost(S)$ that is computed by using the cost models described in Section 6.2, the objective cost function should give a smaller value to the edge containing more users; and thus, the objective cost function adjusts $QCost(S)$ by dividing it by a quality factor $NumUser(S)/k$. On the other hand, when the k-anonymity requirement is satisfied, the number of users in S does not affect the quality of answers, so the objective cost function no longer considers the k-anonymity privacy requirement.

For the minimum length L_{min} privacy requirement, if this requirement is not yet achieved, we should select some longer edges to S. Similar to the k-anonymity privacy requirement, the objective cost function adjusts $QCost(S)$ by dividing it by a quality factor $Length(S)/L_{min}$. On the other hand, if the minimum length privacy requirement is satisfied, the objective cost function gives a larger value to longer edges, i.e., dividing $QCost(S)$ by another quality factor $L_{min}/Length(S)$.

Since the quality factors of these two privacy requirements are normalized to the corresponding privacy requirement, we can encapsulate them in our objective cost function. Hence, the quality factor is:

$$Quality(S) = \min\left(\frac{NumUser(S)}{k}, 1\right) \times \min\left(\frac{Length(S)}{L}_{min}, \frac{L_{min}}{Length(S)}\right).$$

Therefore, for each edge e_i, we consider a new potential cloaked set of road segments $S = S \cup \{e_i\}$, and we calculate the objective cost $Cost(S, Q)$ as:

$$Cost(S, Q) = \frac{QCost(S, Q)}{Quality(S)}, \text{ where}$$

$$QCost(S, Q) = \begin{cases} Cost_{P\mathcal{K}NN}(S, \mathcal{K}), \text{ if } Q \text{ is a } \mathcal{K}\text{-NN query;} \\ Cost_{PRange}(S, r), \text{ if } Q \text{ is a range query.} \end{cases}$$

6.3.3 Greedy Approaches

Trying to find the optimal set of cloaked road segments S that minimizes a certain cost function would require an exhaustive search process. As the underlying application of

road network anonymization (e.g., location-based services) is a real-time application in which it is crucial to efficiently process the anonymization and query processing in a minimal time, we avoid trying to get an optimal set S. Instead, we use a greedy approach to minimize the objective cost function developed in Section 6.3.2. In particular, we present two efficient greedy approaches, namely *pure greedy* and *randomized greedy* approaches, that rely on the objective cost function designed for balancing a trade-off between query execution cost and query quality.

Pure Greedy Approach

The idea of our greedy approach is to start from the road segment in which the querying user is residing. If this road segment satisfies the user's privacy requirements, we return it to a location-based database server as the cloaked road segment S. Otherwise, we check all adjacent road segments of S and greedily pick the road segment that minimizes the objective cost function. We keep adding these adjacent road segments greedily to S until S satisfies the user privacy requirements. As the objective cost function is heavily dependent on the underlying query execution cost model, such approach may result in different S for different query types.

Algorithm 5 depicts the pseudo code of the pure greedy approach of our query-aware location anonymization algorithm. The algorithm has two input parameters, the identifier of the user U who issues the query and the issued query Q. The algorithm starts by initializing a cloaked set of road segments S with the edge e that includes the user U (Line 3 in Algorithm 5). If the current S does not satisfy U's privacy requirements, i.e., $U.k$ and $U.L_{min}$, we do the following three steps (Lines 4 to 8 in Algorithm 5): (1) We construct the set R that consists of all road segments that are adjacent to some road segment in S. (2) For each road segment $e_i \in R$, we calculate the objective cost to decide whether e_i should be added to S for the input query Q based on the objective cost function designed in Section 6.3.2. Then, we choose the best edge as the one that minimizes the objective cost function should it have been added to S. (3) We add that best edge to the current cloaked set of road segments S. We keep doing these three steps until S satisfies U's privacy requirements, i.e., $NumUser(S) \geq U.k$ and $Length(S) \geq U.L_{min}$. Finally, we return S as the cloaked segment set for the user U. It is important to note that S does satisfy the user privacy requirements while it

Algorithm 5 A Greedy Approach

```
1: function GREEDY (User U, Query Q)
2: e ← the road segment contains the user U
3: S ← {e}
4: while NumUser(S) < U.k or Length(S) < U.L_min do
5:    R ← All adjacent road segments of S
6:    BestEdge ← argmin_{e_i ∈ R} (Cost(S ∪ e_i, Q))
7:    S ← S ∪ BestEdge
8: end while
9: return S
```

aims to minimize the query execution cost and maximize the query quality according to our developed objective cost function.

Figure 6.4 gives an example to illustrate the greedy approach for the query-aware location anonymization algorithm where the user issues a $\mathcal{K}$-NN query Q_1 where $\mathcal{K} = 3$ while being five anonymous within a set of connected road segments with a total length of at least five, i.e., $k = 5$ and $L_{min} = 5$. For ease of comparison and discussion, we use the same road network that was used in Figure 6.3. Although we show only part of the road network, we assume that the whole road network has $R = 100,000$ road segments and $T = 1,000$ target objects. Hence, according to the query cost model developed in Section 6.2, we will need to search $R/T \times \mathcal{K} = 300$ edges for each *open vertex* in a cloaked segment set S. Since edge v_4v_6 contains Q_1, we initially set the cloaked set of road segments S to $\{v_4v_6\}$, where vertices v_4 and v_6 are *open vertices* that are enclosed in rectangles. As S cannot satisfy the user privacy requirements, i.e., $NumUser(S) = 1$ and $Length(S) = 1$, we compute the objective cost of the adjacent edges of v_4v_6 and add the edge with the lowest cost to S. The cost of these adjacent edges is $Cost(S \cup v_5v_6) = (3 \times 300 + 2)/(\min(5/5, 1) \times \min(4/5, 5/4)) = 902/(1 \times 4/5) = 1127.5$, $Cost(S \cup v_6v_7) = 902/(2/5 \times 2/5) = 5637.5$, $Cost(S \cup v_3v_4) = 902/(3/5 \times 3/5) = 2505.6$, and $Cost(S \cup v_4v_9) = 902/(1 \times 5/10) = 1804$. Since edge v_5v_6 has the smallest objective cost, we add v_5v_6 to S (Figure 6.4a).

However, $S = \{v_4v_6, v_5v_6\}$ satisfies only the k-anonymity requirement, i.e., $NumUser(S) = 5$ and $Length(S) = 4$, so we compute the objective cost of the adjacent edges of the edges in S. The cost of these adjacent edges is $Cost(S \cup v_6v_7) = (3 \times 300 + 3)/(\min(6/5, 1) \times \min(5/5, 5/5)) = 903/(1 \times 5/5) = 903$, $Cost(S \cup v_3v_4) =$

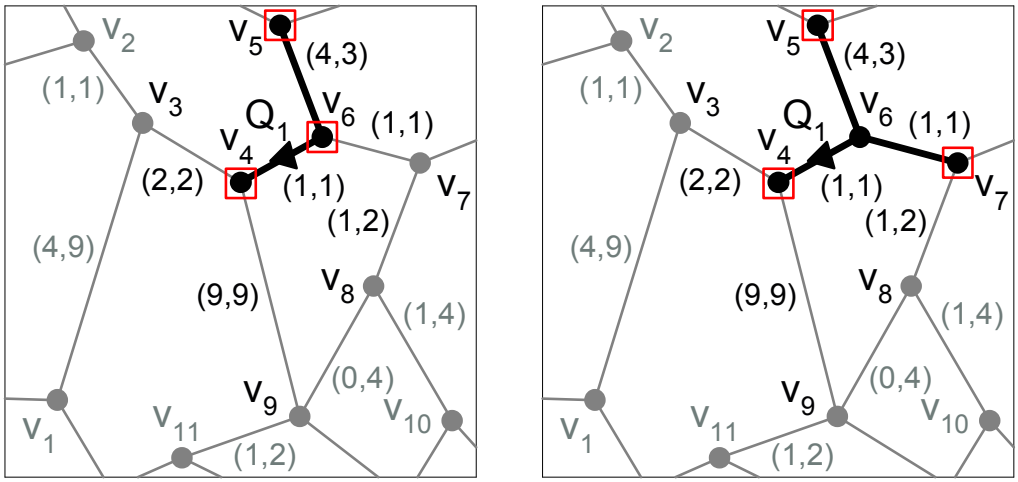

(a) Add v_5v_6 to $S = \{v_4v_6\}$ (b) Add v_6v_7 to S=$\{v_4v_6, v_5v_6\}$

Figure 6.4: Example of the greedy approach.

$(4 \times 300 + 3)/(\min(7/5, 1) \times \min(6/5, 5/6)) = 1203/(1 \times 5/6) = 1443.6$, and $Cost(S \cup v_4v_9) = (4 \times 300 + 3)/(\min(14/5, 1) \times \min(13/5, 5/13)) = 1203/(1 \times 5/13) = 3127.8$. Since edge v_6v_7 has the smallest objective cost, we add v_6v_7 to S (Figure 6.4b). Finally, $S = \{v_4v_6, v_5v_6, v_6v_7\}$ satisfies the user privacy requirements, i.e., $NumUser(S) = 6 \geq k$ and $Length(S) = 5 \geq L_{min}$, and there are three *open vertices* in S, i.e., v_4, v_5, and v_7, that are enclosed in rectangles. This example shows that the developed objective cost function effectively balances between query execution cost and query quality, because the cloaked segment set S has the maximal query $Length(S) = l = 5$, and the query execution cost of S (i.e., cost of S (i.e., $V_o(S) = 3$ and $E(S) = 3$) is only slightly deteriorated compared to the optimal query cost (i.e., $V_o(S_c) = 3$ and $E(S_c) = 2$) given in Section 6.3.1.

Randomized Greedy Approach

Although the greedy approach is simple and effective in terms of achieving privacy requirements, minimizing query execution cost, and maximizing query quality, the greedy approach is vulnerable to adversary attacks. Basically, we assume the worst case that an adversary knows the number of users and length of each road segment, and the adversary is able to crack the system to know or guess the used objective cost function.

Then, the adversary can know the road segment in which the user issuing the query is residing through a reverse engineering process. For example, given a cloaked set of road segments S, the adversary performs two main steps. (1) The adversary selects a certain edge $e_i \in S$, and then applies the revealed cost function in a greedy manner for e_i to compute another cloaked set of road segments S'. (2) If there is an edge e_j where $e_j \in S'$ and $e_j \notin S$, the adversary knows that the user is not in e_i. The main idea is that if the user is in e_i, S' should always be included in S, i.e., $S' \subseteq S$, before S' is equal to S. The adversary can repeat these two steps for each edge in S for all possible combinations of the user's privacy requirements, i.e., k and L_{min}. When the adversary achieves a case that $S' = S$, it is likely that the user who issued the query is in e_i.

The main reason of having such a privacy attack is that the greedy approach relies on a deterministic cost function to determine a cloaked set of road segments S. To this end, we propose a randomized greedy approach for our query-aware location anonymization algorithm. The idea is to inject some randomness into the process of selecting road segments to S. Rather than solely relying on a greedy approach, we will alternate between greedy and random approaches. Although injecting randomness into the anonymization process may degrade the query processing performance, i.e., query execution cost and query quality, but it significantly reduces, if not prevent, the possibility of the adversary attack. To balance between the query processing performance and the vulnerability of adversary attacks, we introduce a user parameter, *random factor* ($Rand_F$), that controls the level of randomness injected into the greedy approach. When $Rand_F$ is set to 0, our randomized greedy approach acts exactly as the pure greedy approach. On the other hand, when $Rand_F$ is set to 1, our randomized greedy approach acts in a purely random way where we keep randomly selecting the adjacent edges of a current cloaked segment set S until S satisfies the user privacy requirements. In general, a larger $Rand_F$ provides more secure privacy for the user, yet it results in lower query processing performance. It is important to note that both the pure greedy and randomized greedy approaches are guaranteed to generate a cloaked set of road segments satisfying both the k-anonymity and minimum length L_{min} privacy requirements.

Algorithm 6 gives the pseudo code of our randomized greedy approach. The pseudo code is similar to that of the pure greedy approach in Algorithm 5 except for the part of choosing an edge in the set of adjacent edges of S, R, to be added to the current cloaked

Algorithm 6 A Randomized Greedy Approach

```
1: function RandomizedGreedy (User U, Query Q, Float Rand_F)
2: e ← the road segment contains the user U
3: S ← {e}
4: while NumUser(S) < U.k or Length(S) < U.L_min do
5:    R ← All adjacent road segments of S
6:    Rand_N ← a random number between 0 and 1, i.e., [0, 1)
7:    if Rand_F > Rand_N then
8:       BestEdge ← a road segment is randomly selected from R
9:    else
10:      BestEdge ← argmin_{e_i ∈ R} (Cost(S ∪ e_i, Q))
11:   end if
12:   S ← S ∪ BestEdge
13: end while
14: return S
```

set of road segments S (Lines 6 to 11 in Algorithm 6). Basically, the randomized greedy approach has an option to randomly select road segments to S. Thus, we generate a random number between 0 and 1. If the input parameter $Rand_F$ is greater than the generated random number, we opt to randomly select a road segment among the ones stored in R, i.e., the adjacent road segments of S. On the other hand, if the input parameter $Rand_F$ is less than the generated random number, we use our greedy approach to select the road segment from R that minimizes the objective cost function described in Section 6.3.2. By injecting randomness to the anonymization process, we can prevent the reverse engineering attack as an adversary cannot guess the generated random numbers.

6.4 Shared Execution Paradigm

As a location-based database server is likely to receive a numerous number of concurrent queries, processing these queries individually would pose a system bottleneck. To tackle this scalability issue, we propose a *shared execution* paradigm that aims to minimize the number of queries executed by the database server for a set of private queries. The main idea is to maximize the number of common vertices and edges in the cloaked set of road segments of a set of similar queries issued from nearby users. Two or more queries

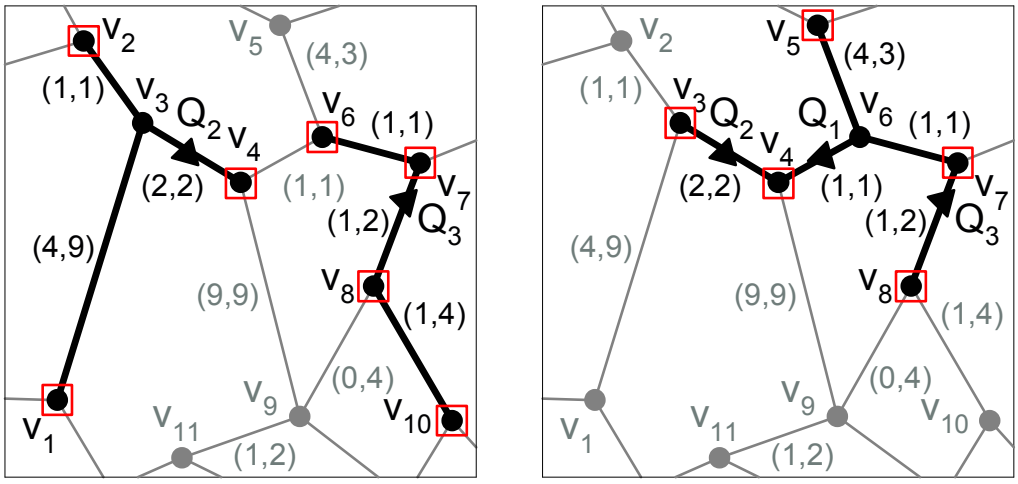

(a) Non-shared execution (b) Shared execution

Figure 6.5: Motivating example of shared execution.

are similar if they belong to the same query type and interested in the same target object type. It is important to note that the proposed shared execution paradigm can be incorporated into both the *pure greedy* and *randomized greedy* approaches for query-aware location anonymization. In this section, we first give the motivation of the shared execution paradigm, and then present the algorithm with a running example.

6.4.1 Motivation

Figure 6.5 depicts a motivating example of the proposed shared execution paradigm, in which the location anonymizer receives three similar queries $\mathcal{Q} = \{Q_1, Q_2, Q_3\}$ at the same time. The privacy requirements of these queries are ($Q_1.k$=5, $Q_1.L_{min}$=5), ($Q_2.k$=6, $Q_2.l$=7), and ($Q_3.k$=3, $Q_3.$=6). Without the concept of shared execution, we use the use the pure greedy approach to anonymize the location information of these queries individually. Figure 6.4b gives the cloaked set of road segments S_1 of Q_1, while the cloaked segment sets S_2 and S_3 of Q_2 and Q_3 are depicted in Figure 6.5a. Anonymizing these queries individually results in three cloaked segment sets $S_1 = \{v_4v_6, v_5v_6, v_6v_7\}$, $S_2 = \{v_1v_3, v_2v_3, v_3v_4\}$, and $S_3 = \{v_6v_7, v_7v_8, v_8v_{10}\}$ that contain a total of nine edges (represented as black lines) and ten *open vertices* (enclosed in rectangles), i.e., $\{v_4, v_5, v_7\}$ in S_1, $\{v_1, v_2, v_4\}$ in S_2, and $\{v_6, v_7, v_8, v_{10}\}$ in S_3. Thus,

Algorithm 7 A Greedy Approach with Shared Execution

```
1: function SharedExecutionGreedy (QuerySet 𝒬)
2: 𝒮 ← {∅}
3: Sort 𝒬 by the query parameter in decreasing order
4: for Each query Q_i ∈ 𝒬 do
5:    e ← the road segment contains the user U_i of Q_i
6:    S_i ← {e}
7:    while NumUser(S_i) < U_i.k or Length(S_i) < U_i.L_min do
8:       R ← All adjacent road segments of S_i
9:       if R ∩ 𝒮 is empty then
10:         e ← argmin_{e_j ∈ R} (Cost(S_i ∪ e_j, Q_i))
11:      else
12:         e ← argmax_{e_j ∈ {R ∩ 𝒮}} (Quality(S_i ∪ e_j))
13:      end if
14:      S_i ← S_i ∪ e
15:   end while
16:   𝒮 ← 𝒮 ∪ S_i
17: end for
18: return 𝒮
```

the database server has to retrieve the target objects of these nine edges and execute the requested query at each of these ten *open vertices*.

With the proposed shared execution paradigm, the location anonymization algorithm aims to maximize the number of common *open vertices* and edges of the cloaked segment sets of a set of similar queries. Figure 6.5b depicts the set $\mathcal{S}$ of distinct edges in the cloaked segment sets S_1, S_2, and S_3 that are computed by the pure greedy approach with our shared execution paradigm, in which $S_1 = \{v_4v_6, v_5v_6, v_6v_7\}$, $S_2 = \{v_3v_4, v_4v_6, v_5v_6, v_6v_7\}$, and $S_3 = \{v_3v_4, v_4v_6, v_6v_7, v_7v_8\}$. Hence, $\mathcal{S}$ contains five distinct edges (represented as black lines), i.e., $v_3v_4, v_4v_6, v_5v_6, v_6v_7$, and v_7v_8, and five distinct *open vertices* (enclosed in rectangles), i.e., v_3, v_4, v_5, v_7, and v_8. This example shows that the shared execution paradigm reduces the number of edges and *open vertices* among the cloaked segment sets of the three queries by 44.4% (i.e., from nine edges to $E(\mathcal{S}) = 5$) and 50% (i.e., from ten *open vertices* to $V_o(\mathcal{S}) = 5$), respectively. As a result, the database server needs to retrieve the target objects of five edges and execute the requested query at five *open vertices*, and then share the answer of these queries among Q_1, Q_2, and Q_3.

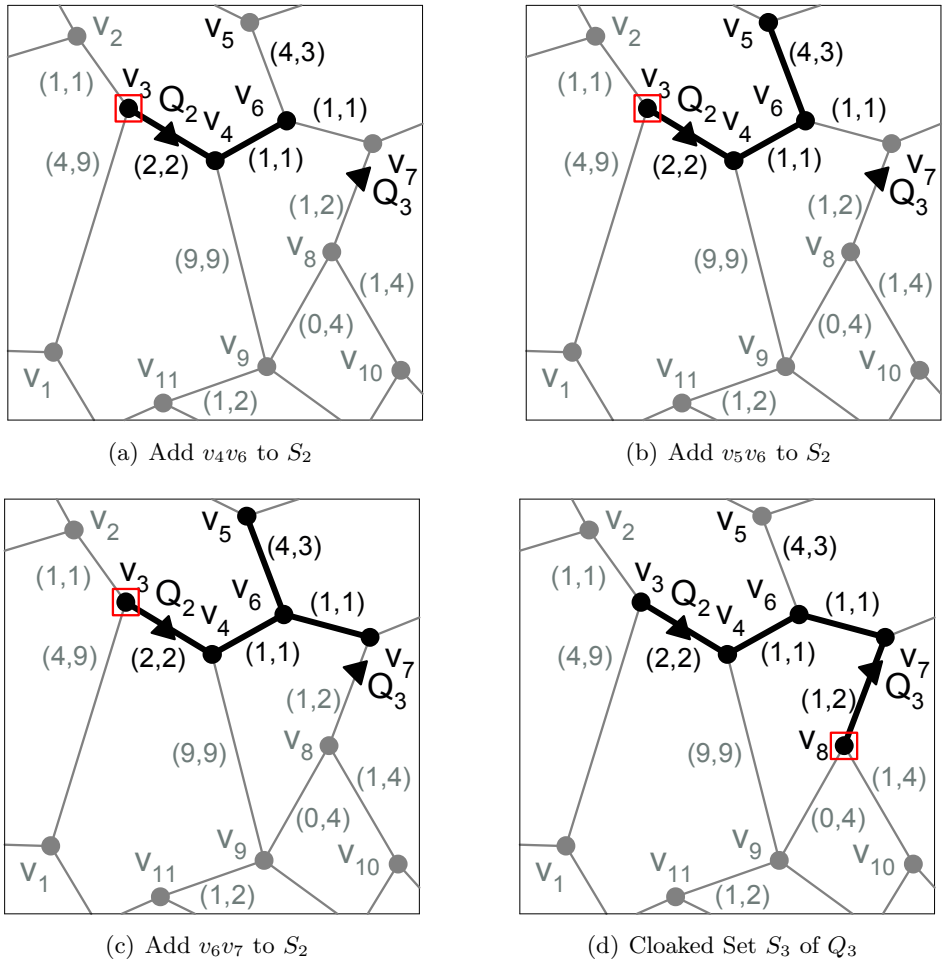

(a) Add v_4v_6 to S_2

(b) Add v_5v_6 to S_2

(c) Add v_6v_7 to S_2

(d) Cloaked Set S_3 of Q_3

Figure 6.6: An example of the shared execution scheme for a query set $\mathcal{Q} = \{Q_1, Q_2, Q_3\}$.

6.4.2 Algorithm

Main idea. Given a set of n similar queries $\mathcal{Q} = \{Q_1, Q_2, \ldots, Q_n\}$ received by the location anonymizer at the same time or within a short time interval, the shared execution paradigm aims to maximize the number of common *open vertices* and edges in the cloaked segment sets $S_1, S_2, \ldots, S_n$ for the queries in $\mathcal{Q}$. $\mathcal{S}$ is a set of distinct edges in the cloaked segment sets $S_1, S_2, \ldots, S_n$, i.e., $\mathcal{S} = \bigcup_{1 \le i \le n} S_i$. The main idea is that when we compute a cloaked set S_i of a query Q_i, we always give a higher priority to select the edges that are in the set of adjacent edges of S_i, R, and have been selected

by other preceding queries in $\mathcal{Q}$ to S_i, i.e., these edges are in the set $\{R \cap \mathcal{S}\}$. The main reason is that adding any edge from $\mathcal{S}$ will have a zero query execution cost because the query execution cost of the edges in $\mathcal{S}$ is absorbed by other queries in $\mathcal{Q}$. Thus, by using the quality function described in Section 6.3.2, we add the edge that gives the highest quality of answers among the set $\{R \cap \mathcal{S}\}$ to S_i. However, in case that $\{R \cap \mathcal{S}\}$ is empty, we simply employ our objective cost function to select the best candidate edge to S_i. Although the shared execution paradigm would incur longer anonymization time for some queries, it improves the average anonymization time of the queries in the similar query set, and this sacrifice will be paid off by the significant gain in the query processing at the database server. Experimental results in Section 7.4 give more details on this performance gain.

Algorithm. Algorithm 7 depicts the pseudo code of the shared execution paradigm applied to the pure greedy approach (or the randomized greedy approach with the same modifications). The input of the algorithm is a set of similar queries $\mathcal{Q}$. We maintain a set $\mathcal{S}$ to store the distinct edges in the cloaked set of road segments of each query in $\mathcal{Q}$. Initially, we set $\mathcal{S}$ to empty and sort the queries in $\mathcal{Q}$ by their parameters in decreasing order, i.e., the value of $\mathcal{K}$ of $\mathcal{K}$-NN queries or the network range distance r of range queries (Lines 2 to 3 in Algorithm 7). The main idea behind this sorting is to ensure that the answer of the requested query at a selected *open vertex* can be used by a database server to answer the subsequent queries in $\mathcal{Q}$. For example, a $\mathcal{K}$-NN query answer can be used to answer another $\mathcal{K}'$-NN query if $\mathcal{K} \geq \mathcal{K}'$. For each query Q_i in $\mathcal{Q}$, the proposed shared execution paradigm is applied to the pure greedy approach (or the randomized greedy approach) to find a cloaked set of road segments S_i. First, we set the edge that contains the querying user U_i to S_i (Line 6 in Algorithm 7). If S_i does not satisfy the user privacy requirements, i.e., $U_i.k$ and $U_i.L_{min}$, we repeatedly select the adjacent edges of S_i, R, to S_i until S_i satisfies the user privacy requirements. We distinguish between two cases of selecting the best edge to S_i. Case 1: $\{R \cap \mathcal{S}\}$ *is empty.* In this case, there is no adjacent edge of S_i in $\mathcal{S}$. Thus, we simply use the objective cost function to select an edge with the best cost among the set of adjacent edges of S_i, R (Line 10 in Algorithm 7). Case 2: $\{R \cap \mathcal{S}\}$ *is not empty.* In this case, there are some adjacent edges of S_i are in $\mathcal{S}$. We select an edge with the largest quality from the set $\{R \cap \mathcal{S}\}$ (Line 12 in Algorithm 7). It is important to note that choosing any edge from

$\{R \cap \mathcal{S}\}$ just adds a zero cost to the query processing. After we find a cloaked set of road segments S_i for Q_i, we update $\mathcal{S}$ accordingly (Line 16 in Algorithm 7). Finally, we send the queries in $\mathcal{Q}$ along with their cloaked segment sets S_i in a batch to the database server.

Example. Figure 6.6 depicts an example of the shared execution paradigm applied to the pure greedy approach where the query set contains three similar queries $\mathcal{Q} = \{Q_1, Q_2, Q_3\}$ that are sorted by their query parameters in decreasing order. The privacy requirements of these queries are the same as in Section 6.4.1. First, we compute the cloaked set of road segments S_1 of Q_1. Since Q_1 is the first query in $\mathcal{Q}$, i.e., $\mathcal{S}$ is empty, we compute S_1 based on the pure greedy approach, as depicted in Figure 6.4; and hence, $\mathcal{S} = S_1 = \{v_4v_6, v_5v_6, v_6v_7\}$. Then, we process Q_2 residing in edge v_3v_4, i.e., $S_2 = \{v_3v_4\}$. Since only one of the adjacent edges of S_2 is in $\mathcal{S}$, i.e., v_4v_6, we add v_4v_6 to S_2 (Figure 6.6a). Selecting v_4v_6 results in two adjacent edges of S_2 in $\mathcal{S}$, so we compute the quality of these two edges, i.e., $Quality(S_2 \cup v_5v_6) = \min(7/6, 1) \times \min(6/7, 7/6) = 1 \times 6/7 = 0.857$ and $Quality(S_2 \cup v_6v_7) = \min(4/6, 1) \times \min(4/7, 7/4) = 4/6 \times 4/7 = 0.381$. Thus, we add the edge with the highest quality, i.e., v_5v_6, to S_2 (Figure 6.6b). Since v_6v_7 is the only adjacent edge of S_2 in $\mathcal{S}$, we add v_6v_7 to S_2 (Figure 6.6c). After that, $S_2 = \{v_3v_4, v_4v_6, v_5v_6, v_6v_7\}$ satisfies the user privacy requirements, i.e., $NumUser(S_2) = 8$ and $Length(S_2) = 7$. The anonymization process of Q_2 results in adding only one *open vertex* v_3 (enclosed in a rectangle) and one edge v_3v_4 to $\mathcal{S}$. Similarly, we anonymize the location information of Q_3 residing in edge v_7v_8. The cloaked segment set of Q_3 is $S_3 = \{v_3v_4, v_4v_6, v_6v_7, v_7v_8\}$ (Figure 6.6d) that results in only one *open vertex* v_8 and edge v_7v_8 to be added to $\mathcal{S}$. Finally, the cloaked segment sets of these three queries contain five distinct *open vertices* (enclosed in rectangles) and five distinct edges (represented as black lines), as depicted in Figure 6.5b.

6.5 Experiment Results

In this section, we experimentally evaluate the performance of the two versions of our proposed query-aware location anonymization algorithm, i.e., *pure greedy* (denoted as PG) and *randomized greedy* (denoted as RG). We also evaluate the performance of the proposed shared execution paradigm incorporated into the *pure greedy* (denoted as SPG)

Table 6.1: Parameter settings.

Parameter	Default Value	Range
Number of users	100K	100K - 500K
Number of queries	5K	2K - 10K
Anonymity levels (k)	200	100 - 500
Min. total segment length (L_{min})	$10 \times l$, $l = 1590.6$	$10 \times l$ - $50 \times l$
Random factor $Rand_F$	0.2	0.1 - 0.5
Requested no. of objects $\mathcal{K}$	10	1 - 20
Required range distance r	$10 \times l$	$5 \times l$ - $30 \times l$

and *randomized greedy* (denoted as SRG) approaches.

Baseline approach. We compare our approaches with the closest work [100] (denoted as BL) that is the only related work considering location anonymization and privacy-preserving query processing in road networks. However, this work uses the *Casper*'s location anonymization algorithm [12] that is designed for the Euclidean space to blur users' locations into k-anonymous spatial regions. After determining a cloaked spatial region, the set of road segments intersecting the spatial region forms a cloaked segment set.

Experiment settings. We use a network-based generator [88] to generate moving objects on an actual road map that has 57,020 edges and 42,135 vertices in which the average length of the edges (l) is 1,590.6 and the the average degree of connectivity of the vertices (d) is 2.7. At the database server, we employ an *incremental network expansion* algorithm [103] and a depth-first search algorithm to process $\mathcal{K}$-NN and range queries in the road network, respectively. We evaluate our algorithms with respect to two performance measures, *CPU time* and *total segment length*. The CPU time is the sum of the average time consumed in the anonymization process (i.e., cloaking time) and the average query processing time at the database server. The total segment length is the sum of the length of all road segments in a cloaked segment set S, $Length(S)$. Since a cloaked segment set with a larger total segment length is more likely to give a larger candidate answer set, this measure indicates the query quality of S.

Parameter settings. Unless mentioned otherwise, the experiments in this section consider 100,000 mobile users and 500 target objects in the road network in which

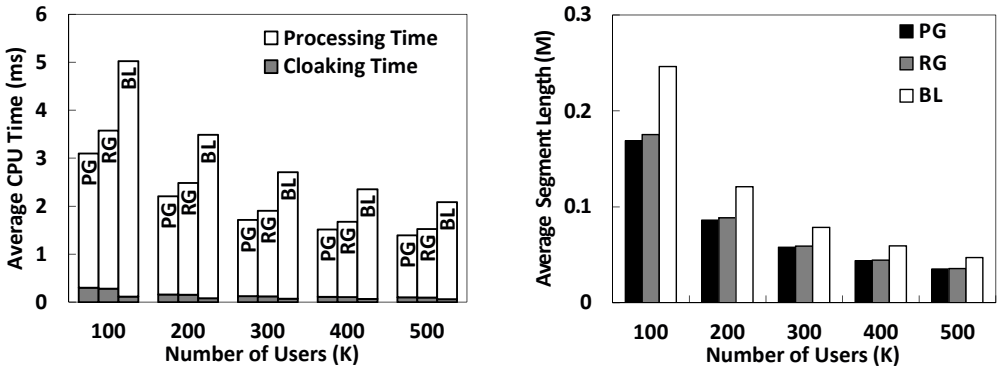

(a) CPU Time (b) Total Segment Length

Figure 6.7: Number of mobile users ($\mathcal{K}$-NN queries).

5,000 users issue queries at each time interval. The default user privacy requirements, anonymity level k and minimum length (L_{min}), are $k = 200$ and $L_{min} = 10 \times l$, where l is the average length of the road segments in the road network. The random factor $Rand_F$ for our randomized greedy approach is set to 0.2. The query parameters of $\mathcal{K}$-NN and range queries are $\mathcal{K} = 10$ and $r = 10 \times l$, respectively. Table 6.1 gives a summary of the parameter settings.

6.5.1 Scalability

Figures 7.8a and 7.8b depict the scalability of our *pure greedy* (PG) and *randomized greedy* (RG) approaches with respect to increasing the number of users from 100K to 500K for $\mathcal{K}$-NN queries in terms of two performance measures, the average CPU time per query (Figure 7.8a) and average total segment length per cloaked segment set S (Figure 7.8b). Figure 7.8a gives the overall CPU time which includes the location anonymization time at the location anonymizer (represented by shaded bars) and the query processing time at the database server (represented by white bars). Focusing on the *baseline* algorithm (BL), although it has better anonymization time than our proposed greedy approaches, it suffers from bad query processing performance and low quality of answers. The main reason is that BL always generates cloaked segment sets with a larger number of *open vertices* and larger total segment length than our

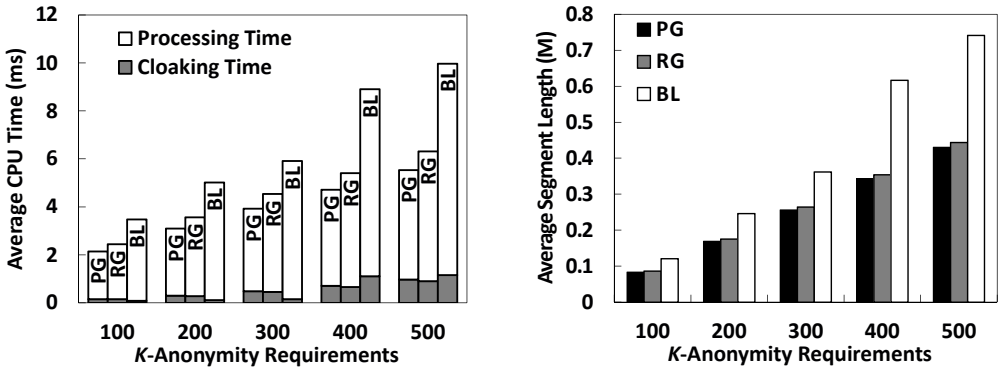

(a) CPU Time (b) Total Segment Length

Figure 6.8: k-anonymity ($\mathcal{K}$-NN queries).

approaches (Figures 7.8b). That was the motivation behind our location anonymization algorithm in which we focus on the road network environment and having the anonymization process as a "query-aware", i.e., enhancing system usability by providing better support for privacy-preserving query processing. With respect to the CPU time, the performance of all approaches is enhanced with the increase of the number of users. By increasing the number of users, the k-anonymity privacy requirement is satisfied with few numbers of road segments in S; and thus, the anonymization process takes a shorter time to find S. In general, a smaller cloaked set contains few numbers of *open vertices*, so the query processing time improves with the increase of the number of users.

6.5.2 Privacy Requirements

Figures 6.8 and 6.9 give the effect of the k-anonymity and minimum length (L_{min}) privacy requirements for $\mathcal{K}$-NN queries, respectively. Figure 6.8 depicts the result with respect to the spectrum of the acceptable values of k from a moderate anonymity level, i.e., $k = 100$, to a very strict level, i.e., $k = 500$. For all approaches, stricter privacy result in increasing the cloaking and query processing time (Figure 6.8a). Increasing the privacy requirement is likely to have more *open vertices* and road segments (Figure 6.8b) in cloaked segment sets. Thus, the anonymization process has to spend more time to find the cloaked segment set and the database server has higher query processing overhead

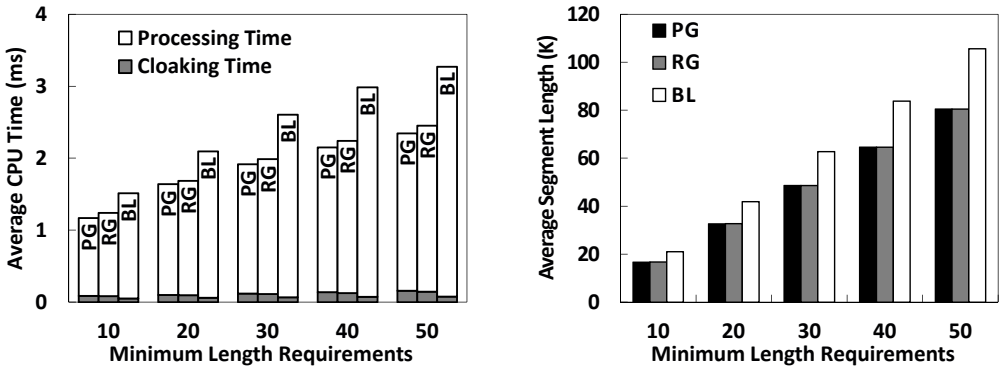

(a) CPU Time (b) Total Segment Length

Figure 6.9: Minimum length L_{min} ($\mathcal{K}$-NN queries).

to compute the candidate answer set. With a higher anonymity level, the improvement of our approaches (i.e., PG and RG) over the *baseline* algorithm (BL) significantly increases in both the CPU time and query quality.

Figure 6.9 gives the performance of our approaches with respect to varying the minimum length privacy requirement from $L_{min} = 10 \times l$ to $50 \times l$, where l is the average length of the segments in the road network. Similar to the k-anonymity privacy requirement, the cloaking and processing time increases as the value of l gets larger. Our greedy-based approaches also perform better than the *baseline* algorithm (BL) in terms of both the CPU time (Figure 6.9a) and query quality (Figure 6.9b) when the user specifies a stricter minimum length privacy requirement.

6.5.3 Query Parameters

Figures 6.10a and 6.10b give the performance of our greedy-based approaches, PG and RG, for various query parameters of $\mathcal{K}$-NN and range queries (r) in terms of the CPU time, respectively. Figures 6.10a and 6.10b give the CPU time of all approaches with respect to varying the value of $\mathcal{K}$ of $\mathcal{K}$-NN queries from 1 to 20 and the network range distance r of range queries from $5 \times l$ to $30 \times l$, respectively. With a larger query parameter, the query processing time increases as the database server needs to spend

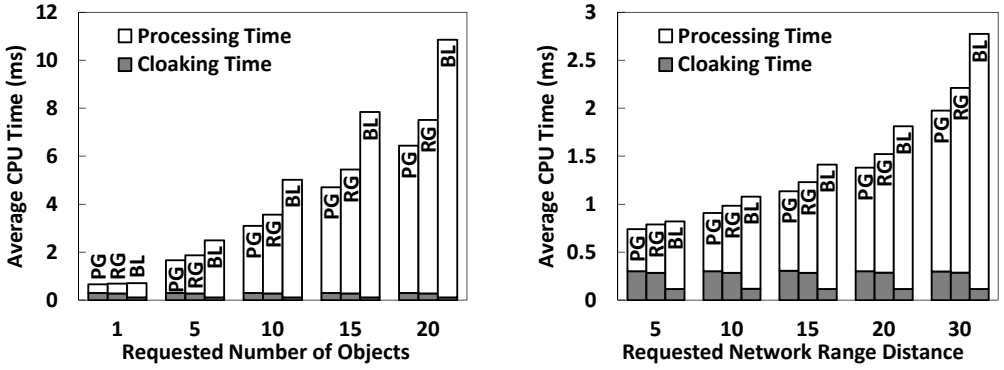

(a) $\mathcal{K}$-NN Queries ($\mathcal{K}$) (b) Range Queries (r)

Figure 6.10: Query parameters.

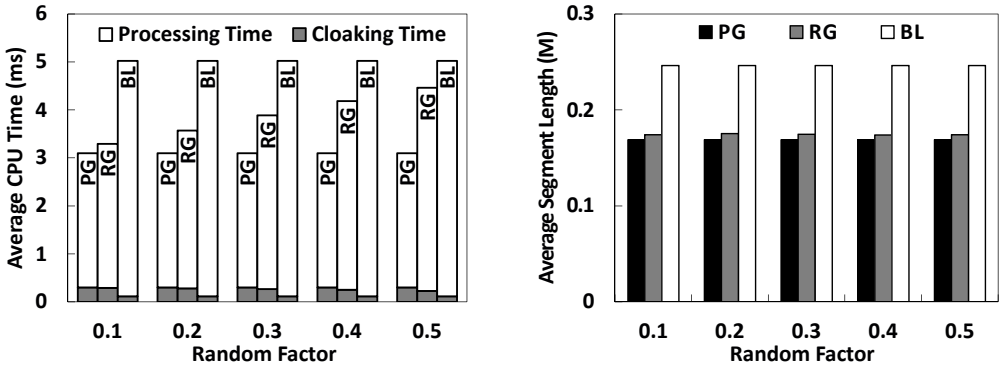

(a) CPU Time (b) Total Segment Length

Figure 6.11: Random factor $Rand_F$ ($\mathcal{K}$-NN queries).

more time to compute a query answer. For both $\mathcal{K}$-NN and range queries, our greedy-based approaches, PG and RG, perform better than the *baseline* algorithm (BL) as the query parameter gets larger. Thus, the user can get better performance from our "query-aware" location anonymization algorithm if her location-based queries require more computation, i.e., a large value of $\mathcal{K}$ for $\mathcal{K}$-NN queries or r for range queries.

6.5.4 Randomness Factor

Figure 6.11 depicts the effect of the amount of randomness injected to the anonymization process for $\mathcal{K}$-NN queries by varying a *random factor*, $Rand_F$, from 0.1 to 0.5. As

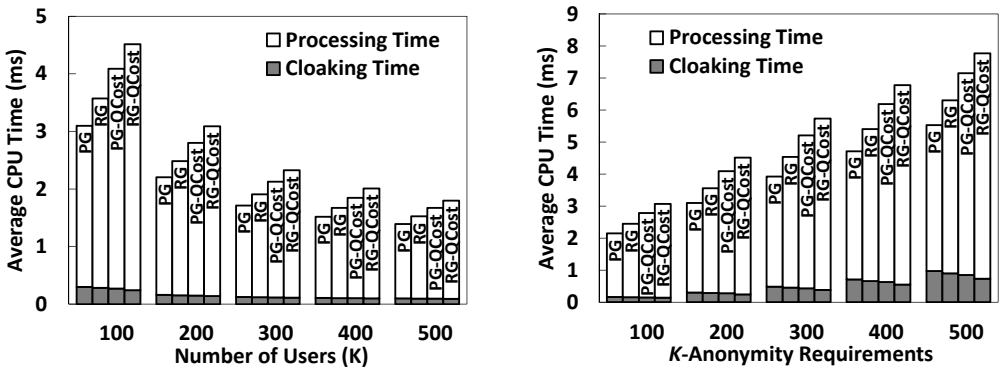

(a) Number of Users (b) k-Anonymity

Figure 6.12: Objective cost function ($\mathcal{K}$-NN queries).

a reference, we plot the result of the *pure greedy* approach (PG) and *baseline* algorithm (BL), though they are not affected by the *random factor*. The cloaking time of the *randomized greedy* approach (RG) gets better with more injected randomness, i.e., a larger $Rand_F$. The main reason for this is that increasing the randomness alleviates the need for the more expensive computation of the best edge (i.e., the objective cost function) to be added to a cloaked segment set S. However, injecting randomness to the anonymization process degrades query processing performance and query quality, as depicted in Figures 6.11a and 6.11b, respectively. Since injecting more randomness into the anonymization process only slightly increases the total segment length (Figure 6.11b), the main reason of the query performance deterioration is due to a larger number of *open vertices* in the cloaked segment sets. Thus, we should limit the *random factor* such that we can have moderate sacrifice of query processing performance in order to obtain more secure privacy.

6.5.5 Objective Cost Function

Figure 6.12 depicts the effectiveness of our objective cost function described in Section 6.3.2 with respect to increasing the number of users from 100K to 500K (Figure 6.12a) and the k-anonymity privacy requirement from $k = 100$ to 500 (Figure 6.12b) for $\mathcal{K}$-NN queries. To evaluate the objective cost function used by the *pure greedy* (PG) and *randomized greedy* (RG) approaches, we compare them with the *pure greedy* and

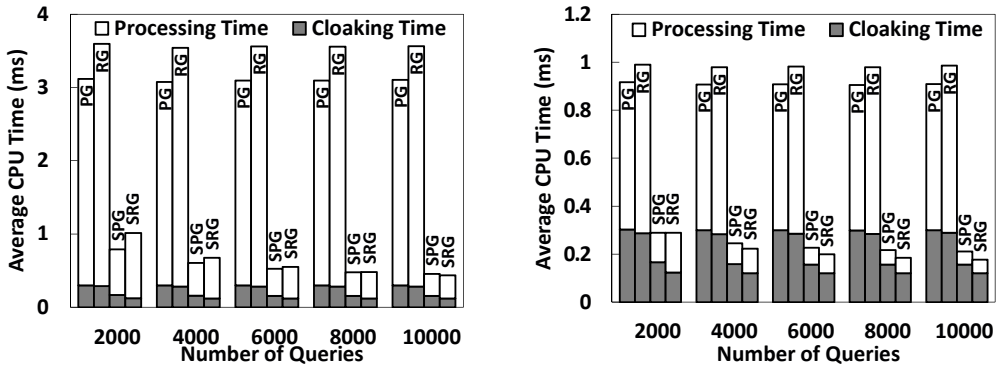

(a) $\mathcal{K}$-NN Queries (b) Range Queries

Figure 6.13: Number of queries.

randomized greedy approaches that rely solely on the *query execution cost model* described in Section 6.2 (denoted as PG-QCost and RG-QCost, respectively). The results show that our objective cost function consistently performs better than the greedy approaches based on the query execution cost model. However, the cloaking time of the greedy approaches using our objective cost function PG and RG is worse than the PG-QCost and RG-QCost approaches. The main reason for this is that our objective cost function incurs higher computational overhead than the query execution cost model. By using our objective cost function, i.e., PG and RG approaches, the cloaked segment set results in lower query processing cost that pays off the computational overhead of the anonymization process. Furthermore, when we need to find a cloaked segment set with more road segments, i.e., in a case of fewer numbers of users (Figure 6.12a) or stricter privacy requirements (Figure 6.12b), the objective cost function is clearly more effective than using only the query execution cost model.

6.5.6 Shared Execution Paradigm

In this section, we evaluate the performance of the shared execution paradigm incorporated into the *pure greedy* (denoted as SPG) and *randomized greedy* (denoted as SRG) approaches with respect to workload, privacy requirements, and query parameters for both $\mathcal{K}$-NN and range queries.

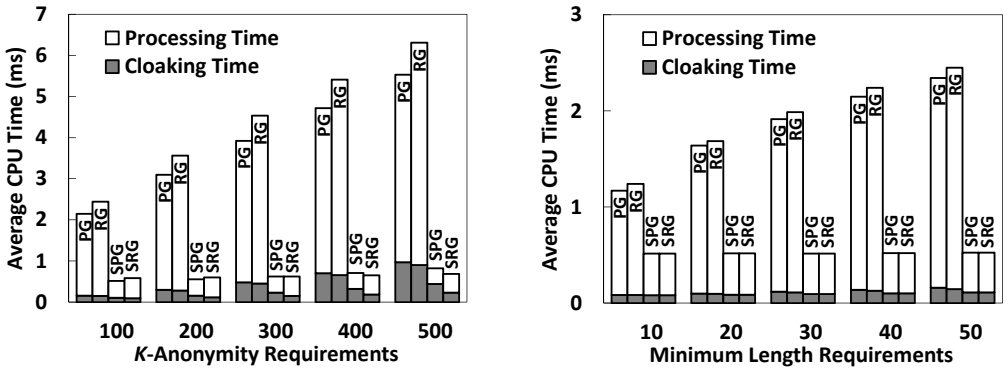

(a) k-Anonymity (b) Minimum Length (L_{min})

Figure 6.14: Privacy requirements ($\mathcal{K}$-NN queries).

Workload. Figure 6.13 depicts the effect of the query workload on the *shared execution* approaches, SPG and SRG, by varying the number of queries received by the location anonymizer within a short time period from 2K to 10K. Since the *non-shared execution* approaches, PG and RG, process the queries individually, their performance is not affected by varying the workload. On the other hand, the query processing cost of the *shared execution* approaches significantly reduces as the workload increases. This is because when the workload increases, it is likely to have more nearby similar queries; and thus, there are more common *open vertices* and edges in their cloaked segment sets. The results clearly indicate that our proposed *shared execution* paradigm effectively improves system scalability, especially when the system encounters a high query workload.

Privacy requirements. Figures 6.14a and 6.14b give the performance of the *shared execution* approaches with respect to increasing the anonymity levels from $k = 100$ to 500 and the minimum length requirement from $L_{min} = 10 \times l$ to $50 \times l$ for $\mathcal{K}$-NN queries, respectively. When the privacy requirement gets stricter, the anonymization process spends more time to find cloaked segment sets; and hence, the cloaking time of all approaches increases. For *non-shared execution* approaches, PG and RG, the query processing time increases as the privacy requirement gets stricter. Increasing the privacy requirement results in cloaked segment sets with more road segments. Since these cloaked segment sets are likely to contain more *open vertices* and road segments, the query processing cost increases. On the other hand, it is interesting to see that

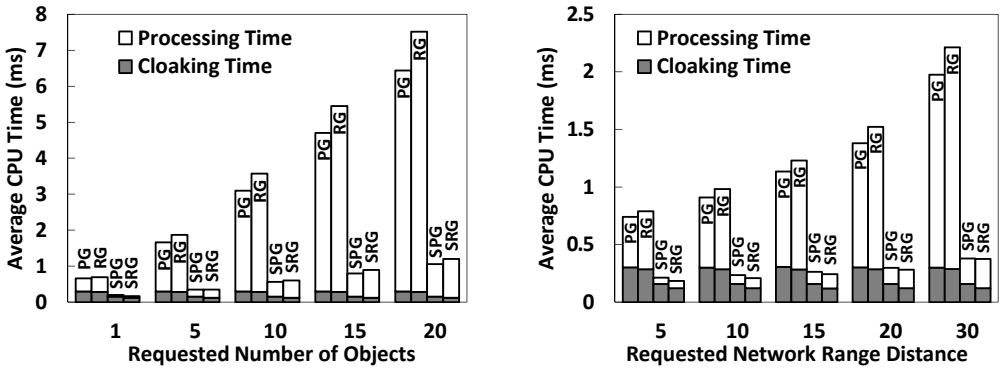

(a) $\mathcal{K}$-NN Queries ($\mathcal{K}$) (b) Range Queries (r)

Figure 6.15: Query parameters.

the query processing cost of the *shared execution* approaches, SPG and SRG, slightly improves as the privacy requirement gets stricter. The main reason for this is that it is likely to have more common *open vertices* and edges of a set of similar queries, when their cloaked segment sets incur more road segments.

Query parameters. Figure 6.15 depicts the effect of query parameters on the performance of the *shared execution* approaches, SPG and SRG, with respect to varying the requested number of nearest target objects ($\mathcal{K}$) of $\mathcal{K}$-NN queries from 1 to 20 and the requested network range distance (r) of range queries from $5 \times l$ to $30 \times l$. Since these two query parameters do not influence the anonymization process, the cloaking time of all approaches is not affected. As discussed in Section 6.5.3, the query processing time of all approaches increases when the query parameter gets larger. The results show that the *shared execution* approaches clearly perform better than the *non-shared execution* approaches in terms of the query processing time as the query parameters get larger. This is because it is likely to have more common *open vertices* and edges in larger cloaked segment sets. The results indicate that our *shared execution* paradigm is more effective to enhance system scalability when the issued location-based queries require more computation.

6.6 Summary

This chapter presents a *query-aware* location anonymization algorithm for road networks. The proposed algorithm distinguishes itself from all previous location anonymization algorithms in the sense that it is *query-aware* and is designed specifically for the road network environment. The proposed *query-aware* location anonymization algorithm aims to blur a user location on a road network into a set of connected road segments S such that: (a) there exist at least k users in S, and the total segment length of the road segments in S is at least L_{min}, (b) the processing cost of the requested query over S is minimized, and (c) the query quality of S is maximized. Based on a developed objective cost function that takes into account privacy requirements, query processing cost, and query quality, we propose two greedy-based approaches for location anonymization in road networks. To accommodate intervals with a high workload, we also propose a *shared execution* paradigm to improve the scalability of our anonymization process to support larger numbers of quires in a short time period. Extensive experimental results show that our proposed location anonymization algorithm with the two proposed approaches is efficient and scalable while preserving users' location privacy and enabling high quality services through minimizing the developed objective cost function. The results also indicate that the *shared execution* paradigm significantly improves system scalability and query processing performance.

Chapter 7

Location Anonymization in Peer-to-Peer Environments

In this chapter, we extend the location anonymization functionality of the Casper system in mobile peer-to-peer (P2P) environments. A mobile P2P network is a highly ad-hoc environment in which mobile users can only communicate with other peers through multi-hop routing without any support of fixed communication infrastructure or centralized/distributed servers. There are many unique limitations in the mobile P2P environment, e.g., user mobility, limited transmission range, multi-hop communication, scarce communication resources, and network partitions[1] . In terms of system architecture, existing spatial cloaking techniques can be classified into three main categories, *centralized* (e.g., [32, 36, 37, 44, 12, 47, 48]), *distributed* (e.g., [38, 39]), and *peer-to-peer* approaches (e.g., [19]). Since the spatial cloaking algorithms proposed for the *centralized* or *distributed* approach rely on fixed communication infrastructure and centralized/distributed servers, they cannot be applied to the mobile P2P environment. To our best knowledge, our previous work is the only spatial cloaking algorithm for the mobile P2P environment [19]. The main idea of the P2P spatial cloaking algorithm is that when a mobile user wants to obtain services from an LBS provider, she collaborates with other peers via multi-hop communication to blur her location into a cloaked area. Our algorithm guarantees that the cloaked area satisfies the user's k-anonymity

[1] In a partitioned network, mobile users are partitioned into disjoint networks, in which a mobile user is only able to communicate with other peers residing in her network partition.

and minimum area A_{min} privacy requirements. Then, the user sends her location-based query along with the cloaked area to the LBS provider to obtain her desired services. Since the location-based database server does not know the exact user location, it can only return an answer set that includes the exact answer to the user. Thus, after the user gets the answer set from the database server, she has to compute the exact answer from the answer set.

In this chapter, we propose three key features to enhance the scalability, efficacy and privacy protection of our P2P spatial cloaking algorithm. Since the mobile P2P environment has limited communication resources and constrained transmission range, excessively searching the network for peers would pose a scalability issue. To this end, we propose an *information sharing scheme* for our P2P spatial cloaking algorithm to enable mobile users to share their gathered peer location information with nearby peers. If the mobile user can get enough peer location information from a peer, she does not need to search the network; and therefore, the *information sharing scheme* can reduce communication overhead. In addition, the mobile user may encounter a network partition problem in the mobile P2P environment, i.e., the number of users residing in her network partition is less than her required anonymity level, i.e., k, she cannot find enough peer location information to satisfy her k-anonymity privacy requirement. To alleviate the network partition problem, we design a *historical location scheme* that allows users to utilize the peer location information cached by the peers residing in their network partition. We use a consecutive approach to adjust such stale location information to capture its uncertainty. Furthermore, the mobile user needs to search the network for an adequate number of peers to satisfy her required anonymity level. Since the peer search process usually starts at the user and spreads out from her nearby peers to farther peers, the user may be close to the center of the cloaked area. Thus, an adversary could guess that the user who is the closest to the center of a cloaked area is the actual query issuer, i.e., a "center-of-cloaked-area" privacy attack. To avoid such a privacy breach, we propose a *cloaked area adjustment scheme* that adjusts a cloaked area such that the probability of the actual query issuer being the closest to the center of a cloaked area is $1/K$.

We evaluate the performance of our proposed features through simulated experiments. The experimental results show that these features enhance the scalability of our

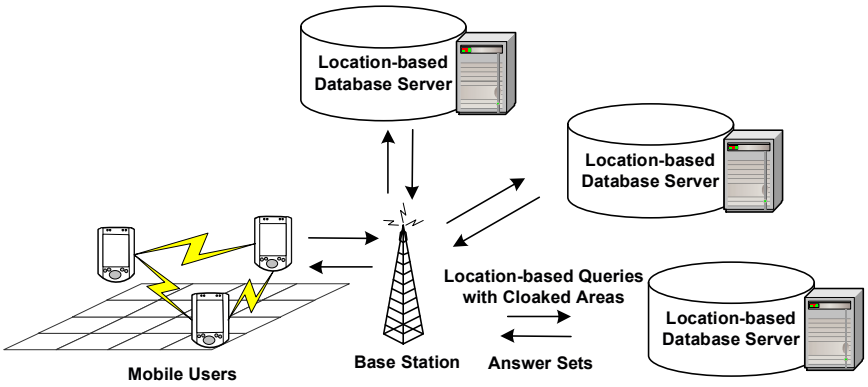

Figure 7.1: System architecture.

P2P spatial cloaking algorithm while guaranteeing the user's location privacy protection. In general, the contributions of this chapter can be summarized as follows:

- We propose a spatial cloaking algorithm for mobile peer-to-peer environments. (Section 7.2.1)
- We introduce an *information sharing scheme* for our spatial cloaking algorithm to enable mobile users to share their gathered peer location information with other peers in order to reduce communication overhead. (Section 7.2.2)
- We design a *historical location scheme* for our algorithm to overcome the network partition problem. (Section 7.2.3)
- We propose a *cloaked area adjustment scheme* for our algorithm to avoid the "center-of-cloaked-area" privacy attack. (Section 7.2.4)
- We experimentally evaluate our P2P spatial cloaking algorithm with the three enhancement schemes. The experimental results show that the enhanced algorithm is scalable while guaranteeing the user's location privacy protection. (Section 7.4)

7.1 System Model

Figure 7.1 depicts the system architecture of our peer-to-peer (P2P) spatial cloaking algorithm that consists of two entities, *mobile users* and *location-based database servers*.

We will first discuss our privacy threat model and privacy settings in *user privacy profiles*, and then describe each entity in our system.

Privacy threat model. We assume that mobile users are trusted, so they do not use their gathered peer location information to attack our system. However, we do not have any assumption about the trustworthiness of the location-based service providers. Thus, we assume that an adversary can utilize the information gathered by the service provider to make privacy attacks. In addition, we only focus on snapshot location-based queries, and each query is assigned a unique pseudonymous identity that is completely unrelated to the user's personal identity in order to ensure the pseudonymity of the user's location information [9].

User privacy profiles. Each user specifies her privacy requirements in a *privacy profile* in a form of (K, A_{min}), where k indicates the required anonymity level and A_{min} indicates the required minimum area of her cloaked areas. In other words, the user wants to find a cloaked area that includes at least k users and has an area of at least A_{min}. A_{min} is particularly useful in a dense area where a large k would not achieve high privacy protection. For example, a user in a stadium with $K = 100$ may result in a very small cloaked area. It is important to note that the user can change her privacy profile at any time to guarantee that her specified privacy settings achieve her desired privacy protection in different situations.

The privacy profile can be extended to support temporal, spatial, and/or interdependent constraints on the required anonymity level and the required cloaked area size.

- *Temporal constraint.* The user can specify her privacy requirements for different time intervals. For example, a user is willing to reveal her location information during office hours, e.g., ($K = 1, A_{min} = 0$ mile) between 8:00 AM and 5:00 PM, but she needs high privacy protection after office hours, e.g., ($K = 100, A_{min} = 5$ miles) after 5:00 PM.

- *Spatial constraint.* The user can specify her privacy requirements for different geographic regions. For example, a user needs a small A_{min} in downtown areas, e.g., ($K = 50, A_{min} = 1$ mile), but a large A_{min} in rural areas, e.g., ($K = 50, A_{min} = 10$ miles). This is because a high density of geographic features in a downtown area can make the adversary very difficult to infer anything

about the user even a small cloaked area of a couple of city blocks.

- *Interdependent constraint.* The user can specify an interdependence between the anonymity level and the size of a cloaked area. For example, a user can specify a maximum area A_{max} requirement of her cloaked areas, i.e., she is happy with a cloaked area of a size A_{max} regardless of the number of users within the cloaked area. A_{max} also ensures the query utility of our spatial cloaking algorithm.

Since it is straightforward to extend our P2P spatial cloaking algorithm to support temporal, spatial, and/or interdependent constraints, we only discuss how our algorithm finds cloaked areas satisfying both k and A_{min} in this paper.

Mobile users. Each mobile user is equipped with two wireless network interface cards; one of them is dedicated to connect to a mobile base station to communicate with *location-based database servers*, while the other one is devoted to communicate with other peers via multi-hop routing without any support of fixed communication infrastructure or centralized/distributed servers. This multi-interface approach has been adopted in location-based services (e.g., [19, 105]) and mobile peer-to-peer information access applications (e.g., [106, 107]). Each user is also equipped with a positioning device, e.g., GPS, to determine her location that is represented as a coordinate (x, y). It is important to note that we do not have any assumption about the transmission range of the user mobile device, i.e., the mobile users can have different transmission ranges, and the network topology.

Location-based database servers. A privacy-aware query processor embedded inside the *location-based database server* has the ability to deal with location-based queries with cloaked areas. When a mobile user wants to obtain services from a location-based service provider, she executes our P2P spatial cloaking algorithm to blur her location into a cloaked area that satisfies her privacy requirements. Then, the user sends her location-based query along with the cloaked area to the database server. Since the query processor does not know the exact user location, it can only compute an answer set that includes the exact answer to the user. Then, the database server sends the answer set to the user, and the user computes the exact answer from the answer set.

7.2 Peer-to-Peer Spatial Cloaking Algorithm

We now present our spatial cloaking algorithm in mobile peer-to-peer (P2P) environments where no fixed communication infrastructure or centralize/distributed servers are available. Thus, the mobile users are only able to collaborate with each other through multi-hop routing to execute our algorithm. Such a highly ad-hoc mobile network poses many limitations to the computing environment, e.g., user mobility, limited transmission range, multi-hop communication, scarce communication resources, and network partition problems. In this section, we first describe our P2P spatial cloaking algorithm (Section 7.2.1). Then, we present the three key features proposed for our algorithm. Section 7.2.2 describes the *information sharing scheme* that enables users to share their gathered peer location information with nearby peers in order to reduce communication overhead. Section 7.2.3 gives the *historical location scheme* that allows users to utilize stale peer location information to alleviate the network partition problem. Section 7.2.4 presents the *cloaked area adjustment scheme* that guarantees our algorithm to be free from the "center-of-cloaked-area" privacy attack. We start by assuming that the network partition problem does not take place, i.e., all mobile users can communicate with each other through multi-hop routing in the network. The network partition problem will be addressed in Section 7.2.3.

7.2.1 Spatial Cloaking Algorithm

The basic idea of our P2P spatial cloaking algorithm is that a mobile user communicates with other peers via multi-hop routing to find at least $K-1$ peers. Then, the user determines a cloaked area that includes the $K-1$ nearest peers and herself. The cloaked area is k-anonymous because the user is indistinguishable among k users within the cloaked area. After satisfying the k-anonymity privacy requirement, the user extends the cloaked area to have an area of at least A_{min}, in order to satisfy the minimum area privacy requirement. To obtain location-based services, the user sends her location-based query along with the result cloaked area as her blurred location information to a database server. We will discuss how the database server computes an answer set that includes the exact answer to the user based on the cloaked area in Section 7.3.

Algorithm 8 Peer-to-Peer Spatial Cloaking

1: **function** P2PSpatialCloaking(User U)
2: //***Step 1: Peer Search Step***
3: $List \leftarrow \{\emptyset\}$
4: $h \leftarrow 1$
5: **while** $NumUser(List) < U.K - 1$ **do**
6: Broadcast a request to the peers within h hop(s) from U
7: $List \leftarrow List \cup \{$the received peer location information$\}$
8: $h \leftarrow h + 1$
9: **end while**
10: //***Step 2: Cloaked Area Step***
11: $S \leftarrow \{U\} \cup \{$the $K - 1$ nearest peers of U in $List\}$
12: $A \leftarrow$ a minimum bounding rectangle of all users in S
13: **if** $Area(A) < U.A_{min}$ **then**
14: $\alpha \leftarrow \frac{-2(w+l)+\sqrt{4(w+l)^2-16(Area(A)-U.A_{min})}}{8}$, where w and l are the width and length of A, respectively
15: Expand each edge of A by α
16: **end if**
17: **return** A

Algorithm. Algorithm 8 depicts the pseudo code of our P2P spatial cloaking algorithm. Figure 7.2 depicts a running example to illustrate the algorithm where 15 mobile users are labeled from m_1 to m_{15}. m_8 who executes the algorithm is represented by a triangle, and other peers are represented by circles. We assume that m_8's required anonymity level is five, i.e., $K = 5$, and her required minimum area is A_{min}. In general, the P2P spatial cloaking algorithm consists of two main steps.

Step 1: ***Peer search step.*** The user U starts this step by enlisting her neighbor peers for help. First, U broadcasts a request to her neighbor peers, i.e., the hop distance between U and her neighbor peers is one ($h = 1$). Each neighbor peer replies her identity and location information to U. Then, U stores the received peer information in a list $List$. If U has at least $K - 1$ neighbor peers, U gets enough peer information, so U proceeds to the next step. However, if U does not have at least $K - 1$ neighbor peers, U has to enlist multi-hop peers for help. U increases h by one, i.e., $h = 2$, and broadcasts the request to the peers within two hop distance. When a peer receiving the request, if $h > 1$, the peer replies her identity and location information to U, decreases h by one, and forwards the request with the updated h to her neighbor peers. However, if $h = 1$,

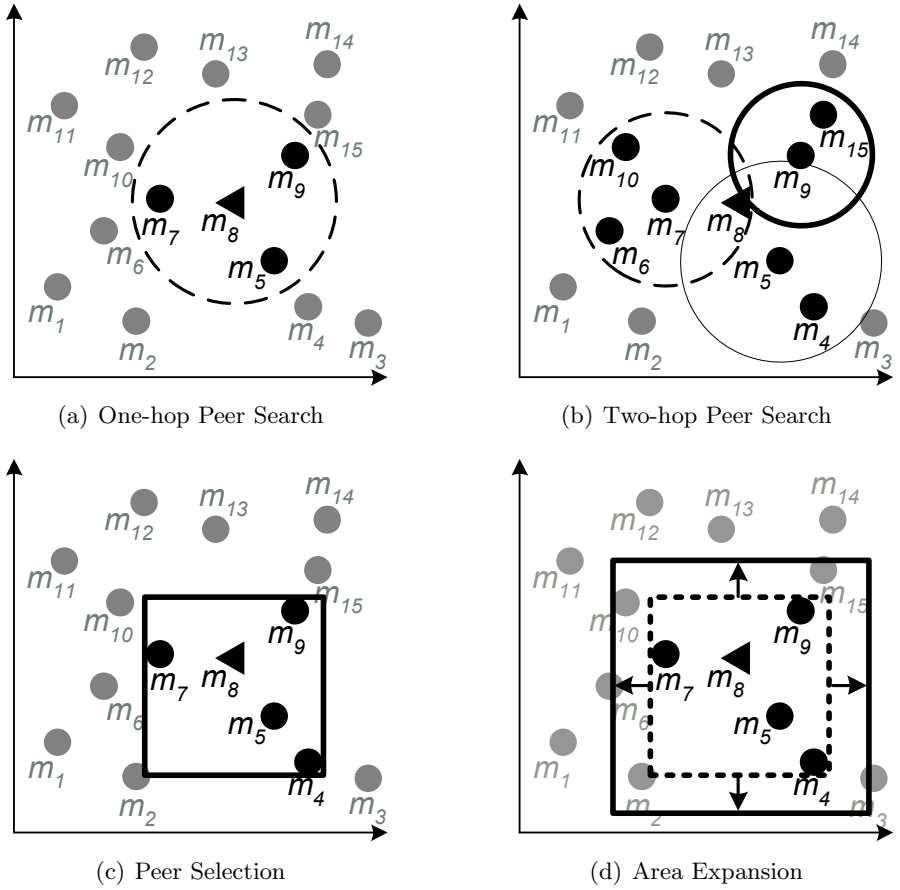

(a) One-hop Peer Search

(b) Two-hop Peer Search

(c) Peer Selection

(d) Area Expansion

Figure 7.2: Example of the peer-to-peer spatial cloaking algorithm.

the peer simply replies her identity and location information to U. U also stores the received peer information in $List$. In case that U still cannot find an adequate number of peers within h hop distance, i.e., $NumUser(List) < K - 1$, where $NumUser(List)$ returns the total number of peers included in $List$, U repeats this peer search process until U finds at least $K - 1$ peers, as depicted in Lines 5 to 9 in Algorithm 8. After U finds enough peer location information, it proceeds to the *cloaked area step*.

Figures 7.2a and 7.2b illustrate the *peer search step*, where m_8 executes the algorithm. The transmission range of m_8 is represented by a dotted circle (Figure 7.2a). Thus, m_8 finds three neighbors peers, m_5, m_7, and m_9, that are represented by black circles, when m_8 searches for her neighbor peers (i.e., $h = 1$). Since m_8 cannot find an

adequate number of peers to satisfy her required anonymity level, i.e., $m_8.K = 5$, m_8 has to enlist more peers for help. m_8 broadcasts a request with $h = 2$ to her neighbor peers. After the neighbor peers m_5, m_7, and m_9 receive the request with $h > 1$, they send their identity and location information to m_8, decrease h by one, and forward the request with $h = 1$ to their neighbor peers. In Figure 7.2b, the transmission ranges of m_5, m_7, and m_9 are represented by thin, dotted, and bold circles, respectively. Thus, the two-hop peers m_4, m_6, m_{10}, and m_{15} receive the request with $h = 1$. Since $h = 1$, they simply send their identity and location information to m_8. After the two-hop search, m_8 has the location information of seven peers, m_4, m_5, m_6, m_7, m_9, m_{10}, and m_{15}, m_8 has enough peer location information to proceed to the *cloaked area step*.

Step 2: ***Cloaked area step.*** This step takes the peer location information stored in *List* from the previous step as an input, and determines a cloaked area A that satisfies both the user k-anonymity and minimum area privacy requirements, i.e., $NumUser(A) \geq K$ and $Area(A) \geq A_{min}$, where $Area(A)$ returns the area of A. We find a set of users S that includes U and the $K - 1$ nearest peers to U in *List* (Line 11 in Algorithm 8). Then, A is a minimum bounding rectangle of U and the selected peers in S (Line 12 in Algorithm 8). A is represented by its bottom-left vertex (x_s, y_s) and top-right vertex (x_e, y_e).

Although A already satisfies the k-anonymity privacy requirement, we still need to check for the minimum area privacy requirement. If the area of A is larger than or equal to A_{min}, i.e., $Area(A) \geq A_{min}$, the algorithm simply returns A as U's blurred location information. However, if $Area(A) < A_{min}$, we extend each edge of A by a distance α such that the area of the extended A is equal to A_{min}. Let w and l be the width (i.e., $x_e - x_s$) and height (i.e., $y_e - y_s$) of A, respectively. We can determine α by solving the following equation:

$$\begin{aligned} (w + 2\alpha)(l + 2\alpha) &= A_{min} \\ 4\alpha^2 + 2(w + l)\alpha + w \times l - A_{min} &= 0 \\ 4\alpha^2 + 2(w + l)\alpha + Area(A) - A_{min} &= 0 \end{aligned} \tag{7.1}$$

Since $Area(A) - A_{min} < 0$, $[2(w + l)]^2 - 4(4)(Area(A) - A_{min}) \geq 0$, i.e., the discriminant of Equation 7.1 is non-negative; hence, α is equal to the non-negative root of Equation 7.1, i.e., $\alpha = \frac{-2(w+l)+\sqrt{4(w+l)^2-16(Area(A)-A_{min})}}{8}$, as depicted in Line 14

in Algorithm 8. After determining α, we extend each edge of A by α to form a new cloaked area that satisfies both the k-anonymity and minimum area privacy requirements. Thus, the bottom-left and top-right vertices of the extended A are $(x_s-\alpha, y_s-\alpha)$ and $(x_e+\alpha, y_e+\alpha)$, respectively.

Figures 7.2c and 7.2d illustrate the *cloaked area step*, where m_8 knows the location information of seven peers, i.e., $List = \{m_4, m_5, m_6, m_7, m_9, m_{10}, m_{15}\}$. We find a set of users S that includes m_8 and the four nearest peers of m_8 in $List$, i.e., m_4, m_5, m_7, and m_9. The selected peers in S are represented by black circles in Figure 7.2c. Then, we determine a minimum bounding rectangle of the users in S as a cloaked area A that is represented by a rectangle. In this example, we assume that the area of A is less than A_{min}. Thus, we determine α and extend each edge of A by α. In Figure 7.2d, the distance of α is indicated by arrows, and the extended A is represented by a rectangle, while the original A is represented by a dotted rectangle.

7.2.2 Information Sharing Scheme

As described in the previous section, when a mobile user wants to obtain anonymous location-based services from a service provider, she executes our P2P spatial cloaking algorithm to blur her location into a cloaked area. Due to scarce communication resources in mobile P2P environments, excessively searching the network for peers could pose a scalability issue. For example, if many nearby users search the network for peers within a short time period, they would suffer from long searching time. In the mobile P2P network, the user has to enlist her neighbor peers for help to forward messages to multi-hop peers, in order to search the network for enough peer information. Thus, a set of nearby mobile users would have a similar set of peers within the same hop distance. To this end, we propose the *information sharing scheme* for our P2P spatial cloaking algorithm to improve system scalability. The main idea is to enable a group of nearby mobile users to share their gathered peer location information with others. If the user obtains enough peer location information from her neighbor peer, she can blur her location without performing the *peer search step* in Algorithm 8. Thus, the *information sharing scheme* can reduce communication and computational overhead.

Algorithm. Algorithm 9 depicts the pseudo code of the *information sharing scheme*. In this scheme, after the mobile user has found enough peer information through

Algorithm 9 Information Sharing Scheme

1: **function** InformationSharingScheme(User U, Tolerance tol_s)
2: //***Step 1: Peer Search Step***
3: $List$ stores the received peer location information of the last peer search
4: **if** the timestamp of the last peer search $< t_{now} - tol_s$ **then**
5: Request the neighbor peers to turn in their $List$ size and the timestamp of their last peer search t_{search}
6: **if** some neighbor peer has $List$ with a size of at least $U.K$ and the timestamp of her last peer search $\geq t_{now} - tol_s$ **then**
7: Select the neighbor peer P with the latest peer search timestamp
8: Request P to turn in the cached location information of the k-nearest peers to U
9: $List \leftarrow$ the received peer location information
10: **else**
11: **return** P2PSpatialCloaking(User U) (i.e., Algorithm 8)
12: **end if**
13: **end if**
14: //***Step 2: Cloaked Area Step***
15: Adjust the peer location information in $List$
16: $A \leftarrow$ a minimum bounding rectangle includes U and the adjusted location region of the $K-1$ nearest P of U in $List$
17: Execute Lines 13 to 16 in Algorithm 8 to ensure that A satisfies the minimum area privacy requirement
18: **return** A

the *peer search step* in Algorithm 8, she maintains the received peer information in $List$ and records the timestamp, t_{search}, when the last *peer search step* started. Since this scheme only provides the cached peer location information for the user, the information could be cached a long time ago. The older the cached information, the lower the quality of a cloaked area (i.e., the cloaked area size) will be obtained. To this end, the *information sharing scheme* enables the user to control the staleness of the cached information through a user specified parameter tol_s. In other words, the user only utilizes the peer's stored information cached not earlier than tol_s. The *information sharing scheme* can be incorporated into our P2P spatial cloaking algorithm (i.e., Algorithm 8) with the following modifications.

Step 1: *Peer search step.* The user U starts this step by checking whether she can use her cached information and/or her neighbor peers' cached information to blur her

location. U first checks the freshness of her cached peer information. If the timestamp of the last peer search is larger than or equal to $t_{now} - tol_s$, where t_{now} is the current time, U can reuse her cached peer information. Otherwise, U requests her neighbor peers to reply with the size of their *List* along with t_{search} (Line 5 in Algorithm 9). If more than one neighbor peer caches enough peer location information and $t_{search} \geq t_{now} - tol_s$, U selects the peer P caching the freshest information, i.e., the largest t_{search} (Line 7 in Algorithm 9). Then, U requests P to turn in the $K-1$ nearest peer information to U. However, if no neighbor peer caches enough peer location information or the cached information is too stale, U simply executes the original *peer search step* in Algorithm 8 (Line 11 in Algorithm 9). After U receives enough peer information, U stores the peer information in *List*.

Step 2: ***Cloaked area step.*** Due to user mobility, i.e., mobile users are continuously moving, the only modification to this step is to capture the location uncertainty of the cached peer information. The basic idea is that given a peer's location cached at time t, we use a conservative approach to determine a location region that includes all possible locations of the peer at current time t_{now}. Since the current location of the peer could be at any point within a circular area centered at the peer's cached location with a radius of $(t_{now} - t) \times v_{max}$, where v_{max} is the maximum possible speed of the peer and t is the time when the peer's location information was cached, such a circular area constitutes the peer's *adjusted location region*. For a peer P with an adjusted location region, we consider the maximum distance between U and P's adjusted location region, i.e., $d_{max}(U, P) = d(U, P) + (t_{now} - t) \times v_{max}$, as their distance. In reality, v_{max} can be set to the maximum legal speed in the system area. Then, we form a k-anonymous cloaked area A as a minimum bounding rectangle of U and the adjusted location region of the $K-1$ peers (Line 16 in Algorithm 9). If A does not satisfy the minimum area privacy requirement, we extend A as in the original *cloaked area step* in Algorithm 8 (Line 17 in Algorithm 9).

7.2.3 Peer-to-Peer Spatial Cloaking in a Partitioned Network

Since we consider a highly ad hoc mobile environment, where no fixed communication infrastructure or centralized/distributed servers are available, mobile users can only communicate with each other via multi-hop peer-to-peer routing. Due to user mobility,

mobile users may be partitioned into disjoint networks. When a network partition takes place, a mobile user can only communicate with other peers residing in her network partition. If a user's required anonymity level is larger than the number of users residing in her network partition, the user cannot find enough peer location information to blur her location information; and thus, the user suffers from a network partition problem. In this section, we first discuss how to detect a network partition problem and two straightforward approaches to alleviate it, and then propose the *historical location scheme* to better alleviate the network partition problem.

We now discuss how to detect a network partition problem in the *peer search step* in Algorithm 8. Let $List_h$ be the set of peer location information that is found by the *peer search step* with a hop distance h. It is expected to find more peers as h increases, i.e., $|List_h| > |List_{h-1}|$. Thus, we know that a network partition takes place when $|List_h| = |List_{h-1}|$. It is important to note that we only need to record the size of $List_{h-1}$ without maintaining the peer location information. There are two straightforward approaches that a user can use to overcome the network partition problem. (1) After the user suffers from the network partition problem, she periodically performs the *peer search step* until she can find enough peer location information. (2) After the user cannot find an adequate number of peers in her network partition, she simply reduces her required k-anonymity level to the number of users residing in her network partition. However, these two straightforward approaches have drawbacks. The first approach would incur very long searching time while the second one requires the user to degrade her privacy protection. To this end, we propose the *historical location scheme* that enables the users to utilize their or other peers' cached information to better alleviate the network partition problem.

Algorithm. Algorithm 10 depicts the pseudo code of the *historical location scheme*, and Figure 7.3 gives an example to illustrate this scheme. Similar to the *information sharing scheme*, the user can control the staleness of the historical peer location information through a tolerance parameter tol_h. Thus, this scheme only uses the historical peer location information that was cached not earlier than $t_{now} - tol_h$. When U suffers from the network partition problem in the *peer search step* in Algorithm 8, i.e., $|List_h| = |List_{h-1}|$ and $List_{h-1} < K$, U sets $h_{last} = h - 1$ and executes the *historical location scheme*. In general, the *historical location scheme* can be incorporated into our

Algorithm 10 Historical Location Scheme

1: **function** HISTORICALLOCATIONSCHEME(*User* U, Tolerance tol_h)
2: //***Step 1: Peer Search Step***
3: **if** U detects $|List_h| = |List_{h-1}|$ in the *peer search step* in Algorithm 8 **then**
4: $h_{last} \leftarrow h - 1$
5: $h \leftarrow 1$
6: **while** $|List| < U.K - 1$ **or** $h \leq h_{last}$ **do**
7: Send a request with $U.K$ and tol_h to the peers within h hops
8: $List \leftarrow List \cup$ {the "*uncertain*" cached location information returned by the peers}
9: $h \leftarrow h + 1$
10: **end while**
11: **end if**
12: //***Step 2: Cloaked Area Step***
13: Adjust the *uncertain* peer location information in $List$
14: **if** $|List| \geq K - 1$ **then**
15: $S \leftarrow \{U\} \cup \{$the $K - 1$ peer nearest to U in $List\}$
16: **else**
17: $S \leftarrow \{U\} \cup List$
18: **end if**
19: $A \leftarrow$ a minimum bounding rectangle includes U, the peers with *exact* location information in S, and the adjusted location region of the peers with *uncertain* location information
20: Execute Lines 13 to 16 in Algorithm 8 to insure that A satisfies the minimum area privacy requirement
21: **return** A

P2P spatial cloaking algorithm with the following modifications.

Step 1: *Peer search step.* As $List$ already stores the *exact* location information of the peers residing in U's network partition through the previous peer search process, U only needs to ask them to turn in their cached peer location information. Initially, U sends a request with a parameter tol_h and a hop distance $h = 1$ to her neighbor peers. Then, the neighbor peer sends the location information cached not earlier than $t_{now} - tol_h$ to U. U stores this cached location information in $List$ and marks it as *uncertain*. When U receives duplicate peer location information, U only keeps the freshest one. Similar to the original *peer search step* in Algorithm 8, if U cannot find enough peer location information in $List$ with a hop distance h, U increases h by one and rebroadcasts the request. This peer search process repeats until U finds enough

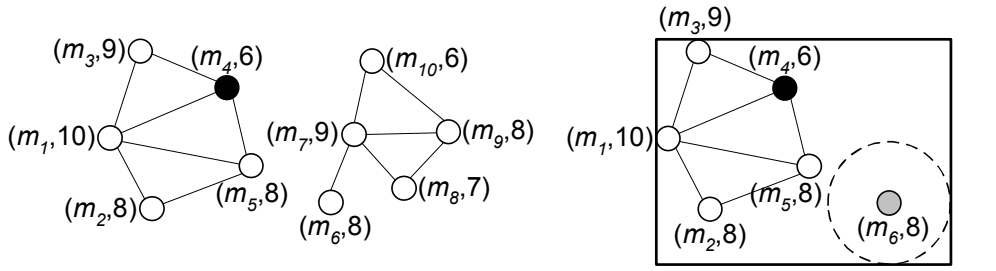

(a) Partitioned Network (b) Historical Location Scheme

Figure 7.3: Example of peer-to-peer spatial cloaking in a partitioned network.

peer location information or $h = h_{last}$ (Lines 6 to 10 in Algorithm 10). After U finishes the peer search process, she proceeds to the next step regardless of whether $List$ stores enough peer location information.

Step 2: *Cloaked area step.* The user U starts this step by adjusting the *uncertain* peer location information in $List$ as in the *information sharing scheme*. If $|List| \geq U.K-1$, U adds the $K-1$ nearest peers in $List$ and herself to S (Line 15 in Algorithm 10). For a peer P with *uncertain* location information, the distance between U and P is the maximum distance between U and the adjusted location region of P, i.e., $d_{max}(U, P) = d(U, P) + (t_{now} - t) \times v_{max}$. However, if $|List| \leq U.K$, we use the second straightforward approach to temporally reduce $U.K$ to $|List| + 1$ (Line 17 in Algorithm 10); and thus, U simply adds all peers in $List$ and herself to S. Then, U forms a cloaked area A that includes the peers with the *exact* location information and the adjusted location region of the peers with the *uncertain* location information in S (Line 19 in Algorithm 10). If A does not satisfy the minimum area privacy requirement, we extend A as in the original *cloaked area step* in Algorithm 8 (Line 20 in Algorithm 10).

Example. Figure 7.3 depicts an example of a partitioned network where the mobile users are partitioned into two disjoint networks. One network partition includes five mobile users m_1 to m_5, while the other partition includes five mobile users m_6 to m_{10} (Figure 7.3a). Each user is labeled with a pair of values, where the first value is her identity and the second value is her required anonymity level. In this example, m_4 (represented by a black circle) executes the P2P spatial cloaking algorithm to blur her location into a cloaked area. Since the number of users residing in m_4's network

partition is less than her required anonymity level, i.e., $m_4.K = 6$, m_4 suffers from the network partition problem. After m_4 performs the peer search process with a hop distance of $h = 3$, she detects the network partition problem because $|List_2| = |List_3|$ (i.e., $h_{last} = 2$). We assume that m_5 caches the location information of m_6. Thus, m_4 can find enough peer location information after she enlists the peers within two hop distance for help to turn in their cached location information. *List* stores the location information of five peers, i.e., $List = \{m_1, m_2, m_3, m_5, \underline{m_6}\}$, where the peer with *uncertain* location information is underlined. Then, m_4 adjusts m_6's location information, and the adjusted location region of m_6 is represented by a dotted circle, as depicted in Figure 7.3b. The cloaked area A of m_4 that is represented by a rectangle includes m_4, the peers with *exact* location information in *List*, i.e., m_1, m_2, m_3, and m_5, and the adjusted location region of m_6 (i.e., the dotted circle). We assume that A satisfies m_4's minimum area privacy requirement, so A is returned to m_4 as her cloaked area.

7.2.4 Cloaked Area Adjustment Scheme

As discussed in Section 7.2.1, our P2P spatial cloaking selects the nearest peers of a mobile user to form her cloaked area A. This peer selection process may pose a privacy breach that the query issuer tends to be the closest to the center of A, i.e., the "center-of-cloaked-area" privacy attack [39, 44, 108]. Such a privacy breach may give more information to an adversary to infer the query issuer's actual location. To prevent this privacy breach, we should adjust A such that the probability of the query issuer being the closest to the center of A is $1/K$. To this end, we propose the *cloaked area adjustment scheme* that prevents the "center-of-cloaked-area" privacy attack if the user knows the exact location information of the peers residing in A. In case that the user only knows the historical location information of some peers residing in A, the *cloaked area adjustment scheme* can still alleviate the "center-of-cloaked-area" privacy attack. We will evaluate the resistance of our *cloaked area adjustment scheme* to this privacy attack through extensive experiments in Section 7.4.1.

Algorithm. Algorithm 11 gives the pseudo code of the *cloaked area adjustment scheme*. This algorithm is called by Algorithm 8 after executing Line 12; thus, we

Algorithm 11 Cloaked Area Adjustment Scheme

1: **function** CloakedAreaAdjustment(*User* U, *UserSet* S, *Area* A)
2: $C'_A \leftarrow C_A$; $A' = \{(x'_s, y'_s), (x'_e, y'_e)\} \leftarrow A = \{(x_s, y_s), (x_e, y_e)\}$
3: $P_C \leftarrow$ the nearest user in S to C_A
4: $P \leftarrow$ a randomly selected user in S
5: **if** $P \neq P_C$ **then**
6: //***Step 1: Center Adjustment Step***
7: $P_N \leftarrow$ the nearest user in S to P
8: $M \leftarrow$ the intersection point between line $\overline{PC_A}$ and the circle centered at P with a radius of $d(P, P_N)/2$
9: $R \leftarrow$ a random value within a range of $(d(M, C_A), d(P, C_A)]$
10: $C'_A \leftarrow \left(\frac{[d(P,C_A)-R]\times C_A.x + R\times P.x}{d(P,C_A)}, \frac{[d(P,C_A)-R]\times C_A.y + R\times P.y}{d(P,C_A)}\right)$
11: //***Step 2: Area Adjustment Step***
12: $\Delta_x \leftarrow |C'_A.x - C_A.x|$
13: $\Delta_y \leftarrow |C'_A.y - C_A.y|$
14: **if** $C'_A.x < C_A.x$ **then** $x'_s \leftarrow x_s - 2\Delta_x$; **else** $x'_e \leftarrow x_e + 2\Delta_x$
15: **if** $C'_A.y < C_A.y$ **then** $y'_s \leftarrow y_s - 2\Delta_y$; **else** $y'_e \leftarrow y_e + 2\Delta_y$
16: **end if**
17: **return** A'

add the statement "$A \leftarrow$ CloakedAreaAdjustment(U, S, A)" after Line 12 in Algorithm 8. The inputs to the algorithm include a user U, a set of users S selected by the *cloaked area step* in Algorithm 8, and a minimum bounding box of the users in S, A. A is represented by its bottom-left vertex (x_s, y_s) and top-right vertex (x_e, y_e), and the center of A is $C_A = ((x_s + x_e)/2, (y_s + y_e)/2)$. The output of this algorithm is an adjusted cloaked area A' that is represented by its bottom-left vertex (x'_s, y'_s) and top-right vertex (x'_e, y'_e), and C'_A is the center of A'. Initially, we set $A' = A$ (Line 2 in Algorithm 11). For the peer with historical location information in S, we consider the center of her adjusted location region as her location. We start this algorithm by randomly selecting a user P in S and finding the nearest user P_C in S to the center of A, C_A. If $P = P_C$, we simply return the original A to Algorithm 8; otherwise, we have to adjust A by the following two main steps.

Step 1: ***Center adjustment step.*** Figure 7.4a illustrates this step where the gray and black squares represent the center of the input A (C_A) and the center of the adjusted A' (C'_A), respectively. The user U starts this step by finding the nearest user P_N in S to P. Then, U computes the intersection point M between line $\overline{PC_A}$ and the

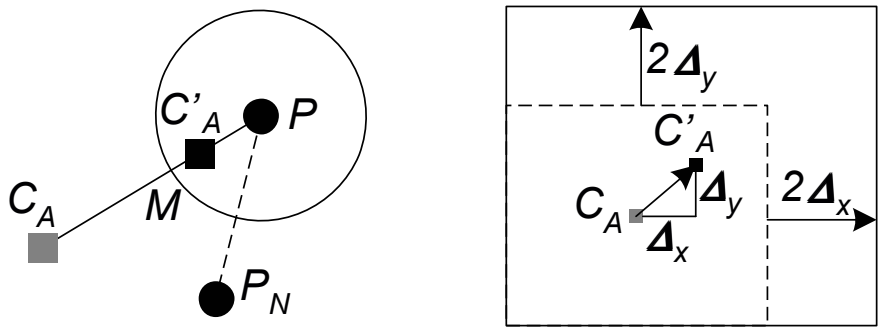

(a) Center Adjustment (b) Cloaked Area Adjustment

Figure 7.4: Examples of the cloaked area adjustment scheme.

circle centered at P with a radius of $d(P, P_N)/2$ (Line 8 in Algorithm 11). To guarantee that P will be the closest one to C'_A, C_A has to be moved towards P by a distance of greater than $d(M, C_A)$. We can set the upper bound of the adjustment distance to $d(P, C_A)$. If the adjustment distance is $d(P, C_A)$, C'_A will be located at P. To avoid revealing any location information of the user residing in A, we randomly select a value R within a range $(d(M, C_A), d(P, C_A)]$ (Line 9 in Algorithm 11). Then, C_A is moved towards P by a distance of R; hence, the adjusted center C'_A is:

$$\left(\frac{[d(P, C_A) - R] \times C_A.x + R \times P.x}{d(P, C_A)}, \frac{[d(P, C_A) - R] \times C_A.y + R \times P.y}{d(P, C_A)} \right).$$

Step 2: ***Area adjustment step.*** Figure 7.4b illustrates this step where the solid and dotted rectangles represent the adjusted A' and the input A, respectively. After the user U determines the center of the adjusted A, C'_A, we adjust A such that C'_A is the center of A'. To form A', we can determine the difference between the coordinates of C_A and C'_A, i.e., $\Delta_x = |C'_A.x - C_A.x|$ and $\Delta_y = |C'_A.y - C_A.y|$ (Lines 12 to 13 in Algorithm 11). Then, we extend the nearest vertical edge of A to C'_A by a distance of $2\Delta_x$, and the nearest horizontal edge of A to C'_A by a distance of $2\Delta_y$. Mathematically, we can compute the coordinates of A' by using the equations given in Lines 14 to 15 in algorithm 11.

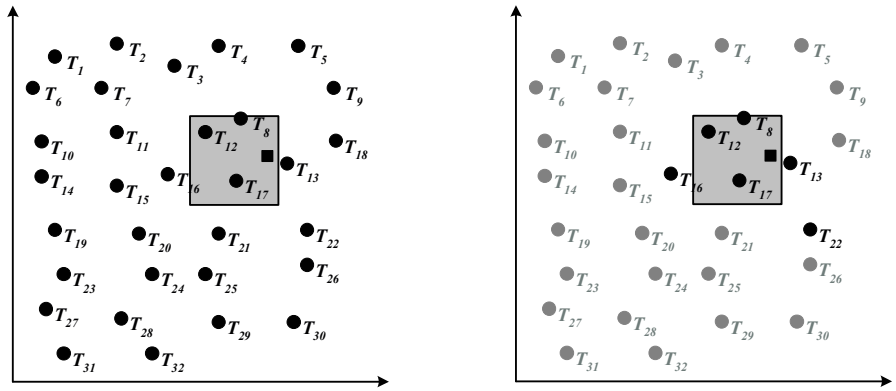

(a) Server Side (b) Client Side

Figure 7.5: Privacy-aware nearest-neighbor query processing.

7.3 Anonymous Location-based Services

To enable location-based database servers to support privacy-aware location-based queries with cloaked areas rather than with exact location points, the database server needs to be equipped with a privacy-aware query processor [17, 80, 44, 12]. In this paper, we adopt the work [80] as our privacy-aware query processor because it minimizes the communication overhead of sending a minimal answer set from the database server to the user while guaranteeing the user can get the exact answer. When a user wants to issue a privacy-aware location-based queries, she executes our P2P spatial cloaking algorithm to blur her location into a cloaked area. Then, the user sends the query along with the cloaked area to the location-based database server. After the privacy-aware query processor computes a minimal answer set that includes the exact answer to the user, the database server sends the answer set to the user. Finally, the user computes the exact answer from the answer set. The smaller the cloaked area, the smaller the answer set will be returned to the user. However, the user may need to relax her privacy requirements to achieve a smaller cloaked area. Thus, a trade-off between the user privacy protection and the quality of services can be achieved.

Figure 7.5 illustrates the privacy-aware nearest-neighbor query processing. Figure 7.5a depicts the data objects, e.g., gas stations, stored at the server side. There are 32 data objects T_1 to T_{32} represented by black circles, the shaded area represents

Table 7.1: Summary of the features of our algorithms.

	P2P	P2P-IS	P2P-IS-CA	P2P-IS-CA-HL
Peer-to-Peer Spatial Cloaking (P2P)	√	√	√	√
Information Sharing Scheme (IS)	×	√	√	√
Cloaked Area Adjustment Scheme (CA)	×	×	√	√
Historical Location Scheme (HL)	×	×	×	√

the cloaked area of the mobile user who issued the query. For clarification, the actual mobile user location is plotted in Figure 7.5 as a black square inside the cloaked area A, i.e., the shaded area. However, such information is neither stored at the server side nor revealed to the server. The privacy-aware query processor determines a minimal answer set that includes the nearest object to every point within A. It has been proved that the minimal answer set includes all objects within A and the nearest object to every point of each edge of A [80]. In this example, the server returns the answer set that includes six objects, i.e., T_8, T_{12}, T_{13}, T_{16}, T_{17}, and T_{22}, to the user. Then, the user computes the exact answer, i.e., T_{13}, from the answer set. The algorithmic detail of the privacy-aware query processor is beyond the scope of this paper. Interested readers are referred to [80] for more details.

7.4 Experiment Results

In this section, we evaluate the performance of our P2P spatial cloaking algorithm (denoted as P2P) with the three key features, *information sharing scheme* (denoted as IS), *historical location scheme* (denoted as HL), and *cloaked area adjustment scheme* (denoted as CA) through simulated experiments. Our P2P spatial cloaking algorithm (P2P) corresponds to the *on-demand* approach of the state-of-the-art P2P spatial cloaking algorithm [19]. We do not consider the *proactive* approach because its communication overhead is much higher than the *on-demand* approach. Table 7.1 summaries the features of our algorithms.

We evaluate our algorithms with respect to five important performance measures. (1) *Number of messages.* This measure gives the average number of messages incurred

by our algorithms per each query. It indicates the network bandwidth consumption and the power consumption on user devices. (2) *Cloaked area size.* This measure gives the average size of cloaked areas generated by our algorithms. The smaller the cloaked area, the more accurate the location is reported to the location-based database server; the thus, this measure can indicate the location utility of our algorithms. (3) *Answer set size.* This measure indicates the average number of objects included in answer sets returned by the location-based database server. It also indicates the communication overhead of sending the answer set from the database server to the user. (4) *Anonymization success rate.* This is a ratio of the number of times that the anonymization algorithm can find enough peer location information to satisfy the user's k-anonymity privacy requirement to the total number of queries. (5) *Privacy attack probability.* This measure gives the resilience of our algorithms to the "center-of-cloaked-area" privacy attack by measuring the probability of the nearest user to the center of a cloaked area (U_c) being the actual query issuer, i.e., P(U_c is the query issuer).

We use a networked generator to generate moving objects on the road map of Hennepin County, Minnesota, USA. The road map consists of 57,020 edges and 42,135 vertices. Unless mentioned otherwise, all our experiments consider 100,000 mobile users in which 10% of them are randomly selected to issue nearest-neighbor queries (e.g., "*where is my nearest gas station*") at each time instance. The mobile users are moving at speeds between 50 and 70 miles per hour. Their required k-anonymity levels are uniformly selected from a range $[50, 100]$, while their required minimum areas are set to zero. There are 20,000 data objects that are uniformly distributed within the underlying road map. The default uncertainty tolerance for the *information sharing scheme* (tol_s) and *historical location scheme* (tol_h) is set to zero and 50 seconds, respectively. We consider a heterogeneous network environment where the transmission range of each user is uniformly selected within a range $[100, 200]$ meters. Table 9.1 summarizes the parameter settings.

7.4.1 Anonymization Strength

Figure 7.6 depicts the resilience of our algorithms to the "center-of-cloaked-area" privacy attack with respect to varying (a) the k-anonymity level from 100 to 300, (b) the number of users from 100,000 to 500,000, (c) the transmission range from $[100, 100]$ to $[100, 300]$

Table 7.2: Parameter settings.

Parameters	Default values	Ranges
Number of users	200K	100K to 500K
Number of querying users	20K	10K to 50K
Number of data objects	20K	10K to 50K
Transmission range	$[100, 200]$ meters	$[100, 100]$ to $[100, 300]$ meters
k-anonymity	$[50, 100]$	$[50, 100]$ to [50, 300]
Minimum area A_{min}	0	1 to 5 km^2
tol_s	0	0 to 50 seconds
tol_h	50 seconds	-
Movement speed	$[50, 70]$ miles per hour	-

meters, and (d) the uncertainty tolerance for the *information sharing scheme*, i.e., tol_s, from 0 to 50 seconds. The default k-anonymity level for (b)-(d) is 100. The results of P2P-IS-CA-HL, P2P-IS-CA, P2P-IS, and P2P are represented by black, gray, light gray, and white bars, respectively. The pattern bars represent the value of $1/K$ which indicates the ideal probability of the actual query issuer being the nearest user to the center of the cloaked area U_c, i.e., P(U_c is the query issuer). Although P2P is more vulnerable to the "center-of-cloaked-area" attack than P2P-IS (Figures 7.6a-7.6d), the probability of both P2P and P2P-IS are way above the ideal probability. The results show that our *cloaked area adjustment scheme* (CA) gives the probability of U_c being the actual query issuer is equal to or very close to $1/K$. Thus, our *cloaked area adjustment scheme* can effectively prevent the "center-of-cloaked-area" privacy attack.

7.4.2 Scalability

In this section, we evaluate the scalability of our algorithms with respect to large numbers of querying users, large numbers of users, and large numbers of data objects.

Figure 7.7 depicts the performance of our algorithms with respect to varying the number of querying users from 10,000 to 50,000 users, i.e., from 5% to 25% of 200,000 users. The performance of P2P is not affected by the number of querying users because there is no information sharing among users in P2P. The results show that our *information sharing scheme* (i.e., P2P-IS, P2P-IS-CA, and P2P-IS-CA-HL) effectively reduces

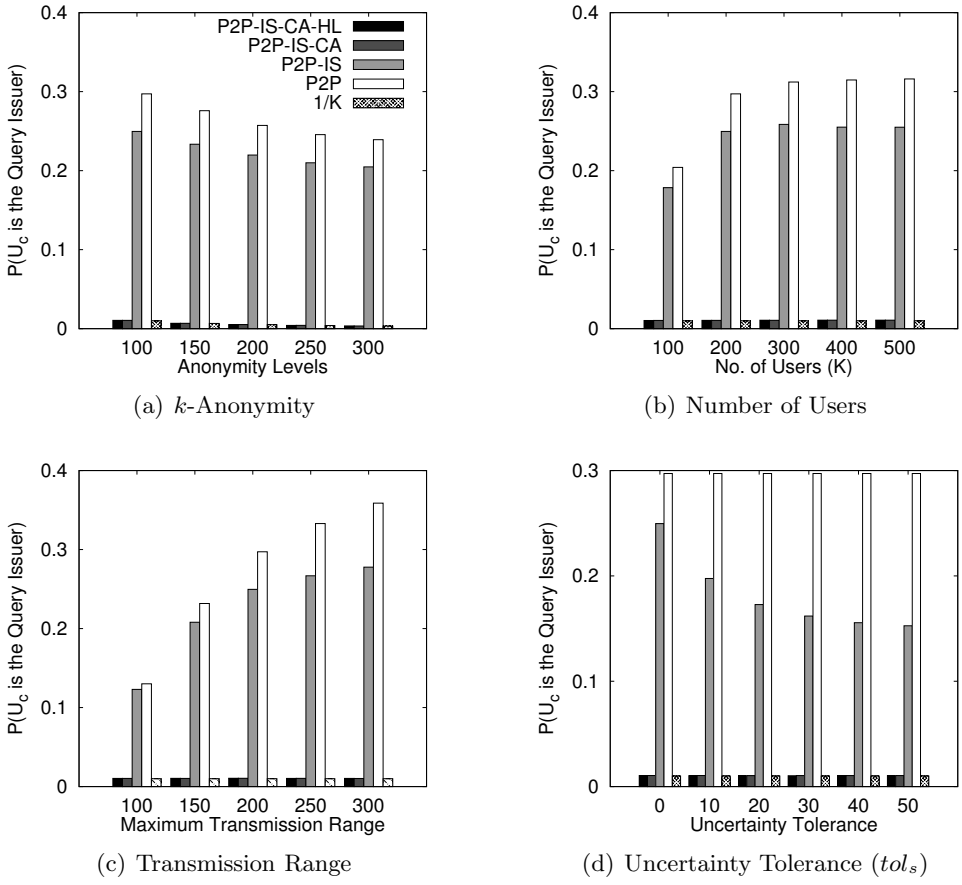

(a) k-Anonymity (b) Number of Users

(c) Transmission Range (d) Uncertainty Tolerance (tol_s)

Figure 7.6: "Center-of-cloaked-area" privacy attack.

communication overhead as there are more querying users (Figure 7.7a). The main reason is that when the number of querying users increases, there is a higher chance for a user to obtain enough peer location information from her neighbor peers without searching the network. Likewise, when a user encounters a network partition problem, she is more likely to get enough peer location information from other peers residing in her network partition, as there are more querying users. Thus, the anonymization success rate of P2P-IS-CA-HL improves with more querying users (Figure 7.7b). Since P2P-IS-CA-HL requires the users to adjust historical peer location to capture location uncertainty, they get larger cloaked areas than P2P-IS-CA (Figure 7.7c). Processing such larger cloaked areas at the database server results in larger answer sets (Figure 7.7d). It is important

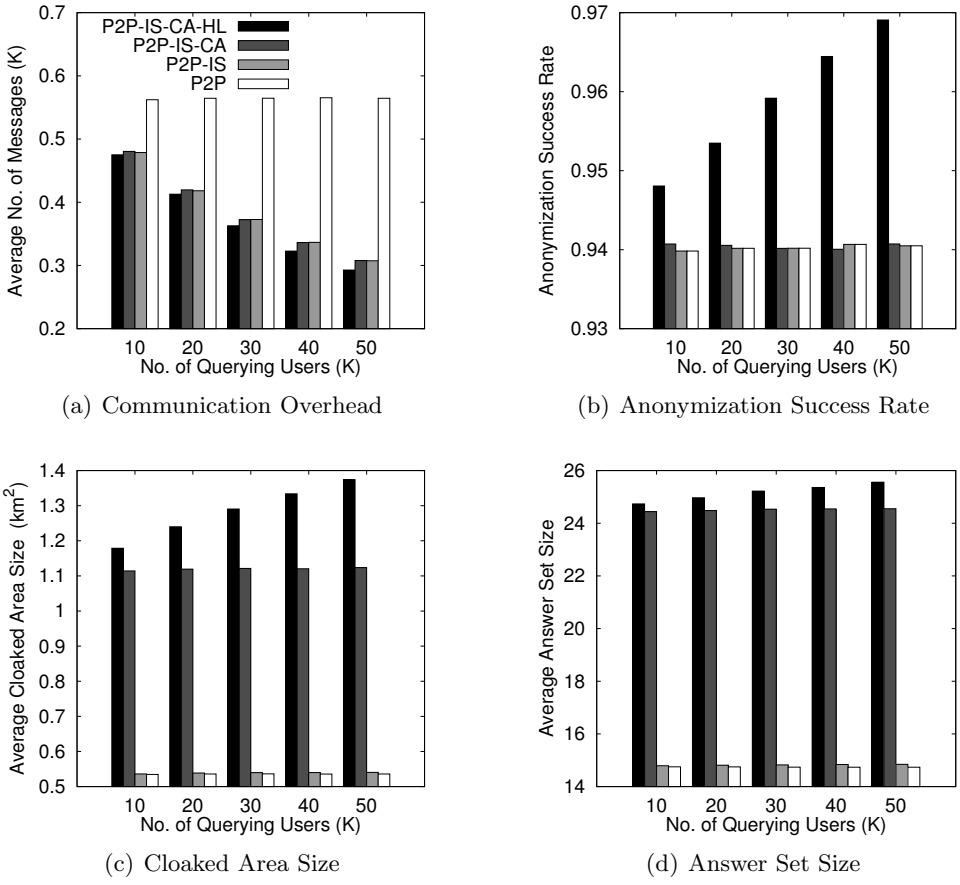

(a) Communication Overhead

(b) Anonymization Success Rate

(c) Cloaked Area Size

(d) Answer Set Size

Figure 7.7: Number of querying users.

to note that although our algorithms with the *cloaked area adjustment scheme*, i.e., P2P-IS-CA and P2P-IS-CA-HL, result in larger cloaked areas and answer sets than P2P and P2P-IS, P2P-IS-CA and P2P-IS-CA-HL are free from the "center-of-cloaked-area" privacy attack.

Figure 7.8 depicts the scalability of our algorithms with respect to increasing the number of users from 100,000 to 500,000. The results show that the performance of all algorithms gets better when there are more users. In a denser network, the user can find enough peer information to blur her location with a smaller hop distance, i.e., a smaller searching area; and hence, the communication overhead reduces (Figure 7.8a). When the number of users increases, there are more users in a network partition. Thus,

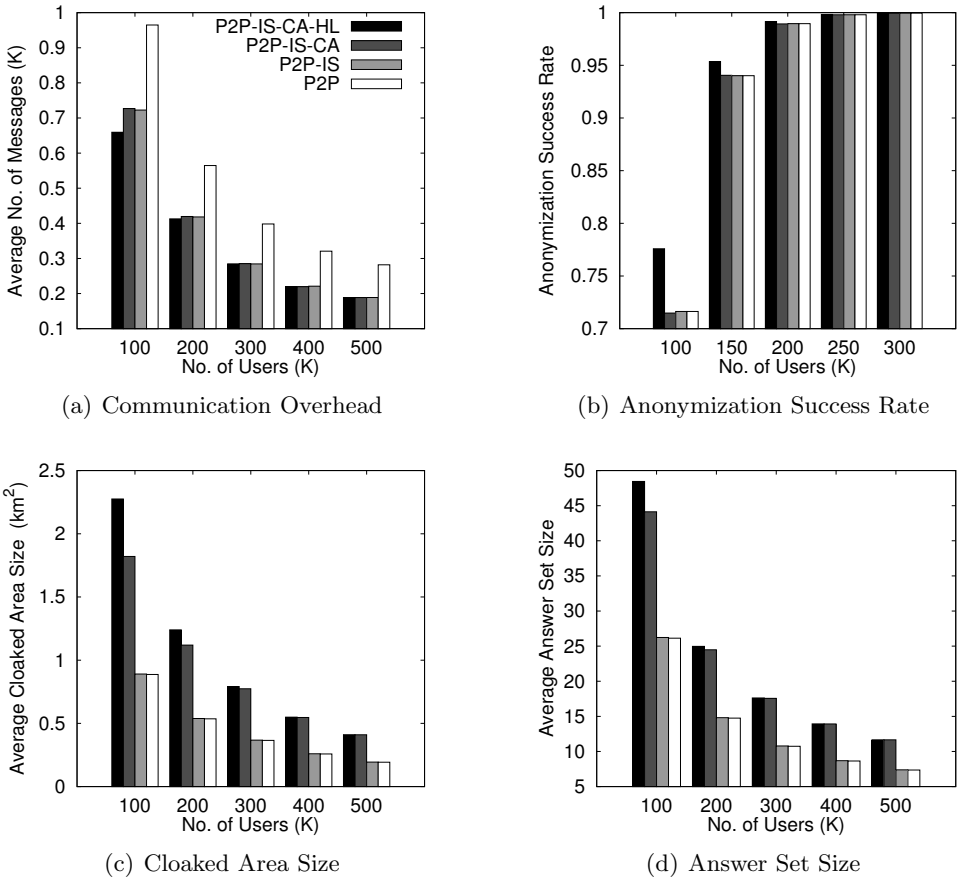

(a) Communication Overhead

(b) Anonymization Success Rate

(c) Cloaked Area Size

(d) Answer Set Size

Figure 7.8: Number of users.

it is more likely that the user can find enough peer location information in her network partition, i.e., the anonymization success rate improves (Figure 7.8b). Since the users can blur their locations into smaller cloaked areas in the denser network (Figure 7.8c), the database server returns smaller answer sets to them (Figure 7.8d).

Figure 7.9 depicts the scalability of our algorithms with respect to varying the number of data objects from 10,000 to 50,000. Since increasing the number of data objects at the database server only affects the answer set size, the performance of the peer search process and the spatial cloaking process of all algorithms is not affected. Figure 7.9b gives that the answer set size of all algorithms linearly increases as there are more data objects.

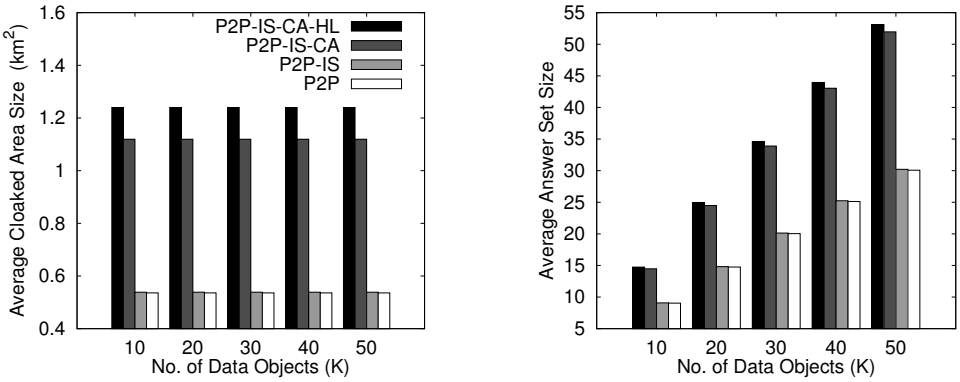

(a) Cloaked Area Size (b) Answer Set Size

Figure 7.9: Number of data objects.

7.4.3 Effect of Privacy Requirements

In this section, we evaluate the performance of our algorithms with respect to the user specified k-anonymity and minimum area A_{min} privacy requirements.

Figure 7.10 depicts the performance of our algorithms with the increase of the strictness of the k-anonymity privacy requirement from $[50, 100]$ and $[50, 300]$. It is expected that the performance of all algorithms becomes worse as the k-anonymity privacy requirement gets stricter. When k increases, the user needs to enlist more peers for help to gather enough peer location information, so the communication overhead gets higher (Figure 7.10a). Our algorithms with the *information sharing scheme* (i.e., P2P-IS, P2P-IS-CA, and P2P-IS-CA-HL) perform better than P2P as k gets larger. Since the user with a stricter k-anonymity privacy requirement needs to gather more peer location information to blur her location, she is more likely to encounter the network partition problem (Figure 7.10b). The results show that the user adopting our *historical location scheme* (i.e., P2P-IS-CA-HL) records a higher anonymization success rate than other algorithms. Figure 7.10c depicts that all algorithms generate larger cloaked areas to satisfy stricter privacy requirements. With larger cloaked areas, it is expected that the database server returns larger answer sets to the user (Figure 7.10d).

Figure 7.11 gives the performance of our algorithms with respect to increasing the required minimum area A_{min} of cloaked areas from 1 to 5 km^2. In this experiment, we set the anonymity level to a smaller value, i.e., $K = 10$, so the results mainly depend

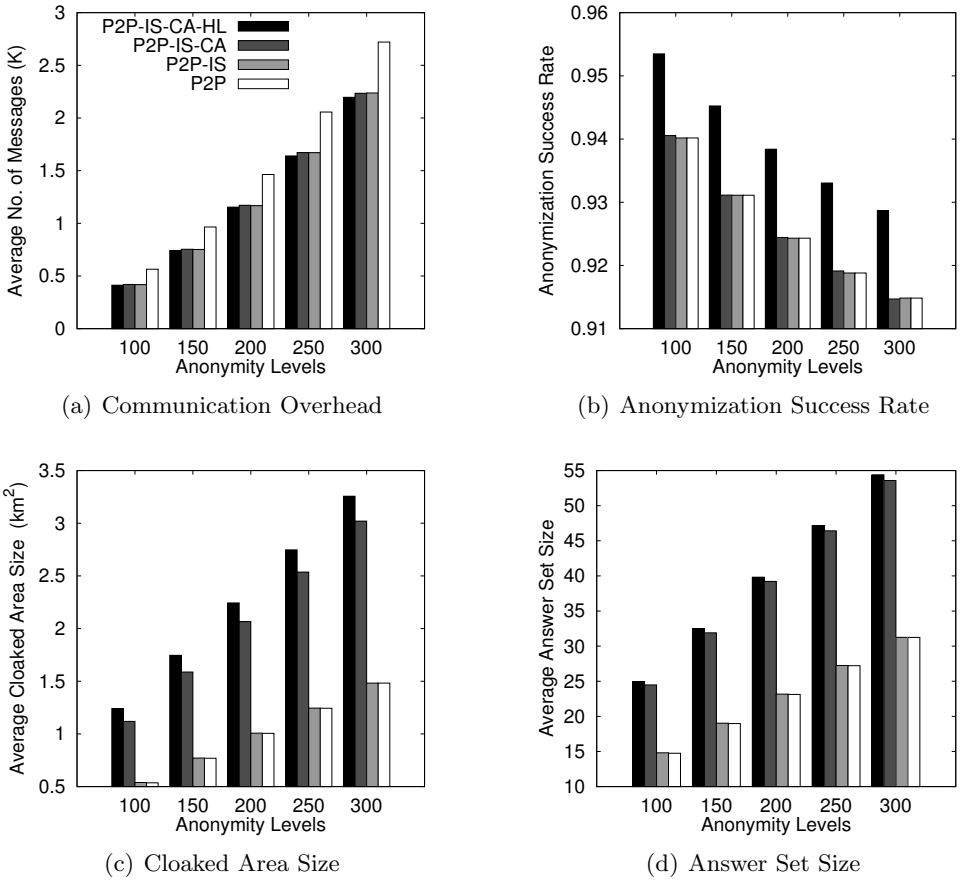

(a) Communication Overhead

(b) Anonymization Success Rate

(c) Cloaked Area Size

(d) Answer Set Size

Figure 7.10: k-anonymity privacy requirements.

on A_{min}. Varying A_{min} only affects the cloaked area size and the answer set size. It is interesting to see that when A_{min} is stricter than the k-anonymity privacy requirement, all algorithms give similar results in terms of cloaked area size and answer set size, as depicted in Figures 7.11a and 7.11b, respectively. It is expected that all algorithms generate larger cloaked areas as A_{min} gets stricter. When a cloaked area A gets larger, it is more likely that A includes a larger set of data objects and each edge of A has a larger set of nearest data objects. Thus, the answer set size increases as A_{min} gets stricter.

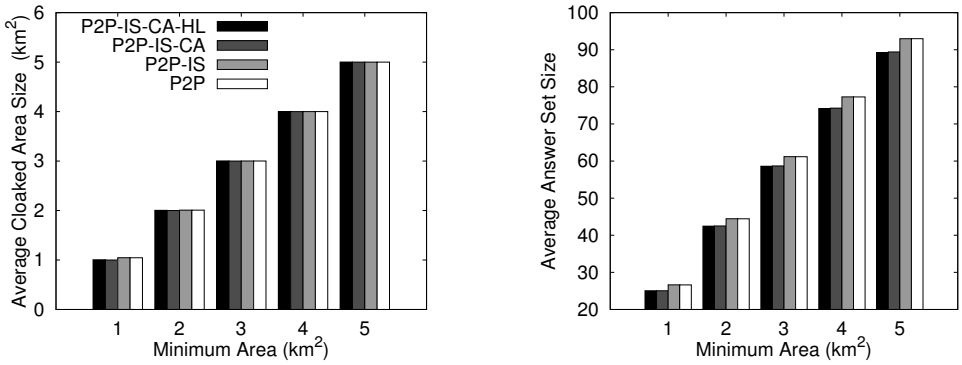

(a) Cloaked Area Size

(b) Answer Set Size

Figure 7.11: Minimum area privacy requirements.

7.4.4 Effect of Transmission Range

Figure 7.12 depicts the performance of our algorithms respect to increasing the transmission range of user mobile devices from $[100, 100]$ to $[100, 300]$ meters. If the transmission range gets larger, the user can find enough peer location information within a smaller hop distance; and thus, the communication overhead reduces (Figure 7.12a). As the transmission range gets larger, our algorithms can find k-anonymized cloaked areas for the users with stricter anonymity levels, so the anonymization success rate improves (Figure 7.12b). However, the stricter the anonymity level, the lager the cloaked area size is generated by our algorithms, so all algorithms generates larger cloaked areas as the transmission range increases (Figure 7.12c). Since the increase of the cloaked area size is small, the answer set size is slightly affected (Figure 7.12d).

7.4.5 Effect of Uncertainty Tolerance

Figure 7.13 gives the performance of our algorithms respect with to varying the user uncertainty tolerance level for the *information sharing scheme*, i.e., tol_s, from 0 to 50 seconds. Since P2P does not support information sharing among users, varying tol_s does not affect its performance. When the user is willing to utilize staler peer location information, it is easier for her to obtain enough peer location information from her neighbor peers without searching the network. Thus, the communication overhead of

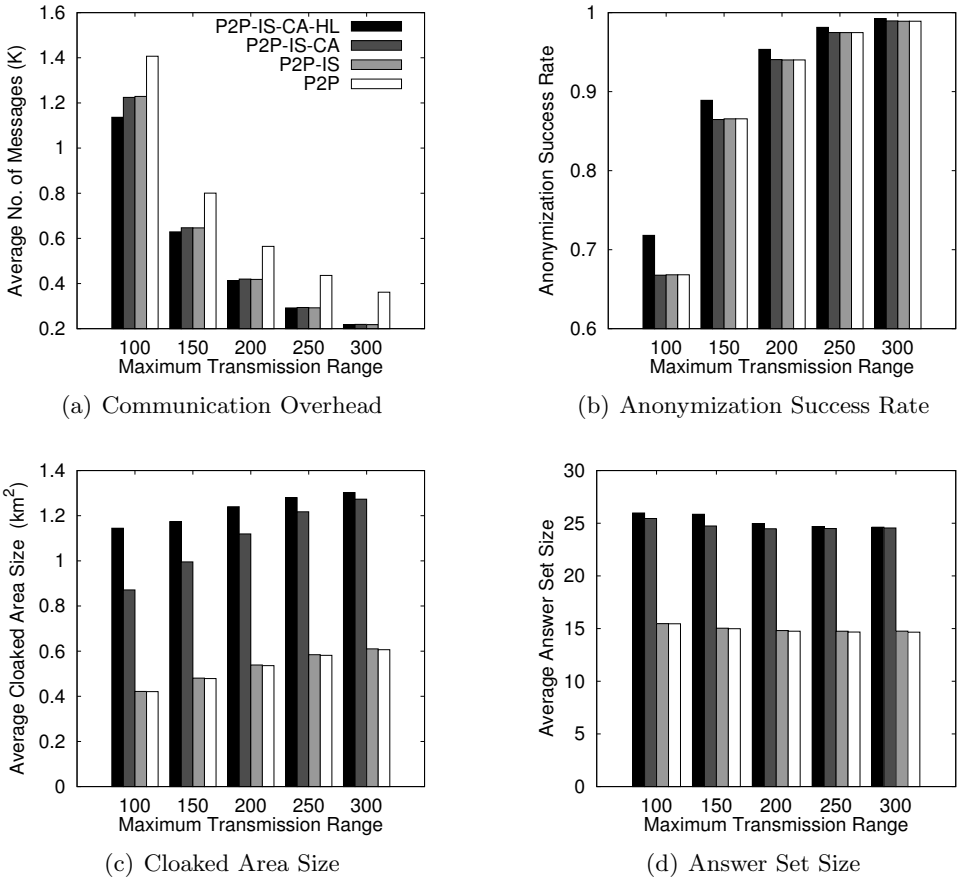

(a) Communication Overhead

(b) Anonymization Success Rate

(c) Cloaked Area Size

(d) Answer Set Size

Figure 7.12: Transmission range.

the algorithms with the *information sharing scheme* (i.e., P2P-IS, P2P-IS-CA, and P2P-IS-CA-HL) reduces, as tol_s gets larger (Figure 7.13a). Likewise, when the user accepts a larger tol_s, there is a higher chance for her to find enough peer location information within her network partition; and therefore, the user experiences a higher anonymization success rate as tol_s increases (Figure 7.13b). With respect to cloaked area size, all algorithms generate larger cloaked areas, as tol_s increases (Figure 7.13c). This is due to the fact that we need larger adjusted location regions for staler peer location information in order to capture its uncertainty. It is expected that the answer set size increases as the cloaked area gets larger (Figure 7.13d).

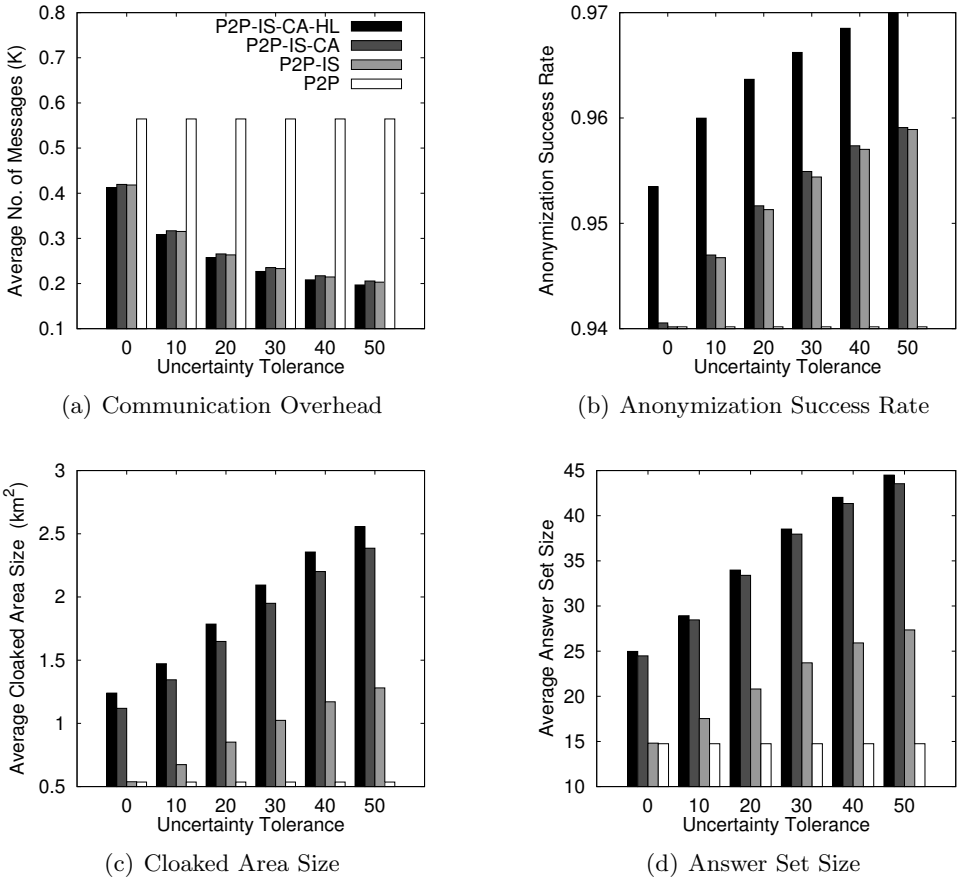

(a) Communication Overhead

(b) Anonymization Success Rate

(c) Cloaked Area Size

(d) Answer Set Size

Figure 7.13: Uncertainty tolerance for the information sharing scheme (tol_s).

7.5 Summary

In this chapter, we present a peer-to-peer (P2P) spatial cloaking algorithm that enables mobile users to obtain location-based services without revealing their exact location information. Our P2P spatial cloaking algorithm is designed for mobile P2P environments in which no fixed communication infrastructure or centralized/distributed servers are available. The main idea of our algorithm is that when a mobile user wants to obtain location-based services, she collaborates with other peers to blur her location into a cloaked area. Our algorithm guarantees the cloaked area satisfies the user specified k-anonymity and minimum area A_{min} privacy requirements, i.e., the cloaked area includes at least k users and has a size of at least A_{min}. To overcome the limitations of mobile

P2P environments, e.g., user mobility, limited transmission range, scarce communication resources, multi-hop communication, and network partition problem, we propose three key features for our algorithm. (1) The *information sharing scheme* enables mobile users to share their gathered peer location information with nearby peers in order to reduce communication overhead. (2) The *historical location scheme* allows users to utilize historical peer location information cached by other peers to alleviate the network partition problem. (3) The *cloaked area adjustment scheme* aims to adjust a cloaked area to guarantee that the adjusted cloaked area is free from a "center-of-cloaked area" privacy attack. We evaluate our P2P spatial cloaking algorithm with the three key features through extensive experiments. The experimental results show that our algorithm is scalable and efficient while guaranteeing the user's location privacy protection.

Chapter 8

The TinyCasper System

This chapter presents the architecture and system model of the *TinyCasper* system; a privacy-preserving location monitoring system in wireless sensor networks. Monitoring personal locations with a potentially untrusted location monitoring system poses privacy threats to the monitored individuals, because an adversary could abuse the location information gathered by the system to infer personal sensitive information [22, 23, 24, 25]. For the location monitoring system using identity sensors, the sensor nodes report the exact location information of the monitored persons to the server; thus using identity sensors immediately poses a major privacy breach. To tackle such a privacy breach, the concept of *aggregate location information*, that is, a collection of location data relating to a group or category of persons from which individual identities have been removed [25, 109], has been suggested as an effective approach to preserve location privacy [23, 25, 109]. Although the counting sensors by nature provide aggregate location information, they would also pose privacy breaches.

Figure 8.1 gives an example of a privacy breach in a location monitoring system with counting sensors. There are 11 counting sensor nodes installed in nine rooms R_1 to R_9, and two hallways C_1 and C_2 (Figure 8.1a). The non-zero number of persons detected by each sensor node is depicted as a number in parentheses. Figures 8.1b and 8.1c give the numbers reported by the same set of sensor nodes at two consecutive time instances t_{i+1} and t_{i+2}, respectively. If R_3 is Alice's office room, an adversary knows that Alice is in room R_3 at time t_i. Then the adversary knows that Alice left R_3 at time t_{i+1} and went to C_2 by knowing the number of persons detected by the sensor nodes in R_3 and

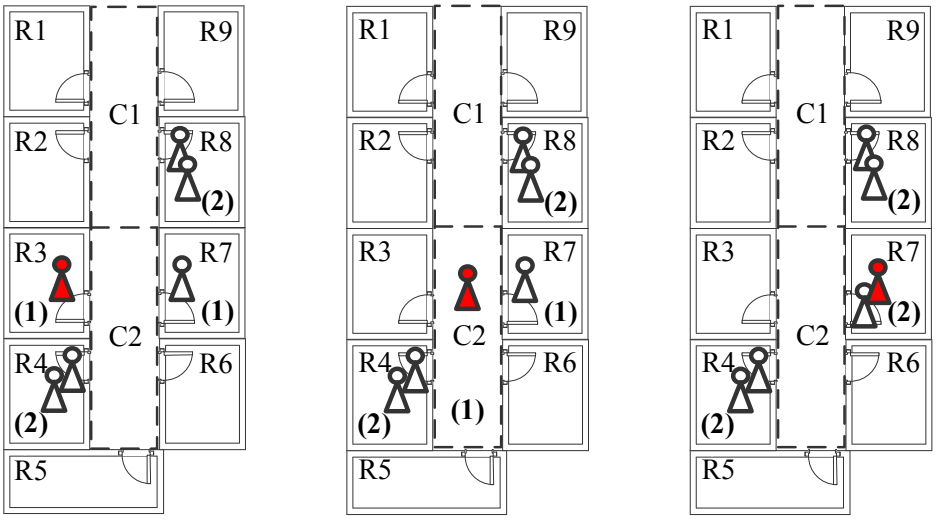

(a) At time t_i (b) At time t_{i+1} (c) At time t_{i+2}

Figure 8.1: A location monitoring system using counting sensors.

C_2. Likewise, the adversary can infer that Alice left C_2 at time t_{i+2} and went to R_7. Such knowledge leakage may lead to several privacy threats. For example, knowing that a person has visited certain clinical rooms may lead to knowing the her health records. Also, knowing that a person has visited a certain bar or restaurant in a mall building may reveal confidential personal information.

This paper proposes a privacy-preserving location monitoring system for wireless sensor networks to provide monitoring services. Our system relies on the well established k-anonymity privacy concept, which requires each person is indistinguishable among k persons. In our system, each sensor node blurs its sensing area into a *cloaked area*, in which at least k persons are residing. Each sensor node reports only aggregate location information, which is in a form of a cloaked area, A, along with the number of persons, N, located in A, where $N \geq k$, to the server. It is important to note that the value of k achieves a trade-off between the strictness of privacy protection and the quality of monitoring services. A smaller k indicates less privacy protection, because a smaller cloaked area will be reported from the sensor node; hence better monitoring services. However, a larger k results in a larger cloaked area, which will reduce the quality of monitoring services, but it provides better privacy protection. Our system can avoid

the privacy leakage in the example given in Figure 8.1 by providing low quality location monitoring services for small areas that the adversary could use to track users, while providing high quality services for larger areas. The definition of a small area is relative to the required anonymity level, because our system provides better quality services for the same area if we relax the required anonymity level. Thus the adversary cannot infer the number of persons currently residing in a small area from our system output with any fidelity; therefore the adversary cannot know that Alice is in room R_3.

To preserve personal location privacy, we propose two in-network aggregate location anonymization algorithms, namely, *resource-* and *quality-aware* algorithms. Both algorithms require the sensor nodes to collaborate with each other to blur their sensing areas into cloaked areas, such that each cloaked area contains at least k persons to constitute a k-anonymous cloaked area. The resource-aware algorithm aims to minimize communication and computational cost, while the quality-aware algorithm aims to minimize the size of the cloaked areas, in order to maximize the accuracy of the aggregate locations reported to the server. In the resource-aware algorithm, each sensor node finds an adequate number of persons, and then it uses a greedy approach to find a cloaked area. On the other hand, the quality-aware algorithm starts from a cloaked area A, which is computed by the resource-aware algorithm. Then A will be iteratively refined based on extra communication among the sensor nodes until its area reaches the minimal possible size. For both algorithms, the sensor node reports its cloaked area with the number of monitored persons in the area as an aggregate location to the server.

Although our system only knows the aggregate location information about the monitored persons, it can still provide monitoring services through answering aggregate queries, for example, "What is the number of persons in a certain area?" To support these monitoring services, we propose a *spatial histogram* that analyzes the gathered aggregate locations to estimate the distribution of the monitored persons in the system. The estimated distribution is used to answer aggregate queries.

We evaluate our system through simulated experiments in Section 9.4. The results show that the communication and computational cost of the resource-aware algorithm is lower than the quality-aware algorithm, while the quality-aware algorithm provides more accurate monitoring services (the average accuracy is about 90%) than the resource-aware algorithm (the average accuracy is about 75%). Both algorithms only

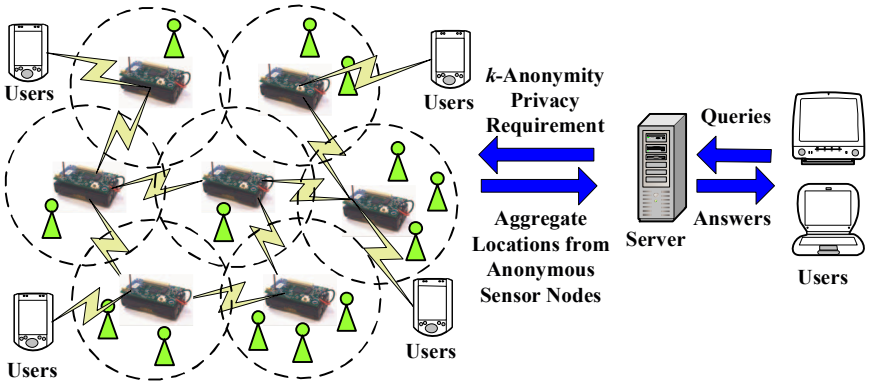

Figure 8.2: System architecture.

reveal k-anonymous aggregate location information to the server, but they are suitable for different system settings. The resource-aware algorithm is suitable for the system, where the sensor nodes have scarce communication and computational resources, while the quality-aware algorithm is favorable for the system, where accuracy is the most important factor in monitoring services.

8.1 System Model

Figure 8.2 depicts the architecture of our system, where there are three major entities, *sensor nodes*, *server*, and *system users*. We will define the problem addressed by our system, and then describe the detail of each entity and the privacy model of our system.

Problem definition. Given a set of sensor nodes $s_1, s_2, \ldots, s_n$ with sensing areas $a_1, a_2, \ldots, a_n$, respectively, a set of moving objects $o_1, o_2, \ldots, o_m$, and a required anonymity level k, (1) we find an aggregate location for each sensor node s_i in a form of $R_i = (Area_i, N_i)$, where $Area_i$ is a rectangular area containing the sensing area of a set of sensor nodes S_i and N_i is the number of objects residing in the sensing areas of the sensor nodes in S_i, such that $N_i \geq k$, $N_i = |\cup_{s_j \in S_i} O_j| \geq k$, $O_j = \{o_l | o_l \in a_j\}$, $1 \leq i \leq n$, and $1 \leq l \leq m$; and (2) we build a spatial histogram to answer an aggregate query Q that asks about the number of objects in a certain area $Q.Area$ based on the aggregate locations reported from the sensor nodes.

Sensor nodes. Each sensor node is responsible for determining the number of objects in its sensing area, blurring its sensing area into a cloaked area A, which includes

at least k objects, and reporting A with the number of objects located in A as aggregate location information to the server. We do not have any assumption about the network topology, as our system only requires a communication path from each sensor node to the server through a distributed tree [110]. Each sensor node is also aware of its location and sensing area.

Server. The server is responsible for collecting the aggregate locations reported from the sensor nodes, using a spatial histogram to estimate the distribution of the monitored objects, and answering range queries based on the estimated object distribution. Furthermore, the administrator can change the anonymized level k of the system at anytime by disseminating a message with a new value of k to all the sensor nodes.

System users. Authenticated administrators and users can issue range queries to our system through either the server or the sensor nodes, as depicted in Figure 8.2. The server uses the spatial histogram to answer their queries.

Privacy model. In our system, the sensor nodes constitute a trusted zone, where they behave as defined in our algorithm and communicate with each other through a secure network channel to avoid internal network attacks, for example, eavesdropping, traffic analysis, and malicious nodes [23, 111]. Since establishing such a secure network channel has been studied in the literature [23, 111], the discussion of how to get this network channel is beyond the scope of this paper. However, the solutions that have been used in previous works can be applied to our system. Our system also provides anonymous communication between the sensor nodes and the server by employing existing anonymous communication techniques [112, 113]. Thus given an aggregate location R, the server only knows that the sender of R is one of the sensor nodes within R. Furthermore, only authenticated administrators can change the k-anonymity level and the spatial histogram size. In emergency cases, the administrators can set the k-anonymity level to a small value to get more accurate aggregate locations from the sensor nodes, or even set it to zero to disable our algorithm to get the original readings from the sensor nodes, in order to get the best services from the system. Since the server and the system user are outside the trusted zone, they are untrusted.

We now discuss the privacy threat in existing location monitoring systems. In an identity-sensor location monitoring system, since each sensor node reports the exact location information of each monitored object to the server, the adversary can pinpoint

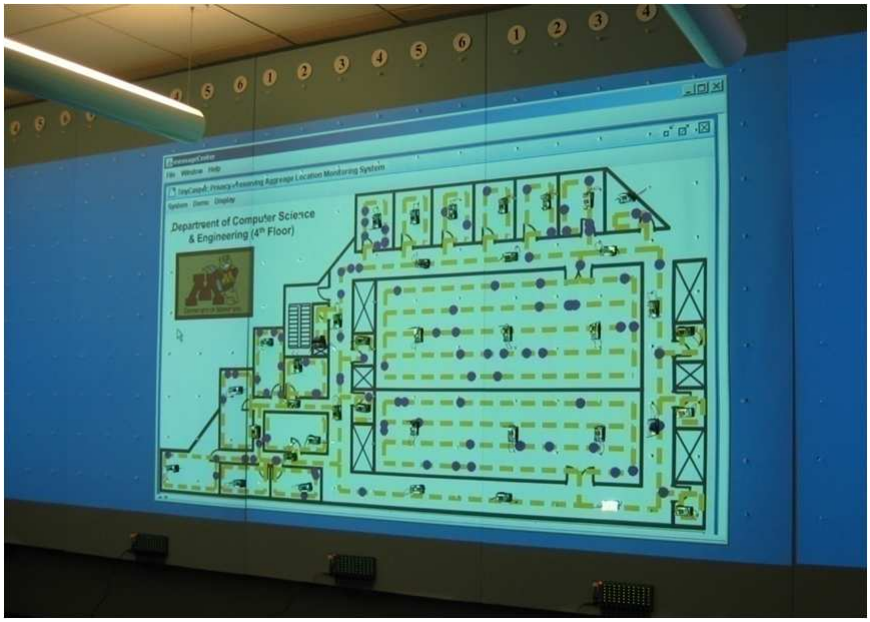

Figure 8.3: The prototype of TinyCasper on a physical test-bed with 39 MICAz motes.

each object's exact location. On the other hand, in a counting-sensor location monitoring system, each sensor node reports the number of objects in its sensing area to the server. The adversary can map the monitored areas of the sensor nodes to the system layout. If the object count of a monitored area is very small or equal to one, the adversary can infer the identity of the monitored objects based on the mapped monitored area, for example, Alice is in her office room at time instance t_i in Figure 8.1.

Since our system only allows each sensor node to report a k-anonymous aggregate location to the server, the adversary cannot infer an object's exact location with any fidelity. The larger the anonymity level, k, the more difficult for the adversary to infer the object's exact location. With the k-anonymized aggregate locations reported from the sensor nodes, the underlying spatial histogram at the server provides low quality location monitoring services for a small area, and better quality services for larger areas. This is a nice privacy-preserving feature, because the object count of a small area is more likely to reveal personal location information. The definition of a small area is relative to the required anonymity level, because our system provides lower quality services for the same area if the anonymized level gets stricter. We will also describe an attack model,

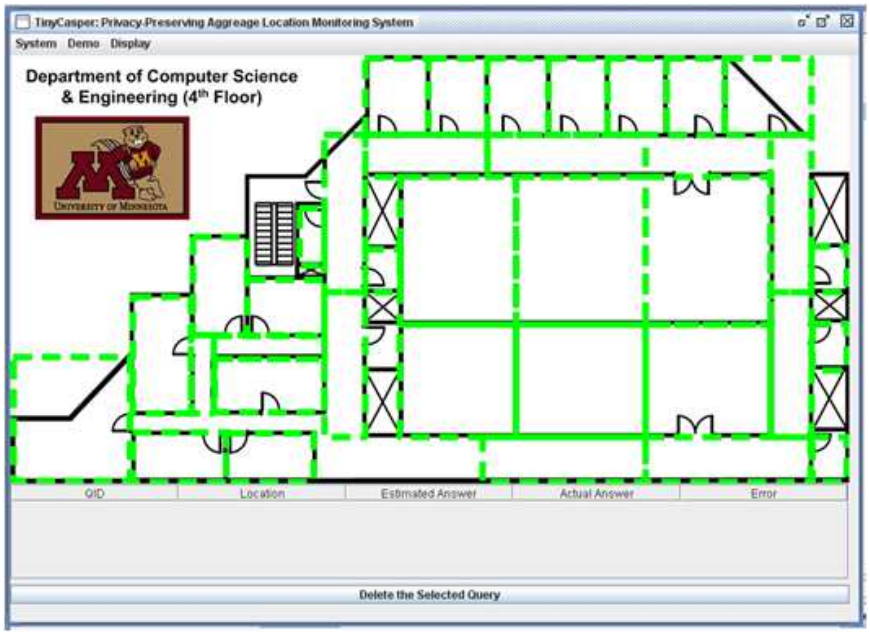

Figure 8.4: Server GUI - aggregate locations reported from sensor nodes.

where we stimulate an attacker that could be a system user or the server attempting to infer the object count of a particular sensor node in Section 9.3.1. We evaluate our system's resilience to the attack model and its privacy protection in Section 9.4.

8.2 System Prototype

Figure 8.3 depicts the prototype of TinyCasper on the TinyOS/Mote platform [114] in nesC [115] with 39 MICAz motes [27]. A floor plan is projected on two 4-foot by 8-foot boards using a projector. Also, we use an MIB510 serial gateway [116] connected to a computer as a base station. This prototype consists of the following three main modules.

1. Floor plan. We use the floor plan of the fourth floor of the Computer Science and Engineering Building at University of Minnesota - Twin Cities. The floor plan is divided into 39 monitoring areas that correspond to faculty offices, student labs, and hallways. A moving object generator is used to generate people movement within the floor plan. The exact locations of the moving objects are represented as red circles

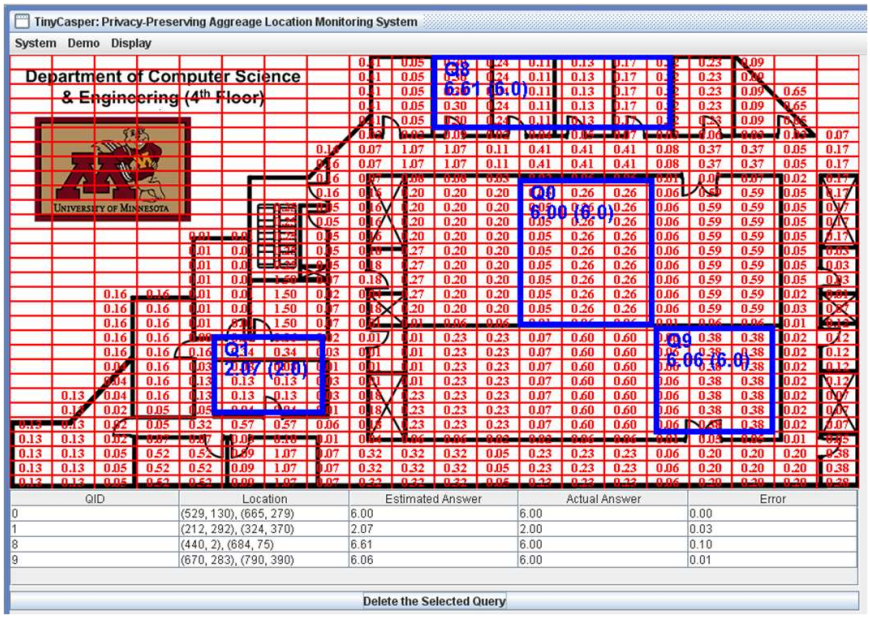

Figure 8.5: Server GUI - a spatial histogram and range queries.

for illustration purposes only. However, these actual locations are not revealed to the server.

2. Wireless sensor nodes. In each of the 39 monitoring areas, we install a wireless sensor that is responsible for detecting the exact location of the users within its monitoring area. In this demo, the wireless sensor nodes get the identity and exact location of the moving objects within their monitoring areas from the *floor plan* module. Also, the sensor nodes get the privacy requirement, i.e., the degree of k-anonymity, from the server. Then, the sensor nodes with a non-zero object count collaborate with each other to find their cloaked spatial regions (represented as blue rectangular regions). Finally, the sensor nodes report their cloaked spatial regions along with the number of objects within the region to the server.

3. Server. Figures 8.4 and 8.5 depict GUI screen shots for the TinyCasper server. The server GUI is used by the system security or administration people where they can change the privacy requirements of the system at anytime. Furthermore, they can get the number of moving objects within a specified area or get an alarm if the number of people in a certain area exceeds a specified threshold. Using the server GUI, users are

able to plot any area within the floor plan as a monitored area. However, they cannot see the exact locations of people, but they can see only the cloaked spatial regions reported by the sensor nodes (depicted as blue rectangles in Figure 8.4). Figure 8.5 visualizes the spatial histogram, where an estimator is maintained for each cell to estimate the number of people located within the cell area. The user can issue range queries through the server GUI by dragging their query regions. The location information and query answer of each range query is displayed in a table at the bottom of the server GUI.

Chapter 9

Location Anonymization and Query Processing in TinyCasper

In this chapter, we present the detail of the *TinyCasper* system; a privacy-preserving location monitoring system designed for wireless sensor networks. Figure 9.1 depicts the system overview of TinyCasper, which consists of two main modules, *location anonymization* and *spatial histogram modules*, whose details will be described in Sections 9.1 and 9.2, respectively. In the location anonymization module, we have two in-network location anonymization algorithms, namely, resource- and quality-aware algorithms. Both algorithms guarantee to provide aggregate locations with k-anonymous cloaked areas. The resource-aware algorithm aims to minimize the communication and computational cost of the anonymization process, while the quality-aware algorithm aims to minimize the cloaked area size to provide more accurate aggregate location information for the system.

In TinyCasper, the sensor node periodically executes the location anonymization module. The sensor node starts with the resource-aware algorithm in the location anonymization module. If the system is satisfied with the resource-aware cloaked areas, the sensor node does not need to perform the quality-aware algorithm. However, if the system requires the sensor node to produce cloaked areas of the minimal size, the sensor node executes the quality-aware algorithm with the resource-aware cloaked area, which is computed by the resource-aware algorithm as, an input. Then, the quality-aware

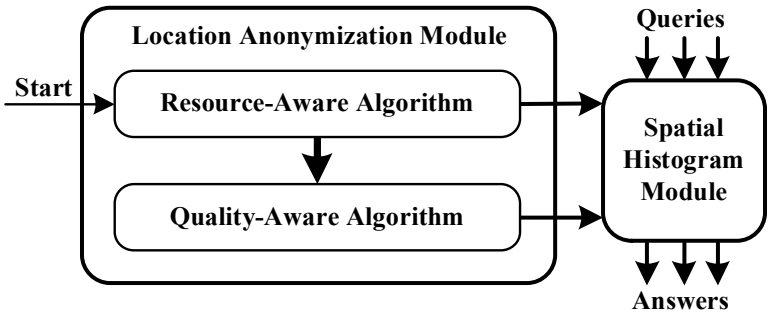

Figure 9.1: System overview.

algorithm requires additional communication and computational overhead to refine the input cloaked area to its minimal possible size. For both algorithms, after the sensor node finds its cloaked area, it sends the cloaked area A with the number of monitored objects located in A as an aggregate location to the spatial histogram module embedded inside the server. The spatial histogram module estimates the distribution of the monitored objects based on the gathered aggregate locations. TinyCasper can provide location monitoring services by using the estimated distribution to answer range queries.

9.1 Location Anonymization Algorithms

In this section, we present our in-network resource- and quality-aware location anonymization algorithms that is periodically executed by the sensor nodes to report their k-anonymous aggregate locations to the server for every reporting period.

9.1.1 The Resource-Aware Algorithm

Algorithm 12 outlines the resource-aware location anonymization algorithm. Figure 9.2 gives an example to illustrate the resource-aware algorithm, where there are seven sensor nodes, A to G, and the required anonymity level is five, $k = 5$. The dotted circles represent the sensing area of the sensor nodes, and a line between two sensor nodes indicates that these two sensor nodes can communicate directly with each other. In general, the algorithm has three steps.

Step 1: ***Broadcast step.*** The objective of this step is to guarantee that each sensor node knows an adequate number of objects to compute a cloaked area. To reduce

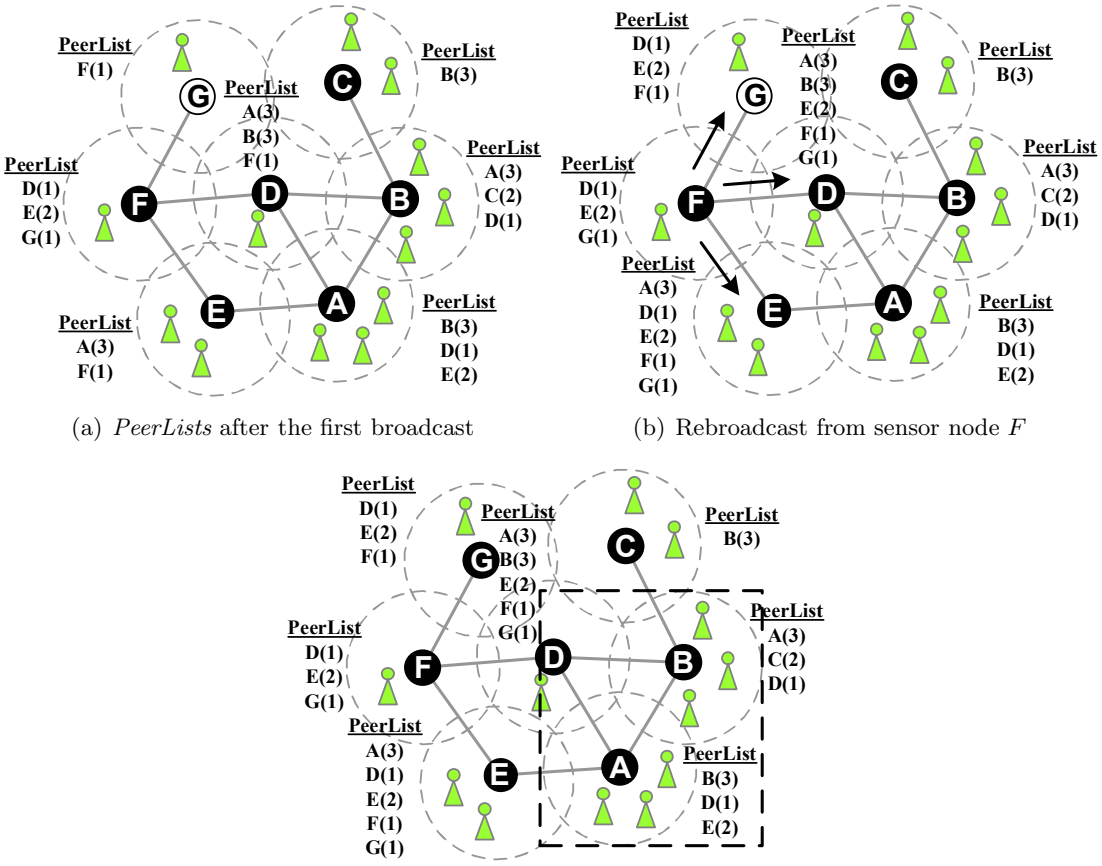

(a) *PeerLists* after the first broadcast

(b) Rebroadcast from sensor node F

(c) *Resource-aware* cloaked area of sensor node A

Figure 9.2: The resource-aware location anonymization algorithm ($k = 5$).

communication cost, this step relies on a heuristic that a sensor node only forwards its received messages to its neighbors when some of them have not yet found an adequate number of objects. In this step, after each sensor node m initializes an empty list *PeerList* (Line 2 in Algorithm 12), m sends a message with its identity $m.ID$, sensing area $m.Area$, and the number of objects located in its sensing area $m.Count$, to its neighbors (Line 3). When m receives a message from a peer p, i.e., $(p.ID, p.Area, p.Count)$, m stores the message in its *PeerList* (Line 5). Whenever m finds an adequate number of objects, m sends a *notification* message to its neighbors (Line 7). If m has not received the notification message from all its neighbors, some neighbor has not found an adequate number of objects; therefore m forwards the received message to its neighbors

Algorithm 12 Resource-aware Location Anonymization

```
1: function ResourceAware (Integer k, Sensor m, List R)
2: PeerList ← {∅}
   // Step 1: Broadcast step
3: Send a message with m's identity m.ID, sensing area m.Area, and object count m.Count to m's
   neighbor peers
4: if Receive a message from a peer p, i.e., (p.ID, p.Area, p.count) then
5:     Add the message to PeerList
6:     if m has found an adequate number of objects then
7:         Send a notification message to m's neighbors
8:     end if
9:     if Some m's neighbor has not found an adequate number of objects then
10:        Forward the message to m's neighbors
11:    end if
12: end if
   // Step 2: Cloaked area step
13: S ← {m}
14: Compute a score for each peer in PeerList
15: Repeatedly select the peer with the highest score from PeerList to S until the total number of
   objects in S is at least k
16: Area ← a minimum bounding rectangle of the senor nodes in S
17: N ← the total number of objects in S
   // Step 3: Validation step
18: if No containment relationship with Area and R ∈ R then
19:    Send (Area, N) to the peers within Area and the server
20: else if m's sensing area is contained by some R ∈ R then
21:    Randomly select a R′ ∈ R such that R′.Area contains m's sensing area
22:    Send R′ to the peers within R′.Area and the server
23: else
24:    Send Area with a cloaked N to the peers within Area and the server
25: end if
```

(Line 10).

Figures 9.2a and 9.2b illustrate the broadcast step. When a reporting period starts, each sensor node sends a message with its identity, sensing area, and the number of objects located in its sensing area to its neighbors. After the first broadcast, sensor nodes A to F have found an adequate number of objects (represented by black circles), as depicted in Figure 9.2a. Thus sensor nodes A to F send a notification message to their neighbors. Since sensor node F has not received a notification message from its neighbor G, F forwards its received messages, which include the information about sensor nodes D and E, to G (Figures 9.2b). Finally, sensor node G has found an adequate number of objects, so it sends a notification message to its neighbor, F. As all the sensor nodes have found an adequate number of objects, they proceed to the next step.

Step 2: *Cloaked area step.* The basic idea of this step is that each sensor node blurs its sensing area into a cloaked area that includes at least k objects, in order to satisfy the k-anonymity privacy requirement. To minimize computational cost, this step uses a greedy approach to find a cloaked area based on the information stored in *PeerList*. For each sensor node m, m initializes a set $S = \{m\}$, and then determines a score for each peer in its *PeerList* (Lines 13 to 14 in Algorithm 12). The score is defined as a ratio of the object count of the peer to the Euclidean distance between the peer and m. The idea behind the score is to select a set of peers from *PeerList* to S to form a cloaked area that includes at least k objects and has an area as small as possible. Then we repeatedly select the peer with the highest score from the *PeerList* to S until S contains at least k objects (Line 15). Finally, m determines the cloaked area ($Area$) that is a *minimum bounding rectangle* (MBR) that covers the sensing area of the sensor nodes in S, and the total number of objects in S (N) (Lines 16 to 17).

An MBR is a rectangle with the minimum area (which is parallel to the axes) that completely contains all desired regions, as illustrated in Figure 9.2c, where the dotted rectangle is the MBR of the sensing area of sensor nodes A and B. The major reasons of our algorithms aligning with MBRs rather than other polygons are that the concept of MBRs have been widely adopted by existing query processing algorithms and most database management systems have the ability to manipulate MBRs efficiently.

Figure 9.2c illustrates the cloaked area step. The *PeerList* of sensor node A contains the information of three peers, B, D, and E. The object count of sensor nodes B, D, and E is 3, 1, and 2, respectively. We assume that the distance from sensor node A to sensor nodes B, D, and E is 17, 18, and 16, respectively. The score of B, D, and E is $3/17 = 0.18$, $1/18 = 0.06$, and $2/16 = 0.13$, respectively. Since B has the highest score, we select B. The sum of the object counts of A and B is six which is larger than the required anonymity level $k = 5$, so we return the MBR of the sensing area of the sensor nodes in S, i.e., A and B, as the resource-aware cloaked area of A, which is represented by a dotted rectangle.

Step 3: *Validation step.* The objective of this step is to avoid reporting aggregate locations with a containment relationship to the server. Let R_i and R_j be two aggregate locations reported from sensor nodes i and j, respectively. If R_i's monitored area is included in R_j's monitored area, $R_i.Area \subset R_j.Area$, or vice versa, $R_j.Area \subset$

$R_i.Area$, they have a containment relationship. We do not allow the sensor nodes to report their aggregate locations with the containment relationship to the server, because combining these aggregate locations may pose privacy leakage. For example, if $R_i.Area \subset R_j.Area$ and $R_i.Area \neq R_j.Area$, an adversary can infer that the number of objects residing in the non-overlapping area, $R_j.Area - R_i.Area$, is $R_j.N - R_i.N$. In case that $R_j.N - R_i.N < k$, the adversary knows that the number of objects in the non-overlapping is less than k, which violates the k-anonymity privacy requirement. As this step ensures that no aggregate location with the containment relationship is reported to the server, the adversary cannot obtain any deterministic information from the aggregate locations.

In this step, each sensor node m maintains a list $\mathcal{R}$ to store the aggregate locations sent by other peers. When a reporting period starts, m nullifies $\mathcal{R}$. After m finds its aggregate location R_m, m checks the containment relationship between R_m and the aggregate locations in $\mathcal{R}$. If there is no containment relationship between R_m and the aggregate locations in $\mathcal{R}$, m sends R_m to the peers within $R_m.Area$ and the server (Line 19 in Algorithm 12). Otherwise, m randomly selects an aggregate location R_p from the set of aggregate locations in $\mathcal{R}$ that contain m's sensing area, and m sends R_p to the peers within $R_p.Area$ and the server (Lines 21 to 22). In case that no aggregate location in $\mathcal{R}$ contains m's sensing area, we find a set of aggregate locations, $\mathcal{R}'$, in $\mathcal{R}$ that are contained by R_m and N' is the number of monitored persons in R_m that is not covered by any aggregate location in $\mathcal{R}'$. If $N' \geq k$, the containment relationship does not violate the k-anonymity privacy requirement; therefore m sends R_m to the peers within $R_m.Area$ and the server. However, if $N' < k$, m cloaks the number of monitored persons of R_m, $R_m.N$, by increasing it by an integer uniformly selected between k and $2k$, and sends R_m to the peers within $R_m.Area$ and the server (Line 24). Since the server receives an aggregate location from each sensor node for every reporting period, it cannot tell whether any containment relationship takes place among the actual aggregate locations of the sensor nodes.

9.1.2 The Quality-Aware Algorithm

Algorithm 13 outlines the quality-aware algorithm that takes the cloaked area computed by the resource-aware algorithm as an *initial solution*, and then refines it until the

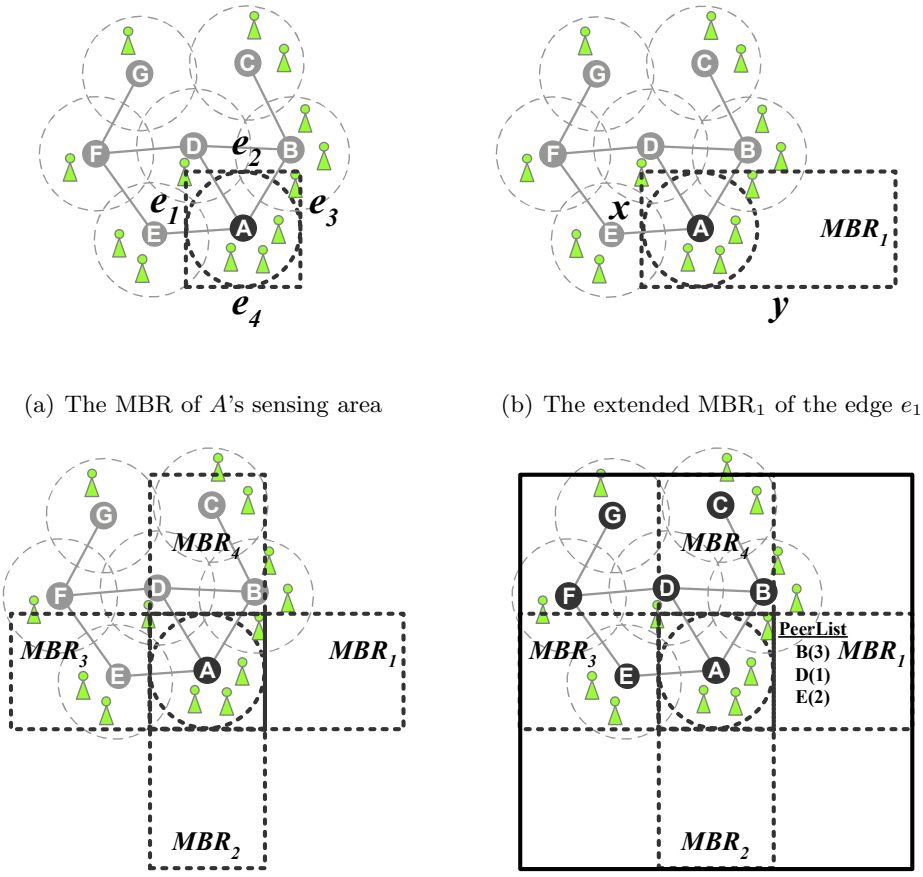

(a) The MBR of A's sensing area

(b) The extended MBR_1 of the edge e_1

(c) The extended MBR_i $(1 \leq i \leq 4)$

(d) The search space $\mathcal{S}$

Figure 9.3: The search space $\mathcal{S}$ of sensor node A.

cloaked area reaches the minimal possible area, which still satisfies the k-anonymity privacy requirement, based on extra communication between other peers. The quality-aware algorithm initializes a variable *current minimal cloaked area* by the input initial solution (Line 2 in Algorithm 13). When the algorithm terminates, the *current minimal cloaked area* contains the set of sensor nodes that constitutes the minimal cloaked area. In general, the algorithm has three steps.

Step 1: ***Search space step.*** Since a typical sensor network has a large number of sensor nodes, it is too costly for a sensor node m to gather the information of all the sensor nodes to compute its minimal cloaked area. To reduce communication and

Algorithm 13 Quality-aware Location Anonymization

```
1: function QualityAware (Integer k, Sensor m, Set init_solution, List R)
2: current_min_cloaked_area ← init_solution
   // Step 1: Search space step
3: Determine a search space S based on init_solution
4: Collect the information of the peers located in S
   // Step 2: Minimal cloaked area step
5: Add each peer located in S to C[1] as an item
6: Add m to each itemset in C[1] as the first item
7: for i = 1; i ≤ 4; i ++ do
8:    for each itemset X = {a_1, ..., a_{i+1}} in C[i] do
9:       if Area(MBR(X)) < Area(current_min_cloaked_area) then
10:         if N(MBR(X)) ≥ k then
11:            current_min_cloaked_area ← {X}
12:            Remove X from C[i]
13:         end if
14:      else
15:         Remove X from C[i]
16:      end if
17:   end for
18:   if i < 4 then
19:      for each itemset pair X={x_1,...,x_{i+1}}, Y={y_1,...,y_{i+1}} in C[i] do
20:         if x_1 = y_1, ..., x_i = y_i and x_{i+1} ≠ y_{i+1} then
21:            Add an itemset {x_1, ..., x_{i+1}, y_{i+1}} to C[i + 1]
22:         end if
23:      end for
24:   end if
25: end for
26: Area ← a minimum bounding rectangle of current_min_cloaked_area
27: N ← the total number of objects in current_min_cloaked_area
   // Step 3: Validation step
28: Lines 18 to 25 in Algorithm 12
```

computational cost, m determines a *search space*, $\mathcal{S}$, based on the input initial solution, which is the cloaked area computed by the resource-aware algorithm, such that the sensor nodes outside $\mathcal{S}$ cannot be part of the minimal cloaked area (Line 3 in Algorithm 13). We will describe how to determine $\mathcal{S}$ based on the example given in Figure 9.3. Thus gathering the information of the peers residing in $\mathcal{S}$ is enough for m to compute the minimal cloaked area for m (Line 4).

Figure 9.3 illustrates the search space step, in which we compute $\mathcal{S}$ for sensor node A. Let $Area$ be the area of the input initial solution. We assume that $Area = 1000$. We determine $\mathcal{S}$ for A by two steps. (1) We find the *minimum bounding rectangle* (MBR) of the sensing area of A. It is important to note that the sensing area can be

in any polygon or irregular shape. In Figure 9.3a, the MBR of the sensing area of A is represented by a dotted rectangle, where the edges of the MBR are labeled by e_1 to e_4. (2) For each edge e_i of the MBR, we compute an MBR_i by extending the opposite edge such that the area of the extended MBR_i is equal to $Area$. $\mathcal{S}$ is the MBR of the four extended MBR_i. Figure 9.3b depicts the extended MBR_1 of the edge e_1 by extending the opposite edge e_3, where $\text{MBR}_1.x$ is the length of MBR_1, $\text{MBR}_1.y = Area/\text{MBR}_1.x$ and $Area = 1000$. Figure 9.3c shows the four extended MBRs, MBR_1 to MBR_4, which are represented by dotted rectangles. The MBR of the four extended MBRs constitutes $\mathcal{S}$, which is represented by a rectangle (Figure 9.3d). Finally, the sensor node only needs the information of the peers within $\mathcal{S}$.

Step 2: ***Minimal cloaked area step.*** This step takes a set of peers residing in the search space, $\mathcal{S}$, as an input and computes the minimal cloaked area for the sensor node m. Although the search space step already prunes the entire system space into $\mathcal{S}$, exhaustively searching the minimal cloaked area among the peers residing in $\mathcal{S}$, which needs to search all the possible combinations of these peers, could still be costly. Thus we propose two optimization techniques to reduce computational cost.

The basic idea of the first optimization technique is that we do not need to examine all the combinations of the peers in $\mathcal{S}$; instead, we only need to consider the combinations of at most four peers. The rationale behind this optimization is that an MBR is defined by at most four sensor nodes because at most two sensor nodes define the width of the MBR (parallel to the x-axis) while at most two other sensor nodes define the height of the MBR (parallel to the y-axis). Thus this optimization mainly reduces computational cost by reducing the number of MBR computations among the peers in $\mathcal{S}$. The correctness of this optimization technique will be discussed in Section 9.1.2.

The second optimization technique has two properties, *lattice structure* and *monotonicity property*. We first describe these two properties, and then present a *progressive refinement* approach for finding a minimal cloaked area.

A. Lattice structure. In a lattice structure, a data set that contains n items can generate 2^{n-1} itemsets excluding a *null* set. In the sequel, since the *null* set is meaningless to our problem, it will be neglected. Figure 9.4 shows the lattice structure of a set of four items $S = \{s_1, s_2, s_3, s_4\}$, where each black line between two itemsets indicates that an itemset at a lower level is a subset of an itemset at a higher level. For our

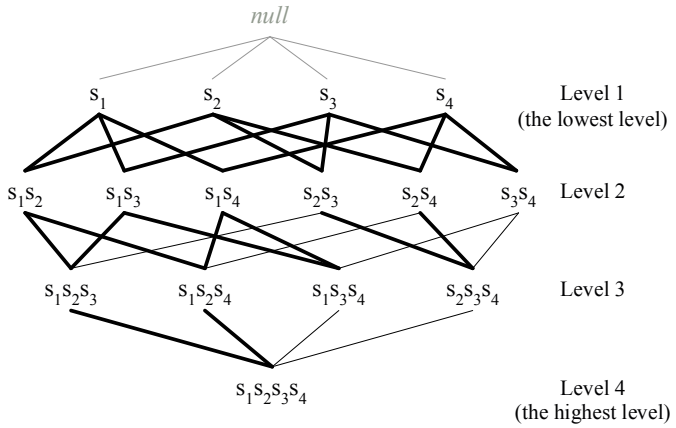

Figure 9.4: The lattice structure of a set of four items.

problem, given a set of sensor nodes $S = \{s_1, s_2, \ldots, s_n\}$, all the possible combinations of these sensor nodes are the non-empty subsets of S; thus we can use a lattice structure to generate the combinations of the sensor nodes in S. In the lattice structure, since each itemset at level i has i items in S, each combination at the lowest level, level 1, contains a distinct item in S; therefore there are n itemsets at the lowest level. We generate the lattice structure from the lowest level based on a simple *generation rule*: given two sorted itemsets $X = \{x_1, \ldots, x_i\}$ and $Y = \{y_1, \ldots, y_i\}$ in increasing order, where each itemset has i items ($1 \leq i < n$), if all item pairs but the last one in X and Y are the same, $x_1 = y_1$, $x_2 = y_2$, ..., $x_{i-1} = y_{i-1}$, and $x_i \neq y_i$, we generate a new itemset with $i + 1$ items, $\{x_1, \ldots, x_i, y_i\}$. In the example, we use bold lines to illustrate the construction of the lattice structure based on the generation rule. For example, the itemset $\{s_1, s_2, s_3, s_4\}$ at level 4 is combined by the itemsets $\{s_1, s_2, s_3\}$ and $\{s_1, s_2, s_4\}$ at level 3, so there is a bold line from $\{s_1, s_2, s_3, s_4\}$ to $\{s_1, s_2, s_3\}$ and another one to $\{s_1, s_2, s_4\}$.

B. Monotonicity property. Let S be a set of items, and P be the power set of S, 2^S. The monotonicity property of a function f indicates that if X is a subset of Y, then $f(X)$ must not exceed $f(Y)$, i.e., $\forall X, Y \in P : (X \subseteq Y) \rightarrow f(X) \leq f(Y)$. For our problem, the MBR of a set of sensor nodes S has the monotonicity property, because adding sensor nodes to S must not decrease the area of the MBR of S or the number

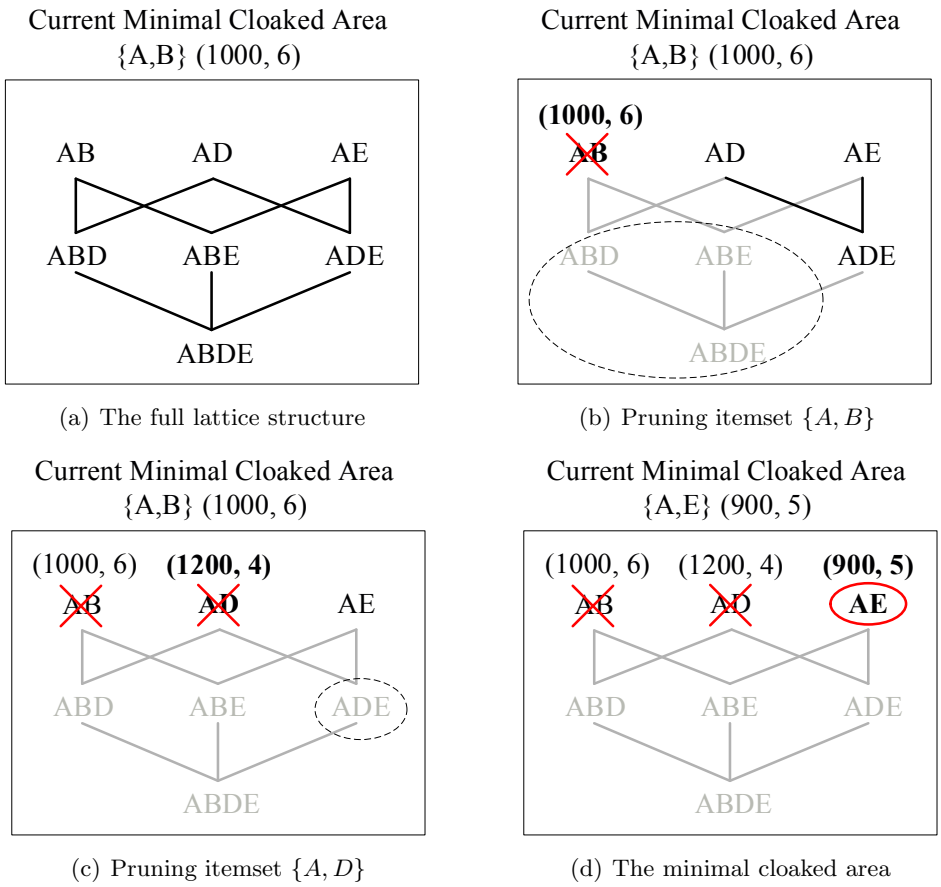

(a) The full lattice structure

(b) Pruning itemset $\{A, B\}$

(c) Pruning itemset $\{A, D\}$

(d) The minimal cloaked area

Figure 9.5: The quality-aware cloaked area of sensor node A.

of objects within the MBR of S. Let $Area(MBR(X))$ and $N(MBR(X))$ be two functions that return the area of the MBR of an itemset X and the number of monitored objects located in the MBR, respectively. Thus, given two itemsets X and Y, if $X \subseteq Y$, then $Area(MBR(X)) \leq Area(MBR(Y))$ and $N(MBR(X)) \leq N(MBR(Y))$. By this property, we propose two pruning conditions in the lattice structure. (1) If a combination $\mathcal{C}$ gives the *current minimal cloaked area*, other combinations that contain $\mathcal{C}$ at the higher levels of the lattice structure should be pruned. This is because the monotonicity property indicates that the pruned combinations cannot constitute a cloaked area smaller than the *current minimal cloaked area*. (2) Similarly, if a combination $\mathcal{C}$ constitutes a cloaked area that is the same or larger than the *current minimal cloaked area*, other combinations that contain $\mathcal{C}$ at the higher levels of the lattice structure should be

pruned.

C. Progressive refinement. Since the monotonicity property shows that we would not need to generate a complete lattice structure to compute a minimal cloaked area, we generate the lattice structure of the peers in the search space, $\mathcal{S}$, progressively from the lowest level of the lattice structure to its higher levels, in order to minimize the computational and storage overhead. To compute the minimal cloaked area for the sensor node m, we first generate an itemset for each peer in $\mathcal{S}$ at the lowest level of the lattice structure, $C[1]$ (Line 5 in Algorithm 13). To accommodate with our problem, we add m to each itemset in $C[1]$ as the first item (Line 6). Such accommodation does not affect the generation of the lattice structure, but each itemset has an extra item, m. For each itemset X in $C[1]$, we determine the MBR of X, $MBR(X)$. If the area of $MBR(X)$ is less than the *current minimal cloaked area* and the total number of objects in $MBR(X)$ is at least k, we set X to the *current minimal cloaked area*, and remove X from $C[1]$ based on the first pruning condition of the monotonicity property (Lines 11 to 12). However, if the area of $MBR(X)$ is equal to or larger than the area of the *current minimal cloaked area*, we also remove X from $C[1]$ based on the second pruning condition of the monotonicity property (Line 15). Then we generate the itemsets, where each itemset contains two items, at the second lowest level of the lattice structure, $C[2]$, based on the remaining itemsets in $C[1]$ based on the generation rule of the lattice structure. We repeat this procedure until we produce the itemsets at the highest level of the lattice structure, $C[4]$, or all the itemsets at the current level are pruned (Lines 19 to 23). After we examine all non-pruned itemsets in the lattice structure, the *current minimal cloaked area* stores the combination giving the minimal cloaked area (Lines 26 to 27).

Figure 9.5 illustrates the minimal cloaked area step that computes the minimal cloaked area for sensor node A. The set of peers residing in the search space is $\mathcal{S} = \{B, D, E\}$. We assume that the area of the MBR of $\{A, B\}$, $\{A, D\}$, and $\{A, E\}$ is 1000, 1200, and 900, respectively. The number of objects residing in the MBR of $\{A, B\}$, $\{A, D\}$, and $\{A, E\}$ is six, four, and five, respectively, as depicted in Figure 9.2. Figure 9.5a depicts the full lattice structure of $\mathcal{S}$ where A is added to each itemset as the first item. Initially, the *current minimal cloaked area* is set to the initial solution, which is the MBR of $\{A, B\}$ 'computed by the resource-aware algorithm. The area of the MBR

of $\{A, B\}$, $Area(MBR(\{A, B\}))$, is 1000 and the total number of monitored objects in $MBR(\{A, B\})$, $N(MBR(\{A, B\}))$, is six. It is important to note that the progressive refinement approach may not require our algorithm to compute the full lattice structure. As depicted in Figure 9.5b, we construct the lowest level of the lattice structure, where each itemset contains a peer in $\mathcal{S}$. Since the area of $MBR(\{A, B\})$ is the *current minimal cloaked area*, we remove $\{A, B\}$ from the lattice structure; hence the itemsets at the higher levels that contain $\{A, B\}$, $\{A, B, D\}$, $\{A, B, E\}$, and $\{A, B, D, E\}$ (enclosed by a dotted oval), will not be considered by the algorithm. Then, we consider the next itemset $\{A, D\}$. Since the area of $MBR(\{A, D\})$ is larger than the *current minimal cloaked area*, this itemset is removed from the lattice structure. After pruning $\{A, D\}$, the itemsets at the higher levels that contain $\{A, D\}$, $\{A, D, E\}$ (enclosed by a dotted oval), will not be considered (Figure 9.5c). We can see that all itemsets beyond the lowest level of the lattice structure will not be considered by the algorithm. Finally, we consider the last itemset $\{A, E\}$. Since the area of $MBR(\{A, E\})$ is less than *current minimal cloaked area* and the total number of monitored objects in $MBR(\{A, E\})$ is $k = 5$, we set $\{A, E\}$ to the *current minimal cloaked area* (Figure 9.5d). As the algorithm cannot generate any itemsets at the higher level of the lattice structure, it terminates. Thus the minimal cloaked area is the MBR of sensor nodes A and E, and the number of monitored objects in this area is five.

Step 3: ***Validation step.*** This step is exactly the same as in the resource-aware algorithm (Section 9.1.1).

Analysis

A *brute-force* approach of finding the minimal cloaked area of a sensor node has to examine all the combinations of its peers. Let N be the number of sensor nodes in the system. Since each sensor node has $N - 1$ peers, we have to consider $\sum_{i=1}^{N-1} C_i^{N-1} = 2^{N-1} - 1$ MBRs to find the minimal cloaked area. In our algorithm, the search space step determines a search space, $\mathcal{S}$, and prunes the peers outside $\mathcal{S}$. Let M be the number of peers in $\mathcal{S}$, where $M \leq N - 1$. Thus the computational cost is reduced to $\sum_{i=1}^{M} C_i^M = 2^M - 1$. In the minimal cloaked area step, the first optimization technique indicates that an MBR can be defined by at most four peers. As we need to consider the combinations of at most four peers, the computational cost is reduced to $\sum_{i=1}^{4} C_i^M =$

$(M^4 - 2M^3 + 11M^2 + 14M)/24 = O(M^4)$. Furthermore, the second optimization technique uses the monotonicity property to prune the combinations, which cannot give the minimal cloaked area. In our example, the brute-force approach considers all the combinations of six peers; hence this approach computes $2^6 - 1 = 63$ MBRs to find the minimal cloaked area of sensor node A. In our algorithm, the search space step reduces the entire space into $\mathcal{S}$, which contains only three peers; hence this step needs to compute $2^3 - 1 = 7$ MBRs. After examining the three itemsets at the lowest level of the lattice structure, all other itemsets at the higher levels are pruned. Thus the progressive refinement approach considers only three combinations. Therefore our algorithm reduces over 95% computational cost of the brute-force approach, as it reduces the number of MBR computations from 63 to 3.

Proof of Correctness

In this section, we show the correctness of the quality-aware location anonymization algorithm.

Theorem 10. *Given a resource-aware cloaked area of size Area of a sensor node s, a search space, $\mathcal{S}$, computed by the quality-aware algorithm contains the minimal cloaked area.*

Proof. Let X be the minimal cloaked area of size equal to or less than *Area*. We know that X must totally cover the sensing area of s. Suppose X is not totally covered by $\mathcal{S}$, X must contain at least one extended MBR, MBR_i, where $1 \leq i \leq 4$ (Figure 9.3c). This means that the area of X is larger than the area of an extended MBR, *Area*. This contradicts to the assumption that X is the minimal cloaked area; thus X is included in $\mathcal{S}$. □

Theorem 11. *A* minimum bounding rectangle *(MBR) can be defined by at most four sensor nodes.*

Proof. By definition, given an MBR, each edge of the MBR touches the sensing area of some sensor node. In an extreme case, there is a distinct sensor node touching each edge of the MBR but not other edges. The MBR is defined by four sensor nodes, which touch different edges of the MBR. For any edge e of the MBR, if multiple sensor nodes

touch e but not other edges, we can simply pick one of these sensor nodes, because any one of these sensor nodes gives the same e. Thus an MBR is defined by at most four sensor nodes. □

9.2 Spatial Histogram

In this section, we present a *spatial histogram* that is embedded inside the server to estimate the distribution of the monitored objects based on the aggregate locations reported from the sensor nodes. Our spatial histogram is represented by a two-dimensional array that models a grid structure $\mathcal{G}$ of N_R rows and N_C columns; hence, the system space is divided into $N_R \times N_C$ disjoint equal-sized grid cells. In each grid cell $\mathcal{G}(i, j)$, we maintain a float value that acts as an estimator $\mathcal{H}[i, j]$ ($1 \leq i \leq N_C$, $1 \leq j \leq N_R$) of the number of objects within its area. We assume that the system has the ability to know the total number of moving objects M in the system. The value of M will be used to initialize the spatial histogram. In practice, M can be computed online for both indoor and outdoor dynamic environments. For the indoor environment, the sensor nodes can be deployed at each entrance and exit to count the number of users entering or leaving the system [117, 118]. For the outdoor environment, the sensor nodes have been already used to count the number of people in a predefined area [119]. We use the spatial histogram to provide approximate location monitoring services. The accuracy of the spatial histogram, which indicates the utility of our privacy-preserving location monitoring system, will be evaluated in Section 9.4.

Algorithm 14 outlines the maintenance of our spatial histogram. Initially, we assume that the objects are evenly distributed in the system, so the estimated number of objects within each grid cell is $\mathcal{H}[i, j] = M/(N_R \times N_C)$. The input of the histogram is a set of aggregate locations $\mathcal{R}$ reported from the sensor nodes. Each aggregate location R in $\mathcal{R}$ contains a cloaked area, $R.Area$, and the number of monitored objects within $R.Area$, $R.N$. First, the aggregate locations in $\mathcal{R}$ are grouped into the same partition $P = \{R_1, R_2, \ldots, R_{|P|}\}$ if their cloaked areas are not overlapping with each other, which means that for every pair of aggregate locations R_i and R_j in P, $R_i.Area \cap R_j.Area = \emptyset$ (Lines 2 to 8). Then, for each partition P, we update its entire set of aggregate locations to the spatial histogram at the same time. For each aggregate location R in P, we

Algorithm 14 Spatial Histogram Maintenance

1: **function** HISTOGRAMMAINTENANCE (AggregateLocationSet $\mathcal{R}$)
2: **for** each aggregate location $R \in \mathcal{R}$ **do**
3: **if** there is an existing partition $P = \{R_1, \ldots, R_{|P|}\}$ such that $R.Area \cap R_k.Area = \emptyset$ for every $R_k \in P$ **then**
4: Add R to P
5: **else**
6: Create a new partition for R
7: **end if**
8: **end for**
9: **for** each partition P **do**
10: **for** each aggregate location $R_k \in P$ **do**
11: $R_k.\widehat{N} \leftarrow \sum_{\mathcal{G}[i,j] \in R_k.Area} \mathcal{H}[i,j]$
12: For every cell $\mathcal{G}(i,j) \in R_k.Area$, $\mathcal{H}[i,j] \leftarrow \frac{R_k.N}{\text{No. of cells within } R_k.Area}$
13: **end for**
14: $P.Area \leftarrow R_1.Area \cup \ldots \cup R_{|P|}.Area$
15: For every cell $\mathcal{G}(i,j) \notin P.Area$,
$\mathcal{H}[i,j] = \mathcal{H}[i,j] + \frac{\sum_{R_k \in P} R_k.\widehat{N} - R_k.N}{\text{No. of cells outside } P.Area}$
16: **end for**

record the estimation error, which is the difference between the sum of the estimators within $R.Area$, $R.\widehat{N}$, and $R.N$, and then $R.N$ is uniformly distributed among the estimators within $R.Area$; hence each estimator within $R.Area$ is set to $R.N$ divided by the total number of grid cells within $R.Area$ (Lines 10 to 13). After processing all the aggregate locations in P, we sum up the estimation error of each aggregate location in P, $\sum_{k=1}^{|P|} R_k.\widehat{N} - R_k.N$, that is uniformly distributed among the estimators outside $P.Area$, where $P.Area$ is the area covered by some aggregate location in P, $P.Area = \cup_{R_k \in P} R_k.Area$ (Line 15). Formally, for each partition P that contains $|P|$ aggregate locations R_k ($1 \leq k \leq |P|$), every estimator in the histogram is updated as follows:

$$\mathcal{H}[i,j] = \begin{cases} \frac{R_k.N}{\text{No. of cells within } R_k.Area}, & \text{for } \mathcal{G}(i,j) \in R_k.Area \\ \\ \mathcal{H}[i,j] + \frac{\sum_{k=1}^{|P|} R_k.\widehat{N} - R_k.N}{\text{No. of cells outside } P.Area}, & \text{for } \mathcal{G}(i,j) \notin P.Area \end{cases}$$

Example. Figure 9.6 depicts an example of maintaining the *spatial histogram* in which the grid structure $\mathcal{G}$ divides the system space into $N_R \times N_C = 5 \times 5$ grid cells. When the *spatial histogram* is initialized, the total number of objects in the system is $M = 100$; and hence, the estimator of each grid cell is initially set to $M/(N_R \times$

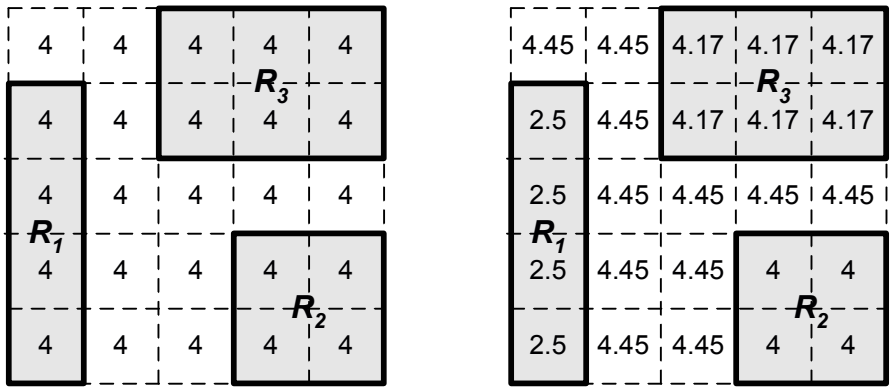

(a) Initial histogram (b) Updated histogram

Figure 9.6: Example of histogram maintenance.

$N_C) = 100/25 = 4$ (Figure 9.6a). In this example, we update a partition that contains three *aggregate locations* $P = \{R_1, R_2, R_3\}$ where their cloaked areas are represented as black rectangles, the shaded cells are the grid cells within their cloaked areas, and the number of monitored objects within their cloaked areas is $R_1.N = 10$, $R_2.N = 16$, and $R_3.N = 25$. For R_1, the estimation error is $R_1.\widehat{N} - R_1.N = 16 - 10 = 6$, and $R_1.N$ is uniformly distributed among the estimators within $R_1.Area$; and hence, each estimator within $R_1.Area$ is set to $R_1.N/4 = 10/4 = 2.5$ (Figure 9.6b). For R_2, the estimation error is $R_2.\widehat{N} - R_2.N = 16 - 16 = 0$, and $R_2.N$ is uniformly distributed among the estimators within $R_2.Area$. Since there is no estimation error, the estimators remain unchanged. For R_3, the estimation error is $R_3.\widehat{N} - R_3.N = 24 - 25 = -1$, and $R_3.N$ is uniformly distributed among the estimators within $R_3.Area$; and hence, each estimator within $R_3.Area$ is set to $R_3.N/6 = 25/6 = 4.17$. The sum of the estimation error of the *aggregate locations* in P is $6 + 0 + (-1) = 5$ that is uniformly distributed among the 11 grid cells outside $P.Area$, i.e., the grid cells outside the shaded areas; and hence, each estimator of these grid cells is added by $5/11 = 0.45$.

9.3 System Evaluation

In this section, we discuss an attacker model, the experiment setting of TinyCasper in a wireless sensor network, and the performance metrics.

9.3.1 Attacker Model

To evaluate the privacy protection of TinyCasper, we simulate an attacker attempting to infer the number of objects residing in a sensor node's sensing area. We will analyze the evaluation result in Section 9.4.1. The key idea of the attacker model is that if the attacker cannot infer the exact object count of the sensor node from our system output, the attacker cannot infer the location information corresponding to an individual object. We consider the worst-case scenario where the attacker has the background knowledge about the system, which includes the map layout of the system, the location of each sensor node, the sensing area of each sensor node, the total number of objects currently residing in the system, and the aggregate locations reported from the sensor nodes. In general, the attacker model is defined as: *Given an area A (that corresponds to the monitored area of a sensor node) and a set of aggregate locations $\mathcal{R} = \{R_1, R_2, \ldots, R_{|\mathcal{R}|}\}$ overlapping with A, the attacker estimates the number of persons within A.* Since the validation step in our location anonymization algorithms guarantees that the containment relationship among the aggregate locations reported to the server does not violate the k-anonymity privacy requirement, we do not consider any containment relationship in $\mathcal{R}$.

Without loss of generality, we use the Poisson distribution as a concrete exemplary distribution for the attacker model [120]. Under the Poisson distribution, objects are uniformly distributed in an area within intensity of λ. The probability of n distinct objects in a region S of size s is $P(N(S) = n) = \frac{e^{-\lambda s}(\lambda s)^n}{n!}$, where λ is computed as the number of objects in the system divided by the area of the system.

Suppose that the object count of each aggregate location R_i is n_i, where $1 \leq i \leq |\mathcal{R}|$, and the aggregate locations in $\mathcal{R}$ and A constitute m non-overlapping subregions S_j, where $1 \leq j \leq m$; hence $N(R_i) = \sum_{S_j \in R_i} N(S_j) = n_i$. Each subregion must either intersect or not intersect A, and it intersects one or more aggregate locations. If a subregion S_k intersects A, but none of the aggregate locations in $\mathcal{R}$, then $N(S_k) = 0$. The probability mass function of the number of distinct objects in A being equal to n_a, $\mathcal{N} = n_a$, given the aggregate locations in $\mathcal{R}$ can be expressed as follows:

$$
\begin{aligned}
&P(\mathcal{N} = n_a | N(R_1) = n_1, \ldots, N(R_{|\mathcal{R}|}) = n_{|\mathcal{R}|}) \\
=&\frac{P(\mathcal{N} = n_a, N(R_1) = n_1, \ldots, N(R_{|\mathcal{R}|}) = n_{|\mathcal{R}|})}{P(N(R_1) = n_1, \ldots, N(R_{|\mathcal{R}|}) = n_{|\mathcal{R}|})} \\
=&\frac{\sum_{V_i \in (V_S \cap V_A)} < v_1^i, v_2^i, \ldots, v_m^i >}{\sum_{V_j \in V_S} < v_1^j, v_2^j, \ldots, v_m^j >},
\end{aligned} \tag{9.1}
$$

where the notation $V =< v_1, v_2, \ldots, v_m >$ represents the joint probability that there are v_i objects in a subregion S_i $(1 \leq i \leq m)$; the joint probability is computed as $\prod_{1 \leq i \leq m} P(N(S_i) = v_i)$. The lower and upper bounds of v_i (denoted as $LB(v_i)$ and $UB(v_i)$, respectively) are zero and the minimum n_j of the aggregate locations intersecting S_i, respectively. Thus the possible value of v_i is within a range of $[0, \min_{R_j \cap S_i \neq \emptyset \wedge 1 \leq i \leq m \wedge 1 \leq j \leq |\mathcal{R}|}(n_j)]$. V_S is the set of $< v_1, v_2, \ldots, v_m >$ that is a solution to the following equations: $V_S : \sum_{S_i \in R_1} v_i = n_1, \sum_{S_i \in R_2} v_i = n_2, \ldots, \sum_{S_i \in R_{|\mathcal{R}|}} v_i = n_{|\mathcal{R}|}$, where $v_i \geq 0$ for $1 \leq i \leq m$. V_A is the set of $< v_1, v_2, \ldots, v_m >$ that satisfies the following equation: $V_A : \sum_{1 \leq i \leq m} v_i = n_a$.

The attacker uses an exhaustive approach to find all possible solutions to V_S, in order to compute the expected value $E(\mathcal{N})$ of Equation 9.1 as the estimated value of n_a. The complexity of computing $E(\mathcal{N})$ is $O(\prod_{1 \leq i \leq m} UB(v_i))$. Since the complexity of the attacker model is an exponential function of m and m would be much larger than $|\mathcal{R}|$, such exponential complexity makes it prohibitive for the attacker model to be used to provide online location monitoring services; therefore we use our spatial histogram to provide online services in the experiments. We will evaluate the resilience of our system to the attacker model in Section 9.4.1.

9.3.2 Simulation Settings

In all experiments, we simulate 30×30 sensor nodes that are uniformly distributed in a 600×600 system space. Each sensor node is responsible for monitoring a 20×20 space. We generate a set of moving objects that freely roam around the system space. Unless mentioned otherwise, the experiments consider 5,000 moving objects that move at a random speed within a range of $[0, 5]$ space unit(s) per time unit, and the required anonymity level is $k = 20$. The spatial histogram contains $N_R \times N_C = 200 \times 200$ grid

Table 9.1: Parameter settings.

Description	Default Value	Range
Histogram size ($N_R \times N_C$)	200×200	50^2 to 250^2
Query region size ratio	[0.001, 0.032]	0.001 to 0.256
Number of moving objects	5,000	2,000 to 10,000
k-anonymity level	20	10 to 30
Object mobility speed	[0,5]	[0,5] to [0,30]

cells, and we issue 1,000 range queries whose query region size is specified by a ratio of the query region area to the system area, that is, a query region size ratio. The default query region size ratio is uniformly selected within a range of $[0.001, 0.032]$. Table 9.1 gives a summary of the parameter settings.

9.3.3 Performance Metrics

We evaluate TinyCasper in terms of five performance metrics. (1) *Attack model error.* This metric measures the resilience of our system to the attacker model by the relative error between the estimated number of objects $\widehat{N}$ in a sensor node's sensing area and the actual one N. The error is measured as $\frac{|\widehat{N}-N|}{N}$. When $N = 0$, we consider $\widehat{N}$ as the error. (2) *Communication cost.* We measure the communication cost of our location anonymization algorithms in terms of the average number of bytes sent by each sensor node per reporting period. This metric also indicates the network traffic and the power consumption of the sensor nodes. (3) *Cloaked area size.* This metric measures the quality of the aggregate locations reported by the sensor nodes. The smaller the cloaked area, the better the accuracy of the aggregate location is. (4) *Computational cost.* We measure the computational cost of our location anonymization algorithms in terms of the average number of *minimum bounding rectangle* (MBR) computations that are needed to determine a resource- or quality-aware cloaked area. We compare our algorithms with a *basic* approach that computes the MBR for each combination of the peers in the required search space to find the minimal cloaked area. The basic approach does not employ any optimization techniques proposed for our quality-aware algorithm. (5) *Query error.* This metric measures the utility of our system, in terms of the relative

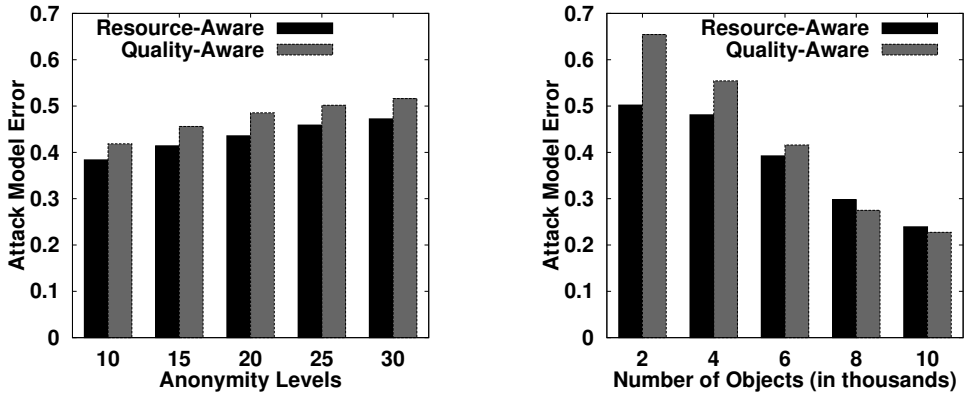

(a) Anonymity levels (b) Number of objects

Figure 9.7: Attacker model error.

error between the query answer $\widehat{M}$, which is the estimated number of objects within the query region based on a spatial histogram, and the actual answer M, respectively. The error is measured as $\frac{|\widehat{M}-M|}{M}$. When $M = 0$, we consider $\widehat{M}$ as the error.

9.4 Experimental Results and Analysis

In this section, we show and analyze the experimental results with respect to the privacy protection and the quality of location monitoring services of TinyCasper.

9.4.1 Anonymization Strength

Figure 9.7 depicts the resilience of our system to the attacker model with respect to the anonymity level and the number of objects. In the figure, the performance of the resource- and quality-aware algorithms is represented by black and gray bars, respectively. Figure 9.7a depicts that the stricter the anonymity level, the larger the attacker model error will be encountered by an adversary. When the anonymity level gets stricter, our algorithms generate larger cloaked areas, which reduce the accuracy of the aggregate locations reported to the server. Figure 9.7b shows that the attacker model error reduces, as the number of objects gets larger. This is because when there are more objects, our algorithms generate smaller cloaked areas, which increase the accuracy of the aggregate locations reported to the server. It is difficult to set a hard quantitative

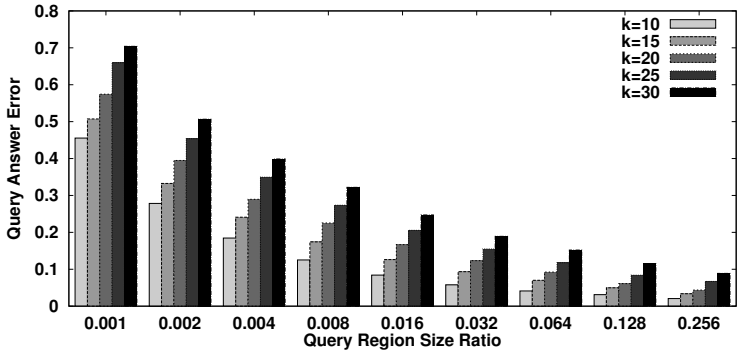

(a) Resource-aware algorithm

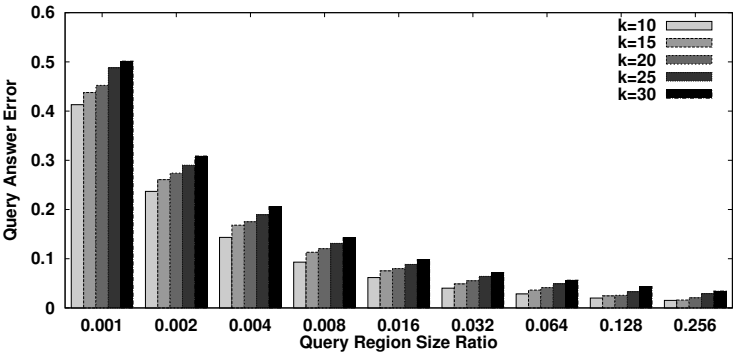

(b) Quality-aware algorithm

Figure 9.8: Query region size.

threshold for the attacker model error. However, it is evident that the adversary cannot infer the number of objects in the sensor node's sensing area with any fidelity.

9.4.2 Effect of Query Region Size

Figure 9.8 depicts the privacy protection and the quality of our location monitoring system with respect to increasing the query region size ratio from 0.001 to 0.256, where the query region size ratio is the ratio of the query region area to the system area and the query region size ratio 0.001 corresponds to the size of a sensor node's sensing area. The results give evidence that our system provides low quality location monitoring services for the range query with a small query region, and better quality services for larger query regions. This is an important feature to protect personal location privacy,

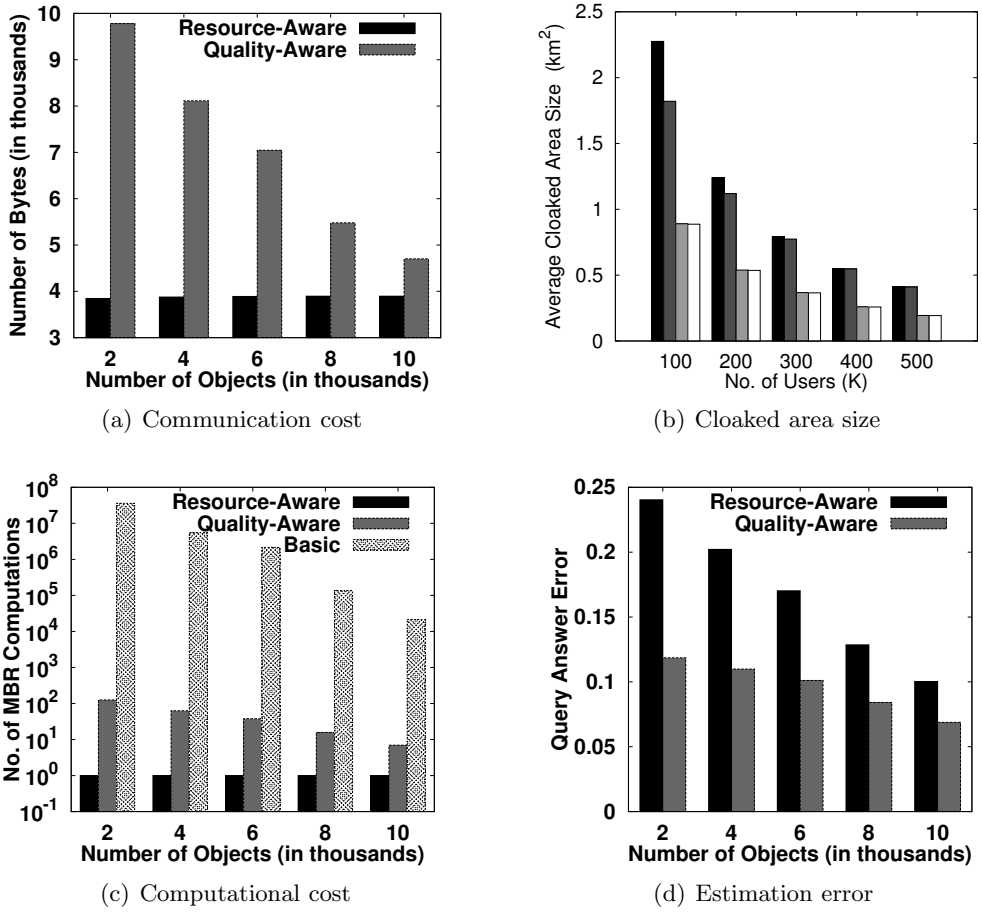

(a) Communication cost

(b) Cloaked area size

(c) Computational cost

(d) Estimation error

Figure 9.9: Number of objects.

because providing the accurate number of objects in a small area could reveal individual location information; therefore an adversary cannot use our system output to track the monitored objects with any fidelity. The definition of a small query region is relative to the required anonymity level k. For example, we want to provide low quality services, such that the query error is at least 0.2, for small query regions. For the resource-aware algorithm, Figure 9.8a shows that when $k = 10$, a query region is said to be small if its query region size is not larger than 0.002 (it is about two sensor nodes' sensing area). However, when $k = 30$, a query region is only considered as small if its query region size is not larger than 0.016 (it is about 16 sensor nodes' sensing area). For the quality-aware algorithm, Figure 9.8b shows that when $k = 10$, a query region is said to be small if

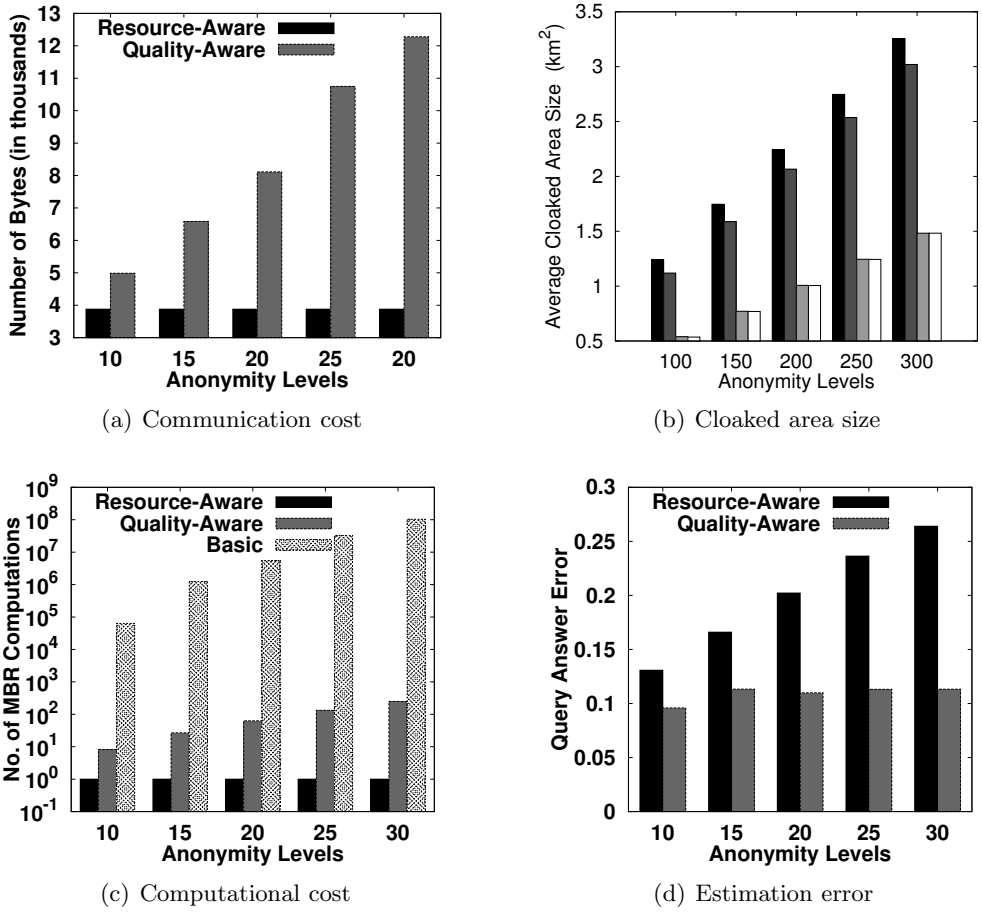

(a) Communication cost

(b) Cloaked area size

(c) Computational cost

(d) Estimation error

Figure 9.10: Anonymity levels.

its query region size is not larger than 0.002, while when $k = 30$, a query region is only considered as small if its query region size is not larger than 0.004. The results also show that the quality-aware algorithm always performs better than the resource-aware algorithm.

9.4.3 Effect of the Number of Objects

Figure 9.9 depicts the performance of our system with respect to increasing the number of objects from 2,000 to 10,000. Figure 9.9a shows that when the number of objects

increases, the communication cost of the resource-aware algorithm is only slightly affected, but the quality-aware algorithm significantly reduces the communication cost. The broadcast step of the resource-aware algorithm effectively allows each sensor node to find an adequate number of objects to blur its sensing area. When there are more objects, the sensor node finds smaller cloaked areas that satisfy the k-anonymity privacy requirement, as given in Figure 9.9b. Thus the required search space of a minimal cloaked area computed by the quality-aware algorithm becomes smaller; hence the communication cost of gathering the information of the peers in such a smaller required search space reduces. Likewise, since there are less peers in the smaller required search space as the number of objects increases, finding the minimal cloaked area incurs less minimum bounding rectangle (MBR) computation (Figure 9.9c). Since our algorithms generate smaller cloaked areas when there are more users, the spatial histogram can gather more accurate aggregate locations to estimate the object distribution; therefore the query answer error reduces (Figure 9.9d). The result also shows that the quality-aware algorithm always provides better quality services than the resource-aware algorithm.

9.4.4 Effect of Privacy Requirements

Figure 9.10 depicts the performance of our system with respect to varying the required anonymity level k from 10 to 30. When the k-anonymity privacy requirement gets stricter, the sensor nodes have to enlist more peers for help to blur their sensing areas; therefore the communication cost of our algorithms increases (Figure 9.10a). To satisfy the stricter anonymity levels, our algorithms generate larger cloaked areas, as depicted in Figure 9.10b. For the quality-aware algorithm, since there are more peers in the required search space when the input (resource-aware) cloaked area gets larger, the computational cost of computing the minimal cloaked area by the quality-aware algorithm and the basic approach gets worse (Figure 9.10c). However, the quality-aware algorithm reduces the computational cost of the basic approach by at least four orders of magnitude. Larger cloaked areas give more inaccurate aggregate location information to the system, so the estimation error increases as the required k-anonymity increases (Figure 9.10d). The quality-aware algorithm provides much better quality location monitoring services than the resource-aware algorithm, when the required anonymity level gets stricter.

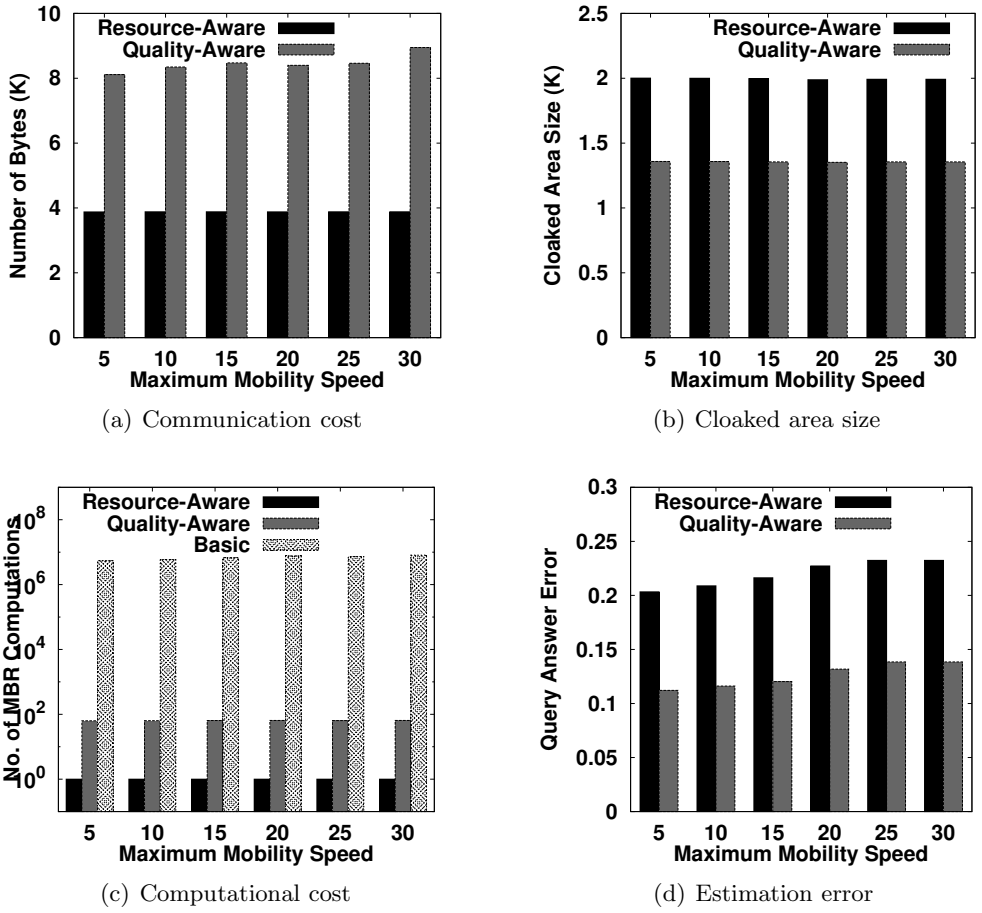

(a) Communication cost

(b) Cloaked area size

(c) Computational cost

(d) Estimation error

Figure 9.11: Object mobility speeds.

9.4.5 Effect of Mobility Speeds

Figure 9.11 gives the performance of our system with respect to increasing the maximum object mobility speed from $[0, 5]$ and $[0, 30]$. The results show that increasing the object mobility speed only slightly affects the communication cost and the cloaked area size of our algorithms, as depicted in Figures 9.11a and 9.11b, respectively. Since the resource-aware cloaked areas are slightly affected by the mobility speed, the object mobility speed has a very small effect on the required search space computed by the quality-aware algorithm. Thus the computational cost of the quality-aware algorithm is also only slightly affected by the object mobility speed (Figure 9.11c). Although Figure 9.11d

shows that query answer error gets worse when the objects are moving faster, the query accuracy of the quality-aware algorithm is consistently better than the resource-aware algorithm.

9.5 Summary

In this chapter, we present the TinyCasper system; a privacy-preserving location monitoring system designed for wireless sensor networks. We design two in-network location anonymization algorithms, namely, *resource-* and *quality-aware* algorithms, that preserve personal location privacy, while enabling the system to provide location monitoring services. Both algorithms rely on the well established k-anonymity privacy concept that requires a person is indistinguishable among k persons. In our system, sensor nodes execute our location anonymization algorithms to provide k-anonymous aggregate locations, in which each aggregate location is a cloaked area A with the number of monitored objects, N, located in A, where $N \geq k$, for the system. The resource-aware algorithm aims to minimize communication and computational cost, while the quality-aware algorithm aims to minimize the size of cloaked areas in order to generate more accurate aggregate locations. To provide location monitoring services based on the aggregate location information, we propose a *spatial histogram* approach that analyzes the aggregate locations reported from the sensor nodes to estimate the distribution of the monitored objects. The estimated distribution is used to provide location monitoring services through answering range queries. We evaluate TinyCasper through simulated experiments. The results show that TinyCasper provides high quality location monitoring services (the accuracy of the resource-aware algorithm is about 75% and the accuracy of the quality-aware algorithm is about 90%), while preserving the monitored object's location privacy.

Chapter 10

Conclusion and Discussion

In this thesis, Chapter 2 presents the Casper system; a privacy-preserving location-based services (LBS) framework. Casper consists of two main components, namely, location anonymizer and privacy-aware query processor. The location anonymizer is a trusted third party placed between the user and the database server to blur a user's exact location into a cloaked area. The location anonymizer guarantees that the cloaked area satisfies the user's k-anonymity and minimum area privacy requirements that are specified by the user in his/her privacy profile. The privacy-aware query processor is embedded inside the database server to deal with location-based queries based on cloaked areas.

In Chapter 3, we present the basic and adaptive location anonymizers of Casper. The basic location anonymizer utilizes a complete pyramid structure to index mobile users and blur their exact locations into cloaked areas. On the other hand, the adaptive location anonymizer uses an incomplete pyramid structure for the location anonymization task. Experiment results show that the adaptive location anonymizer is more effective than the basic one in terms of location anonymization time and location update cost.

Chapter 4 describes the technical details of the privacy-aware query processor of Casper. Casper supports three privacy-aware query types: private queries over public data, public queries over private data, and private queries over private data. Data and/or queries are public, if their exact locations are reported to the database server. However, data and/or queries are private, if only their cloaked location areas are reported to the database server passing through the location anonymizer. Since the

privacy-aware query processor only knows that the locations of queries and/or data are located in their cloaked area, it returns a candidate answer set for a privacy-aware query. The privacy-aware query processor guarantees that the candidate answer set is inclusive, i.e., it contains the exact answer to the querying user, and minimal, i.e., the size of the candidate answer set is minimal. To guarantee system scalability, we design a couple of query performance tuning parameters to trade off between the query execution cost and the minimality of candidate answer sets.

Chapter 5 presents a new query type, called an approximate range nearest-neighbor query, where the location of a query issuer is a rectangular area, i.e., query region, and the locations of data are exact location points. The new query type is not only designed for private queries over public data, but it also supports the query issuer with uncertain location information. Given a query region and a user's specified approximation tolerance level k, the proposed query processing algorithm returns the user a candidate answer set that includes at least one of the k nearest objects of interest of the user, no matter where the user is actually located within the query region.

In Chapter 6, we extend the functionalities of Casper, i.e., location anonymization and privacy-aware query processing, in road network environments. The extended location anonymization algorithm is not only designed for road network environments, i.e., a user's location is blurred into a set of connected road segments, but it is also "query-aware" as it aims to find a cloaked road segment set that minimizes the query execution cost and the size of candidate answer sets. The extended query processing algorithm supports both privacy-aware range and nearest-neighbor queries. To further improve system performance, we also design a shared execution paradigm for nearby privacy-aware queries.

Chapter 7 describes a location anonymization algorithm designed for mobile peer-to-peer (P2P) environments. Mobile P2P environments have many unique limitations, e.g., limited battery power, limited communication bandwidth, and network partition problems. To tackle these limitations, we design an P2P information sharing scheme that allows mobile users to share their cached information with other peers. Since mobile P2P environments rely on multi-hop communication, the cloaking user tends to be the nearest one to the center of a cloaked area. Thus, we propose a cloaked area adjustment scheme to guarantee that the probability of the cloaking user being the closest to the

center of a cloaked area is $1/k$, where the required anonymity level of the cloaking user is k.

In Chapters 8 and 9, we present the TinyCasper system; a privacy-preserving location monitoring system designed for wireless sensor networks. Given a required anonymity level k, the sensor nodes work together to blur their sensing areas into cloaked areas, where each cloaked area contains at least k monitored objects. Then, each sensor node reports an aggregate location, which includes its cloaked area and the number of monitored objects located within the cloaked area, to a server. On the server side, we design a spatial histogram that estimates the object distribution based on the aggregate locations reported from the sensor nodes. TinyCasper provides location monitoring services through answering range queries based on the estimated object distribution.

10.1 Future Research Directions

In this section, we outline some major open issues related to location privacy in LBS that should be addressed in the future.

New privacy-aware query types. Existing privacy-preserving LBS frameworks support only range and/or $\mathcal{K}$-nearest-neighbor queries. To provide comprehensive privacy protection for users, it is important to extend the query processing functionality of existing frameworks to support other popular location-based queries. Examples of these location-based queries include shortest path queries [10], where we should protect the privacy of the source and destination locations, reverse nearest-neighbor queries [121], aggregate nearest-neighbor queries [122], and spatial matching queries [123].

PIR for privacy-preserving LBS. Spatial cloaking techniques have been recently drawn a lot of attention for privacy-preserving LBS. There is a new approach for privacy-preserving LBS that utilizes private information retrieval (PIR) techniques to preserve the location privacy of query issuers. PIR allows a user to gain access to a specific record of a database but it does not reveal the record to the service provider in which the user is interested. Although PIR techniques have been proposed for nearest-neighbor queries, they are limited to only snapshot queries over static data [78, 79, 124]. It is important to investigate new PIR techniques for continuous queries over moving data, and other

query types, e.g., shortest path queries and spatial matching queries.

Probabilistic privacy-preserving LBS. Location perturbation is the most popular technique for privacy-preserving LBS. Since this technique does not allow a database server to know the exact location information of query issuers and/or data, the database server can only returns a candidate answer set to the query issuer. In many mobile environments, the communication bandwidth between the user and the database server is very limited, especially, in the case that the user is moving at a high speed. Thus, it is important to reduce the size of candidate answer sets to improve transmission time. Given a user specified threshold, using probabilistic techniques to compute the probability of each object in a candidate answer set being the exact answer to the user, and then the database server only sends the objects with probabilities larger than the threshold to the user. Although such probabilistic techniques have been designed for public nearest-neighbor (NN) queries over private data [125, 126], we should extend them for other privacy-aware query types, i.e., public queries over private data and private queries and private data, and other spatial query types, e.g., aggregate NN queries and reverse NN queries.

Privacy-preserving trajectory publication. Many organizations have collected huge amount of personal trajectory data through deploying GPS-enabled devices in vehicles. This personal trajectory data is very useful for many important applications, e.g., traffic analysis, travel time estimation, city planning, and customer behavior analysis [127]. However, this personal trajectory data cannot be published to third parties for analysis due to privacy concerns. Thus, we should develop effective techniques that anonymize personal trajectory data and maintain its usability for spatial and spatio-temporal query processing, e.g., *"How many cars have travelled from location A to location B last year"* and *"What is the average travel time from location A to location B during rush hours"*, and analysis, e.g., data mining.

References

[1] Christian S. Jensen. Database Aspects of Location-Based Services. In *Location-Based Services*, pages 115–148. Morgan Kaufmann, 2004.

[2] Mohamed F. Mokbel and Walid G. Aref. PLACE: A Scalable Location-aware Database Server for Spatio-temporal Data Streams. *IEEE Data Engineering Bulletin*, 28(3):3–10, 2005.

[3] Kyriakos Mouratidis, Dimitris Papadias, and Marios Hadjieleftheriou. Conceptual Partitioning: An Efficient Method for Continuous Nearest Neighbor Monitoring. In *Proceedings of the ACM International Conference on Management of Data, SIGMOD*, 2005.

[4] Ouri Wolfson, Hu Cao, Hai Lin, Goce Trajcevski, Fengli Zhang, and Naphtali Rishe. Management of Dynamic Location Information in DOMINO. In *Proceedings of the International Conference on Extending Database Technology, EDBT*, 2002.

[5] Foxs News. Man Accused of Stalking Ex-Girlfriend With GPS. `http://www.foxnews.com/story/0,2933,131487,00.html`. September 4, 2004.

[6] John Voelcker. Stalked by Satellite: An Alarming Rise in GPS-enabled Harassment. *IEEE Spectrum*, 47(7):15–16, 2006.

[7] USA Today. Authorities: GPS System Used to Stalk Woman. `http://www.usatoday.com/tech/news/2002-12-30-gps-stalker$_$x.htm`. December 30, 2002.

[8] BBC News. Privacy Worry Over Location Data. `http://news.bbc.co.uk/2/hi/technology/7559731.stm`. August 14, 2008.

[9] Andreas Pfitzmann and Marit Kohntopp. Anonymity, Unobservability, and Pseudonymity - A Proposal for Terminology. In *Proceedings of the Workshop on Design Issues in Anonymity and Unobservability*, 2000.

[10] Google Maps. `http://maps.google.com`.

[11] Intelius. `http://www.intelius.com/people-search-address.html`.

[12] Mohamed F. Mokbel, Chi-Yin Chow, and Walid G. Aref. The New Casper: Query Procesing for Location Services without Compromising Privacy. In *Proceedings of the International Conference on Very Large Data Bases, VLDB*, 2006.

[13] Chi-Yin Chow, Mohamed F. Mokbel, and Walid G. Aref. Casper*: Query Processing for Location Services without Compromising Privacy. *ACM Transactions on Database Systems, TODS*, 34(4), 2009.

[14] Mohamed F. Mokbel, Chi-Yin Chow, and Walid G. Aref. The New Casper: A Privacy-Aware Location-Based Database Server (Demo). In *Proceedings of the International Conference on Data Engineering, ICDE*, 2007.

[15] Mohamed F. Mokbel, Xiaopeng Xiong, Walid G. Aref, Susanne Hambrusch, Sunil Prabhakar, and Moustafa Hammad. PLACE: A Query Processor for Handling Real-time Spatio-temporal Data Streams (Demo). In *Proceedings of the International Conference on Very Large Data Bases, VLDB*, 2004.

[16] Mohamed F. Mokbel, Xiaopeng Xiong, Moustafa A. Hammad, and Walid G. Aref. Continuous Query Processing of Spatio-temporal Data Streams in PLACE. *GeoInformatica*, 2005.

[17] Chi-Yin Chow, Mohamed F. Mokbel, Joe Nap, and Suman Nath. Evaluation of Range Nearest-Neighbor Queries with Quality Guarantee. In *Proceedings of the International Symposium on Advances in Spatial and Temporal Databases, SSTD*, 2009.

[18] Chi-Yin Chow, Mohamed F. Mokbel, and Xuan Liu. Query-Aware Location Anonymization in Road Networks. *GeoInformatica*, 2010, Under submission.

[19] Chi-Yin Chow, Mohamed F. Mokbel, and Xuan Liu. A Peer-to-Peer Spatial Cloaking Algorithm for Anonymous Location-based Services. In *Proceedings of the ACM Symposium on Advances in Geographic Information Systems, ACM GIS*, 2006.

[20] Chi-Yin Chow, Mohamed F. Mokbel, and Xuan Liu. Spatial Cloaking for Anonymous Location-based Services in Mobile Peer-to-Peer Environments. *GeoInformatica*, To appear.

[21] Chi-Yin Chow, Mohamed Mokbel, and Tian He. A Privacy-Preserving Location Monitoring System for Wireless Sensor Networks. *IEEE Transactions on Mobile Computing, TMC*, To appear.

[22] Nissanka B. Priyantha, Anit Chakraborty, and Hari Balakrishnan. The Cricket Location-Support System. In *Proceedings of the International Conference on Mobile Computing and Networking, MobiCom*, 2000.

[23] Marco Gruteser, Graham Schelle, Ashish Jain, Rick Han, and Dirk Grunwald. Privacy-Aware Location Sensor Networks. In *Proceedings of the USENIX International Workshop on Hot Topics in Operating Systems, HotOS*, 2003.

[24] Gundars Kaupins and Robert Minch. Legal and Ethical Implications of Employee Location Monitoring. In *Proceedings of the Hawaii International Conference on System Sciences, HICSS*, 2005.

[25] Location Privacy Protection Act of 2001, `http://www.techlawjournal.com/cong107/privacy/location/s1164is.asp`.

[26] Chi-Yin Chow, Mohamed Mokbel, and Tian He. TinyCasper: A Privacy-Preserving Aggregate Location Monitoring System in Wireless Sensor Networks (Demo). In *Proceedings of the ACM International Conference on Management of Data, SIGMOD*, 2008.

[27] Crossbow Technology Inc. MICAz 2.4GHz. `http://www.xbow.com/Products/productdetails.aspx?sid=164`.

[28] Linda Ackerman, James Kempf, and Toshio Miki. Wireless Location Privacy: A Report on Law and Policy in the United States, the European Union, and Japan. Technical Report DCL-TR2003-001, DoCoMo Commuinication Laboratories, USA, 2003.

[29] Louise Barkhuus and Anind K. Dey. Location-Based Services for Mobile Telephony: a Study of Users' Privacy Concerns. In *Proceedings of the IFIP Conference on Human-Computer Interaction, INTERACT*, 2003.

[30] Alastair R. Beresford and Frank Stajano. Location Privacy in Pervasive Computing. *IEEE Pervasive Computing*, 2(1):46–55, 2003.

[31] Jay Warrior, Eric McHenry, and Kenneth McGee. They Know Where You Are. *IEEE Spectrum*, 40(7):20–25, 2003.

[32] Bhuvan Bamba, Ling Liu, Peter Pesti, and Ting Wang. Supporting Anonymous Location Queries in Mobile Environments with PrivacyGrid. In *Proceedings of the International World Wide Web Conference, WWW*, 2008.

[33] Chi-Yin Chow and Mohamed F. Mokbel. Enabling Private Continuous Queries For Revealed User Locations. In *Proceedings of the International Symposium on Advances in Spatial and Temporal Databases, SSTD*, 2007.

[34] R. Cheng, Y. Zhang, E. Bertino, and S. Prabhakar. Preserving User Location Privacy in Mobile Data Management Infrastructures. In *Proceedings of Privacy Enhancing Technology Workshop, PET*, 2006.

[35] Matt Duckham and Lars Kulik. A Formal Model of Obfuscation and Negotiation for Location Privacy. In *International Conference on Pervasive Computing, PERVASIVE*, 2005.

[36] Bugrg Gedik and Ling Liu. Protecting Location Privacy with Personalized k-Anonymity: Architecture and Algorithms. *IEEE Transactions on Mobile Computing, TMC*, 7(1):1–18, 2008.

[37] Marco Gruteser and Dirk Grunwald. Anonymous Usage of Location-Based Services Through Spatial and Temporal Cloaking. In *Proceedings of the International Conference on Mobile Systems, Applications, and Services, MobiSys*, 2003.

[38] Gabriel Ghinita, Panos Kalnis, and Spiros Skiadopoulos. PRIVÉ: Anonymous Location-Based Queries in Distributed Mobile Systems. In *Proceedings of the International World Wide Web Conference, WWW*, 2007.

[39] Gabriel Ghinita1, Panos Kalnis, and Spiros Skiadopoulos. MobiHide : A Mobile Peer-to-Peer System for Anonymous Location-Based Queries. In *Proceedings of the International Symposium on Advances in Spatial and Temporal Databases, SSTD*, 2007.

[40] Marco Gruteser and Xuan Liu. Protecting Privacy in Continuous Location-Tracking Applications. *IEEE Security and Privacy*, 2(2):28–34, 2004.

[41] Tanzima Hashem and Lars Kulik. Safeguarding Location Privacy in Wireless Ad-Hoc Networks. In *Proceedingds of the International Conference on Ubiquitous Computing, UBICOMP*, 2007.

[42] Urs Hengartner and Peter Steenkiste. Protecting Access to People Location Information. In *Proceedings of the International Conference on Security in Pervasive Computing, SPC*, 2003.

[43] Jason I. Hong and James .A. Landay. An Architecture for Privacy-Sensitive Ubiquitous Computing. In *In Proceedings of The International Conference on Mobile Systems, Applications, and Services, MobiSys*, 2004.

[44] Panos Kalnis, Gabriel Ghinita, Kyriakos Mouratidis, and Dimitris Papadias. Preventing Location-Based Identity Inference in Anonymous Spatial Queries. *IEEE Transactions on Knowledge and Data Engineering, TKDE*, 19(12):1719–1733, 2007.

[45] Hidetoshi Kido, Yutaka Yanagisawa, and Tetsuji Satoh. An Anonymous Communication Technique using Dummies for Location-based Services. In *Proceedings of the IEEE International Conference on Pervasive Services, ICPS*, 2005.

[46] Po-Yi Li, Wen-Chih Peng, Tsung-Wei Wang, Wei-Shinn Ku, and Jianliang Xu. A Cloaking Algorithm based on Spatial Networks for Location Privacy. In *Proceedingds of the International Conference on Sensor Networks, Ubiquitous, and Trustworthy Computing, SUTC*, 2008.

[47] Toby Xu and Ying Cai. Location Anonymity in Continuous Location-based Services. In *Proceedings of the ACM Symposium on Advances in Geographic Information Systems, ACM GIS*, 2007.

[48] Toby Xu and Ying Cai. Exploring Historical Location Data for Anonymity Preservation in Location-based Services. In *Proceedings of the International Conference of Computer Communications, INFOCOM*, 2008.

[49] Asim Smailagic and David Kogan. Location Sensing and Privacy in a Context-aware Computing Environment. *IEEE Wireless Communication*, 9(5):10–17, 2002.

[50] Pierangela Samarati. Protecting Respondents Identities in Microdata Release. *IEEE Transactions on Knowledge and Data Engineering, TKDE*, 13(6), 2001.

[51] Latanya Sweeney. Achieving k-anonymity Privacy Protection using Generalization and Suppression. *International Journal on Uncertainty, Fuzziness and Knowledge-based Systems, IJUFKS*, 10(5):571–588, 2002.

[52] Latanya Sweeney. k-anonymity: A Model for Protecting Privacy. *International Journal on Uncertainty, Fuzziness and Knowledge-based Systems, IJUFKS*, 10(5):557–570, 2002.

[53] Marios Hadjieleftheriou, George Kollios, Petko Bakalov, and Vassilis J. Tsotras. Complex Spatio-temporal Pattern Queries. In *Proceedings of the International Conference on Very Large Data Bases, VLDB*, 2005.

[54] Bin Lin and Jianwen Su. Shapes Based Trajectory Queries for Moving Objects. In *Proceedings of the ACM Symposium on Advances in Geographic Information Systems, ACM GIS*, 2005.

[55] Dimitris Papadias, Qiongmao Shen, Yufei Tao, and Kyriakos Mouratidis. Group Nearest Neighbor Queries. In *Proceedings of the International Conference on Data Engineering, ICDE*, 2004.

[56] Jimeng Sun, Dimitris Papadias, Yufei Tao, and Bin Liu. Querying about the Past, the Present and the Future in Spatio-temporal Databases. In *Proceedings of the International Conference on Data Engineering, ICDE*, 2004.

[57] Yufei Tao and Dimitris Papadias. Historical Spatio-temporal Aggregation. *ACM Transactions on Information Systems, TOIS*, 23(1):61–102, 2005.

[58] Yufei Tao, Jimeng Sun, and Dimitris Papadias. Analysis of Predictive Spatio-temporal Queries. *ACM Transactions on Database Systems, TODS*, 28(4):295–336, 2003.

[59] Ouri Wolfson, Bo Xu, and Sam Chamberlain. Location Prediction and Queries for Tracking Moving Objects. In *Proceedings of the International Conference on Data Engineering, ICDE*, 2000.

[60] Bugra Gedik and Ling Liu. MobiEyes: Distributed Processing of Continuously Moving Queries on Moving Objects in a Mobile System. In *Proceedings of the International Conference on Extending Database Technology, EDBT*, 2004.

[61] Haibo Hu, Jianliang Xu, and Dik Lun Lee. A Generic Framework for Monitoring Continuous Spatial Queries over Moving Objects. In *Proceedings of the ACM International Conference on Management of Data, SIGMOD*, 2005.

[62] Glenn S. Iwerks, Hanan Samet, and Ken Smith. Continuous k-Nearest Neighbor Queries for Continuously Moving Points with Updates. In *Proceedings of the International Conference on Very Large Data Bases, VLDB*, 2003.

[63] Mohammad R. Kolahdouzan and Cyrus Shahabi. Alternative Solutions for Continuous K Nearest Neighbor Queries in Spatial Network Databases. *GeoInformatica*, 9(4):321–341, 2005.

[64] Iosif Lazaridis, Kriengkrai Porkaew, and Sharad Mehrotra. Dynamic Queries over Mobile Objects. In *Proceedings of the International Conference on Extending Database Technology, EDBT*, 2002.

[65] Mohamed F. Mokbel, Xiaopeng Xiong, and Walid G. Aref. SINA: Scalable Incremental Processing of Continuous Queries in Spatio-temporal Databases. In *Proceedings of the ACM International Conference on Management of Data, SIGMOD*, 2004.

[66] Jun Zhang, Manli Zhu, Dimitris Papadias, Yufei Tao, and Dik Lun Lee. Location-based Spatial Queries. In *Proceedings of the ACM International Conference on Management of Data, SIGMOD*, 2003.

[67] Kyriakos Mouratidis, Man Lung Yiu, Dimitris Papadias, and Nikos Mamoulis. Continuous Nearest Neighbor Monitoring in Road Networks. In *Proceedings of the International Conference on Very Large Data Bases, VLDB*, 2006.

[68] Ying Cai, Kien A. Hua, and Guohong Cao. Processing Range-Monitoring Queries on Heterogeneous Mobile Objects. In *Proceedings of the International Conference on Mobile Data Management, MDM*, 2004.

[69] Sunil Prabhakar, Yuni Xia, Dmitri V. Kalashnikov, Walid G. Aref, and Susanne E. Hambrusch. Query Indexing and Velocity Constrained Indexing: Scalable Techniques for Continuous Queries on Moving Objects. *IEEE Trans. on Computers*, 51(10), 2002.

[70] Wenliang Du and Mikhail J. Atallah. Secure Multi-Party Computation Problems and their Applications: A Review and Open Problems. In *Proceedings of the New Security Paradigms Workshop*, 2001.

[71] Laura M. Haas, Renèe J. Miller, B. Niswonger, Mary Tork Roth, Peter M. Schwarz, and Edward L. Wimmers. Transforming Heterogeneous Data with Database Middleware: Beyond Integration. *IEEE Data Engineering Bulletin*, 22(1), 1999.

[72] Rakesh Agrawal, Alexandre V. Evfimievski, and Ramakrishnan Srikant. Information Sharing Across Private Databases. In *Proceedings of the ACM International Conference on Management of Data, SIGMOD*, 2003.

[73] Fatih Emekci, Divyakant Agrawal, Amr El Abbadi, and Aziz Gulbeden. Privacy Preserving Query Processing using Third Parties. In *Proceedings of the International Conference on Data Engineering, ICDE*, 2006.

[74] Gagan Aggarwal, Mayank Bawa, Prasanna Ganesan, Hector Garcia-Molina, Krishnaram Kenthapadi, Nina Mishra, Rajeev Motwani, Utkarsh Srivastava, Dilys Thomas, Jennifer Widom, and Ying Xu. Vision Paper: Enabling Privacy for the Paranoids. In *Proceedings of the International Conference on Very Large Data Bases, VLDB*, 2004.

[75] Nigel Jefferies, Chris J. Mitchell, and Michael Walker. A Proposed Architecture for Trusted Third Party Services. In *Proceedings of the International Conference on Cryptography: Policy and Algorithms*, 1995.

[76] Anonymous surfing. `http://www.anonymizer.com`.

[77] Paypal. `http://www.paypal.com`.

[78] Gabriel Ghinita, Panos Kalnis, Ali Khoshgozaran, Cyrus Shahabi, and Kian-Lee Tan. Private Queries in Location Based Services: Anonymizers Are Not Necessary. In *Proceedings of the ACM International Conference on Management of Data, SIGMOD*, 2008.

[79] Ali Khoshgozaran and Cyrus Shahabi. Blind Evaluation of Nearest Neighbor Queries Using Space Transformation to Preserve Location Privacy. In *Proceedings of the International Symposium on Advances in Spatial and Temporal Databases, SSTD*, 2007.

[80] Haibo Hu and Dik Lun Lee. Range Nearest-Neighbor Query. *IEEE Transactions on Knowledge and Data Engineering, TKDE*, 18(1):78–91, 2006.

[81] Man Lung Yiu, Christian Jensen, Xuegang Huang, and Hua Lu. SpaceTwist: Managing the Trade-Offs Among Location Privacy, Query Performance, and

Query Accuracy in Mobile Services. In *Proceedings of the International Conference on Data Engineering, ICDE*, 2008.

[82] Yufei Tao, Dimitris Papadias, and Qiongmao Shen. Continuous Nearest Neighbor Search. In *Proceedings of the International Conference on Very Large Data Bases, VLDB*, 2002.

[83] Eija Kaasinen. User Needs for Location-Aware Mobile Services. *Personal and Ubiquitous Computing*, 7(1):70–79, 2003.

[84] Mohamed F. Mokbel. Towards Privacy-Aware Location-Based Database Servers. In *Proceedings of the International Workshop on Privacy Data Management, PDM*, 2006.

[85] Bugra Gedik and Ling Liu. A Customizable k-Anonymity Model for Protecting Location Privacy. In *Proceedings of the IEEE International Conference on Distributed Computing Systems, ICDCS*, 2005.

[86] Steven L. Tanimoto and Theodosios Pavlidis. A Hierarchical Data Structure for Picture Processing. *Computer Graphics and Image Processing*, 4(2), 1975.

[87] Walid G. Aref and Hanan Samet. Efficient Processing of Window Queries in The Pyramid Data Structure. In *Proceedings of the ACM Symposium on Principles of Database Systems, PODS*, 1990.

[88] Thomas Brinkhoff. A Framework for Generating Network-Based Moving Objects. *GeoInformatica*, 6(2):153–180, 2002.

[89] U.S. Census Bureau. TIGER/Line Census Files `http://www.census.gov/geo/www/tiger/`, 2006.

[90] Rimantas Benetis, Christian S. Jensen, Gytis Karciauskas, and Simonas Saltenis. Nearest and Reverse Nearest Neighbor Queries for Moving Objects. *The International Journal on Very Large Data Bases, VLDB Journal*, 15(3):229–249, 2006.

[91] Baihua Zheng, Jianliang Xu, Wang-Chien Lee, and Dik Lun Lee. Grid-Partition Index: A Hybrid Method for Nearest-Neighbor Queries in Wireless Location-based

Services. *The International Journal on Very Large Data Bases, VLDB Journal*, 15(1):21–39, 2006.

[92] Victor Teixeira de Almeida and Ralf Hartmut Güting. Supporting Uncertainty in Moving Objects in Network Databases. In *Proceedings of the ACM Symposium on Advances in Geographic Information Systems, ACM GIS*, 2005.

[93] Reynold Cheng, Dmitri V. Kalashnikov, and Sunil Prabhakar. Querying Imprecise Data in Moving Object Environments. *IEEE Transactions on Knowledge and Data Engineering, TKDE*, 16(9), 2004.

[94] Dieter Pfoser and Christian S. Jensen. Capturing the Uncertainty of Moving-Object Representations. In *Proceedings of the International Symposium on Advances in Spatial Databases, SSD*, 1999.

[95] Goce Trajcevski, Ouri Wolfson, Klaus Hinrichs, and Sam Chamberlain. Managing Uncertainty in Moving Objects Databases. *ACM Transactions on Database Systems, TODS*, 29(3), September 2004.

[96] Man Lung Yiu, Nikos Mamoulis, Xiangyuan Dai, Yufei Tao, and Michail Vaitis. Efficient Evaluation of Probabilistic Advanced Spatial Queries on Existentially Uncertain Data. *IEEE Transactions on Knowledge and Data Engineering, TKDE*, 21(1):108–122, 2009.

[97] Haibo Hu and Jianliang Xu. Non-Exposure Location Anonymity. In *Proceedings of the International Conference on Data Engineering, ICDE*, 2009.

[98] Der-Tsai Lee. On k-Nearest Neighbor Voronoi Diagrams in the Plane. *IEEE Transactions on Computers*, 31(6):478–487, 1982.

[99] Thomas H. Cormen, Charles E. Leiserson, Ronald L. Rivest, and Clifford Stein. *Introduction to Algorithms, 2nd Edition*. MIT Press, Cambridge, MA, 2001.

[100] Wei-Shinn Ku, Roger Zimmermann, Wen-Chih Peng, and Sushama Shroff. Privacy Protected Query Processing on Spatial Networks. In *Proceedings of the International Workshop on Privacy Data Management, PDM*, 2007.

[101] Haibo Hu, Dik Lun Lee, and Jianliang Xu. Fast Nearest Neighbor Search on Road Networks. In *Proceedings of the International Conference on Extending Database Technology, EDBT*, 2006.

[102] Mohammad Kolahdouzan and Cyrus Shahabi. Voronoi-Based k Nearest Neighbor Search for Spatial Network Databases. In *Proceedings of the International Conference on Very Large Data Bases, VLDB*, 2004.

[103] Dimitris Papadias, Jun Zhang, Nikos Mamoulis, and Yufei Tao. Query Processing in Spatial Network Databases. In *Proceedings of the International Conference on Very Large Data Bases, VLDB*, 2003.

[104] Christian S. Jensen, Jan Kolář, Torben Bach Pedersen, and Igor Timko. Nearest Neighbor Queries in Road Networks. In *Proceedings of the ACM Symposium on Advances in Geographic Information Systems, ACM GIS*, 2003.

[105] Wei-Shinn Ku, Roger Zimmermann, and Haixun Wang. Location-Based Spatial Query Processing with Data Sharing in Wireless Broadcast Environments. *IEEE Transactions on Mobile Computing, TMC*, 7(6):778–791, 2008.

[106] Chi-Yin Chow, Hong Va Leong, and Alvin T. S. Chan. GroCoca: Group-based Peer-to-Peer Cooperative Caching in Mobile Environment. *The IEEE Journal on Selected Areas in Communications: Special Issue on Peer-to-Peer Communications and Applications, J-SAC*, 25(1):179–191, 2007.

[107] Wei Wu and Kian-Lee Tan. Global Cache Management in Nonuniform Mobile Broadcast. In *Proceedings of the International Conference on Mobile Data Management, MDM*, 2006.

[108] Chengyang Zhang and Yan Huang. Cloaking Locations for Anonymous Location based Services: A Hybrid Approach. *GeoInformatica*, 13(2):159–182, 2009.

[109] Title 47 United States Code Section 222 (h) (2), `http://frwebgate.access.gpo.gov/cgi-bin/getdoc.cgi?dbname=browse_usc&docid=Cite:+47USC222`.

[110] David Culler and Mani Srivastava Deborah Estrin. Overview of Sensor Networks. *IEEE Computer*, 37(8):41–49, 2004.

[111] Adrian Perrig, Robert Szewczyk, Victor Wen, David E. Culler, and J. D. Tygar. SPINS: Security Protocols for Sensor Netowrks. In *Proceedings of the International Conference on Mobile Computing and Networking, MobiCom*, 2001.

[112] Jiejun Kong and Xiaoyan Hong. ANODR: ANonymous On Demand Routing with Untraceable Routes for Mobile Adhoc Networks. In *Proceedings of the ACM International Symposium on Mobile Ad Hoc Networking and Computing, MobiHoc*, 2003.

[113] Pandurang Kamat, Yanyong Zhang, Wade Trappe, and Celal Ozturk. Enhancing Source-Location Privacy in Sensor Network Routing. In *Proceedings of the IEEE International Conference on Distributed Computing Systems, ICDCS*, 2005.

[114] UC Berkeley WEBS Project. TinyOS: Operating System Support for Sensor Tiny Networked Sensors. `http://www.tinyos.net`.

[115] David Gay, Phil Levis, Rob von Behren, Matt Welsh, Eric Brewer, and David Culler. The nesC Language: A Holistic Approach to Networked Embedded Systems. In *Proceedings of the International Conference on Programming Language Design and Implementation, PLDI*, 2003.

[116] Crossbow Technology Inc. MIB510 Serial Gateway. `http://www.xbow.com/Products/productdetails.aspx?sid=226`.

[117] Onesystems Technologies. Counting People in Buildings. `http://www.onesystemstech.com.sg/index.php?option=com_content&task=view&id=10`.

[118] Traf-Sys Inc. People Counting Systems. `http://www.trafsys.com/products/people-counters/thermal-sensor.aspx`.

[119] Byungrak Son, Seungchan Shin, Junggyu Kim, and Yongsork Her. Implementation of the Real-Time People Counting System using Wireless Sensor Networks. *International Journal of Multimedia and Ubiquitous Engineering, IJMUE*, 2(2):63–80, 2007.

[120] Shuo Guo, Tian He, Mohamed F. Mokbel, John A. Stankovic, and Tarek F. Abdelzaher. On Accurate and Efficient Statistical Counting in Sensor-based Surveillance Systems. In *Proceedings of the International Conference on Mobile Ad Hoc and Sensor Systems, MASS*, 2008.

[121] James M. Kang, Mohamed F. Mokbel, Shashi Shekhar, Tian Xia, and Donghui Zhang. Continuous Evaluation of Monochromatic and Bichromatic Reverse Nearest Neighbors. In *Proceedings of the International Conference on Data Engineering, ICDE*, 2007.

[122] Man Lung Yiu, Nikos Mamoulis, and Dimitris Papadias. Aggregate Nearest Neighbor Queries in Road Networks. *IEEE Transactions on Knowledge and Data Engineering, TKDE*, 17(6), 2005.

[123] Leong Hou U, Man Lung Yiu, Kyriakos Mouratidis, and Nikos Mamoulis. Capacity Constrained Assignment in Spatial Databases. In *Proceedings of the ACM International Conference on Management of Data, SIGMOD*, 2008.

[124] Wai Kit Wong, David Cheung, Ben Kao, and Nikos Mamoulis. Secure k-NN Computation on Encrypted Databases. In *Proceedings of the ACM International Conference on Management of Data, SIGMOD*, 2009.

[125] Reynold Cheng, Jinchuan Chen, Mohamed F. Mokbel, and Chi-Yin Chow. Probabilistic Verifiers: Evaluating Constrained Nearest-Neighbor Queries over Uncertain Data. In *Proceedings of the International Conference on Data Engineering, ICDE*, 2008.

[126] Jinchuan Chen, Reynold Cheng, Mohamed F. Mokbel, and Chi-Yin Chow. Scalable Processing of Snapshot and Continuous Nearest-Neighbor Queries over One-Dimensional Uncertain Data. *The International Journal on Very Large Data Bases, VLDB Journal*, 18(5):1219–1240, 2009.

[127] Osman Abul, Francesco Bonchi, and Mirco Nanni. Never Walk Alone: Uncertainty for Anonymity in Moving Objects Databases. In *Proceedings of the International Conference on Data Engineering, ICDE*, 2008.